INTERACTION BETWEEN DIETARY IRON OVERLOAD AND AFLATOXIN B_1 IN HEPATOCARCINOGENESIS USING AN EXPERIMENTAL RAT MODEL

Michelle Saltão Bronze

Dissertation submitted to the Faculty of Health Sciences, University of the Witwatersrand, Johannesburg, in fulfilment of the requirements for the degree of Master of Science in Medicine

Johannesburg, 2006

Declaration

I, Michelle Saltão Bronze declare that this dissertation is my own work. It is being submitted for the degree of Master of Science in Medicine in the University of the Witwatersrand, Johannesburg. It has not been submitted before for any degree or examination at this or any other University.

Signature

7th day of April, 2006.

In memory of an angel

Benji

1989 - 2006

Abstract

Hepatocellular carcinoma (HCC) is the most common primary malignant tumour of the liver. Aflatoxin B_1 (AFB_1) is a potent hepatocarcinogen, and dietary iron overload has been shown to contribute to HCC development in black africans. Both are well studied hepatotoxins. The aim of this study was to use a Wistar rat model over a 12 month period to investigate synergy and the extent thereof between AFB_1 ingestion and dietary iron overload. 25ug/day of AFB_1, reconstituted in DMSO, was administered by gavaging the animals, over a period of 10 days with a 2 day interval in between. The chow diet was supplemented with 0.75% (w/w) ferrocene iron. Experimental subjects were divided into 4 groups. Group 1 was fed the normal chow diet. Group 2 was fed 0.75% (w/w) ferrocene iron alone. Group 3 was gavaged 250µg AFB_1 alone. Group 4 was fed the 0.75% (w/w) ferrocene iron and gavaged 250µg AFB_1. A number of assays were conducted to investigate synergy. Colorimetric assays were used to measure serum iron, total-iron binding capacity, ALT, AST, GGT, nitrite production, lipid peroxidation and hydroxyproline concentrations. ELISA's were used to determine ferritin, 8-isoprostane and 8-hydroxyguanosine concentrations. Non-transferrin bound iron was measured using an HPLC method. A chemiluminescent assay was used to measure superoxide anion production. Cytokines were measured using a suspension array system. Mutagenicity was assessed using the Ames mutagenicity assay using *salmonella typhimirium* strains TA97, TA98, TA100 and TA102. Iron profiling indicated that iron overloading occurred with the ingestion of the ferrocene diet. Biomarkers of oxidative stress, as illustrated by the measurement of 8-hydroxyguanosine and lipid peroxidation, showed additive synergistic effects between the two carcinogens. The anti-inflammatory interleukin-10 was shown to be markedly elevated with the co-administration of the two carcinogens, indicating the

elevated inflammatory processes. Additive synergistic effects were noted in terms of the liver disease marker ALT. The *salmonella typhimirium* strain TA102 used in the Ames mutagenicity test showed increased colony counts with respect to the co-administration of carcinogens ($P<0.05$), although no synergistic effect was noted. In a few of the presented parameters, the AFB_1 group was not significantly different to the control group, although significant differences between the Fe group and the Fe + AFB_1 groups were noted. The implication of which is that the presence of AFB_1 is increasing the activity of Fe as a carcinogen, thereby acting as a co-carcinogen. Examples of such parameters illustrating this are presented in the results section including serum ALT, serum nitrite, liver and serum lipid peroxidation, liver and serum 8-hydroxyguanosine, some of the mutagenicity assays, and interleukin-10. The conclusion of this study suggests that AFB_1 acts as a co-carcinogen in the presence of iron overloading, implying that a synergistic relationship between these two toxins exists.

Acknowledgments

- Professor MC Kew for his supervision, guidance and support throughout the project and for his aid in editing this dissertation.
- Dr GA Asare for his supervision and for being my mentor in the lab and in writing this dissertation
- Professor AC Paterson for preliminary histological analysis of liver samples
- Professor CP Kahler-Venter at the University of Limpopo –Medunsa Campus for allowing me to use equipment in her lab to perform the superoxide anion chemiluminescent assay
- Dr H Steel at the Institute of Pathology in Pretoria for allowing me the use of the BioPlex Suspension Array System in her laboratory
- Ms L McNamara for helping me with the quantitation of non-transferrin bound iron
- Mr P Dawson and the staff members of the Central Animal Unit (CAS) at the medical school of Witwatersrand University for housing the experimental animals and guidance in handling and care of animals. Dr L Meyer, the veterinary doctor in charge at the CAS, for his assistance and guidance throughout the project
- Mrs Lisa Loram for helping me with the statistical analysis.
- My family, friends and colleagues, who motivated me to work to my full potential at all times and reminded me of the importance of being passionate about my work
- Professor A Kramvis for hours of philosophizing in the lab and for guiding me to think outside the box, not only in terms of science but also in terms life.
- Yoda for saying “Do, or do not. There is no try”.

TABLE OF CONTENTS

LIST OF FIGURES

Figure **Page**

In Appendix

LIST OF TABLES

Tables **Page**

In Appendix

Nomenclature

$^1O_2$	: singlet oxygen
4-HNE	: 4-hydroxynonel
8IP	: 8-isoprostane
8OHdG	: 8-oxo-7,8-dihydro-2-deoxyguanosine
AA	: arachidonic acid
AF	: aflatoxins
AFB_1	: aflatoxin B_1
AFB_1-FAPY	: aflatoxin B_1 formamidopyrimidine
AFB_1-N^7-Gua	: 8,9-dihydro-8-(N7-guanyl)-9-hydroxyaflatoxin B_1
AFP	: alpha feta protein
ALT	: alanine aminotransferase
AP	: apurinic
AST	: aspartate aminotransferase
ATP	: adenosine triphosphate
CAT	: catalase
CD	: conjugated dienes
CGD	: chronic granulomateous disease
CI	: carbonyl iron
Cl^-	: chloride
CO_2	: carbon dioxide
DMSO	: Dimethyl sulphoxide
DMT1	: divalent metal transporter
DNA	: deoxynucleic acid
ELISA	: enzyme-linked immunosorbent assay
ESR	: electron spin resonance
ETC	: electron transport chain
Fe	: iron
FOX	: ferrous xylenol orange
GC/MS	: gas chromatography/mass spectrometry
GGT	: γ-glutamyl transferase
GST	: glutathione S-transferase
H_2O_2	: hydrogen peroxide
Hb	: haemoglobin
HBsAg	: hepatitis B s-antigen
HBV	: hepatitis B virus
HCC	: hepatocellular carcinoma
HH	: hereditary haemochromatosis
HIF	: hypoxia inducible factors
HMdU	: 5-hydroxymethul-2'- deoxyuridine
$HO^{\bullet}$	**:** hydroxyl radical
HOCl	: hypochlorous acid
HOMO	: highest occupied molecular orbitals
HPLC/ECD	: high performance liquid chromatography with electrochemical detector
IARC	: International Agency for Research on Cancer
IFF	: iron free foci
IL	: interleukin

IRE	: iron responsive element
IREG1	: iron-regulated transporter 1
IRP	: iron regulatory protein
LDL	: low density lipoprotein
LOO^-	: lipid radical
$LOO^\bullet$	: alkoxyl radicals
LOOH	: lipid hydroperoxides
LPO	: lipid peroxidation
Mb	: myoglobin
MDA	: malondialdehyde
MHC	: major histocompatability complex
MPV	: mean platelet volume
mRNA	: messenger ribonucleic acid
MTP1	: metal transporter protein 1
NADH	: nicotinamide adenine dinucelotide, reduced form
NAGA	: N-acetyl-glucosaminidase
$NO^\bullet$	**:** nitric oxide
NO_2	: nitrogen dioxide
NO_3^-	: nitrate
NOS	: nitric oxide synthase
Nramp1	: natural resistance-associated macrophage protein 1
NTBI	: non-transferrin binding iron
$O_2^{-\cdot}$	: superoxide anion
O_3	: ozone
$ONOO^-$	: peroxynitrite
ORAC	: oxygen radical absorbance capacity
PSAT	: percentage saturation
PUFA	: polyunsaturated fatty acid
RBC	: red blood cells
RNS	: reactive nitrogen species
$ROO^\bullet$	**:** peroxyl
$ROO^\bullet$	: peroxyl radicals
ROS	: reactive oxygen species
RR	: relative risk
$RS^\bullet$	: thyl
SOD	: superoxide dismutase
TBA	: thiobarbituric acid
TBARS	: thiobabituric acid-reactants
TfR	: transferrin receptor
TIBC	: total iron-binding capacity
TMH-ferrocene	: 3,5,5-trimethylhexanoyl ferrocene
TNF-α	: tumour necrosis factor alpha
TRAP	: total $ROO^\bullet$ trapping
UV	: ultraviolet
WBC	: white blood cells

1.0. Introduction

1.1.HCC, Dietary Iron Overload and Aflatoxin B_1 exposure

1.1.1. Historical and Clinical Perspective

Hepatocellular carcinoma (HCC) is the most common primary malignant tumour of the liver, it ranks as the 5th and 8th most common cancer among men and women, respectively. HCC also accounts for 4% of all newly diagnosed cancers in both sexes and is regarded as one of the major malignant diseases in the world today (Stewart *et al.*, 2003). Among the reasons for this are its high incidence in several of the world's most populous regions, its grave prognosis, and the fact that a number of potentially preventable risk factors for the turnover have been identified. Men are more likely than women to develop HCC, and its prevalence generally increases with increasing age, except in black Africans where there is a shift towards younger age groups (Kew, 1994). Certain viral, environmental, and hereditary causes of cirrhosis have a strong correlation with HCC. Chronic viral hepatitis as a cause of cirrhosis and HCC is well known. Hepatitis B virus infection is the leading cause HCC around the world and is the predominant cause of cancer in high-risk areas including China and Africa (Yeh *et al.*, 1989; Kew *et al.,* 1997). Hepatitis C virus (HCV) is the major cause of HCC in industrialized countries (Dana *et al.*, 1994). Alcohol use is also a common cause of cirrhosis, which can indirectly lead to HCC. A direct carcinogenic effect of alcohol on liver has, however not been proved (Donato F *et al.*, 2002).

Aflatoxin B_1 (AFB_1) is a hepatocarcinogen produced by the fungi *Aspergillus flavus* and *A. parasiticus*, which contaminates food stuffs in certain areas of the world. Exposure to aflatoxins and the rest of the mycotoxins occurs through the ingestion of mouldy foods which is a consequence of contamination of crops in the ground or poor

storage of susceptible grains. A causal association between repeated dietary exposure to AFB_1 and the development of HCC is supported by epidemiological evidence from Africa and the Far East (Adamson *et al.*, 1979). A prospective population-based cohort study in Shanghai, China, provided the first set of compelling human data linking dietary aflatoxin exposure to the development of HCC (Ross *et al.*, 1992; Qian *et al.*, 1994). The carcinogenic effects of HCV and AFB_1 are synergistic (Ross *et al.*, 1992; Qian *et al.*, 1994).

Iron overloading has also been shown to be a high risk-factor in the development of HCC, whether it arises on a genetic basis or as a result of dietary exposure (Bradbear *et al.*, 1985; Strachan, 1929). Hereditary haemochromatosis (HH) is an inherited disorder that increases the amount of iron that the body absorbs from a normal iron diet. HCC has been recognized as one of the major life-threatening complications of the disease. The risk for development of HCC in patients with HH has been estimated to be over 200 (Bradbear *et al.*, 1985; Strohmeyer *et al.*, 1988). A mutation in the HFE gene is the most common cause of haemochromatosis. Other mutations involving the body's iron transport system have also been implicated. The HFE gene is located on chromosome 6, and a mutation leading to a cysteine to tyrosine substitution at position 282, is designated a C282Y mutation. In the mature HFE protein, the mutation is called C260Y, because during transcription 22 amino acids are cleaved to produce the mature protein. Mutant HFE is unable to bind to the iron-loaded transferrin receptor. Without this interaction, the receptor brings more iron into the cells. A H63D mutation in the HFE gene has also been denoted as causing haemochromatosis, albeit to a lesser extent. H63D heterozygotes have hepatic iron concentrations significantly higher than control subjects, but lower than C282Y homozygotes. No biochemical or histological evidence

of liver disease or clinical manifestations is present in H63D heterozygotes (Hellerbrand *et al.*, 2003). Most HH patients who are not appropriately treated develop progressive iron overload and cirrhosis (Harrison & Bacon, 2005). It was originally believed that cirrhosis and not the iron itself was the cause of HCC, but there are reports that suggest HCC development may occur in the absence of cirrhosis in an HH patient (Brage *et al.,* 2002). Such cases are relatively rare and continue to be the topic of case reports (Kowdley, 2004).

Another major risk factor for developing HCC is the dietary form of iron overload. It was first described by Strachan in 1929, and it was known as Bantu visceral siderosis (Strachan, 1929). Strachan carried out necropsy analysis of blacks from southern and central Africa, and concluded that haemosiderosis was a common disease in this population. These findings were substantiated through a number of studies performed thereafter. (Higginson *et al*., 1953; Walker, 1953; Bothwell *et al*., 1960, 1962, 1964; Buchanan 1966, 1967, 1969; MacPhail *et al*., 1979a, 1979b; Gordeuk *et al*., 1986; Friedman *et al*., 1990; Gordeuk 1992b; Mandishona *et al*., 1998). The source of iron overload was shown to be derived from iron drums and pots used in brewing traditional alcoholic beverages, which were consumed in large quantities by the blacks (Bothwell *et al.*, 1964). It was found that the bulk of iron deposition was in the liver and the mononuclear-macrophage system (Bothwell *et al.*, 1965).

The prevalence of dietary iron overload is still high in rural sub-Saharan African populations (Gordeuk *et al.*, 1986), where the prevalence of this disease has been shown to be greater than 10%, and carries a relative risk factor for developing HCC of 10.6, and a population attributable risk of 29 (Mandishona *et al.*, 1998).

1.2. Putative Mechanisms of Iron-induced Carcinogenesis

Dietary iron overload has recently been demonstrated to be a direct cause of HCC in experimental rat model (Asare *et al.*, 2006a). Both direct and indirect effects of iron overload are considered to contribute to carcinogenesis. Direct mechanisms include the effects of iron on cellular proliferation, direct damage by non-transferrin-bound iron to DNA, with resultant inactivation of tumour suppressor genes such as *p53* or their products through post transcriptional or posttranslational changes (Britton *et al*., 2002). Indirect causes include the effects of iron on the formation of reactive oxygen species, iron-induced lipid peroxidation, and acceleration of fibrogenesis in the liver (Kowdley, 2004). There is also evidence that iron overload could lead to immunologic abnormalities that may be associated with decreased immune surveillance for malignancy (Deugnier *et al.,* 2001; Green et *al.*, 1988).

1.3.Putative Mechanisms of AFB_1-induced Carcinogenesis

Metabolism plays a major role in deciding the degree of AFB_1 toxicity (Eaton *et al.,* 1994). After ingestion, AFB_1 is metabolized by the cytochrome P450 group of enzymes in the liver, where it is converted into various metabolic products, depending on the genetic predisposition of the species. The amount of the metabolite, aflatoxin 8,9 epoxide formed, determines the species susceptibility. This metabolite forms adducts with the guanine moiety in the DNA (Smela *et al.*, 2001). A GC to TA transversion at the third position of codon 249 of the *p53* gene is a striking mutational hotspot caused by the intercalation of this epoxide. This observation was made in most experimental HCC models, and it is presumed that this is the major reason for AFB_1 carcinogenicity (Smela *et al.*, 2001).

During its metabolic process an enhanced production of reactive oxygen species (ROS) has been reported (Sivakumar *et al.*, 2001), and ROS have a major role in the mediation of cell damage. Furthermore, ROS damage initially induced by mycotoxins can be propagated and magnified by lipid peroxidation chain reactions (Atroshi *et al.*, 2000). The induction of lipid peroxidation by mycotoxins such as T-2 toxin, AFB_1, and fumonisin B_1, has been clearly elucidated by previous studies (Rizzo *et al.*, 1994; Shen *et al*., 1994; Becognee *et al.*, 1998, Lemmer *et al*., 1999. In addition, the role of ROS in the induction of chromosomal damage by AFB_1 was significantly inhibited by ROS scavenging agents such as superoxide dismutase (SOD), catalase (CAT), and mannitol (Amstad *et al*., 1984).

AFB_1 has also been shown to influence the functioning of the immune system. It was found to markedly inhibit tumour necrosis factor alpha (TNF-α), interleukin-1 (IL-1) and interleukin-6 (IL-6) production by lipopolysaccharide stimulated macrophages. AFB_1 was also found to inhibit the killing ability of murine macrophages (Moon *et al.*, 1999), decreasing various secretory molecules in those cells.

It is clear that both iron overloading and AFB_1 exposure individually have clear involvement in the pathology and induction of HCC.

1.4. Research Hypothesis

1.4.1. Aims and Objectives

It has been suggested that dietary iron overload leads to increased generation of ROS with mutagenic and carcinogenic activity, leading to DNA strand breaks and unwinding, and ultimately malignant transformation (Kowdley, 2004, Asare *et al*., 2006b). AFB_1 is a well known carcinogen, and is one of the most potent liver cancer-forming chemicals known (Smela *et al*., 2001). Iron overloading and the presence of AFB_1 have separately been shown to be carcinogenic, but a possible carcinogenic interaction between the two agents has not been studied**.** The primary aims of this study are to identify synergism between AFB_1, and dietary iron overload in the development of HCC, using an experimental rat model. The objectives therefore are:

1) to show if dietary iron overload and AFB_1 exposure have synergistic effects on the pathogenesis of HCC.
2) to determine the extent of the potential synergy, whether super additive or multiplicative.

1.4.2. Experimental Design

1.4.2.1. Subjects

The Wistar albino rat (*Rattus norvegicus*) was selected for the study based on its higher growth and survival rate compared to the Fischer 344 and the Sprague Dawley rats (Figure 1.1.).

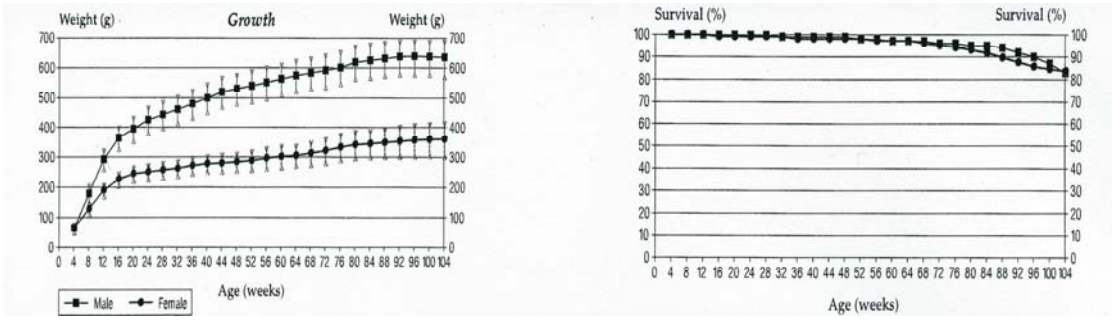

Wistar albino: Growth and Survival Curves

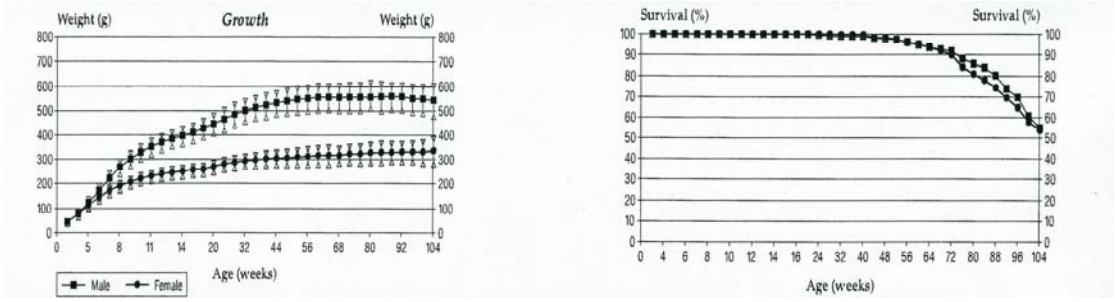

Sprague Dawley: Growth and Survival Curves

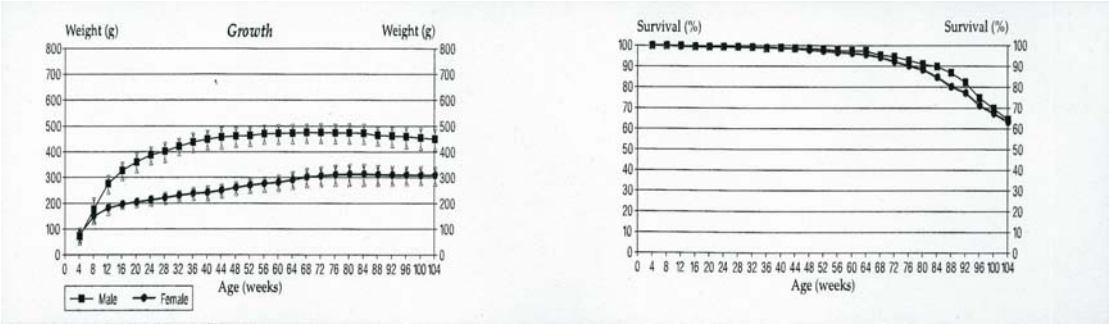

Fischer 344: Growth and Survival Curves

Figure 1.1. Growth Curves of three types of commonly used experimental rats (Harlan, 2000)

Two hundred and twenty (220) Wistar albino rats were divided into 4 groups: Group 1 was the control group consisting of 30 subjects; Group 2, the Fe group with 40 subjects; Group 3, the AFB_1 group with 40 subjects; Group 4, the AFB_1 group with 110 subjects (Figure 1.2.). Group 4 had a larger group of subjects because no previous data was available to indicate how these two carcinogens would interact. A high casualty

rate was expected. To determine synergy, of which no previous data was available, a high sample size was required to enable statistical accuracy. Group 1 was fed the normal chow diet. Group 2 was fed 0.75% (w/w) ferrocene iron alone. Group 3 was gavaged 250µg AFB_1 alone. Group 4 was fed the 0.75% (w/w) ferrocene iron and gavaged 250µg AFB_1.

The AFB_1 was administered, in groups 2 and 4 as 25µg/day for 10 days in total; 5 days at a time, with a 2 day break in-between (Roebuck, 2004). 5 rats per group were sacrificed at 6 months and 12 months after commencement of the project. Rats were anaesthetized with anneket and chanazine, and then euthanased with euthanasia, and blood and liver samples were then harvested. The rats were studied for a total period of 12 months. The remaining rats were kept for disease progression analysis to be conducted in further studies.

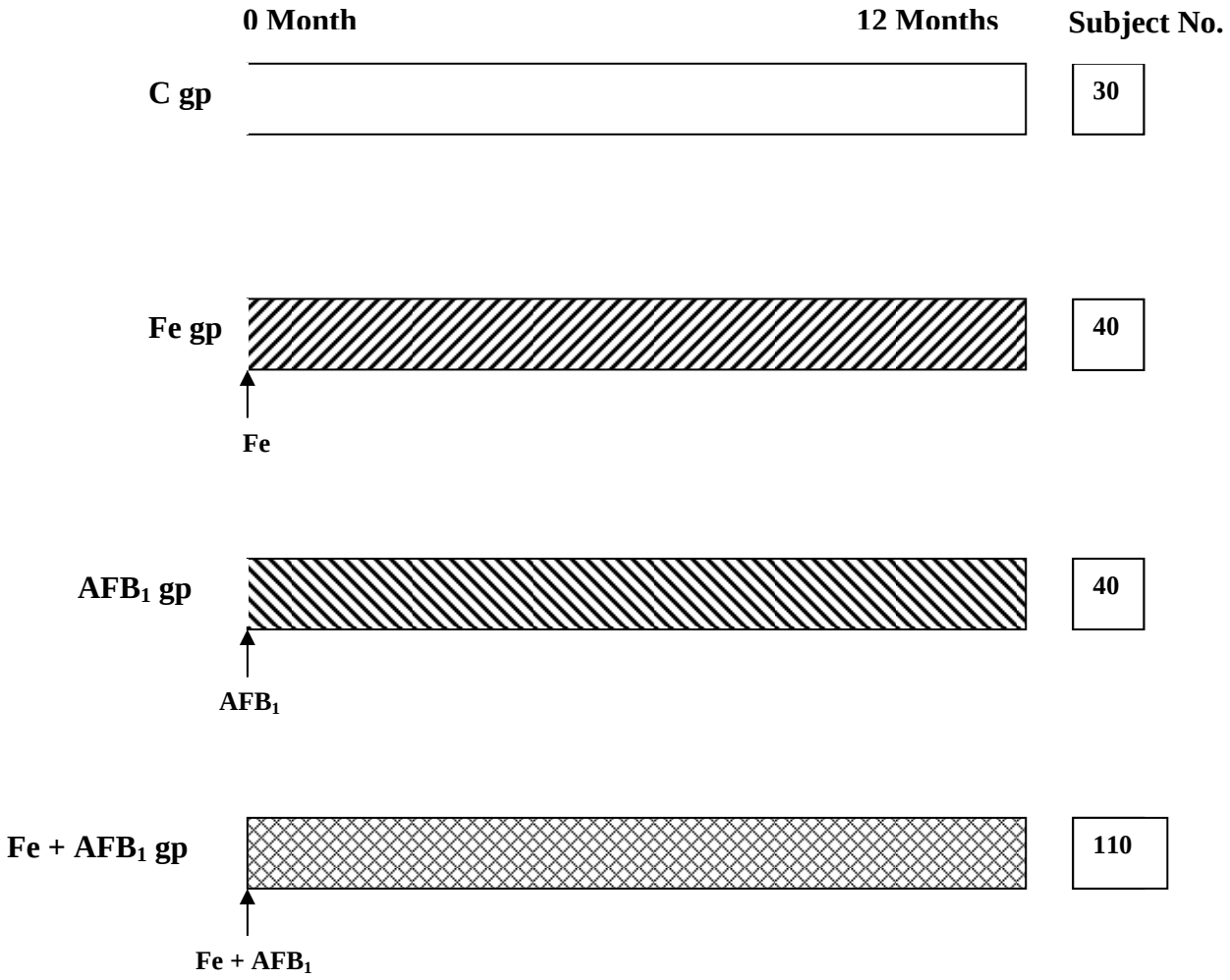

Figure 1.2. Subject Categories

KEY:
C gp = Control group
Fe gp = Iron group
AFB_1 gp = aflatoxin B_1 group
Fe + AFB_1 gp = Iron + Aflatoxin B_1 gp
Fe = Iron
AFB_1 = Aflatoxin B_1

1.4.2.2. Diet

1.4.2.2.1. Iron Diet (Ferrocene)

Ferrocene $Fe(C_5H_5)_2$ is a prototypical metallocene, a type of organometallic chemical compound, consisting of two cyclopentadienyl rings bound on opposite sides of a central iron atom and forming an organometallic sandwich compound.

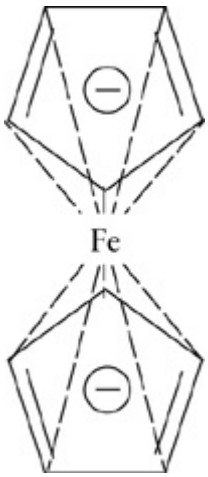

Figure 1.3. Ferrocene molecule

In ferrocene, the pi electrons of both aromatic cyclopentadienyl rings are shared with the central iron ion, giving it an inert gas electron configuration, which makes ferrocene particularly stable. The redox behaviour of ferrocene is not easily influenced by external factors such as temperature and solvents. This stability makes ferrocene an attractive molecule for both basic study and applications. This redox behaviour exists because the highest occupied molecular orbitals (HOMO-1) of ferrocene have almost non-bonding characteristics, and the change of the coordination environment around the iron centre by oxidation is small.

The aromatic cyclopentadienyl rings of ferrocene are just like those of benzene and hence the reactivities of both molecules are similar to each other. Substitution groups can therefore be easily introduced to ferrocene by using an organosynthetic method.

Large numbers of compounds utilizing ferrocene have been synthesized and their relative properties studied. Ferrocenium salts have an anticancer activity (Swarts *et al.*, 2001; Vashisht *et al.*, 2000), and a drug has been reported which is a ferrocenyl version of tamoxifen (Top *et al*., 2003).

A dietary model for severe iron overload was produced by enriching rat diets with (3,5,5-trimethylhexanoyl) ferrocene (TMH-ferrocene) (Nielsen & Heinrich, 1993). Three ^{59}Fe-labelled ferrocene compounds with different lipophylic characters were synthesized. Ferrocene had a bioavailability twice lower than that of TMH-ferrocene, but exhibited similar advantageous characteristics. These advantages included the observation that ferrocene iron is relatively independent of dose, indicating that absorption is not regulated by body iron stores. It is transported through portal blood to the liver, independent of transferrin (Nielsen & Heinrich, 1993). 0.5% TMH-ferrocene was found to be an adequate dosage. In this study a slightly higher dose of 0.75% ferrocene was incorporated and compounded into the chow diet because of ferrocene's slightly lower bioavailability than TMH-Ferrocene. Epol (SA) certified that this diet was mutagen free. Ferrocene was obtained from Sigma, Germany.

1.4.2.2.2. Aflatoxin B_1

1000µg of lyophilized AFB_1 was dissolved in 1000µl of 3% DMSO. AFB_1 was administered to the subjects through the process of gavaging with the aid of a gavage needle. 250µg/day of AFB_1 was administered per rat; hence 25µl/day for 10 days was

dispensed by gavaging from the reconstituted AFB_1. AFB_1 was obtained from Alexis Corporation, UK.

1.4.2.3. Laboratory Methods

A variety of methods was implored to determine the presence and quantitation of reactive oxygen and nitrogen species, lipid peroxidation, DNA mutagenicity bioassays, and iron profiling. Figure 1.4 is a depiction of parameters measured.

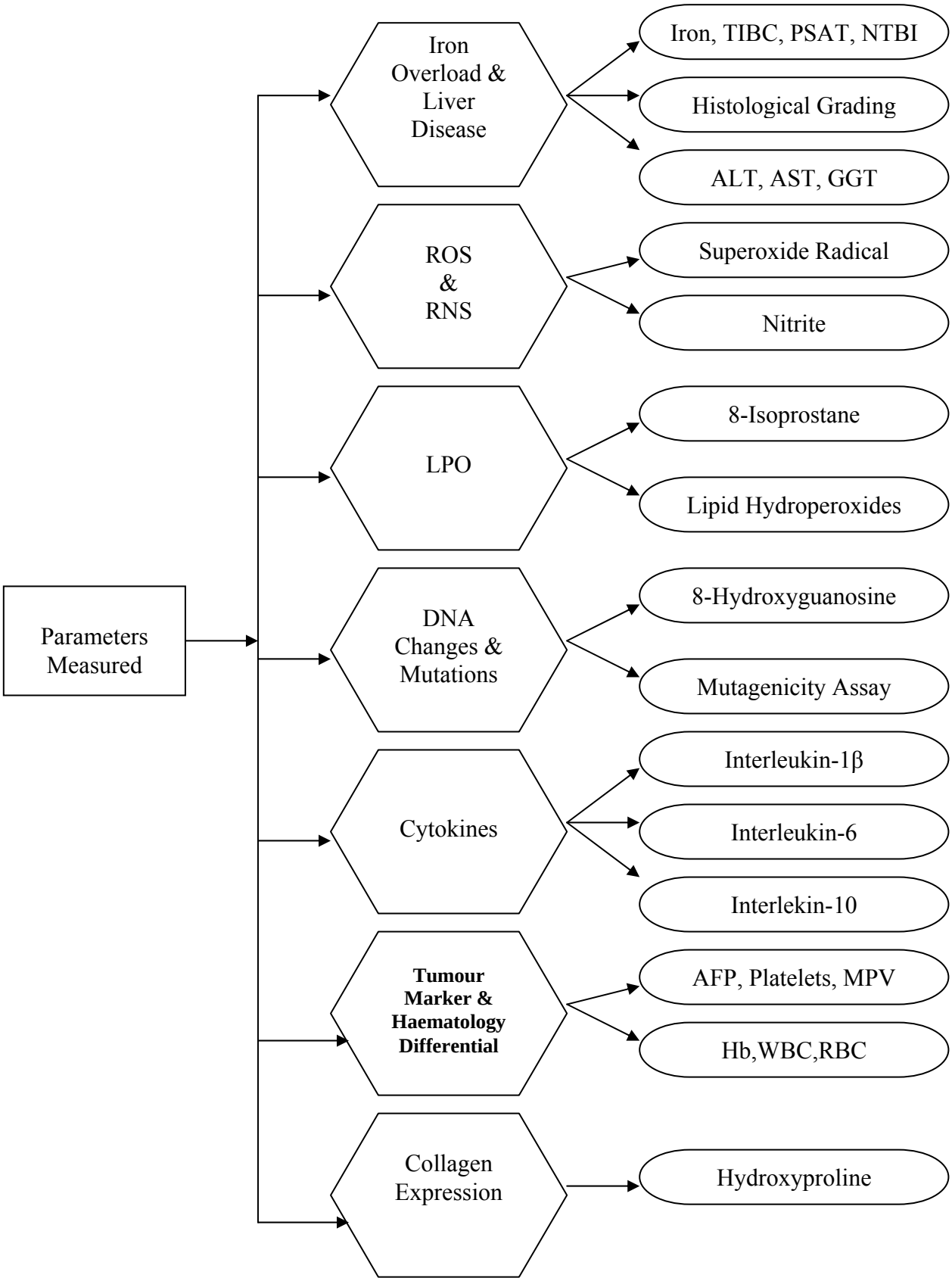

Figure 1.4. Parameters Measured

2.0. Iron

2.1. Iron Chemistry

Iron is of fundamental importance for the growth, development and well being of almost all living organisms. Multiple biological systems have been developed for the uptake, utilization, storage and homeostasis of iron in microbes, plants and mammals. Its bioavailability is generally limited and higher species often exhibit deficiency states. Paradoxically, iron overload conditions occur.

In quantitative terms, iron is the most important essential trace element, being an important mineral for essential nutrition. Adult men and women contain approximately 55 and 45mg per kilogram of body weight of iron, respectively (Halliwell & Gutteridge, 1989).

Iron is a d-block transition element that can exist in oxidation states ranging from -2 to +6. Within biological systems, iron exists in 3 oxidation states, namely ferrous (+2), ferric (+3) and ferryl (+4) states. Iron participates in reactions where there is a transfer of electrons (redox reactions), and in so doing it can reversibly bind to ligands by virtue of its unoccupied d orbitals. The electronic spin state and biological redox potential of iron can change according to the ligand to which it is bound. Iron is therefore particularly suited to participate in a large number of biochemical reactions (Webb,1992).When iron is complexed with water, it is readily hydrolysed and polymerized at a physiological pH of 7 (Spiro & Saltman, 1974). When water molecules are replaced by other chelating ligands, stable complexes are formed. Under conditions of neutral or alkaline pH, iron is found in the Fe^{3+} state and at an acidic pH the Fe^{2+} state is favoured. The strongest complexes of Fe^{3+} tend to be with oxygen donor ligands, e.g. citrates, phosphates, phenols or carbohydrates, whereas Fe^{2+} prefers nitrogen or nitrogen with oxygen donors. The

complexes formed with Fe^{3+} are large, have poor solubility and upon their aggregation lead to pathological consequences (Halliwell & Gutteridge, 1989).

2.2. Biochemical Functions of Iron

The biochemical role of iron is largely manifest in the activity of its metalloproteins. These can be categorized into four main groups (Figure 2.1.). The first consists of those proteins that form reversible complexes with iron and whose primary function is one of iron transport and storage (transferrin and ferritin). The second group can be classified by their ability to bind oxygen reversibly (haemoglobin and myoglobin). The third and most extensive group, the iron-sulfur enzymes, is involved with redox reactions. The fourth group of iron-containing enzymes is a catch-all group in which iron is not bound to a porphyrin ring structure or in iron-sulfur complexes.

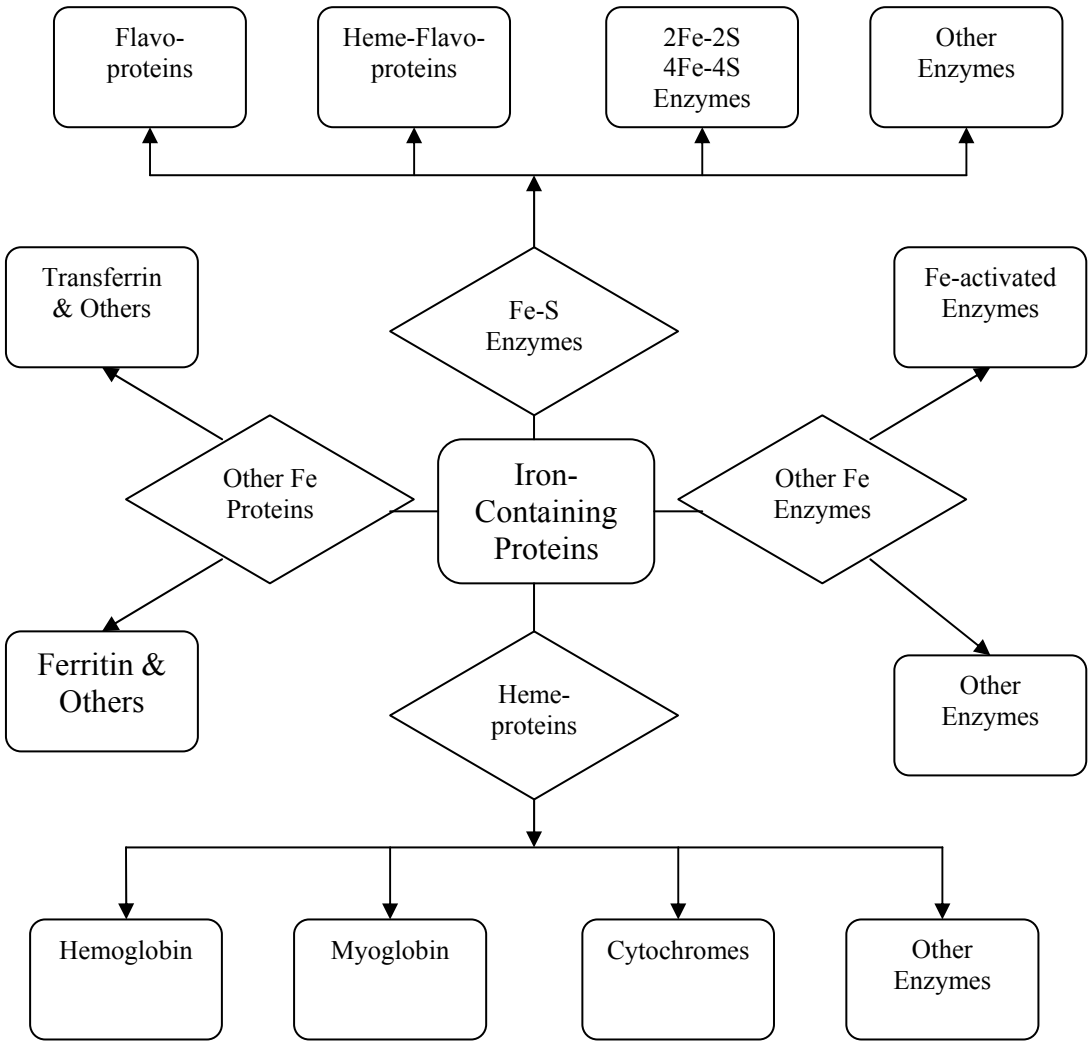

Figure 2.1. Iron-containing Proteins.

These metalloproteins are either metabolically active and functional or metabolically inactive and used for iron storage.

2.2.1. Metabolically Active/ Functional Iron

Metabolically active iron can be divided into three major groups, including iron involved in oxygen transport and storage, iron transport and the iron-containing enzymes.

2.2.1.1. Oxygen transport and storage

2.2.1.1.1. Myoglobin

Myoglobin (Mb) is a monomeric haem protein found mainly in muscle tissue where it serves as an intracellular storage site for oxygen. During periods of oxygen deprivation, oxyhaemoglobin releases its bound oxygen which is then used for metabolic purposes. Its tertiary structure is that of a typical water soluble globular protein. It has an α -helical secondary structure, comprising eight separate right-handed α-helices that are connected by short non-helical regions. Amino acid R-groups are packed into the interior of the molecule. They are predominantly hydrophobic in character, whereas those exposed on the surface of the molecule are generally hydrophilic, thus making the molecule relatively water soluble (Voet & Voet, 1995).

Each Mb molecule contains a haem prosthetic group. Each haem residue contains one central coordinately bound iron atom that is normally in the ferrous state. Oxygen carried by haem proteins is bound directly to this ferrous iron atom. When the iron is oxidized to the ferric state, the molecule is rendered incapable of normal oxygen binding (Voet & Voet, 1995).

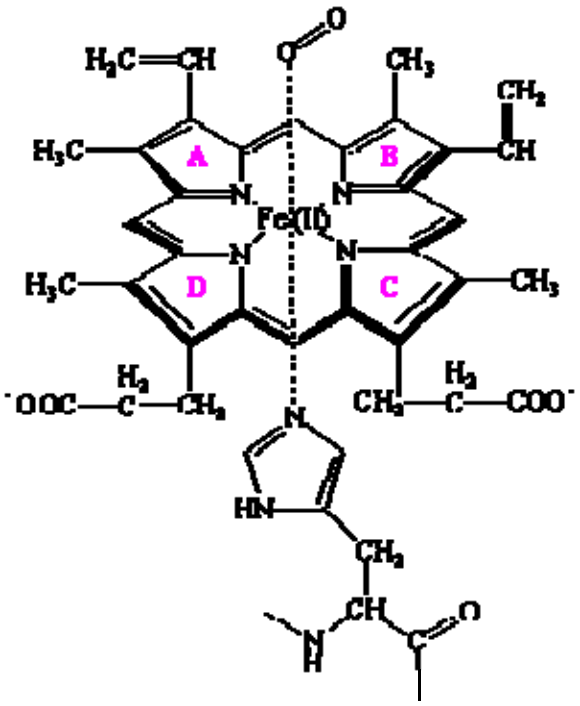

Figure 2.2. Haem Molecule (Voet &Voet, 1995)

2.2.1.1.2. Haemoglobin

Haemoglobin (Hb) is a haemprotein found in erythrocytes and is responsible for binding oxygen in the lung and transporting the bound oxygen throughout the body, where it is used in metabolic pathways. It is the largest iron compartment. Iron binds to protoporphyrin to form haem, which then binds with globin chains to form haemoglobin.

Hb is a tetrameric protein, consisting of two α and two β units. The α and β subunits are structurally and evolutionarily related to each other and to Mb. Each subunit has a haem prosthetic group identical to that of Mb.

The four subunits are not covalently attached to each other but do react cooperatively with dioxygen with specific modulation of pH, pCO_2, organic phosphates and temperature. These modulators of the affinity of haemoglobin for iron determine the efficiency of

transport of oxygen from the alveoli capillary interface in the lung to red cell – capillary – tissue interface in peripheral tissues. The allosteric effect of decreasing pH, the well-known Bohr Effect, decreases the binding affinity of haem-Fe for dioxygen through protonation of His-146 on β chains and Val-1 on α chains in the presence of Cl^- and CO_2. CO_2 forms a Schiff base with terminal amino acids of each chain and decreases dioxygen affinity. This favors the unloading of oxygen in tissues in which the pH is lower and pCO_2 is higher than in arterial blood. 2,3-Diphosphoglycerate is a product of a side pathway within erythrocytes and binds to a specific region of the β chain to decrease Hb-O_2 binding affinity (Voet & Voet, 1995).

2.2.1.2. Iron Transport compartments in blood

2.2.1.2.1. Transferrin

The major function of transferrin is to transport iron into cells. Eventually all circulating plasma iron is bound to transferrin. The amount of iron both attached to transferrin or free from transferrin is measured as the serum iron. The sum of all iron binding sites on transferrin constitutes the total iron binding capacity (TIBC) of plasma. Under normal circumstances, about one third of transferrin iron-binding pockets are filled. Consequently, with the exception of iron overload when all the transferrin binding sites are occupied, non-transferrin-bound iron (NTBI) in the circulation is virtually nonexistent. In iron overload, plasma iron concentrations rise significantly and leads to the appearance of NTBI. The accumulation of plasma NTBI has been shown to correlate with the appearance of oxidation products and a decrease in plasma antioxidant capacity (Cighetti *et al.*, 2002; De Luca *et al.*, 1999).

The chelation between transferrin and iron serves three purposes: it renders iron soluble under physiological conditions, it prevents iron-mediated free radical toxicity, and it facilitates transport into cells.

Transferrin is the most important physiological source of iron for red cells (Ponka, 1997). It is synthesized in the liver and thereafter secreted into the plasma. Transferrin has also been found to be synthesized locally in the testes and the central nervous system. This local transferrin production could play a role in iron metabolism in these tissues.

Transferrin is an 80kDa glycoprotein with homologous N-terminal and C-terminal iron-binding domains (Huebers & Finch,1987). The molecule is related to several other proteins, including ovotransferrin in bird and reptile eggs (Williams *et al.*, 1982), lactoferrin in extracellular secretions and neutrophil granules (Mazurier *et al.*, 1983; Metz-Boutigue *et al.*, 1984) and melanotransferrin, a protein produced by melanoma cells (Brown *et al.*, 1982). However, their main function is not delivery. Instead, they serve to protect cells from bacteria. Since they mop up any free iron ions, they restrict bacteria of a vital resource, slowing the growth of an infection. All members of the transferrin protein superfamily have similar polypeptide folding patterns. N- and C-terminal domains are globular moieties of about 330 amino acids. Each of these is divided into two sub-domains, with iron- and anion-binding sites in the intersubdomain cleft. The binding cleft opens with iron release, and closes with iron binding (Voet & Voet, 1995).

Figure 2.3. Ribbon Diagram of Mammalian Transferrin

(http://www.iupac.org/news/prize/2005/Dhungana.pdf)

2.2.1.3. Iron-containing Enzymes

2.2.1.3.1. Enzymes involved in Electron Transport and Energy Metabolism

Cytochromes are haem-containing compounds that are critical to cellular energy production through their roles in mitochondrial electron transport. They serve as electron carriers during the synthesis of ATP, the primary energy-storage compound in the cells. Cytochrome P450 is a family of enzymes that functions in the metabolism of a number of important molecules, as well as the detoxification and metabolism of drugs and pollutants. Nonhaem iron-containing enzymes, such as NADH dehydrogenase and succinate dehydrogenase, are also critical to energy metabolism (Yip *et al.*, 1996).

2.2.1.3.2. Enzymes involved in Antioxidant Functions

Catalase and peroxidases are haem-containing enzymes that protect cells against the accumulation of hydrogen peroxide, a ROS, by catalyzing a reaction that converts hydrogen peroxide to water and oxygen. As part of the immune response, some leukocytes engulf bacteria and expose them to ROS in order to kill them. The synthesis of

hypochlorous acid by neutrophils is catalyzed by the haem-containing enzyme myeloperoxidase (Yip *et al.*,1996; Brody, 1999).

2.2.1.3.3. Enzymes Involved in Oxygen Sensing

During a state of hypoxia, compensatory physiological responses are induced. This includes the increased formation of red blood cells, increased angiogenesis, and increased production of enzymes utilized in anaerobic metabolism. Transcription factors known as hypoxia inducible factors (HIF) bind to response elements in genes that encode various proteins involved in compensatory responses to hypoxia and hence increase their synthesis. Iron-dependent prolyl hydroxylase enzymes play a critical role in regulating HIF and consequently, physiological responses to hypoxia. When cellular oxygen tension is adequate, HIF, is targeted by a prolyl hydroxylase enzyme, and is rapidly degraded. When cellular oxygen tension drops below a critical threshold, prolyl hydroxylase can no longer target HIF for degradation, allowing HIF to form active transcription factors that are stable to enter the nucleus and bind to specific elements on genes (Ivan *et al.*, 2001; Jaakkola *et al.*, 2001).

2.2.2. Metabolically Inactive and Storage Iron

2.2.2.1. Ferritin

Unbound iron can be toxic, so the ability to store and release iron in a controlled manner is essential. Cells handle this problem of iron storage by developing ferritin, a family of iron-storage proteins that sequester iron inside a protein coat as hydrous ferric oxide-phosphate mineral.

Ferritin is mainly a cytoplasmic protein and there are generally two or more genes that encode closely related subunits, designated H (heavy) and L (Light). Ferritin has a spherical shell that consists of 24 subunits folded into ellipsoids. Each subunit is an individual molecule that joins its neighbouring subunits through noncovalent interactions. The subunits have a combined molecular weight of 474000. These subunits pack to form a hollow sphere approximately 80 Angstroms ($1.25x10^{-2}$ μm) in diameter with walls that are approximately 10 Angstroms ($1x10^{-3}$ μm) thick. Among the important structural features of ferritin is the presence of two types of channels that occur in the protein wall. After iron enters the ferritin shell, iron ions are converted into the ferric state, where they form small crystallites along with phosphate and hydroxide ions. A ferritin molecule has the capacity to hold 4500 iron ions.

Serum ferritin is measured as part of iron study profiles. The amount of ferritin in plasma is less than one thousandth of total body ferritin, but its concentration is directly proportional to total body iron ferritin quantities in conditions of health, iron deficiency and mild iron overload. An abnormally raised ferritin level is a marker for iron overload disorders. Although ferritin is also synthesized in the liver in response to inflammation (acute phase reactant), a normal C-reactive protein can be used to exclude elevated ferritin caused by acute phase reactions (Halliwell & Gutteridge, 1989).

2.2.2.2. Haemosiderin

Partially degraded and aggregated ferritin is called haemosiderin. It is insoluble in water and is not as accessible for cell use as is ferritin. It is most commonly seen as golden-brown granular material in macrophages and is readily demonstrated to be iron by a Prussian-blue stain. The presence of haemosiderin in small amounts within iron rich tissues

such as the spleen, liver, and bone marrow is considered normal. Large aggregations of haemosiderin or its presence in tissues such as the lung or subcutaneous connective tissue suggest a pathological condition (Selden, 1980).

2.3. Iron Transport Mechanisms

Four major iron transport mechanisms have been identified.

a) The differic-transferrin/transferrin receptor endocytic mechanism through clathrin coated pits.
b) Divalent metal transporter (DMT1) and Natural resistance-associated macrophage protein (Nramp1)
c) Iron-regulated transporter 1 (IREG1) , with the aid of hephaestin
d) Ferrous ATPase

DMT1 and Nramp1 are two homologous divalent metal/proton symport proteins. DMT1, also known as Nramp2, is an integral membrane protein expressed at cell surfaces and in cycling endosomes. It is induced by a low intracellular iron concentration. It appears to be indirectly involved in iron transport between blood plasma and tissues. High concentrations thereof are expressed at the lumenal surface brush border of the mature upper small intestine enterocytes found along the villus (Trinder *et al.*, 2000). It is modestly expressed in the cytoplasm of the same cells. Nramp1 is an integral membrane protein, exclusive to macrophages, monocytes and polymorphonuclear leukocytes. It is induced in phagosomes or lysosomes of macrophages in response to bacterial endotoxins and cytokines (TNFα and IL-1), and transfers iron out of phagosomes into the cytosol of macrophages. Iron provided in the cytoplasm of macrophages by Nramp1 activity appears to enhance the stability of macrophage mRNA encoding cytokines, which in turn are

responsible for the recruitment of leukocytes to the site of an infection and their activation (Govoni & Gros, 1998).

IREG 1 is also known as ferroportin 1 and metal transporter protein 1 (MTP1). It is highly expressed in the placenta and duodenum. It is a transmembrane protein that mediates iron efflux from cells. Iron deficiency increases IREG1 expression in the duodenum but decreases expression in the liver (McKie *et al.*, 2000). The transport of iron by IREG1 requires that Fe^{2+} be oxidized to Fe^{3+}. This oxidation is proposed to be mediated by hephaestin. Hephaestin is a transmembrane-bound homologue of the copper-containing blood plasma ferroxidase caeruloplasmin. It is proposed to be a ferroxidase located at the basolateral membrane of enterocytes and required for transfer of iron from enterocytes to blood in conjunction with some other, unknown iron transport protein (Vulpe *et al.*, 1999).

Iron ATPase is an ATP-dependent Fe^{2+} transporter. It transports iron into microsomal vesicles and is in high concentration in the spleen. Fe^{2+} is its specific substrate. It has been proposed that the iron ATPase mediates the transport of iron from the cytoplasmic compartment of macrophages into the lumen of their microsomal vesicles to allow export of iron derived from the breakdown of haemoglobin (Baranano *et al.*, 2000).

2.4. Cellular uptake of Iron

2.4.1. Iron Absorption

Elemental iron or dietary haem iron is absorbed principally by the mucin lining the duodenum and to a lesser extent, the jejunum. Gastric acid plays an important role in keeping iron soluble and in the ferrous state. The mucin transfers iron to trans-membrane integrins. Once inside the cell, iron is transferred to mobilferritin. The iron passes to

ferritin and then to transferrin bound to the extracellular side of the protein and is then released into the plasma. Transferrin receptor (TfR) bound to the corporeal portion of the mucosal cell functions to bind transferrin from the plasma and bring it into the cell through clathrin-mediated endocytosis, where it may function to regulate iron absorption (Garrick *et al.*, 1993). When the iron-bound transferrin enters the bloodstream, it is reabsorbed mainly by hepatocytes and erythroblasts, again by the TfR.

The TfR is a disulfide-linked homodimer with each subunit containing 760 amino acids (Kuhn *et al.*, 1984; Schneider *et al.*, 1983; Jing & Trowbridge, 1987). It has a molecular mass of 90kDa per subunit, with 5% consisting of oligosaccharides. ^{3}N-linked and ^{1}O-linked glycosylation sites exist (Hayes *et al.*, 1992). The transmembrane domain functions as an internal signal peptide. A molecule of fatty acid covalently links each subunit to the internal edge of the transmembrane domain and could play a role in membrane localization. The expression of the TfR is increased on cells that are iron deficient, and decreased on cells that are iron overloaded.

After binding to its receptor on the cell surface, transferrin is rapidly internalized by invagination of clathrin-coated pits with the formation of endocytic vesicles. A complex mechanism involving recycling endosomes follows. In plasma, differic-transferrin saturates transferrin receptors displayed on the surface of cells. The collection of iron/transferrin/transferrin-receptor complexes and its embedding membrane is internalized through a clathrin-coated pit to become a recycling endosome. Embedded in the membrane is also a DMT1. An ATP-dependent proton pump lowers the pH of the endosome to about 5.5 (Van Renszoude *et al.*, 1982; Dautry-varsat *et al.*, 1983; Paterson *et al.*, 1984; Yamashiro *et al.*, 1984). The acidification of the endosome weakens the association

between iron and transferrin. Even at pH 5.5, Fe^{3+} would not normally dissociate from transferrin in the several minutes between its endocytosis and the return of transferrin apoprotein to the cell surface (Ciechanover *et al.*, 1983). A plasma membrane oxidoreductase reduces transferrin bound iron from the Fe^{3+} state to the Fe^{2+}, directly or indirectly facilitating the removal of iron from the protein (Low *et al.*, 1987; Thorstensen & Romsolo, 1988; Nunez *et al.*, 1990). Conformational changes in the transferrin receptor also play a role in iron release (Bali *et al.*, 1991; Sipe & Murphy, 1991).

The released iron is transferred to the cytoplasm by the DMT1, driven by the high proton concentration of the endosome. The released apotransferrin/transferrin-receptor is recycled back to the cell surface, where the apotransferrin is released into the plasma (Zak *et al.*, 1994). The re-use of transferrin is accomplished by the pH-dependent changes in the affinity of transferrin for its receptor (Van Renswoude *et al.*, 1982; Klausner *et al.*, 1983: Dautry-Varsat *et al.*, 1983). Exported apotransferrin binds additional iron and undergoes further rounds of iron delivery into the cells. The average transferrin molecule, with a half-life of eight days, may be used up to one hundred times for iron delivery (Harford *et al.*, 1994).

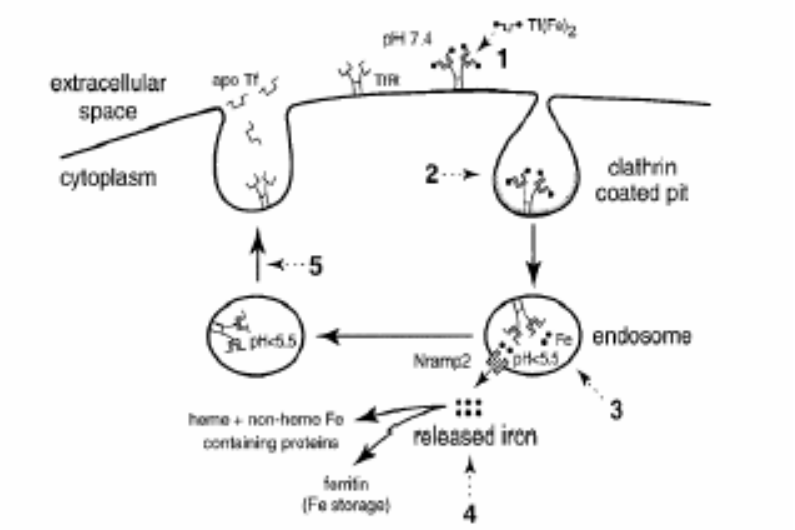

Figure 2.4. Illustration of clathrin-mediated endocytosis.

The primary role of the transferrin-transferrin receptor interaction is to bring iron into the vicinity of the cell surface, thereby increasing the likelihood of iron uptake. Following its release from transferrin within the endosome, iron must traverse the plasma membrane to enter the cytosol proper. The molecules effecting this transport have not been identified, but the process may be carrier-mediated (Egyed, 1988).

Once inside the cell cytoplasm, iron appears to be bound by a low molecular weight carrier molecule, which may assist in delivery to various intracellular locations including the mitochondria (for haem biosynthesis) and ferritin (for storage). The amount of iron in transit within the cell at any given time is miniscule and defies precise measurement. This minute pool of transit iron, which is believed to be in the Fe^{2+} oxidation state, is the biologically active form of the element. Metabolically inactive iron, stored in ferritin and haemosiderin, is in equilibrium with exchangeable iron bound to the low molecular weight carrier molecule.

The function of another protein, produced by a gene called the haemochromatosis gene, HFE, is still incompletely understood. TfR is itself regulated by a MHC type 1-like protein which forms a stable complex with the intracellular portion of TfR and β2-microglobulin. HFE, bound with β2-microglobulin, inhibits the absorption of transferrin, increasing the amount of iron-bound transferrin in the blood and down-regulating iron absorption (Feder *et al.*, 1998).

2.5. Post-transcriptional control of Proteins involved in Iron Metabolism

Induction and repression of several iron-binding proteins are now known to be effected at the level of mRNA stability. Iron regulatory proteins (IRP) can bind iron but, in the

absence of iron they bind to iron responsive elements (IRE) found in mRNA transcripts of specific genes. In the case of mRNA encoding DMT1, transferrin, transferrin receptor and delta-aminolevulinic acid synthase, the IRE is in the untranslated portion at the 3'end of the gene transcript. Each IRE forms a stem-loop structure in which the loop contains five specific bases and the stem contains adenine and uracil rich (AU-rich) sequences similar to those that destabilize cytokine mRNAs. When iron concentrations are adequate, these AU-rich sequences are thought to promote degradation of TfR mRNA by the same mechanism that leads to rapid degradation of cytokine mRNAs. When the iron concentration falls slightly, the conformation of IRE – binding protein (IRP) changes so that it can bind to the IREs. Binding of IRPs to the IREs is thought to block recognition of the destabilizing AU-rich sequences by the proteins that would otherwise degrade TfR mRNA (Eisenstein & Ross, 2003).

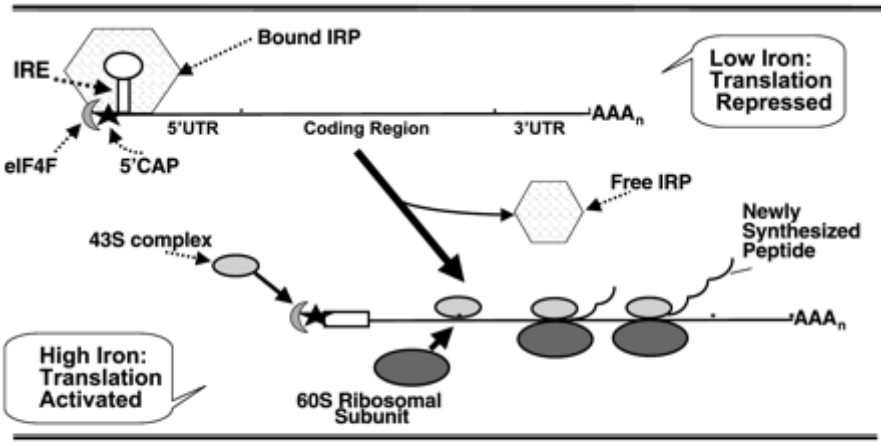

Figure 2.5. Illustration of IRE and IRP activity in high and low iron concentrations (Eisenstein & Ross, 2003).

2.6. Iron Overload

Chronic iron overload is characterized by increased focal or generalized deposition within the tissues. Iron is stored as ferritin and/or haemosiderin. Iron overloading was therefore known as haemosiderosis. When excess iron deposition is associated with tissue injury or the total body iron estimate is greater than 5g, the term haemochromatosis is applied.

Several disorders may lead to pathological accumulation of iron in the body. Hereditary haemochromatosis is the most common genetic iron metabolism disorder. It is characterised by iron overload despite normal dietary iron intake. However, haemochromatosis in Sub-Saharan Africa is caused by increased dietary iron intake. Table 2.1 summarizes many of the heritable and acquired disorders associated with iron overload.

Table 2.1. Heritable and Acquired Disorders Associated with Iron Overload

Heritable Disorder	Cause of Iron Overload
Haemochromatosis	
▪ Haemochromatosis Type 1 (Adult)	HFE gene mutations
▪ Haemochromatosis Type 2A (Juvenile)	Unknown
▪ Haemochromatosis Type 2B (Juvenile)	Hepcidin gene mutations
▪ Haemochromatosis Type 3	Transferrin receptor 2 inactivation
▪ Haemochromatosis Type 4	Ferroportin gene mutations
▪ Haemochromatosis Type 5 (Japanese Iron Overload)	H-ferritin gene mutation
Other Heritable Disorders	
▪ Porphyria cutanea tarda	Heterogenous
▪ African iron overload	Dietary
▪ Neonatal iron overload	In-utero iron transfer
▪ Atransferrinaemia	Transferrin gene mutations & red cell transfusions
▪ Aceruloplasminaemia	Ceruloplasmin gene mutations
▪ Hereditary hyperferritinaemia cataract syndrome	L-ferritin gene mutations
▪ Friedreich ataxia	Frataxin gene mutations
▪ B-Thalassemia major	B-glbin gene mutations, chronic hemolysis, red cell transfusions
▪ Hereditary X-linked sideroblastic anaemia	d-ALA synthase gene mutations
▪ Pyruvate kinase deficiency	Pyruvate kinase gene mutations
▪ G6PD deficiency	G6PD gene mutation
▪ Congenital dyserythropoetic anaemia	Ineffective erythropoeisis
▪ Pantothenate Kinase – Associated Neurodegeneration	Pantothenate kinase 2 gene mutations
Acquired Disorders	
▪ Transfusions	Red Cell iron transfusion
▪ Medicinal Iron	Excessive iron ingestion
▪ Myelodysplasia with ring sideroblasts	Excessive iron absorption
▪ Portocaval Shunt	Excessive iron absorption

2.6.1. Iron overload in Experimental Animals

Iron loading experimental rat models have only recently been optimized. Early studies used Jectofer injections to increase plasma iron concentrations (Hultcrantz *et al.*, 1980). The preferred model, however, included the addition of carbonyl iron (CI) to the diet (Bacon *et al.*, 1983; Pietrangelo *et al.*, 1990; Britton *et al.*, 1990; Tector *et al.*, 1995). This protocol, however, demonstrated adverse side effects to the well-being of the animal, including retarded growth rates and diarrhoea. Various modifications of the feeding regimen were used where CI concentrations were varied throughout the study. No advantages were reported in relation to these modifications.

In the early 1990's investigators experimented with an alternative source of iron, known as ferrocene. A comparative study between ferrocene and CI iron-overload models concluded that ferrocene containing the lipophilic character 3,5,5-trimethylhexanoyl (TMH) was the most encouraging animal model for experimental iron loading (Nielsen *et al.*, 1993). Advantages of this ferrocene above the CI protocol included the indication that the intestinal absorption of TMH-ferrocene is independent from the dose. The absorption of ferrocene is also not regulated by body iron stores, and its bioavailability surpasses any other tried iron-loading agents. TMH-ferrocene showed whole body retention of 48%, twice as high as from ferrocene and six times higher than from (TMH)2-ferrocene and ferrous sulphate (Nielsen & Heinrich, 1993). The most efficient protocol, therefore, for inducing iron overload is a diet containing 0.5% TMH-ferrocene for a period greater or equal to 10 weeks (Nielsen & Heinrich, 1993). However, ferrocene without TMH can be used to achieve a slower iron loading pattern, which is advantageous in studies including synergy with other carcinogens with slower rates of intiation of carcinogenesis.

2.6.2. Iron overload at the ultrastructural level

The study of iron-overloaded organisms at an ultrastructural level has produced certain key observations. Although ferritin has been shown to be the major iron storage protein, haemosiderin is predominant in iron overload (Seldon *et al.*, 1980). Iron loaded cells have abundant and enlarged lysosomes containing ferritin and haemosiderin (Iancu *et al.*, 1994). A close positive correlation has been shown between enhanced lysosomal fragility and haemosiderin content (Seymour & Peters, 1978). It has been suggested that the toxicity of iron could be mediated by haemosiderin-dependent damage to the lysosomal membrane, possibly by a lipid-peroxidation mechanism (Selden *et al.*, 1980). Lysosomal fragility was also investigated through monitoring the activity of N-acetyl-glucosaminidase (NAGA), a lysosomal enzyme. In a study of thalassaemic patients, elevated serum NAGA levels were correlated with the degree of iron overload (Frigerio *et al.*, 1984). When lysosomes increase beyond a cell line-specific concentration, signs of organelle alteration followed by cellular death are noted (Iancu, 1987).

2.7. Iron-Induced Toxicity

In conditions of iron overload, the liver is noted as being the most important organ, where elevated hepatic iron concentrations may result in hepatocellular injury. Two main hypotheses have been postulated to explain this phenomenon: the oxidative injury and lysosomal hypothesis (Arezzini *et al.*, 2003).

2.7.1. The Oxidative Stress Hypothesis

This hypothesis postulates that iron overload results in the formation of oxyradicals in the liver, which induces damage to cellular constituents and hepatocellular function impairment.

Halliwell & Gutteridge (1992) provided initial evidence from *in vitro* experiments that iron in its redox-active state catalyzes the production of oxyradicals such as lipid radicals ($LOO^{\cdot}$) and hydroxyl radicals ($^{\bullet}OH$). Lipid radicals are formed through the decomposition of preformed lipid hydroperoxides (LOOH). Ferrous ions react with LOOH to form alkoxyl radicals ($LOO^{\cdot}$)

$^{\cdot}OH$ radicals are extremely reactive and can attack many cell constituents, including lipids, nucleic acids, carbohydrates and proteins. Polyunsaturated fatty acids (PUFA's) of membrane phospholipids are particularly susceptible to oxidative attack. Peroxidation of PUFA's lead to the formation of highly reactive aldehydes, such as malondialdehyde (MDA) and 4-hydroxynonel (4-HNE), which may then form covalent links to proteins, phospholipids, and DNA (Sodum & Chung, 1989). Other by-products associated with the initiation of lipid peroxidation by $^{\cdot}OH$ have been reported, including conjugated dienes, lipid hydroperoxides, thiobabituric acid-reactants (TBARS). Isoprostanes have been recognised as suitable markers of oxidative stress (Reilly *et al.*, 1998).

Although oxyradicals have the potential to cause damage to cell constituents, protective mechanisms in the form of antioxidants exist in the cell to counteract the hazardous effects of oxyradicals. The net effect of this cellular function depends on the balance between radical production and cytoprotective agent response.

2.7.1.1. Mitochondrial Damage

Mitochondrial oxidative metabolism is susceptible to iron induced impairment. Studies show that chronic iron or copper overload *in vivo* results in an inhibitory defect in the mitochondrial electron transport chain (Sokol *et al*., 1993). Iron overload has been shown to achieve this through lipid peroxidation (LPO), impairing oxidative metabolism, decreasing cytochrome c oxidase, calcium sequestration and release (Britton *et al.*, 1991; Britton *et al.*, 1996), and decreasing the content of reduced pyrimidine nucleotides.

2.7.1.2. Microsomal Damage

Microsomal LPO has been illustrated *in vivo* in rats with chronic dietary iron overload (Bacon *et al.*, 1986). Decreases in cytochromes have been suggested as a result of peroxidation damage (Waller *et al.*, 1983). It has also been shown that calcium sequestration as a part of microsomal function is sensitive to peroxidation. This alters calcium homeostasis and contributes to cell injury.

2.7.1.3. Plasma Membrane Damage

Plasma membranes have also been shown to be affected by LPO. In iron overloaded rats, there is a decrease in unsaturated fatty acid content in the phospholipids for plasma membrane function. It seems that some enzymes in the plasma membrane of hepatocytes may be inhibited by iron overload. In accordance, it has been shown that some thiol-rich enzymes in plasma membranes of heart cells are sensitive to iron (Link *et al.*, 1994).

2.7.1.4. Hepatic DNA Damage

Evidence that chronic iron overload *in vivo* results in damage to hepatic DNA was provided by studies that showed an increased number of strand breaks in hepatic DNA from iron-loaded rats (Edling *et al.*, 1990). Studies have also shown that when iron salts are incubated *in vitro* with purified DNA or isolated rat liver mitochondria or nuclei, DNA strand breaks are produced (Imlay *et al.*, 1988; Hruszkewycz, 1988). Furthermore endogenous iron plays a key role in the DNA damage produced by hydrogen peroxide in mammalian cells (Mello *et al.*, 1984). Finally, it has been suggested that when iron is bound to DNA in the presence of $\cdot^{-}O_2$ and H_2O_2, the formation of "site-directed" $\cdot OH$ radicals that cause DNA damage is catalysed by iron (Halliwell *et al.*, 1990).

2.7.2. Lysosomal Injury Hypothesis

The lysosomal injury hypothesis postulates that excess iron accumulation within lysosomes leads to lysosomal fragility, impaired lysosomal function, and eventually cellular injury through the release of hydrolytic enzymes and stored metals into the cytoplasm (Peters *et al.*, 1985).

During iron overload, the accumulation of iron in lysosomes is a common feature. It is thought that iron sequestration within lysosomes serves a protective role by removing redox-active iron from the cytoplasm and by providing a route for removal from the liver through lysosome-mediated biliary excretion (La Russo, 1989).

2.8. Iron Induced Hepatocarcinogenesis

The clinical, biological and pathological features of HCC complicating haemochromatosis are similar to those of other HCC's (Deugnier *et al.*, 1993). Iron free foci (IFF) are proliferative regions and as such are preneoplastic foci (Deugnier *et al.*, 1993). They are

defined as clear-cut sublobular nodules of hepatocytes free of iron or significantly less iron than the surrounding parenchyma (Deugnier *et al.*, 1993). Experimental (Hirota & Williams, 1979) and clinical (Deugnier *et al.*, 1993) evidence has shown the involvement of IFF as an early step towards HCC development. It has been shown that cirrhosis is no longer a prerequisite for HCC development and hence that iron itself is a carcinogenic factor (Asare *et al.*, 2006a). As stated previously, iron in its redox-active state is capable of inducing oxidative stress. Excessive oxidative stress as seen in iron overload may also cause DNA alterations and alter the methylation status of DNA and may lead to potentially mutagenic effects, such as oncogene activation and tumour suppressor gene inactivation. In one study, HH patients showed tumour suppressor gene mutations (60% A:T to G:C and 40% A:T to T:A) (Vautier *et al.*, 1999), suggesting that etheno-deoxyguanine or etheno-deoxyadenine DNA adducts may be responsible for DNA damage. These DNA modifications are produced by the reaction with LPO products in the liver of HH patients (Nair *et al.*, 1998).

3.0. Aflatoxin

3.1. Introduction

Aflatoxins (AFs) represent a group of mycotoxins produced by the common fungi *Aspergillus flavus* and *Aspergillus parasiticus*. Most mycotoxins have not been implicated in any health problems in animals or humans. However AFs, certain trichothecenes, fumonisins, and ochroatoxins have been associated with episodic outbreaks of lethal poisoning in animal and human populations (Beardall & Miller, 1994; Busby & Wogan, 1985).

AFs are found on improperly stored foods, such as peanuts, corn and to a lesser extent rice (Busby & Wogan, 1985). Figure 3.1 illustrates the conidial head of *A.flavus*. Because conidiophores and conidia of *A.flavus* are produced in abundance, their colour is the predominant one of the foodstuff they cover (Alexopoulos *et al.*, 1996). (Figure 3.2). Conidia are conveyed by wind or insects to nearby plants (Dienier *et al*., 1987)). The major route for AF contamination is through ingestion, but occupational exposure to AF in agricultural workers, people working in oil mills, and granaries have been reported (Sorenson *et al.*, 1984).

Figure 3.1. Conidial Head of *A.flavus*

(www.denniskunkel.com)

Figure 3.2. Conidia and Conidiophores of *A.flavus* on groundnuts.
(www.nri.org/images/foodsafety1.jpg)

Among at least 16 structurally related AFs characterized, there are only 4 major AFs, B_1, B_2, G_1 and G_2 that contaminate agricultural commodities and pose a potential risk to livestock and human health (Bennett & Klich, 2004; Yu *et a*l., 2004). Numerous epidemiological investigations have consistently indicated that dietary aflatoxin B_1 (AFB_1) exposure is one of the main etiologic factors causing human HCC (Groopman *et al.*, 1988; Wogan, 1992; Eaton & Gallagher, 1994). Based on this evidence, the International Agency for Research on Cancer (IARC) designated AFB_1 as a human carcinogen and later classified AFB_1 a Group I carcinogen in humans (IARC, 1993).

3.2. General Toxicity

The adverse effects of AFB_1 can be categorized into two general groups. Exposure to doses greater than 6000mg may cause acute toxicity with lethal effects, whilst exposure to smaller doses for prolonged periods (chronic toxicity) is carcinogenic (Groopman *et al.*, 1988). The severity of effects in animals varies with dose, length of exposure, species, breed, and diet or nutritional status (Eaton & Groopman, 1994). The metabolism of AFB_1, however, plays a major role in deciding the degree of toxicity (Eaton & Gallagher, 1994). AFB_1 has been shown to inhibit DNA synthesis, DNA dependent RNA polymerase

activity, messenger RNA synthesis, and protein synthesis (Busby & Wogan, 1985; McLean & Dutton, 1995). The liver is the major target organ (Busby & Wogan, 1985), although tumours have been found in lung, kidney and colon. AFB_1 can be metabolically activated by cultured intact human tracheal epithelium from the bronchus, in human epitheliod lung cells, and by rabbit lung microsomes (Coulombe, 1994).

3.3. AFB_1 Metabolism

AFB_1-DNA adduct formation is the most important step in AFB_1 carcinogenesis and mutagenesis (Eaton & Gallagher, 1994).

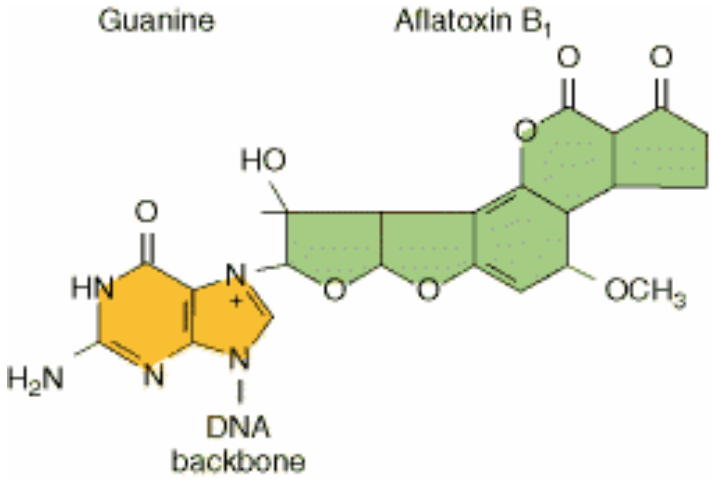

Figure 3.3. Aflatoxin B_1 DNA Adduct (Griffiths *et al.*, 2000)

The initial step requires metabolic conversion of AFB_1 to its exo-8,9-epoxide (Busby & Wogan, 1984), a process known as epoxidation. Two isomers of AFB_1-8,9-epoxide exist. The intercalation of the AFB_1 exo-epoxide in DNA orients the molecule properly for attack by N7 of guanine on C8 of the epoxide. Intercalation of the more chemically stable endo-epoxide does not allow for this configuration (Figure 3.4).

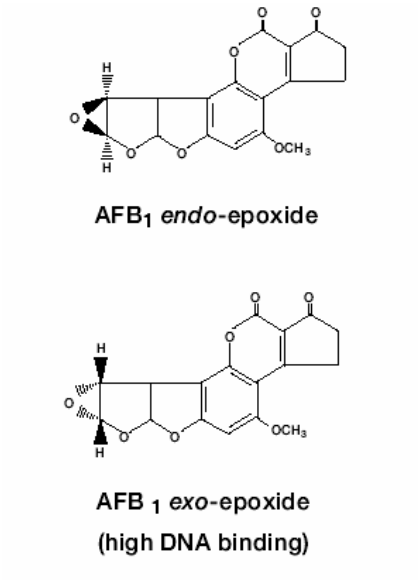

Figure 3.4. AFB1 endo- and exo-epoxide (Massey, 1996)

The bioactivation of AFB_1 to AFB_1-8,9-exo-epoxide is believed to be the ultimate DNA binding mutagenic/carcinogenic metabolite (Gurtoo & Dave, 1975; Essigmann *et al.*, 1982). The group of enzymes responsible for this conversion is known as the cytochrome P450's. In addition to epoxidation, the primary metabolism of AFB_1 also includes hydroxylation to aflatoxin M_1 (AFM_1) and aflatoxin Q_1 (AFQ_1), demethylation to aflatoxin P_1 (AFP_1), and reduction to aflatoxicol (Hsieh *et al.*, 1977). All of these primary metabolites contain vinyl ether double bonds in the dihydrobisfuran ring, and can therefore be epoxidated and activated to form mutagenic species (Wong & Hsieh, 1976) (Figure 3.5).

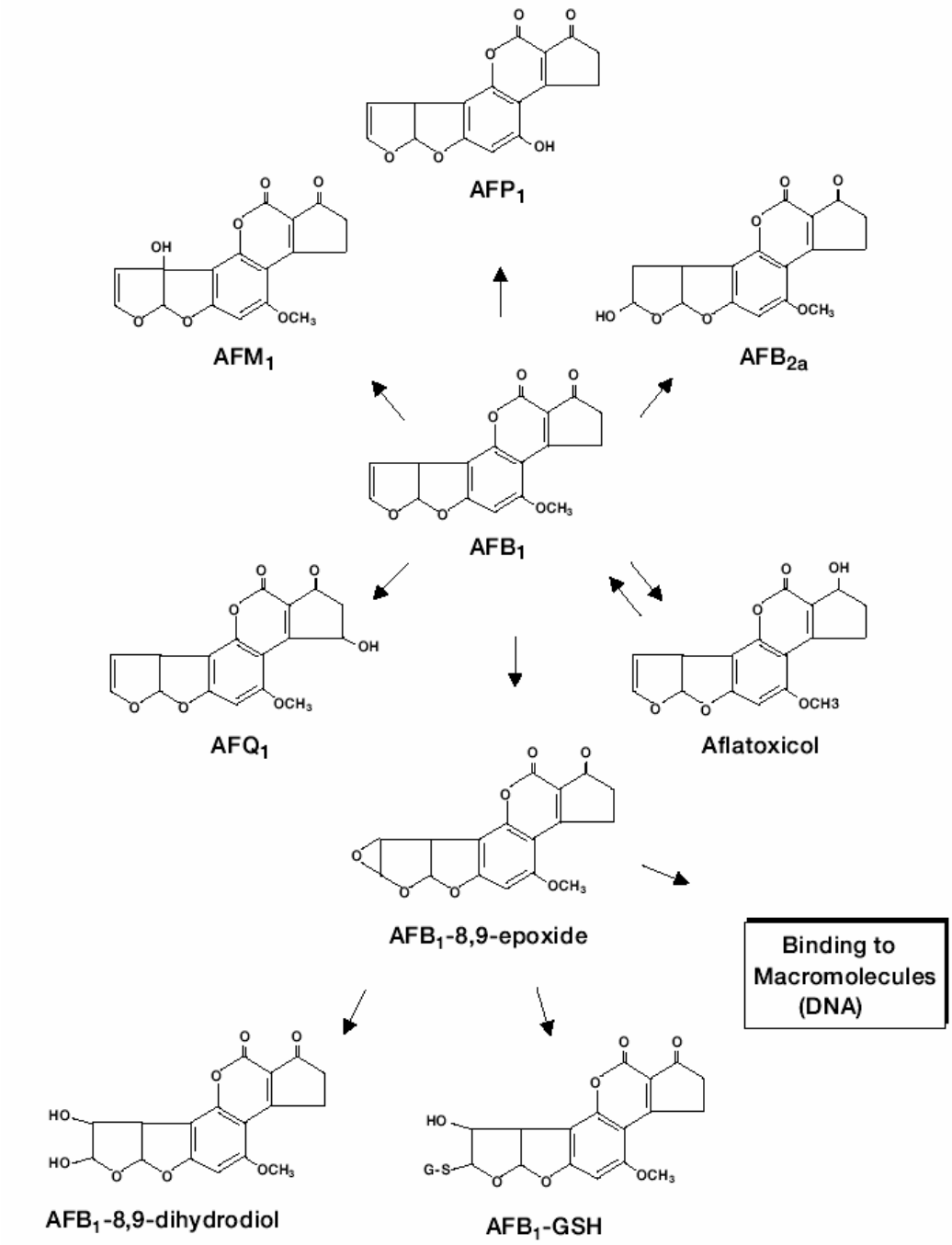

Figure 3.5. Primary Metabolites of AFB_1 Metabolism (Massey, 1996)

The amount of exo-8,9-epoxide formed decides the species susceptibility, as this metabolite has been identified as the active form of AFB_1 which can induce mutations by intercalating into DNA, to form an adduct with the guanine moiety in the DNA (Smela *et al.*, 2001; Essigmann *et al.*, 1983). As a result of steric hinderence of the DNA backbone structure, exo-8,9-epoxide forms adducts with guanine in DNA specifically at the N7 position (Loechler *et al.*, 1988) forming the principal adduct 8,9-dihydro-8-(N7-guanyl)-9-hydroxyaflatoxinB1 (AFB_1-N^7-Gua). A number of other DNA adducts are formed, but their mutational spectrum is dominated by one genetic change: the GC to TA transversion. These mutations are presumed to have arisen from a guanine adduct, because nearly all AFB_1 adducts occur at the same base (Smela *et al.*, 2001).

The positively charged imidazole ring of this adduct promotes depurination, resulting in apurinic (AP) site formation (Fig 3.6). Alternately, under slightly basic conditions the imidazole ring of AFB_1-N^7-Gua opens to form the chemically and biologically stable AFB_1 formamidopyrimidine (AFB_1-FAPY) (Busby & Wogan, 1984) (Fig 3.6). The epoxide also hydrolyses spontaneously or enzymatically to form a diol, which in turn undergoes ring opening to form a dialdehyde intermediate leading to a Schiff base formation with the primary amino groups of proteins (Sabbioni *et al.*, 1987). Plasma albumin adducts of AFB_1 are potential markers of molecular dosimetry of AFB_1 in humans (Gan *et al.*, 1988).

3.4. Mutagenicity and Carcinogenicity

3.4.1. AFB_1 Adducts

The initial AFB_1-N^7-Gua adduct, the AFB1-FAPY and the AP site, individually or collectively, represent the likely chemical precursors to the genetic effects of AFB_1.

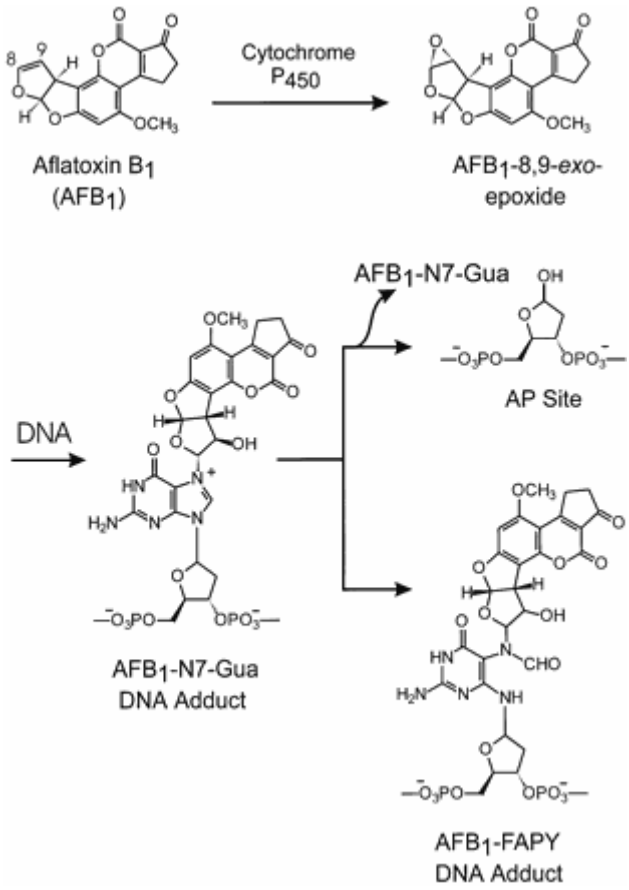

Figure 3.6. AFB_1 Adducts (Smella *et al.*, 2001)

The AP site tends to pair preferentially with adenine, resulting in a guanine to thymine transversion (Foster *et al.*, 1983: Schaaper *et al.*, 1983). The FAPY adducts, being resistant to repair and removal of the adduct, becomes a persistant lesion in the modified DNA that may possibly represent a non-conformational site. It is also preferentially paired by adenine during DNA replication (Wogan, 1989). DNA replication and chromosomal aberrations may also be impaired. The FAPY adducts in RNA may conceivably impair transcription and translation processes thereby altering gene expression.

AFB_1-DNA adducts' mutagenic capacity can be summarized as being capable of forming subsequent repair-resistant adducts, depurination, or lead to error-prone DNA repair resulting in single-strand breaks, base pair substitution, or frameshift mutations (Hsieh, 1986).

One of the most accurate and non-invasive methods for monitoring of AFB_1 exposure lies in the detection of AFB_1-DNA adducts in the urine. A dose-dependent correlation exists between AFB_1 and AFB_1-N^7-Gua adducts excreted in urine of male F344 rats (Bennett *et al.*, 1981). The AFB_1-N^7-Gua adducts have a half-life of about 7,5 hours in rats and are rapidly removed and exclusively excreted in urine. Only 80% of these adducts appear in urine and the remaining 20% of the DNA adduct is converted to AFB_1-FAPY within 24hrs after initial dosing in the rat (Croy *et al.*, 1981). Other processes such as DNA repair and apoptosis of heavily damaged cells are suggested to account for the low concentration of AFB_1-N^7-Gua adducts in urine (Loechler, 1994).

The continuous presence of AFB_1-DNA adducts in the body eventually leads to tumour formation has been well demonstrated in several experimental models (Yu *et al.*, 1996; Schrager *et al.*, 1990). This is accentuated by the roles these adducts play in the multistage carcinogenic processes such as tumour promotion and progression (Wang *et al.*, 1995). A study correlating AFB_1-FAPY persistence with AFB_1 exposure and the risk of human hepatocellular carcinomas (HHC) was demonstrated by Santella *et al.* (1993).

The formation of DNA adducts has been shown to be unevenly distributed. Niranjan *et al.* (1982) showed that AFB_1-adducts bind covalently to liver mitochondrial DNA at concentrations of three to four times higher than nuclear DNA. Irvin & Wogan (1984) demonstrated the preferential binding of AFB_1 adducts to ribosomal RNA gene sequences of rat liver DNA. It was hypothesized that ribosomal RNA regions are preferentially accessible to carcinogen modification because of the diffuse conformation maintained within transcribed genes. Yu (1983) showed that transcriptionally active regions of rat liver nucleolar chromatin had a higher susceptibility to AFB_1-DNA adduct binding.

3.4.2. AFB_1 and HCC

In many epidemiological studies, increased AFB_1 ingestion corresponded to increased HCC incidence (IARC, 1993; Wang & Groopman, 1999). In regions where exposure to AFB_1 is high, such as China, India, Gambia and Senegal, 44% of total HCC cases examined showed a GC to TA mutation predominance at the third position of codon 249 of the *p53* gene (Katiyar *et al.*, 2000; Kirk *et al.*, 2000; Yang *et al.*, 1997; Rashid *et al.*, 1999). This mutation is considered a hotspot for AFB_1 modification and AFB_1-induced mutation. However, 1% of HCC samples examined from populations in regions of low AFB_1 exposure had this mutation (Katiyar *et al.*, 2000; Shimizu *et al.*, 1999; Vautier *et al.*, 1999; Boix-Ferrero *et al.*, 1999).

Aguilar *et al.*, (1994) examined the role of AFB_1 and *p53* mutations in HCCs and in normal liver samples from the US, Thailand, and China where AFB_1 exposures are negligible, low and high, respectively. It was found that the frequency of the AGG to AGT mutation at codon 249 paralleled the level of AFB_1 exposure.

AFB_1 exposure occurs in the presence of other toxins and viruses. The most widely studied being the interaction between hepatitis B virus (HBV) infection and dietary AFB_1 exposure (Kew, 2003). Epidemiological studies carried out in the Guangxi Autonomous Region of China yielded the following results: Individuals who were Hepatitis B s-antigen (HBsAg) positive and found to have heavy AFB_1 exposure had an HCC incidence of 649 cases per 100 000 (0.649%) compared with 66 cases per 100 000 (0.066%) in AFB_1 lightly contaminated areas. HBsAg negative persons eating highly contaminated AFB_1 diets had an HCC rate of 99 per 100 000 (0.099%). The relative risk (RR) factor for HCC in

individuals in Shanghai with both urinary AFB's and positive HBsAg status was shown to be 59. The RR for HCC cases where only urinary AFB_1 metabolites were detected was 3.4 whilst for HBsAg positive only people was 7. These results clearly illustrate a causal relationship between the presence of HBV and AFB_1 with HCC risk (Qian *et al.*, 1994; Ross *et al.*, 1992).

3.4.3. *p53* Tumour Suppressor Gene Mutations

The relationship between AFB_1 exposure and HCC development is highlighted by *p53* tumour suppressor gene mutations. The *p53* protein encoded by this gene has vital biological functions including the control of the cell cycle, DNA repair and synthesis, cell differentiation, genomic plasticity, and apoptosis (Hollstein *et al.*, 1991; Harris & Hollstein, 1993).

3.4.4. AFB_1 Attributed Activation of Protooncogenes

The activation of protoncogenes after AFB_1 exposure has been substantiated in a variety of studies using both animal and *in vitro* models (Tashiro *et al.*, 1986; Bauer-Hofmann *et al.*, 1990; Bailey *et al.*, 1996). Activated *ras* genes predominate the family of oncogenes isolated from solid tumours in animal models. *ras* genes code for small G-proteins of molecular weight 21000, and are related to proteins known as p21. These membrane bound proteins have GTPase activity and form complexes with other proteins. Additionally they play a crucial role in signal transduction, cell proliferation and differentiation (Barbacid, 1990; Lowy & Willumsen, 1993).

Three *ras* genes, designated H-*ras*, K-*ras* and N-*ras*, have been identified (Barbacid, 1990). It was shown that putative activating mutations in the c-K-*ras* genetic locus

involved a single-base modification of either G-C base pair in codon 12 leading to aspartate or cysteine substitutions for glycine (Wogan, 1992). Although *ras* oncogene mutations have frequently been found in AFB_1-induced liver cancer in experimental animal models, the occurrence of these mutations in human HCC's is relatively rare (Bos, 1989; Wogan, 1992). A report by Leon & Kew (1995) found no mutations in all 12 HCC's from Southern African blacks, despite the fact that dietary AFB_1 exposure is an important risk factor in this population. Other oncogenes such as *myc* and *c-erb* have been shown to be over-expressed in human primary liver cancer tissue (Tiniakos *et al.*, 1989; Tashiro *et al.*, 1986).

3.4.5. AFB_1 and Oxidative Stress

Free radical damage initially induced by mycotoxins can be propagated and magnified by LPO chain reactions (Atroshi *et al.*, 2000). LPO is one of the factors responsible for liver damage and necrosis induced by AFB_1 (Souza *et al.*, 1999). Oxidative DNA damage may be defined as structural and functional changes of DNA as a result of the interaction of reactive oxygen species (ROS) with DNA (Shen *et al.*, 1994). During the biotransformation process of forming guanyl adducts, an enhanced production of ROS is reported (Heinonen & Fisher, 1996). ROS such as superoxide radicals ($\cdot^{-}O_2$), hydrogen peroxide (H_2O_2), and hydroxyl radicals ($\cdot OH$) could be generated by many pathways including aerobic cellular metabolism and the metabolic processes of many xenobiotics by cytochrome P450 system (Ames *et al.*, 1995; Frenkel & Gleichauf, 1995; Boelsterli *et al.*, 1993). It is believed that the increased formation of ROS caused by AFB_1 is closely related to the metabolic processing of AFB_1 by cytochrome P450.This increased oxidative stress leads to increased LPO and the formation of the mutagenic 8-oxo-7,8-dihydro-2-deoxyguanosine (8-OHdG) adducts with DNA (Shen *et al.*, 1994; Shen *et al.*, 1995).

8-OHdG adduct formation is one of the well studied consequences of ROS, and is widely considered a key biomarker of oxidative DNA damage (Frenkel, 1992), and capable of changing the fidelity of DNA replication to induce mutations. Furthermore, various mutations caused by 8-OHdG (mainly G to T transversions) are located at the second position of codon 12 of the H-*ras* oncogene (Kamiya *et al.*,1992). Additionally, ROS and 8-OHdG possess essentially the same mutagenic specificity as AFB_1 in causing *p53* and *ras* mutations (Aguilar *et al.*, 1993).

In conclusion, in addition to the well-known mechanisms of AFB_1-DNA adduct formation, AFB_1-induced ROS and 8-OHdG formation may also be involved in the induction of the hot-spot mutations found in human HCCs from AFB_1-endemic regions (Shen & Ong, 1996).

3.4.6. AFB_1 and Cytokines

Cellular components produce various cytokines. Cytokines play a key role in the host resistance and protection against tumour progression. When an organ has been damaged by a toxic assault, cytokines are involved in the inflammatory mechanisms initiated by this damage (Batey & Wang, 2002). Dugyala & Sharma (1996) showed that AFB_1 had a marked effect on macrophage-produced cytokines in a murine model. The mRNA levels of IL-1 and IL-6 were increased at low (0.03mg/kg) and high (0.7mg/kg) AFB_1 doses respectively. Their corresponding protein levels were generally suppressed. Moon *et al.* (1999) found that AFB_1 markedly inhibited TNF-α, IL-1 and IL-6 production by lipopolysaccharide stimulated macrophages. Hence, AFB_1 inhibited the killing ability of murine macrophages.

IL-10 inhibits the synthesis of type 1 helper T cell (Th1) – derived cytokines, which includes IL-1β and IL-6 (Cortes & Kurzrock, 1997). In accordance with those studies showing a decrease in these cytokines, AFB_1 weaned piglets also showed an increased IL-10 mRNA expression. The down-regulation of inflammatory cytokines such as IL-1β and IL-6 could be a consequence of the induction of IL-10 (Marin et al., 2002).

A considerable body of evidence from animal studies exists, suggesting that AFB_1 suppresses immune functions by affecting T-cell dependent immunity (Ghosh *et al.*, 1990; Jakab *et al.*, 1994; Raissuddin *et al.*, 1993). A toxicant can induce immunosuppression through various mechanisms including decreased protein and/or DNA sythesis, changes or loss in enzymatic activity, and changes in metabolism or cell cycles, which may result in apoptosis or necrosis (Hinton *et al.*, 2003). Studies conducted in a pig model show that AFB_1 decreases the blastogenesis response to the mitogen, reduces complement titres, decreases macrophage activation, and depresses delayed hypersensitivity (Miller *et al.*, 1978; Sillvoti *et al.*, 1997; Mocchegiani *et al.*, 1998). Toxic effects on T-lymphocytes and other related lymphoid cells can have pronounced effects on tumourigenesis (Dugyala & Sharma, 1996). This is because these cells are involved with the direct or indirect killing of tumour cells. Immunosuppression can therefore result in a greater rate of tumour progression (Raisuddin *et al.*, 1993).

3.5. Animal models of AFB_1-induced HCC

A large variability in susceptibility toward AFB_1-induced hepatocarcinogenesis has been observed (Wogan, 1973). Mice were found to be resistant, and hamsters were moderately resistant, whereas rats readily develop liver cancer on exposure to AFB_1 (Eaton & Gallagher, 1994). The major detoxification mechanisms for AFB_1 oxides in rodents is catalyzed by glutathione S-transferase (GST) (Eaton & Gallagher, 1994). It is apparent that mice are protected from AFB_1-induced hepatocarcinogenesis because of the relatively high constitutive expression of a hepatic GST isozyme (GST Yc) which has a high catalytic activity for AFB_1 oxides (Buetler *et al.*, 1992). In the rat model, a related enzyme (GST Yc2, subunit 10) is produced. It is also highly active towards AFB_1 oxides. This enzyme is expressed however, only at very low levels in adult rat liver (Hayes *et al.*, 1992). This is one of the reasons why the rat is of greater use as a model for AFB_1-induced HCC.

The use of animal models in the study of AFB_1-related *p53* mutations is a common practice. The homology of the *p53* gene needs to be taken into consideration however. *p53* is at least 92% homologous across commonly used laboratory animal species, such as primates, rats, mice, tree shrews etc. (Duflot *et al.*, 1994; Smela *et al.*, 2001). However, there are no analogous mutations to the human *p53* codon 249 mutation (Arg to Ser) in these animals. A possible reason for the lack of analogous mutations may be attributed to a GC to TA transversion in the third position of the codon which may result in a silent mutation (Smela *et al.*, 2001). In the rat model, codon 243 of the *p53* gene corresponds to codon 249 in the human gene. Although a third base mutation of codon 243 does not result in an amino acid sequence change, mutations in codon 250, as seen in *in vitro* human systems, would be expressed in the rat *p53* protein (Stanley *et al.*, 1999). An *in vivo* and an *in vitro* variation in the oncogene activation in the same target organ or cell lines derived

from that organ does exist. This was demonstrated using a rat liver-derived cell line which was transformed with AFB_1 *in vitro*, and an *in vivo* AFB_1-induced hepatocarcinogenic rodent model (F344 male rats). It is therefore essential to verify and use well investigated extrapolation of data when using *in vitro* and non-human models to study *p53* mutations (Stanley *et al.*, 1999).

A well characterized and quantitative, short-term rat model of liver cancer has been used extensively in studies of AFB_1-induced hepatic carcinogenesis (Appleton & Campbell, 1982; Kensler *et al.*, 1986; Kensler *et al.*, 1987; Roebuck *et al.*, 1991; Kensler *et al.*, 1992; Maxuitenko *et al.*, 1993; Bolton *et al.*, 1993). This protocol includes gavaging the rat 5 days per week with 25μg AFB_1/day. This is followed by a 2 day break, and a second 5-day series of AFB_1 dosing. One of the major advantages of using this short term model is that studies can be completed in a short period of time and fewer rats are required to yield quantitative results (Roebuck, 2004).

3.6. Modulation of AFB_1-induced DNA damage

Considering the mechanisms of AFB_1-induced DNA damage, a variety of chemical agents including nutrients, antioxidants, herbs and pharmaceutical agents have been used to modulate this damage (Eaton & Gallagher, 1994). Furthermore, chemopreventative agents including phenolic antioxidants, ethoxyquin and dithiolethiones have been used to modulate AFB_1 hepatocarcinogenesis in animals (Kensler *et al.*, 1986).

Oltipraz is a synthetic dithiolethione derivative initially used as an antischistosomal agent (Benson, 1993). However, it has been shown to protect laboratory animals from the hepatocarcinogenic effects of AFB_1 (Kensler *et al.*, 1995; Kensler *et al.*, 1992; Roebuck *et*

al., 1991). Oltipraz induces Phase II drug-metabolizing enzymes in laboratory animals, most notably GSTs (Davidson *et al.*, 1990; Meyer *et al.*, 1993; Morel *et al.*, 1993). GST-catalyzed conjugation of activated AFB_1 is the most important detoxification system for prevention of epoxide binding to target macromolecules (Garner & Wright, 1973; Gurtoo & Bejba, 1974).

The inclusion of a 0.03% oltipraz in the diet, beginning 1 week prior to dosing with AFB_1, resulted in substantially lower levels of hepatic AFB_1-DNA adducts throughout the exposure period. Binding was reduced by 76% over the initial 18-day period (Kensler *et al.* 1992). Rats fed with a diet supplemented with 0.075% oltipraz for a 4-week period around the time of AFB_1 exposure, afforded complete protection against AFB_1-induced HCC and hyperplastic nodules (Roebuck *et al.* 1991). In terms of AFB_1-N^7-Gua adduct excretion in the urine, it was found that the feeding of Oltipraz produced an overall reduction of 62% in the elimination of this adduct. This mirrored data on overall levels of hepatic AFB_1-DNA adducts (Groopman *et al.*, 1992).

Ethoxyquin (1,2-dihydro-6-ethoxy-2,2,4-trimethylquinoline) is a powerful antioxidant commonly used as a preservative in the food processing industry. Ethoxyquin was shown to produced a dramatic reduction in AFB_1 binding to hepatic DNA. Rats fed 0.4% ethoxyquin for 7 days showed a 5-fold increase in hepatic cytosolic GST specific activity (Kensler *et al.* 1986). This lead to the hypothesis that ethoxyquin's inhibitory effect on AFB_1 binding to DNA and tumourigenesis appeared to be related to the induction of detoxification enzymes.

4.0. Free Radicals

Atoms are most stable in the ground state. An atom is considered to be "ground" when every electron in the outermost shell has a complimentary electron that spins in the opposite direction. A free radical is any atom with at least one unpaired electron in the outermost shell, and is capable of independent existence (Karlsson, 1997). A free radical may be formed through three major groups of reactions:

1 – The loss of a single electron from a non-radical

$$A: \rightarrow A\cdot + \cdot$$

2 – By the gain of a single electron by a non-radical

$$A: + \cdot \rightarrow A:\cdot$$

3 – When a covalent bond is broken one electron from each pair shared remains with each atom resulting in the formation of two radicals. This process is known as homolytic fission.

$$A:B \rightarrow A\cdot + B\cdot$$

Chemical substances may be converted into free radical by irradiation, or by additives called inhibitors. The ionizing process is well known for producing free radicals in biological systems, which consequently plays a role in the etiology of radiation injuries.

In organic molecules of biological systems, there are many atoms which can exist as free radicals including oxygen, nitrogen, carbon, phosphorous and sulphur. With respect to tissue injury, the prevalence of oxygen makes the oxygen-centered radicals the most common and relevant in biological systems. The ground state of the oxygen molecule (O_2) is itself a radical, with 2 unpaired electrons each located in a π

antibonding orbital. Most biomolecules are covalently bonded non-radicals, and the two electrons forming a covalent bond have opposite spins. Hence, the reaction of oxygen with biomolecules is spin restricted. In living organisms therefore, oxidative enzymes have developed, which circumvent the law of spin restriction and catalyze divalent and tetravalent reduction of oxygen, so that only small amounts of ROS & reactive oxygen intermediates (ROI) are formed. Spin restriction slows down the reaction of molecular oxygen.

4.1. Reactive Oxygen Species (ROS)

Any free radical involving oxygen can be referred to as ROS. Oxygen centered radicals contain two unpaired electrons in the outer shell. When free radicals abstract an electron from a surrounding compound or molecule a new free radical is formed in its place. In turn, the newly formed unstable radical then tends to its ground state by abstracting electrons with antiparallel spins from cellular structures or molecules (Goldfarb, 1999). The electron transport chain (ETC), found in the inner mitochondrial membrane, utilizes oxygen to generate energy in the form of adenosine triphosphate (ATP). Oxygen acts as the terminal electron acceptor within the ETC. Two to 5% of the total oxygen intake during both rest and exercise have the ability to form the highly damaging superoxide radical ($O_2^{-\cdot}$) through electron escape (Sjodin *et al.,* 1990). Free radicals of importance in living organisms include the hydroxyl radical ($HO^{\bullet}$), superoxide anion ($O_2^{-\cdot}$), nitric oxide ($NO^{\bullet}$), thyl ($RS^{\bullet}$) and peroxyl ($ROO^{\bullet}$). Peroxynitrite ($ONOO^-$), hypochlorous acid (HOCl), hydrogen peroxide (H_2O_2), singlet oxygen ($^1O2$) and ozone (O_3) are not free radicals. They can, however, lead to a free radical reaction. The most common ROS involved in iron overload

include the superoxide anion ($O_2^{-\cdot}$), the hydroxyl radical ($OH^{\bullet}$), singlet oxygen ($^1O_2$), and hydrogen peroxide (H_2O_2).

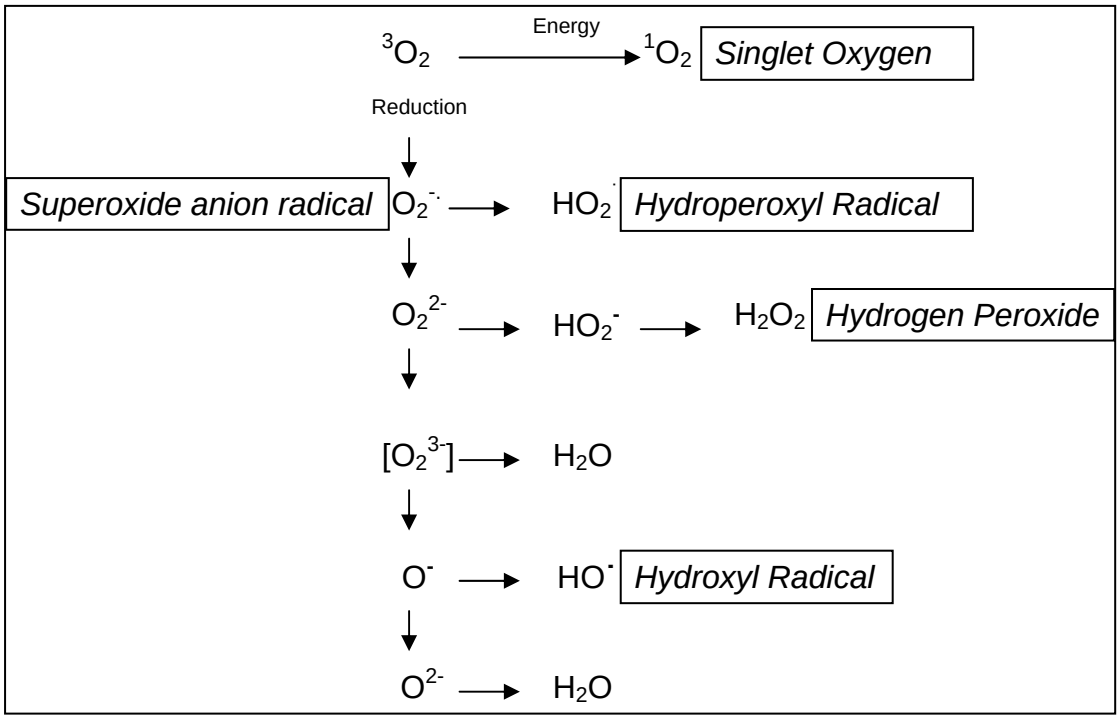

Figure 4.1. Formation of Reactive Oxygen Species (ROS).

4.1.1. Singlet Oxygen ($^1O_2$)

Excitation of O_2 to the singlet states can be achieved when several pigments are illuminated in the presence of O_2. The pigment absorbs light, enters a higher electronic excitation state, and transfers energy onto the O_2 molecule to make a singlet O_2. $^1O_2$ is thus likely to occur in many pigmented systems exposed to light, the lens of the eye and illuminated chloroplasts. As mentioned above, $^1O_2$ is not theoretically termed a ROS. Two denotations of this molecule occur, namely $^1\Delta gO_2$ or $^1\sum g^+O_2$. The former has no unpaired electrons and hence doesn't qualify as a free radical. $^1\sum g^+O_2$ has a set of unpaired electrons, so is theoretically a free radical, although short-lived since it decays to $^1\Delta gO_2$ before it has a chance to exert its free radical effects on other

molecules. Porphyrias are defects usually attributed to inborn errors of porphyrin metabolism, which may be a result of excessive $^1O_2$ formation.

4.1.2. Superoxide Anion Radical ($O_2^{\bullet-}$)

When oxygen acts as an oxidizing agent, it gains one or more electrons from a substance. One electron reduction of oxygen produces the $O_2^{-\cdot}$. This species is produced by a number of enzyme systems, by autooxidation reactions, and by non-enzymatic electron transfers that univalently reduce molecular oxygen. The "leakage" of electrons onto oxygen from various components of the cellular ETC such as those in the mitochondria, endoplasmic reticulum and chloroplasts (in plants) is one of the electron sources triggering the required oxygen reduction to produce $O_2^{-\cdot}$. $O_2^{-\cdot}$ is also produced during respiratory bursts of phagocytic cells such as neutrophils, monocytes, macrophages and eosinophils.$O_2^{-\cdot}$ production is activated when foreign particles touch the neutrophil surface and some $O_2^{-\cdot}$ escapes into the extracellular fluid. Extracellular fluid has little SOD activity, which results in an overproduction of $O_2^{-\cdot}$ and HOCl by activated phagocytes, hence imposing an oxidative stress on surrounding tissues. Its production in this case plays a key role in the killing of several bacterial strains. If this process is hampered, a syndrome of persistant infection, results as is the case of Chronic Granulomateous Disease (CGD) (Curnutte & Babior, 1987).

4.1.3. Hydroperoxyl Radical ($HO_2^{\bullet}$)

The $HO_2^{\bullet}$ radical results from the protonation of $O_2^{-\cdot}$. At physiological pH values close to 7, only around 1% of $O_2^{-\cdot}$ radicals are in the $HO_2^{\bullet}$ form. The production of $HO_2^{\bullet}$ is favoured at a lower pH. A lowered pH occurs around phagocytic surfaces, and so some of the $O_2^{-\cdot}$ they generated exists as the more active $HO_2^{\bullet}$ radical. The

$HO_2^{\bullet}$ radical is considered a more active radical due to its ability to diffuse across lipid membranes with greater ease. The $O_2^{-\cdot}$ diffuses very slowly across lipid membranes, unless an anion channel is present. Charged species generally have a much lower solubility in lipids than uncharged molecules.

4.1.4. Hydrogen Peroxide (H_2O_2)

H_2O_2 has no unpaired electrons, and is not considered to be a free radical. The damage observed is due to the conversion of H_2O_2 into a more highly reactive species, the hydroxyl radical ($HO^{\bullet}$). Pure H_2O_2 has limited reactivity, but it can cross biological membranes, unlike the $O_2^{-\cdot}$. H_2O_2 has been shown to be produced *in vivo* when O_2^{-}dismutates and also by many oxidase enzymes, including amino acid oxidases. Xanthine oxidase converts hypoxanthine and xanthine to urate, O_2 being simultaneously reduced to both $O_2^{-\cdot}$ and H_2O_2 (Granger, 1988). Levels of xanthine oxidase are normally low in human tissues, but they may increase after injury, such as trauma and ischaemia (Buckley, 1994). High levels of H_2O_2 have been shown to inactivate the glycolytic glyceraldehydes-3-phosphate dehydrogenase, an enzyme involved in the energy-producing system. H_2O_2 also forms the $HO^{\bullet}$ in the presence of transition metal ions and O_2 and can facilitate this reaction (Miller *et al.*, 1990). While H_2O_2 is itself an oxidizing agent, it is the combination of H_2O_2 and $O_2^{-\cdot}$ which yields a much more reactive oxidizing agent, the $HO^{\bullet}$.

4.1.5. Hydroxyl Free Radicals ($HO^{\bullet}$)

$HO^{\bullet}$ is produced when H_2O_2 and $O_2^{-\cdot}$ react together:

$O_2^{-\cdot} + H_2O_2 \rightarrow O2 + HO^{\bullet} + OH^{-}$ ----------*Haber-Weiss Reaction*

Human neutrophils and monocytes have been shown to generate $HO^{\bullet}$ through myeloperoxidase-dependent mechanism, which could have microbicidal implications (Ramos *et al.*, 1995). Most radical generation *in vivo*, except during excessive exposure to ionizing radiation, comes from the metal-dependent breakdown of H_2O_2 according to the general equation based on the Fenton reaction:

$$M^{n+} + H_2O_2 \rightarrow M^{n+1} + HO^{\bullet} + OH^-$$

$$Fe^{2}+ + H_2O_2 \rightarrow Fe^{3+} + HO^{\bullet} + OH^- \text{ ----------} \textit{Fenton Reaction}$$

In terms of this Fenton-type chemistry, the extent of $HO^{\bullet}$ formation is largely determined by the availability and location of the metal ion catalyst.

The availability of free Fe is controlled in physiological systems. Fe that is not incorporated into iron-utilizing proteins is rendered largely unavailable for participation in free-radical reactions by sequestration in storage or transport proteins (Aisen & Listowsky, 1980). A minute pool of Fe is solubilized through chelation to low molecular weight biomolecules such as citrate and adenine nucleotides. This intermediate pool of Fe is considered available for pathological free-radical reactions. This is most likely only to occur in conditions of Fe overload.

The $HO^{\bullet}$ radical is several orders of magnitude more reactive towards cellular constituents than $O_2^{\cdot -}$, and H_2O_2. $HO^{\bullet}$ is a highly reactive free radical with an estimated half-life of 10^{-9} seconds.

4.1.6. Peroxyl Radicals (ROO•)

The peroxyl radicals (ROO•) are formed during LPO chain reactions, such as the oxidation of polyunsaturated (PUFA) and unsaturated fatty acids. Any ROS can initiate LPO, provided it has sufficient reactivity to abstract a hydrogen atom from a PUFA side chain. Arachidonic acid (AA), a PUFA, is a precursor of prostaglandins and leukotriens. It is particularly prone to hydrogen abstraction because of multiple methylene-interrupted double bonds (Dix & Aitkens, 1993; Esterbauer *et al.*, 1993). AA peroxidation through ROO• isomers results in F_2 isoprostane formation. F_2 isoprostane formation *in vivo* appears to be enhanced under conditions of oxidative stress (Nourooz-Zadeh *et al.*, 1995; Morrow & Roberts, 1996). The end products of LPO have been linked with DNA damage, faulty DNA repair, protooncogene activation and hence the promotion of carcinogenesis (Cheeseman, 1993).

Low-density lipoproteins (LDLs) contain PUFAs which, when oxidized results in numerous structural and functional changes (Esterbauer *et al.*, 1993). LDL oxidation results in a hydrogen abstraction from a PUFA double bond. This results in the formation of conjugated double bonds, referred to as conjugated dienes (CD) (Esterbauer *et al.*, 1993). LDL cholesterol can be oxidized to oxysterols. The propagation is followed by a decomposition phase, in which there is cleavage of double bonds resulting in the formation of aldehydes such as malondialdehyde (MDA) and 4-hydroxynonenal (4-HNE). These aldehydes are commonly used as biomarkers for LPO (Houglum *et al.*, 1990). The aldehydic products of LDL oxidation are diffusible cytotoxins (Chisolm, 1991).

4.1.7. Nitric Oxide (NO)

Intracellular Fe levels can regulate inducible (nitric oxide synthase) NOS transcription and nitric oxide (NO) formation, through binding to Fe-containing proteins, such as cytosolic Fe regulatory protein-1 (IRP-1), and activation of the Fe response element (IRE) (Weiss *et al.*, 1997). Under these circumstances, post-transcriptional synthesis of ferritin is decreased and the intracellular Fe pool is increased (Cairo & Pietrangelo, 2000). This allows for Fenton reactions to occur more readily, hence increasing $HO^{\bullet}$ radical concentration.

An alternative way for cells to generate $HO^{\bullet}$ radicals requires the formation of NO through NOS. NO reacts in the presence of $O_2^{\cdot -}$ to form a peroxynitrite ($ONOO^-$), which either spontaneously rearranges to form nitrate (NO_3^-) or undergoes cleavage to generate $HO^{\bullet}$-like radicals and nitrogen dioxide (NO_2) (Beckman *et al.*, 1990).

$$O_2^{\cdot -} + NO = ONOO^-$$

In severe inflammatory events, increased NO levels have been shown to induce severe hypotension, along with pronounced cellular damage with subsequent loss of vital organ functions. Important metabolic mechanisms such as protein synthesis, glycogenolysis and detoxification capacity are impaired, which may lead to liver failure (Kuo & Slivka, 1994; Wang & Chaudry, 1996).

4.2. Free Radicals and Iron Overload

Fe overload causes substantial tissue damage and predisposes the individual to HCC development (McLaren *et al.,* 1983). Fe is known to accelerate LPO, and also the formation of the highly reactive $HO^{\bullet}$ from H_2O_2 in the presence of a $O_2^{\cdot -}$ (McCord &

Day, 1978; Halliwell, 1978). Fe-overloaded patients are known to have available Fe complexes in the plasma (Gutteridge *et al.* 1985). These complexes have been shown to be effective promoters of radical reactions (Floyd, 1983). Ferritin participates as an Fe source in the Haber-Weiss reaction, hence promoting LPO (Gutteridge *et al.*, 1983; O'Connell *et al.*, 1985). In Fe-overload, however, it is haemosiderin which predominates as the major Fe protein (Selden *et al.*, 1980). Fe released from haemosiderin at pH 4.5 is capable of promoting LPO (O'Connell *et al.*,1985). Excessive haemosiderin accumulation within tissues could provoke lysosomal damage by increasing LPO (Selden *et al.*, 1980).

4.3. Consequences of Free Radical Attack

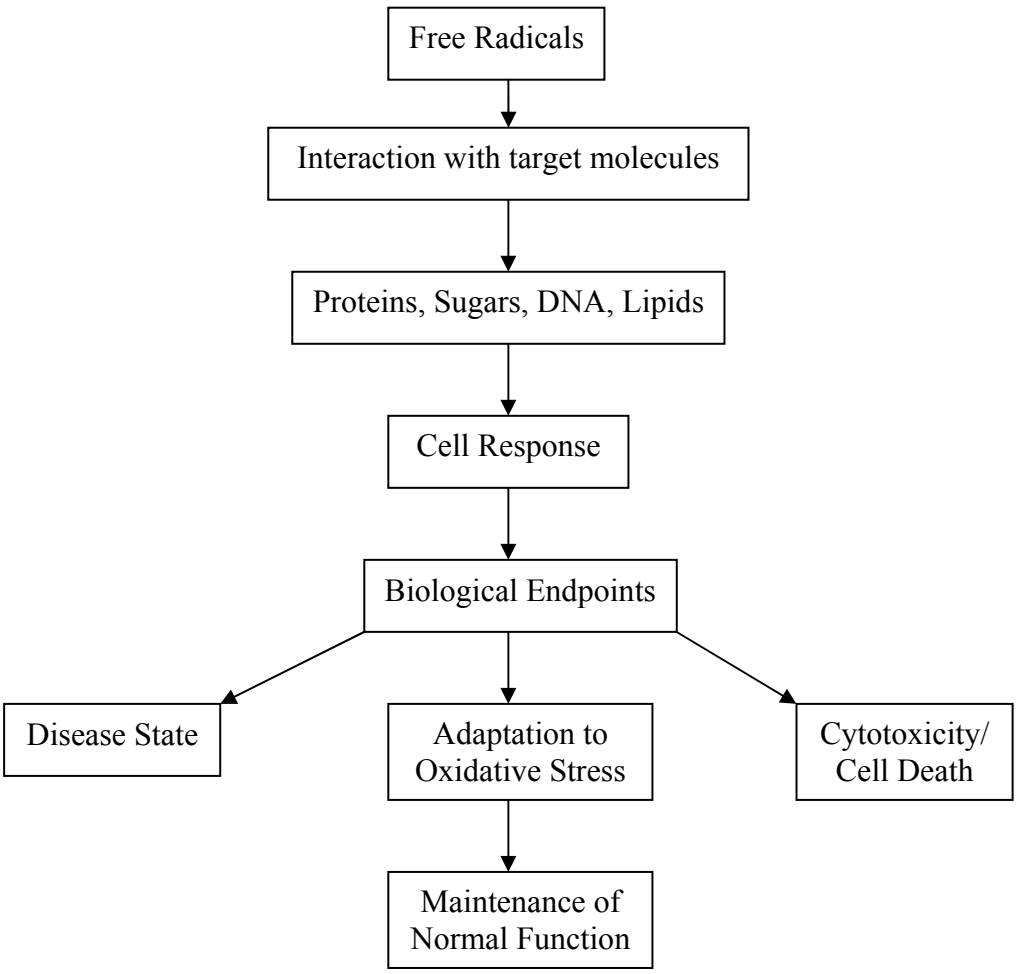

Figure 4.2. Effect of Free Radical Attack

4.3.1. Free Radical Interaction with Target Molecules

Figure 4.2 represents the sequence of events which result in the end-products of free radical attack and oxidative stress. Through free radical attack, the basic building blocks and biomolecules making up proteins, lipids and nucleic acids, are structurally modified and functionally impaired.

The consequence of oxidative stress on proteins include altered enzymatic activities, cellular functions, and altered transport protein functioning. Cellular function alterations may occur resulting from aggregation and cross-linking of receptor

proteins. The alteration of transport proteins occur which affect homeostasis leading to calcium accumulation (Aust et al., 1985).

Free radicals attack electrons from cell membranes, initiating LPO. ROS target the C-C double bond of PUFAs. The double bond of the C weakens the C-H bond, allowing for easy dissociation of the H by a free radical. A free radical acquires the single electron from the H associated with the C at the double bond. This, in turn, leaves the C with an unpaired electron and hence becomes a free radical. The newly arranged molecule is called a conjugated diene (CD). The CD then very easily reacts with oxygen to form a ROO$^{\bullet}$ which abstracts an electron from another lipid molecule in a process called propagation. A chain reaction follows (Halliwell & Gutteridge, 1985). One of the insidious properties of free radicals is that in interacting with other molecules to gain a stable configuration of electrons, they convert that target molecule into a radical. So a chain reaction begins that will propagate until radicals meet each other and each contributes its unpaired electron to form a covalent bond linking the two. The consequence of LPO results in altered lipid fluidity, changes in membrane permeability and the ability of the cell to maintain transmembrane ionic gradients.

DNA radicals can react with protein radicals (in histones) to form crosslinks that interfere with chromatin unfolding, DNA repair, replication, and transcription. It is believed that iron ions complex with negatively charged phosphates in the DNA backbone, thus generating hydroxyl radicals within diffusion distance of reactive bonds in deoxyribose and nitrogen bases. Hydroxyl free radicals attack deoxyribose sugars, leading to single- and double-stranded breaks in DNA. Hydroxyl radicals also deaminate nucleotides, leading to point mutations, notably C>T, G>C and G>T changes (Aust *et al*., 1985).

In terms of cellular response, free radical attack is known to activate transcriptional modification. The activation of NF-κβ leads to increased IL-8 gene expression. Increased levels of *p53*, and proto-oncogenes *c-fos* and *c-myc* have been reported following free radical attack.

4.3.2. Antioxidant Defenses against Free Radicals

Oxidative stress is defined as the state in which the level of toxic ROS overcomes the endogenous antioxidant defences of the host (Bulger & Helton, 1998). Antioxidants are theoretically effective because they readily donate their own electrons to free radicals. When a free radical abstracts the electron from an antioxidant it no longer needs to attack the cell and the chain reaction of oxidation is broken (Dekkers *et al.*, 1996). By definition, an antioxidant becomes a free radical after donating an electron. Antioxidants in this state are not harmful because they have the ability to accommodate the change in electrons without becoming reactive. Two lines of antioxidant defense exist in the cell. The group of antioxidants found in the fat-soluble cellular membrane includes vitamin E, beta-carotene, and coenzyme Q (Kaczmarski *et al.*, 1999). Vitamin E is considered the most potent chain breaking antioxidant within the membrane of the cell. The other group, made up of water soluble antioxidants scavengers includes vitamin C, SOD, CAT and glutathione peroxidase (Dekkers *et al.*, 1996). Antioxidants at certain concentrations can be harmful however, as they can act as pro-oxidants.

4.4. Biomarkers of Oxidative Stress

4.4.1 Biomarkers of LPO

Biomarkers for LPO in particular have been extensively studied. There are more biomarkers available for LPO than for DNA and protein oxidation combined.

4.4.1.1. Thiobarbituric acid-reactive substances (TBARS)

TBARS is one of the earliest markers used in human and animal studies (Buege and Aust, 1978). It may be measured using a spectrophotometric assay that measures the chromogen produced by the reaction of thiobarbituric acid (TBA) with MDA, an end product of LPO. This is an easy method but non-specific because of other substances such as aldehydes reacting with TBA (Handelman and Pryor, 1999). The latter has rendered this approach obsolete. A modified version of this method uses HPLC to separate the MDA-TBA adduct from other interfering chromogens. This improves the specificity, sensitivity and reproducibility (Wong *et al*., 1987).

4.4.1.2. Breath hydrocarbons

The measurement of breath hydrocarbons is another commonly used non-invasive approach for investigating LPO *in vivo* (Knutson *et al*., 2000). Pentane and ethane, which are formed from peroxidation of (n-6) and (n-3) fatty acids, respectively, are volatile compounds released into the breath. Potential errors involve contamination with ambient-air pentane and ethane (Knutson *et al*., 2000).

4.4.1.3. LDL oxidation

The oxidative modification of LDL is thought to enhance atherogenicity. For this reason, susceptibility of LDL to induce oxidative stress *ex vivo* has been used as a possible bio-marker of oxidative defence, at least in the LDL particle itself. Lipid-soluble antioxidants are known to be located in LDL *in vivo*. LDL susceptibility should therefore reflect the antioxidant defence system, particularly as it related to lipid substrates and lipid-soluble antioxidant compounds. When LDL is exposed to Cu^{2+} as a pro-oxidant, the lag time preceding onset of lipid peroxidation formation

indicates resistance of LDL to oxidative stress (Jialal *et al*., 1995). In interpreting results based on LDL oxidation, antioxidant efficacy and the choice of inducing agents used for both metal ion-dependent (i.e.. cupric ions) oxidation and metal ion-independent [e.g. 2,2'-azobis(2-amidinopropane)dihydrochloride or AAPH] oxidation should be taken into account (Gaziano *et al*., 1995).

4.4.1.4. F_2 isoprostanes

F_2 isoprostanes are produced by free-radical induced peroxidation of arachidonic acid (Morrow *et al*., 1990). These compounds are formed in phospholipids and are cleaved and released into the circulation, before excretion into urine as free isoprostanes (Roberts and Morrow,1997). The most abundant F_2 isoprostane is 8-isoprostaglandin $F_{2\alpha}$ (8-iso-$PGF_{2\alpha}$), which has been suggested to be a promising marker of oxidative injury (Sodergren *et al*., 2000). Methods of detection include gas chromatography/ mass spectroscopy (GS/MS) (Handelman and Pryor, 1999). Immunological assays, although available, may sacrifice specificity because of possible cross-reactions with other prostanoids.

4.4.1.5. Ferrous Xylenol Orange (FOX) assay

This method is simple and sensitive. Additionally, it is said to give highly reproducible results for biological samples. It is reported to outperform the iodometric assay, and other assays in terms of simplicity and reproducibility. Finally, very small quantities only of samples are required for this assay (Wolff, 1994).

4.4.1.6. Other Assays for Oxidative Biomarkers

Oxygen radical absorbance capacity (ORAC) (Cao *et al*., 1993) and total $ROO^{\bullet}$-trapping (TRAP) (Wayner *et al*., 1985) take into account the total antioxidant capacity of a system to scavenge or trap oxygen radicals. Assays such as ORAC allow investigators to use different ROS generators to measure total antioxidant capacity of a sample under different conditions. Diene conjugation assays use the principle that the oxidation of unsaturated fatty acids is accompanied by an increase in UV absorbance at 230-235nm. Nitrone adducts of reactive short-lived free radicals may be determined using spin traps, which allow formation of stable nitroxides, which can be examined via electron spin resonance (ESR) (Gutteridge, 1995).

4.4.2. Biomarkers of DNA Oxidation

8OHdG is considered one of the most common markers used in assessing DNA damage. HPLC with electrochemical detectors (HPLC/ECD) and GC/MS methods are most widely used to detect 8-OHdG, although ELISA techniques are also being employed (Santella, 1999). Serum antibodies to 5-hydroxymethyl-2'-deoxyuridine (HMdU), a product of thymine oxidation has been proposed as a possible biomarker of oxidized DNA. Fenkel *et al.* (1998) found that humans produce antibodies to this compound, and titres of anti-HMdU can be measured in simple ELISA assays. The comet assay is able to perform rapid analysis of DNA fragmentation associated with DNA damage. The comet assay or single cell gel electrophoresis assay permits the quantification of DNA damage in individual cells based on the migration of DNA structures in an electric field. As a result of the migration, comets are formed and the amount of DNA in the comet tail as well as the distance of migration, can be a measure of damage. An intermediate step has been introduced using endonulcease III,

which induces breaks in the DNA at sites of oxidized pyrimidines (Collins *et al.*, 1993). Pool-Zobel *et al.* (1997) used this assay to demonstrate that supplementation with antioxidant-rich foods produced significantly reduced endogenous levels of strand breaks in lymphocyte DNA.

4.4.3. Biomarkers of Protein Oxidation

Increased markers of protein oxidation have been associated with several pathologies and diseases such as the aging process, diabetes, atherosclerosis and neurodegenerative diseases (Dean *et al.*, 1997). Protein carbonyls are the biomarkers generally used to estimate protein oxidation. The conventional assay is a colorimetric procedure involving dinitrophenylhydrazine (Levine *et al.*, 1990). Winterbourn & Buss (1999) have developed an ELISA which correlates well with the colorimetric assay. The detection of many other oxidative protein modifications exists including disulfide, thiyl radicals, glutathiolation, methionine sulfoxide and tryptophanyl detection (Dean *et al.*, 1997).

5.0. Materials and Methods

5.1. Serum Iron Determination

5.1.1. Principle

A colorimetric kit manufactured by Randox, UK, was used for the quantitative *in vitro* determination of iron in serum. Ferric iron is dissociated from its carrier protein, transferrin, in an acidic medium and simultaneously reduced to the ferrous form. The ferrous iron is then complexed with the chromogen ferene, a sensitive iron indicator, to produce a blue chromophore which absorbs maximally at 595nm.

5.1.2. Reagents and Preparation

The kit was made up of:

a) Chromogen: Ferene (22.2 mmol/l)

b) Reductant: Ascorbic Acid (1.3 mol/l)

- The contents of one vial of reductant provided were diluted with 15ml of iron-free deionized water.

c) Buffer: Acetate buffer (0.087 mol/l, pH 4.65), Dimethyl sulphoxide, surfactant

d) Iron standard: 35.8 µmol/l or 200µg/dl

5.1.3. Assay Procedure

Disposable labware free of iron was used.

a) The following was pipetted into Eppendorff tubes:

	Reagent Blank	Sample	Standard
Buffer	500µl	500µl	500µl
Reductant	25µl	25µl	25µl
Iron-free water	125µl	-	-
Standard	-	-	125µl
Sample	-	125µl	-

b) The solutions were mixed, and the initial absorbencies of the samples and the standard were read against the reagent blank.

c) 25 µl of the chromogen was added to the reagent blank, standard, and samples.

d) The solutions were vortexed and incubated for at least 15 minutes at room temperature (20 - 25°C).

e) The final absorbance was read against the reagent blank.

5.1.4. Calculations

ΔA = Final Absorbance – Initial Absorbance

$$\text{Concentration} = \frac{\Delta A_{sample}}{\Delta A_{standard}} \times \text{Concentration of Standard}$$

An example of the respective spreadsheet:

	With Chromogen			Without Chromogen				
	Abs1	**Abs2**	**Ave Abs**	**Abs1**	**Abs2**	**Ave Abs**	**Abs1-Abs2**	**Conc**
Blank	0	0	0	0	0	0	0	0
Standard	0.062	0.09	0.076	0.003	0.007	0.005	0.071	35.8
Samples								
4206	0.290	0.372	0.331	0.073	0.093	0.083	0.248	125.1
4208	0.266	0.260	0.263	0.067	0.080	0.074	0.190	95.6
4122	0.144	0.088	0.116	0.057	0.048	0.053	0.064	32.0
4156	0.266	0.260	0.263	0.067	0.080	0.074	0.190	95.6
4123	0.311	0.260	0.286	0.072	0.080	0.076	0.210	105.6

5.2.Total-Iron Binding Capacity (TIBC) Determination

5.2.1. Principle

A colorimetric kit manufactured by Randox, UK, was used to determine the total-iron binding capacity (TIBC) of transferrin in serum samples. An excess of iron was added to the serum to saturate the transferrin. The unbound iron was precipitated with basic magnesium carbonate. After centrifugation the iron in the supernatant was determined using the Randox Serum Iron kit.

5.2.2. Reagents

The kit was made up of:

a) Iron solution: Iron (89.5µmol/l or 500µg/100ml)

b) Basic magnesium carbonate

5.2.3. Assay Procedure

a) The following was pipetted into Eppendorff tubes:

	Reagent Blank	Sample
Iron Solution	100µl	100µl
Sample	-	50µl
Iron free water	50µl	-

b) This mixture was vortexed and allowed to stand for 5-30 minutes at room temperature.

c) One small spatula-full of basic magnesium carbonate was then added to the mixture.

d) This solution stood for 30-60 minutes at room temperature with frequent mixing.

e) The tubes were centrifuged for 10 minutes at 3000 rpm.

f) 25µl of the supernatant was then removed, and assayed for iron.

5.2.4. Calculation for TIBC

$$\text{TIBC (µmol/l)} = \frac{A_{sample}}{A_{standard}} \times 107.4$$

5.2.5. Calculation for PSAT

The percentage saturation (PSAT) was calculated using the following formula:

$$\frac{\text{Total Serum Iron concentration}}{\text{TIBC}} \times 100(\%)$$

5.3. Ferritin Determination

5.3.1. Principle

The ferritin quantitative test kit purchased from IBL, Hamburg, is a solid phase enzyme-linked immunosorbent assay (ELISA) utilizing rabbit anti-ferritin for the solid phase (microtiter wells) immobilization and mouse monoclonal anti-ferritin in the antibody-enzyme (horseradish peroxidase) conjugate solution. The test sample is allowed to react simultaneously with the antibodies, resulting in the ferritin molecules being sandwiched between the solid phase and enzyme-linked antibodies. After 45 minute incubation at room temperature, the wells are rinsed with double-distilled water or buffer to remove unbound labeled antibodies. A solution made-up of 3,3',5,5'-tetramethylbenzidine (TMB) is added and incubated for 20 minutes, resulting in the development of a blue chromophore. The reaction is terminated with the addition of 1N HCl, and the resulting yellow colour is measured spectrophotometrically at 450nm. The concentration of ferritin is directly proportional to the colour intensity of the test sample.

5.3.2. Reagents and Preparations

The kit was made up of:

a) Antibody-coated wells: Microtiter wells coated with rabbit anti-ferritin.
b) Enzyme Conjugate Reagent: Contains mouse monoclonal anti-ferritin conjugated to horseradish peroxidase.
c) Ferritin Standards: Contain 0, 15, 80, 250, 500, and 1000ng/ml human liver or spleen ferritin in bovine serum with preservatives.
d) TMB Reagent: Contains 3,3',5,5'-tetramethylbenzidine stabilized in buffer solution.

e) Stop Solution: Contains diluted hydrochloric acid (1N HCl).

All reagents were allowed to reach room temperature (18-25°C) before use.

Reagents were mixed by gentle inversion or swirling prior to use. (Care was taken not to induce foaming)

5.3.3. Assay Procedure

a) 20µl of standards, samples, and controls was dispensed into the appropriate wells.
b) 100µl of the enzyme conjugate reagent was dispensed into each well.
c) Gentle mixing followed for 30 minutes.
d) The plate was then incubated at room temperature for 45 minutes.
e) The incubation mixture was then removed by flicking the contents into a suitable waste container.
f) The wells were rinsed 5 times with distilled water.
g) The microtiter plate was inverted and struck sharply on absorbent paper to remove residual water droplets from the wells.
h) 100µl of TMB reagent was dispensed into each well, and gently mixed for 5 seconds.
i) The plate was then incubated in the dark for 20 minutes.
j) The reaction was stopped by the addition of 100µl of the stop solution (1N HCl) into each well.
k) Gentle mixing followed for 5 seconds.
l) The absorbance was measured at 450nm within 15 minutes.

5.3.4. Calculations

a) The mean absorbance values for each set of reference standards, controls and samples were calculated.

b) A standard curve was constructed by plotting the mean absorbance obtained for each reference standard against its concentration in ng/ml, as shown below.

c) Using the mean absorbance value for each sample, the corresponding concentration of ferritin in ng/ml was determined from the standard curve. (The graph axis was swopped so as to make calculations easier)

d) A dilution factor of 4 was taken into account.

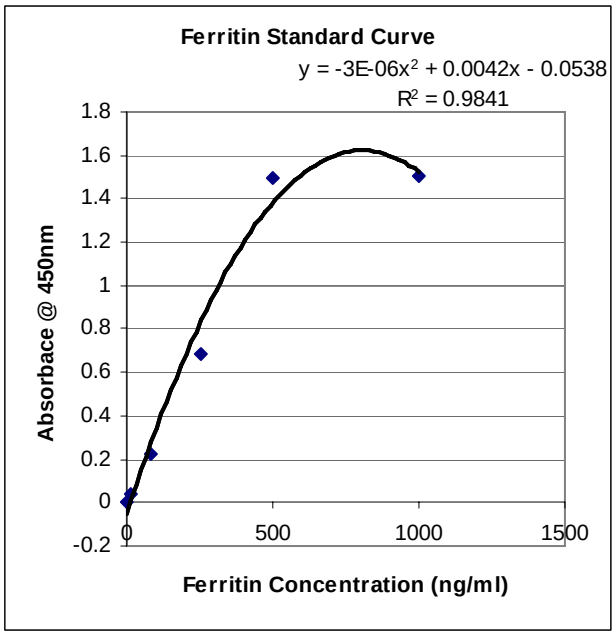

Fig. 5.3.4a. Ferritin Standard Curve

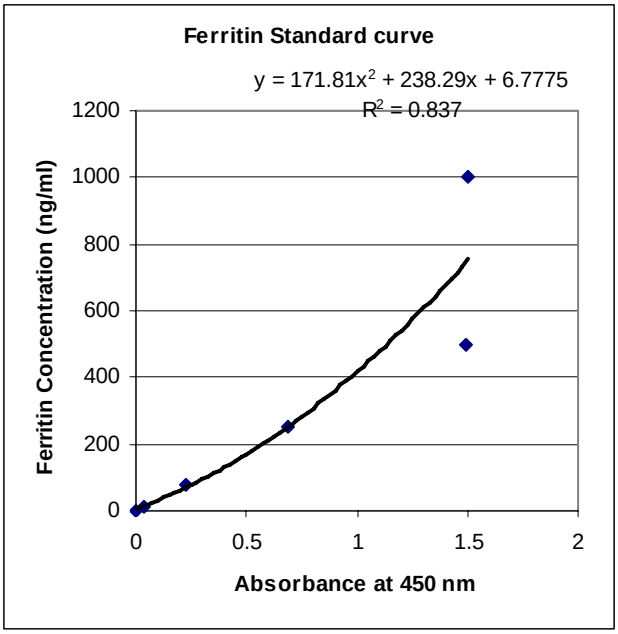

Fig. 5.3.4b. Ferritin Standard Curve

Standards				
Conc.(ng/ml)	Abs			
0	0			
15	0.039			
80	0.223			
250	0.686			
500	1.497			
1000	1.504			
Samples	Abs		Conc. (ng/ml)	(X4-DF)
4206	0.083		27.8	111.0
4208	0.038		16.1	64.3
4122	0.088		29.1	116.3
4156	0.095		31.0	123.9
4123	0.108		34.5	138.1

5.4. Non-transferrin-bound iron (NTBI) Determination

5.4.1. Principle

This is a sensitive assay able to measure the low levels of this NTBI in serum (McNamara *et al.* 1999). The iron-nitrilo-triacetic acid complex formed (iron-NTA) is quantified as a measure of NTBI. NTA does not compete for transferrin-bound iron.

A high-pressure liquid chromatography (HPLC)-based method was used for the quantification of the iron-NTA complex. A flow cell was used to ensure that only the desired complex was measured, excluding the interference from any other substances that may have been present.

5.4.2. Reagents and Preparation

a) Nitrilo-triacetic acid
b) Millipore Ultrafree filter unit
c) HPLC system (The HPLC system used in this study was a Waters Quaternary System with a variable wavelength detector and chromatography data processor using APEX software (Waters Chromatography Products, Milford, MA, USA)).
d) 6mol/l nitric acid
e) 8mm x 10cm Novapak C-18 column (Waters Chromatography Products)
f) 5mmol/l MOPS (4-morpholinpropanesulphonic acid) (Boehringer Mannheim, Mannheim, Germany)
g) 5mmol/l L_1 (1,2-dimethyl-3-hydroxy-pyrid-4-one)
h) 5% acetonitrile, pH 7.0

- Nitrilo-acetic acid: 800mmol/l was made up in iron-free water and adjusted to pH 7.0 with 1mol/l NaOH.
- Millipore Ultrafree filter unit was prewashed with 100µl of 10mmol/l NTA, followed by 100µl of iron-free water.

- The HPLC system was passivated with 6mol/l nitric acid prior to use. An 8mm x 10cm Novapak C-18 column was sued with a mobile phase of 5mmol/l MOPS, 5mmol/l L_1 and 5% acetonitrile at a flow rate of 1ml/min.

5.4.3. Assay Procedure

- 25µl of Nitrilo-acetic acid was added to 225µl serum and the mixture allowed to stand at room temperature for 20 minutes.
- 150µl of the serum solution was then placed in a Millipore Ultrafree unit with a nominal molecular weight of 10 000Da and centrifuged at 8500g for 20 minutes.
- A 20µl aliquot of the ultrafiltrate was then injected directly onto the HPLC system using an iron-free syringe.
- Detection was at 460nm.
- A standard curve was generated by injecting 1,3,5,7 and 10µmol/l iron prepared in 80mmol/l NTA.
- All injections were performed in duplicate and a standard curve was prepared with every run.
- With this method of measurement, concentrations up to 2µmol/l are distinguishable from 0, and the presence of NTBI was therefore taken to be a concentration > 2µmol/l.
-

5.5. Alanine Aminotransferase (ALT)/ Glutamic-Pyruvic Transaminase (GPT) Determination

5.5.1. Principle

A colorimetric kit manufactured by Randox, UK based on the method of Reitman & Frankel (1957) was used for the determination of serum ALT.

$$\alpha\text{-oxoglutarate} + \text{L-alanine} \xrightarrow{\text{GPT}} \text{L-glutamate} + \text{Pyruvate}$$

Glutamic-Pyruvate Transaminase (GPT) is measured by monitoring the concentration of pyruvate hydrazone formed with 2,4-dinitrophenyl-hydrazine.

5.5.2. Reagents and Preparation

The kit contained the following:

a) Sodium Hydroxide

b) GPT Buffer: Phosphate buffer (100 mmol/l, pH 7.4); L-alanine (200 mmol/l); α-oxoglutarate (2 mmol/l)

c) 2,4-dinitrophenyl-hydrazine (4 mmol/l)

d) Pyruvate Standard (2 mmol/l)

- Sodium Hydroxide: 1 vial of the supplied sodium hydroxide was made up to 1000ml with redistilled water in a volumetric flask.

Preparation of Standard Curve:

- Pyruvate Standard was used undiluted as follows:

Tube	Diluted Pyruvate Std (µl)	Redistilled water (µl)	GPT Buffer (µl)	GPT (U/I)
1	0	200	1000	0
2	50	200	950	9
3	100	200	900	18
4	150	200	850	27
5	200	200	800	37
6	250	200	750	46
7	300	200	700	56
8	350	200	650	67
9	400	200	600	77
10	450	200	550	87

a) 1ml of 2,4-dinitrophenyl-hydrazine was pipetted and mixed into each tube

b) Tubes were incubated for 20 minutes at 20-25°C.

c) 10ml of sodium hydroxide solution was added to each tube

d) The solutions were mixed and the absorbance read against the blank (tube 1) after 5 minutes.

5.5.3. Assay Procedure

	Reagent Blank	**Sample**	**Standard**
Sample	-	50 µl	-
Standard	-	-	50 µl
GPT Buffer	250 µl	250 µl	250 µl
Distilled Water	50 µl	-	-

a) The above was mixed and incubated for exactly 30 minutes at 37°C.

b) 250 µl of 2,4-dinitrophenyl-hydrazine was added to each tube being used.

c) Solutions were mixed and allowed to stand for exactly 20 minutes at 20-25°C.

d) 2.5ml of sodium hydroxide was added to each tube.

e) Solutions were mixed and the absorbance read against the reagent blank after 5 minutes.

f)

5.5.4. Calculations

a) The standard curve was obtained by plotting the measured absorbencies against the transaminase concentrations in U/I.

b) Concentrations were calculated using the linear equation of the standard curve.

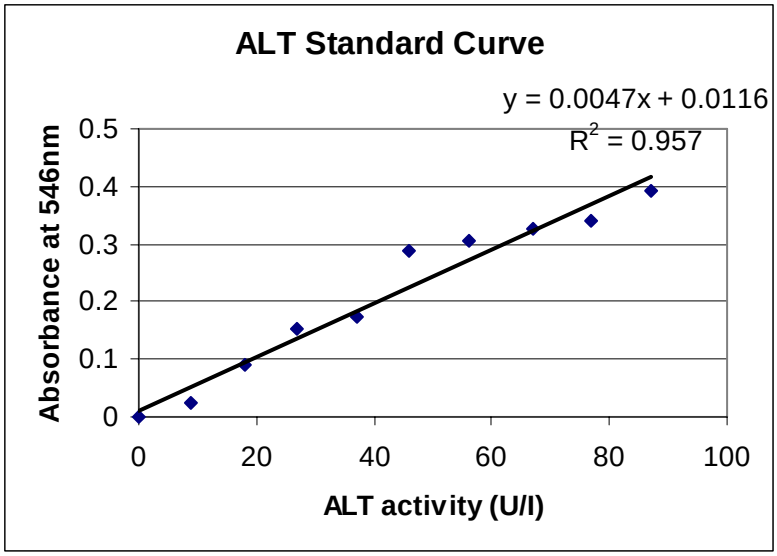

Fig. 5.5.4. ALT Standard Curve

Sample	Abs1	Abs2	Ave Abs	ALT Activity(u/i)
4107	0.122	0.189	0.156	30.6
4108	0.442	0.432	0.437	90.5
4143	0.086	0.222	0.154	30.3
4113	0.128	0.145	0.137	26.6
4114	0.219	0.255	0.237	48.0
4139	0.147	0.168	0.158	31.0
4140	0.079	0.039	0.059	10.1
4142	0.069	0.028	0.049	7.9

5.6. Aspartate Aminotransferase (AST)/ Glutamic-Oxaloacetic Transaminase (GOT) Determination

5.6.1. Principle

A colorimetric kit manufactured by Randox, UK, based on the method of Reitman & Frankel (1957) was used for the determination of serum AST. The principle of the reaction is shown below.

$$\alpha\text{-oxoglutarate} + \text{L-aspartate} \xrightarrow{\text{GOT}} \text{L-glutamate} + \text{Oxaloacetate}$$

Glutamic-Oxaloacetate Transaminase (GOT) is measured by monitoring the concentration of oxaloacetate hydrazone formed with 2,4-dinitrophenyl-hydrazine.

5.6.2. Reagents and Preparation

The kit was made up of:

e) Sodium Hydroxide: 1 vial of the supplied sodium hydroxide was made up to 1000ml with redistilled water in a volumetric flask.

f) GOT Buffer: Phosphate buffer (100 mmol/l, pH 7.4); L-aspartate (100 mmol/l); α-oxoglutarate (2 mmol/l)

g) 2,4-dinitrophenyl-hydrazine (2 mmol/l)

h) Pyruvate Standard (2 mmol/l)

Preparation of Standard Curve:

- 1.5ml Pyruvate Standard was diluted with 4.5ml GOT Buffer.

Tube	Diluted Pyruvate Std (µl)	Redistilled water (µl)	GOT Buffer (µl)	GOT (U/l)
1	0	200	1000	0
2	50	200	950	6
3	100	200	900	11
4	150	200	850	16
5	200	200	800	20
6	250	200	750	25
7	300	200	700	31
8	350	200	650	37
9	400	200	600	44
10	450	200	550	52

e) 1ml of 2,4-dinitrophenyl-hydrazine was pipetted into each tube and mixed

f) Tubes were incubated for 20 minutes at 20-25°C.

g) 10ml of sodium hydroxide solution was added to each tube

h) The solutions were mixed and the absorbance read against the blank (tube 1) after 5 minutes.

5.6.3. Assay Procedure

	Reagent Blank	**Sample**	**Standard**
Sample	-	50 µl	-
Standard	-	-	50 µl
GOT Buffer	250 µl	250 µl	250 µl
Distilled Water	50 µl	-	-

g) The above reactions were prepared and solutions mixed and incubated for exactly 30 minutes at 37°C.

h) 250 µl of 2,4-dinitrophenyl-hydrazine was added to each reaction tube

i) Solutions were mixed and allowed to stand for exactly 20 minutes at 20-25°C.

j) 2.5ml of sodium hydroxide was added to each tube.

k) Solutions were mixed and the absorbance read against the reagent blank after 5 minutes.

5.6.4. Calculations

c) The standard curve was obtained by plotting the measured absorbencies against the transaminase activities in U/I.

d) Concentrations for the test samples were calculated from the linear equation of the standard curve.

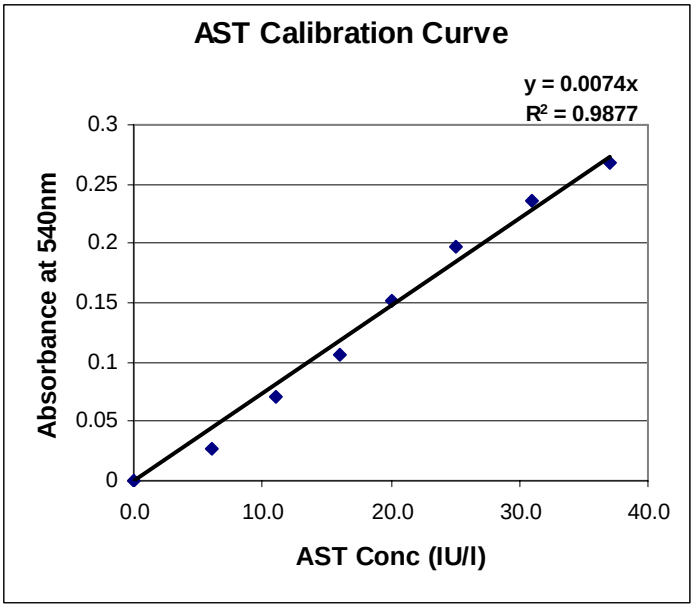

Fig. 5.6.4. AST Standard Curve

Srl	Abs	X 10 (DF)	AST Activity
blank	0		
Samples			
4105	0.034	0.34	44.7
4106	0.029	0.29	38.2
4107	0.032	0.32	42.1
4108	0.028	0.28	36.8
4109	0.029	0.29	38.2
4143	0.019	0.19	24.6

5.7. γ-Glutamyl Transferase (GGT) Determination

5.7.1. Principle

A colorimetric kit manufactured by Kat Medical (PTY) LTD based on the method of Szasz (1976) was used for the determination of plasma GGT. Optimised kinetic determination of γ-glutamyl transferase is dependent on the following reaction:

$$\text{L-}\gamma\text{-Glutamyl-3-carboxy-4-nitroanilide} + \text{glycylglycine} \xrightarrow{\gamma\text{-GT}} \text{L-}\gamma\text{-Glutamyl-glycylglycine} + \text{p-Nitroanilide}$$

The increase of absorbance at 405nm, as a result of the formation of the p-Nitroanilide, is proportional to the Gamma GT activity.

5.7.2. Reagents and Preparation

The kit was made up of:

a) Reagent 1: Tris Buffer, pH 8.25 (100mmol/l); glycylglycerine (100mmol/l).
b) Reagent 2: L-γ-Glutamyl-3-carboxy-4-nitroanilide (40mmol/l).
c) The GGT reagent was made up by adding 1 volume of Reagent 2 to 5 volumes of Reagent 1.

5.7.3. Assay Procedure

a) 50 µl of the sample was mixed with 500 µl of the GGT reagent and incubated for 1 minute at 25°C.
b) The initial absorbance was read at 400nm and the timer started simultaneously.
c) The absorbance was read at 1, 2 and 3 minutes. The change in absorbance was then calculated.

5.7.4. Calculations

a) The average change in absorbance per minute was calculated.
b) The following equation was used to determine the GGT concentration in the sample:

$$U/I = \text{Average } \Delta\text{Absorbance/min} \times 1158$$

	AveAbs-1min	Ave Abs-2min	Ave Abs-3min	Ave Abs difference	U/l
Sample					
4206	0.360	0.361	0.367	0.003	3.6
4208	0.378	0.379	0.380	0.001	1.0
4122	0.492	0.495	0.493	0.003	3.5
4156	0.378	0.379	0.380	0.001	0.1
4123	0.492	0.495	0.493	0.003	3.5

5.8. Superoxide Radical ($^{\cdot}O_2$) Determination

5.8.1. Principle

Luminescence is the emission of light by non-thermal processes. In the case of chemiluminescence analysis, the light is generated by chemical reactions. Molecules responsible for emitting this light absorb free energy released by the chemical reaction and become 'excited'. In this state some of the peripheral electrons of the molecule are raised to a higher energy level. When these electrons lose energy, they return to a lower energy level and the energy lost during this transition is emitted as photons. When the electrons lose all their absorbed energy, the molecule then returns to its stable ground state.

The chemiluminophore used for this research is luminol.

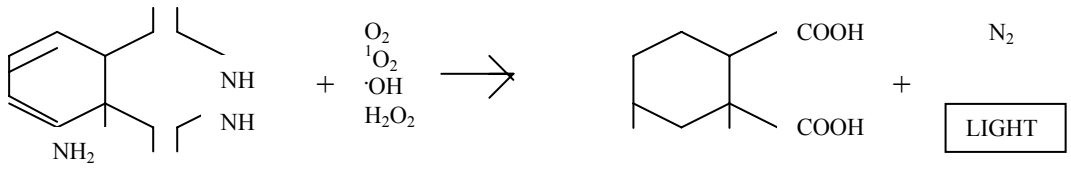

LUMINOL OXIDANT α−AMINOPHTHALATE

The luminol interacts with the oxidizing species to produce larger, more measurable amounts of light at a peak wavelength of approximately 425nm. This was measured by a four-channel luminometer interfaced with a computer.

5.8.2. Reagents and Preparation

a) 10^{-4} M Luminol stock solution was prepared by dissolving 0.177g luminol in 100 ml of 0.1M borate buffer.

b) Borate buffer: 0.1M, pH 9.0 was prepared by dissolving 9.5g / 250 ml dH_20. pH was adjusted to 9.0.

c) 10^{-3} M N-formylmethionylleucinylphenylalanine (fMLP) (stock 10mM in DMSO).

d) Phenol-free HBSS (Sigma).

e) Heparinized whole blood was diluted 1:9 with phenol-free HBSS.

5.8.3. Assay Procedure

Sample and Reagents	Volume	Remarks
1:9 Diluted blood sample	500µl	*In luminometer cuvette*
10mM Luminol solution	200µl	*Resultant solution was loaded onto luminometer*
10mm FMLP	300µl	*After baseline had advanced to about half the length of the next square*

- Graph: 15sec/division was used.
- Temp. setting: 37°C
- Graph was displayed on the screen and ensured that baseline had stabilized halfway across the first square.
- Gain was adjusted as required so that the luminescence curves were within the range on the displayed graph.
- Once the gain was established, the test was performed at that particular gain setting.

- The peak luminescence was recorded in mV from the point of fMLP addition to the end of the graph.
- The results were determined by computer settings.

Sample	Neutrophil	Tmax	Tmax/Neutr	Mean Tmax/Neut
4156	11.0	0.337	0.031	
4123	6.7	0.367	0.055	
4206	3.3	0.216	0.066	
4122	4.9	0.418	0.085	
4208	5.1	0.398	0.078	0.063

5.9. Nitrite Determination – Griess Reagent System

5.9.1. Principle

One means to investigate nitric oxide formation is to measure nitrite (NO_2^-), which is one of two primary, stable and nonvolatile breakdown products of NO. This assay relies on a diazotization reaction that was originally described by Griess (1879). The Griess Reagent System developed by Promega is based on the chemical reaction shown in Figure 5.9.1, which uses sulfanilamide and N-1-napthylethylenediamine dihydrochloride (NED) under acidic (phosphoric acid) conditions to form the Azo compound. This system detects NO_2^- in a variety of biological and experimental liquid matrices such as plasma, serum, urine and tissue culture medium.

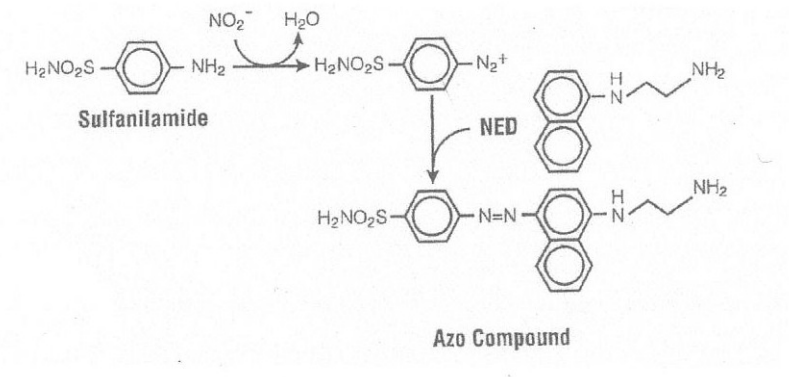

Fig. 5.9.1 Griess Reagent System Reaction

5.9.2. Reagents and Preparation

The following chemicals were used:

- N-1-napthylethylenediamine dihydrochloride (NED)
- Sulfanilamide
- Sodium Nitrite

a) NED Solution: 0.1% NED was prepared by adding 0.1g NED into 100ml distilled water

b) Sulfanilamide Solution: 1% sulfanilamide solution was prepared by adding 1g sulfanilamide into 100ml of 5% phosphoric acid solution

c) Nitrite Standard: Stock 0.1M sodium nitrite was prepared by adding 3.45g sodium nitrite into 100ml of 5% phosphoric acid solution.

d) The solutions for the standard curve was prepared as follows: (Standards were prepared in a 96-well flat-bottom enzymatic assay plate).

- 1ml of a 100µM nitrite solution was prepared by diluting the 0.1M Nitrite Standard 1:1000 in distilled water.

- 3 columns (24 wells) were designated in the 96-well plate for the nitrite standard reference curve. 50µl distilled water was dispensed into well in rows B-H, as follows:

A	100	100	100	ES	ES	ES	ES	ES	ES	ES	ES	ES
B	50	50	50	ES	ES	ES	ES	ES	ES	ES	ES	ES
C	25	25	25	ES	ES	ES	ES	ES	ES	ES	ES	ES
D	12.5	12.5	12.5	ES	ES	ES	ES	ES	ES	ES	ES	ES
E	6.25	6.25	6.25	ES	ES	ES	ES	ES	ES	ES	ES	ES
F	3.13	3.13	3.13	ES	ES	ES	ES	ES	ES	ES	ES	ES
G	1.56	1.56	1.56	ES	ES	ES	ES	ES	ES	ES	ES	ES
H	0	0	0	ES	ES	ES	ES	ES	ES	ES	ES	ES

ES, Experimental Sample

- 100µl of the 100µM nitrite solution was added to the remaining 3 wells in row A.
- A 6 serial 2-fold dilution (50µl/ well) was performed in triplicate down the plate to generate the nitrite standard reference curve:

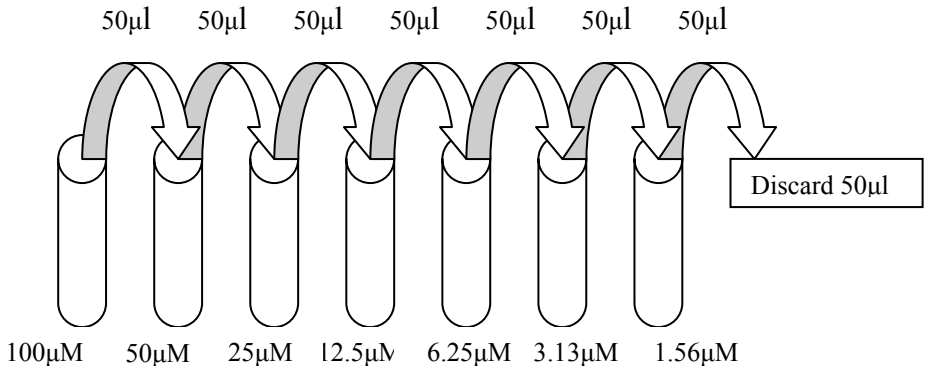

- 50µl from the 1.56µM set of wells was discarded. No nitrite solution was added to the last set of wells (0µM). The final volume in each well was 50µl, and the nitrite concentration range is 0-100µl.

5.9.3. Assay Procedure

	Reagent Blank	Sample	Standard
Sample	-	50µl	-
Standard	-	-	50µl
Sulfanilamide Solution	50µl	50µl	50µl
Plate was protected from light and incubated at room temperature for 5 to 10 minutes			
NED Solution	50µl	50µl	50µl
Plate was protected from light and incubated at room temperature for 5 to 10 minutes			

a) The absorbance of the purple/magenta colour was measured within 30 minutes in the plate reader at a wavelength of 550nm.

b)

5.9.4. Calculations

A nitrite standard reference curve was generated as shown below:

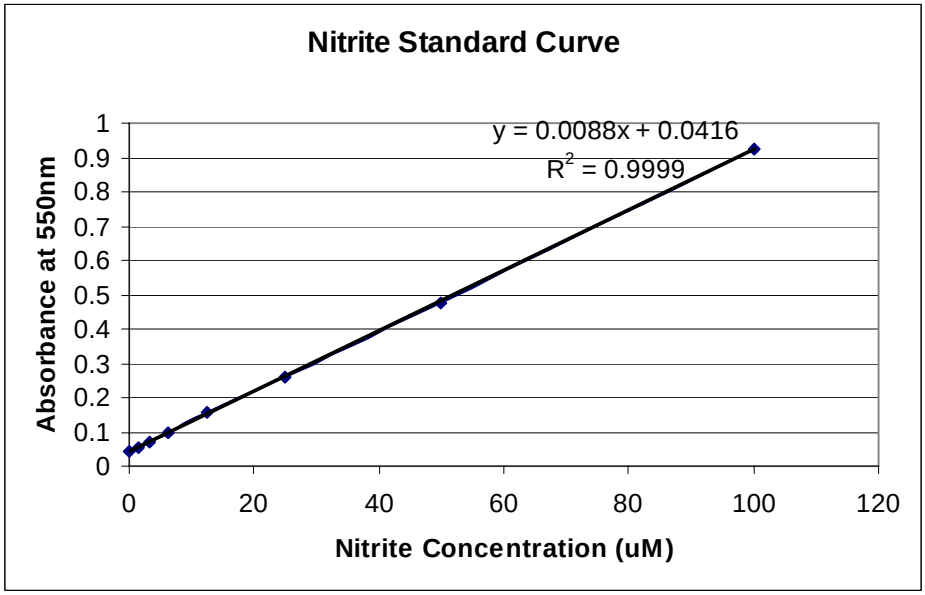

Fig. 5.9.4. Nitrite Standard Curve

- The concentration of the test samples was calculated using the linear equation of the standard curve.

Std	Abs1	Abs2	Abs3	Ave Abs	Conc (uM)
S1	0.912	0.926	0.938	0.925	100
S2	0.476	0.479	0.477	0.477	50
S3	0.261	0.260	0.264	0.262	25
S4	0.155	0.157	0.152	0.155	12.5
S5	0.103	0.097	0.097	0.099	6.25
S6	0.070	0.069	0.069	0.069	3.13
S7	0.054	0.052	0.050	0.052	1.56
S8	0.061	0.031	0.037	0.043	0
Sample					
206	0.155	0.216		0.186	16.4
208	0.149	0.139		0.144	11.6
122	0.133	0.152		0.143	11.5
156	0.109	0.115		0.112	8.0
123	0.11	0.115		0.1125	8.1

5.10. Lipid Hydroperoxide (LPO) Determination

5.10.1. Principle

Ferrous oxidation with xylenol orange (FOX *VERSION II*) is based on the principle of the rapid peroxide-mediated oxidation of the Fe^{2+} to Fe^{3+} under acidic conditions. The latter in the presence of Xylenol Orange, forms an Fe-Xylenol Orange complex which can be measured spectrophotometrically at 560nm (Nourooz-Zadeh *et al.*,1994).

In this method, alkoxyl radicals generated in the ferrous oxidation step react rapidly with native lipid, generating further hydroperoxide in a chain reaction. Eqs. 1-4

$$ROOH + Fe2+ \text{ ------> } Fe3+ + RO^{\bullet} + OH^{-} \quad (1)$$

$$RO^{\bullet} + RH \text{ ------> } ROH + R^{\bullet} \quad (2)$$

$$R^{\bullet} + O_2 \text{ ------> } ROO^{\bullet} \quad (3)$$

$$ROO^{\bullet} + RH \text{ ------> } ROOH + R^{\bullet} \quad (4)$$

$$R^{\bullet} + BHT \text{ ------> } RH + BT \quad (5)$$

Inclusion of the chain-breaking antioxidant butylated hydroxytoluene (BHT) overcomes this problem. As shown in Eq.(5), BHT presumably repairs alkyl radicals produced by the reaction of alkoxyl radicals with unsaturated lipids [Eq. (2)]. Experimentally, BHT at a concentration of 4mM was found to provide a firm endpoint when measuring phosphatidyl-choline and low-density lipoprotein peroxide content. The FOX reagent was further adopted for the measurement of lipid hydroperoxides by the addition of methanol (90%, v/v) in order to solubilize the lipid and BHT. Sorbitol was omitted in the FOX reagent as the high concentration of methanol (>25M) in the revised method made the presence of sorbitol as an oxyl radical scavenger superfluous.

5.10.2. Reagents and Preparation

- Xylenol orange (XO)
- Ferrous ammonium sulfate ($Fe(NH_4)2(SO_4)_2$
- Butylated hydroxytoluene (BHT)
- Sulphuric acid (H_2SO_4)
- Methanol. HPLC grade. (MeOH)

A. 250mM H_2SO_4 was prepared by diluting 13.88ml conc. H_2SO_4 (18M) with ddH_2O to 1L.

B. 4.4mM BHT /MeOH was prepared by dissolving 0.97g BHT in 1L HPLC grade MeOH.

C. Stock FOX solution: 1mM XO / 2.5mM $Fe(NH_4)_2(SO_4)_2$ in 250mM H_2SO_4 was prepared by dissolving 0.76g XO and 0.98g $Fe(NH_4)_2(SO_4)_2$ in 1L 250mM H_2SO_4.

D. Working FOX II solution: 1ml stock FOX II solution was added to 9ml BHT/MeOH solution. This was freshly prepared before use.

E. The following concentrations of H_2O_2 were prepared (using 30% Sigma H_2O_2 which is equivalent to 8.82M):

- Stock standard 8.82mM H_2O_2 was prepared by diluting 1ml 30% H_2O_2 (8.82M) to 1L. Thereafter, the following standards were prepared:

4.4µl of stock standard was made up to 10ml ≡ 3.9µM

8.8µl " ≡ 7.81µM

17.5µl " ≡ 15.62µM

35.0µl " ≡ 31.25µM

70.0µl " ≡ 62.50µM

5.10.3. Assay Procedure

Sample and Reagents	**Volume**	**Remarks**
Plasma / Blank / Std	50µl	*1.5ml microfuge vials were used and work done in duplicate*
Working FOX II reagent	950µl	*The solution was vortexed*
		It was then incubated at room temp. for 30min
		Microfuge vials were centrifuged at 12,000g for 5min. to remove all flocculated materials
Absorbance of supernatant was read at 540nm		

The blank included only the FOXII reagent

5.10.4. Calculation

The concentrations of the samples were calculated from the equation of the standard curve. An example of a spreadsheet follows.

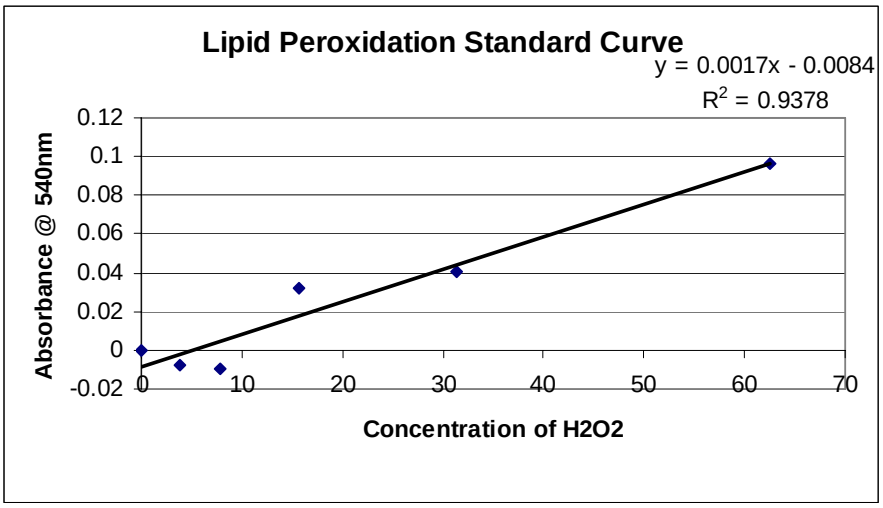

Fig. 5.10.4. Lipid Peroxidation Standard Curve

Standards	Abs1	Abs2	Ave Abs	(- blank)	Conc (uM)
Blank	0.323	0.330	0.327	0	0
S1	0.322	0.350	0.336	0.010	3.9
S2	0.337	0.329	0.333	0.007	7.8
S3	0.345	0.340	0.343	0.016	15.6
S4	0.360	0.392	0.376	0.050	31.3
S5	0.421	0.435	0.428	0.102	62.5
Samples					
4105	0.404	0.381	0.3925	0.066	41.1
4106	0.415	0.474	0.4445	0.118	71.7
4107	0.399	0.449	0.424	0.098	59.7
4108	0.386	0.411	0.3985	0.072	44.7
4109	0.434	0.574	0.504	0.178	106.7
4143	0.469	0.469	0.469	0.143	86.1

5.11. 8-Isoprostane (8-IP)

5.11.1. Principle

This ELISA procedure is based on the competition between 8-IP and an 8-IP-acetylcholinesterase (AChE) conjugate (8-IP tracer) for a limited number of 8-IP-specific rabbit antiserum binding sites. Because the concentration of the 8-IP tracer is held constant while the concentration of 8-IP varies, the amount of 8-IP tracer that is able to bind to the rabbit antiserum will be inversely proportional to the concentration of 8-IP in the well. The rabbit antiserum-8-IP (either free or tracer) complex binds to

the mouse monoclonal anti-rabbit IgG antibody that has been previously attached to the well. The plate is then washed to remove all unbound reagents and the Ellman's reagent (which contains the substrate to AChE) is added to the well. The product of this enzymatic reaction has a distinct yellow colour that is measured spectrophotometrically at 412nm. The absorbance is directly proportional to the [Bound 8-IP Tracer] and inversely proportional to [8-IP].

5.11.2. Reagents

8-IP kit (Cayman Chemicals, USA) was used. The kit contained the following:

a) Mouse anti-rabbit IgG coated plate.

b) 8-IP EIA antisera

c) 8-IP AChE tracer

d) 8-IP EIA standard

e) EIA buffer concentrate

f) Wash buffer concentrate

g) Tween 20

h) Ellman's Reagent

5.11.3. Assay procedure

- Reconstitution of reagents was done according to the manufacturer's instructions using Ultra Pure water (from Cayman). Additionally, the mapping of the plate was designed as recommended by the manufacturer. Wells to cater for blanks, "Non-specific binding" (NSB), "minimum binding" (B_o) and "total activity or maximum binding" (TA) were incorporated. Assay was performed in triplicates.

- 50µl of standards and samples were added to the appropriate wells.
- 50µl of 8-IP AChE Tracer was again added to each well except the TA and the blank wells.
- 50µl 8-IP antiserum was added to each well except the TA, NSB and blank wells.
- The plate was covered with a plastic film and incubated for 18hrs at room temp.
- Wells were emptied and washed 5x with the wash solution.
- 200µl of Ellman's solution was added to each well.
- 5µl of Tracer was then added to the TA wells.
- Plate was again covered with a plastic film and kept in the dark for 60-90 min for the colour to develop.
- The colour typically developed when B_o read 0.3-0.8A.U. at 405nm.

5.11.4. Calculations

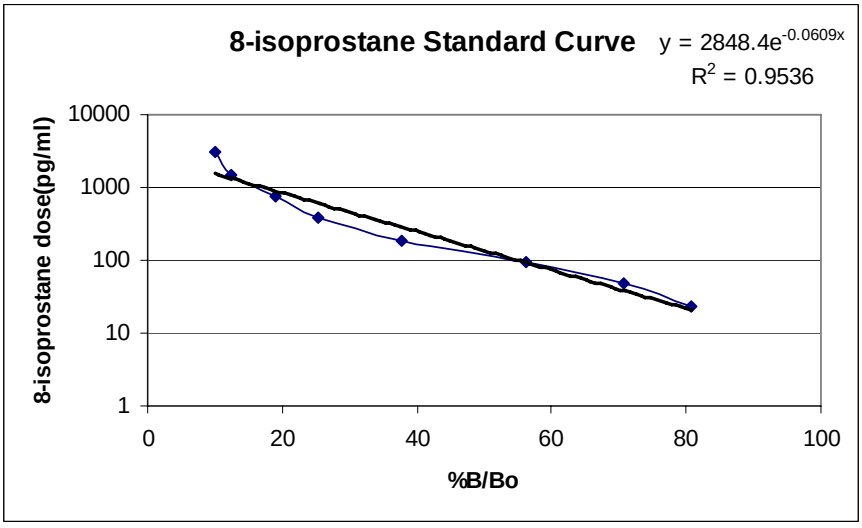

Fig. 5.11.4. 8-Isoprostane Standard Curve

	Abs1(mU)	Abs2(mU)	Corrected	Corrected	%Abs/Abs(max)		Mean A&B	8IP conc.(pg/ml)
			(-Av.NSB)		[%B/Bo]	[%B/Bo]	(%B/Bo)	
			(-0.011)					
S1	139	147	139.0	147.0	21.1	22.3	21.7	3000
S2	283	263	283.0	263.0	42.9	39.9	41.4	1500
S3	342	381	342.0	381.0	51.9	57.8	54.9	750
S4	438	601	438.0	601.0	66.5	91.2	78.8	375
S5	617	766	617.0	766.0	93.6	116.2	104.9	187.5
S6	1048	918	1048.0	918.0	159.0	139.3	149.2	93.8
S7	1160	1063	1160.0	1063.0	176.0	161.3	168.7	46.9
S8	1303	1252	1303.0	1252.0	197.7	190.0	193.9	23.4
	Abs1	Abs2	Abs3	Mean Abs	Corrected	%B/Bo	Mean %B/Bo	8IP conc.(pg/ml)
4124	73	70	73	72.0	72.0	10.9		2973
4156	35	31	35	33.7	33.7	5.1	8.0	3470
4117	51	50	58	53.0	53.0	8.0		3209
4119	42	35	39	38.7	38.7	5.9		3401
4141	15	14	31	20.0	20.0	3.0		3667
4144	56	108	45	69.7	69.7	10.6		3001
4146	66	75	67	69.3	69.3	10.5		3005
4148	22	35	33	30.0	30.0	4.6		3522
4151	64	59	74	65.7	65.7	10.0		3049
4157	54	66	66	62.0	62.0	9.4		3095
4158	68	58	58	61.3	61.3	9.3	7.9	3103

5.12. 8-Hydroxy-2'deoxyguanosine (8OHdG) Determination

5.12.1. Principle

The 8OHdG test is a competitive *in vitro* enzyme-linked immunosorbent assay for the quantitative measurement of the oxidative DNA adduct 8-hydroxy-2'-deoxyguanosine (8OHdG) in tissue, serum and plasma. 8OHdG monoclonal antibody and the sample (liver tissue homogenate) are added to a microtiter plate that has been pre-coated with 8OHdG. The 8OHdG monoclonal antibody reacts competitively with the 8OHdG in the tissue and that immobilized on the microtiter plate. Therefore, higher concentrations of 8OHdG in the tissue sample will lead to a reduced binding of the antibody to the 8OHdG on the plate. The antibodies that are bound to the 8OHdG in the tissue sample are washed away from the antibodies that are bound to the 8OHdG on the microtiter plate.

An enzyme-labelled secondary antibody that is added to the plate, binds to the monoclonal antibody that is bound to the 8OHdG coated on the plate. Unbound enzyme-labelled secondary antibody is removed by a wash step and the addition of a chromatic substrate results in the development of colour in proportion to the amount of antibody bound to the plate. Finally, the reaction is terminated by the addition of 1M phosphoric acid and the absorbance read at 450nm on a microplate plate reader.

5.12.2. Reagent Preparation

8OHdG kit purchased from the Japanese Institute for the Control of Aging, Japan, was used. The kit contained the following:

1. 8OHdG Micrtiter plate : precoated with 8-OHdG (8x12 wells, split type).
2. Primary antibody : monoclonal antibody specific for 8OHdG.
3. Primary antibody solution : phosphate buffered saline.
4. Secondary antibody : horseradish peroxidase-conjugated antibody
5. Secondary antibody solution : phosphate buffered saline.
6. Chromatic solution : 3,3',5,5'-tetramethylbenzidine.
7. Diluting solution : H_2O_2 / citrate-phosphate buffered saline.
8. Washing solution (5 times) : 5 times concentrated phosphate buffered saline.
9. Reaction terminating solution : 1M phosphoric acid
10. 8-OHdG standards : 0.5, 2.0, 8.0, 20.0, 80.0, 200.0 ng/ml

5.12.3. Assay Procedure:

The assay procedure is represented by a flow chart below.

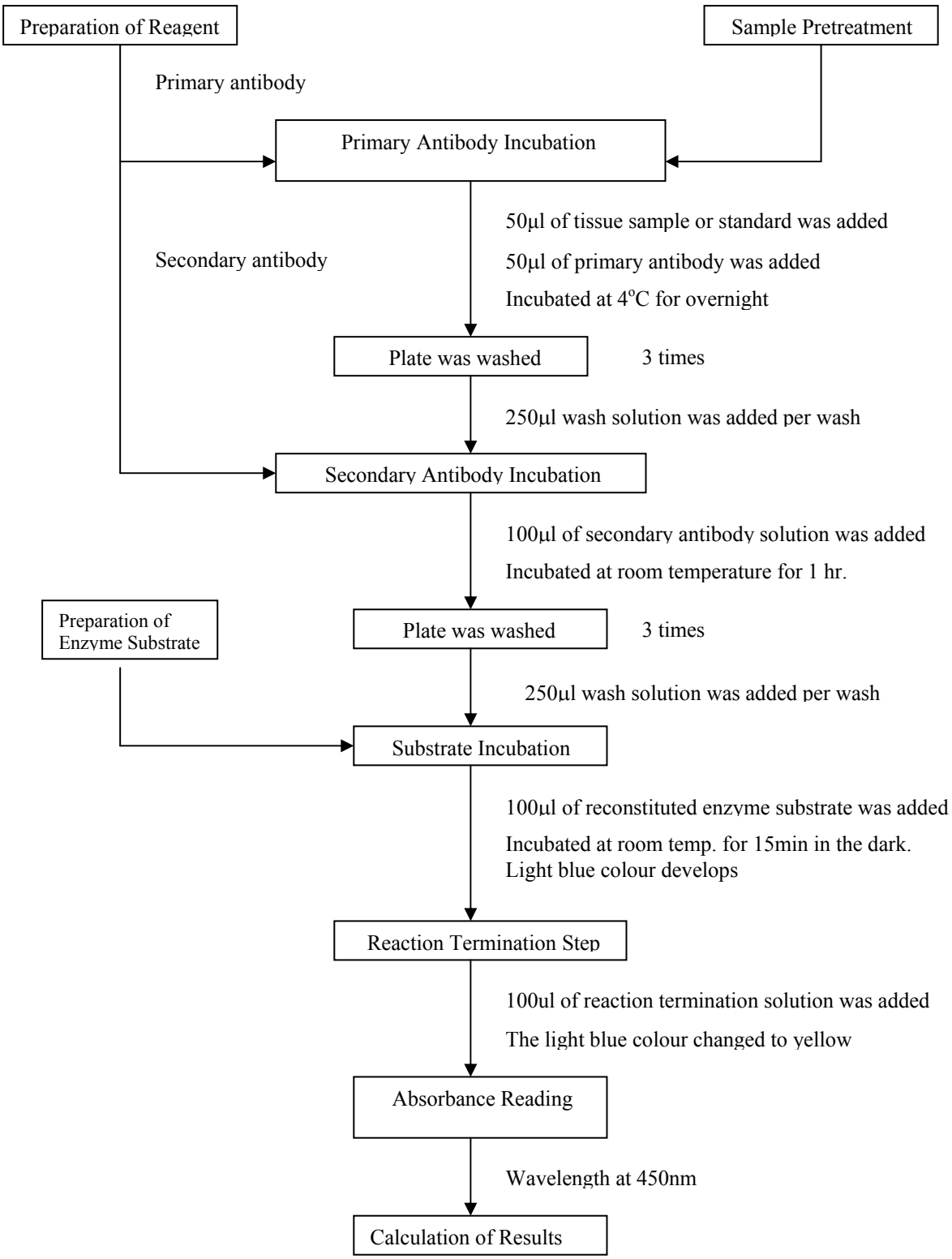

Well A1 on the plate was designated blank. Primary antibody was not added to this well.

5.12.4. Calculation

A standard curve of absorbance against concentration was plotted as shown.

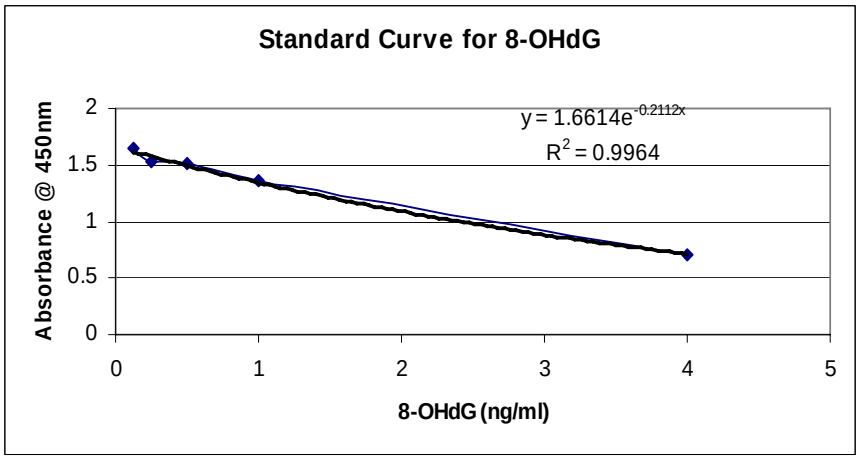

Fig. 5.12.4. 8-Hydroxyguanosine Standard Curve

Standards	Abs1	Abs2	Mean Abs	8-OHdG (ng/ml)
S1	1.683	1.615	1.649	0.125
S2	1.456	1.59	1.523	0.25
S3	1.532	1.49	1.511	0.5
S4	1.396	1.31	1.353	1
S5	0.705	0.721	0.713	4
S6	0.293	0.522	0.408	10
	Abs1	Abs2	Mean Abs	8-OHdG (ng/ml)
Samples				
5	0.44	0.50	0.47	1.01
37	0.83	0.80	0.8	1.08
3	0.42	0.43	0.43	1.01
4	0.48	0.50	0.49	1.02
22	0.25	0.23	0.24	0.97
25	0.44	0.46	0.45	1.01
27	0.26	0.27	0.26	0.98
29	0.53	0.46	0.50	1.02
32	0.34	0.30	0.32	0.99
38	0.62	0.60	0.61	1.04
39	0.22	0.20	0.2	0.97

5.13. Ames Mutagenicity Assay (Maron DM and Ames BN, 1983)

5.13.1. Introduction

Normal metabolism produces oxidants that are by-products. These oxidants such as $^{\bullet}O_2$ and H_2O_2, are the same mutagens produced by irradiation and cause damage to DNA, proteins and lipids. Two factors are critical for the formation of mutagens: lesions in DNA formed when DNA is damaged, and cell division which converts DNA lesions to mutagens.

5.13.2. Principle

A test for determining if a chemical is a mutagen is the *Ames Mutagenecity Test* named after Bruce N Ames. The Ames test is based on the assumption that any substance that is mutagenic (for the bacteria used in this test) may also turn out to be a carcinogen. However, some substances that cause cancer in laboratory animals do not give a positive Ames test (and vice-versa). The low cost of the test makes it invaluable for screening substances in our environment.

The bacterium used in the test is a strain of *Salmonella typhimurium* that carries a defective (mutant) gene, making it unable to synthesize the amino acid histidine (His) from the ingredient in its culture medium. However, some types of mutations (including this one) can be reversed, (a back mutation) with the gene regaining its function. These revertants are able to grow in a medium lacking histidine. Furthermore, many chemicals are not mutagenic (or carcinogenic) by themselves, but become converted to mutagens (and carcinogens) as they are metabolized in the body. For this reason, the Ames test includes a mixture of liver enzymes.

5.13.3. The Bacteria Tester Strain

A set of histidine-requiring strains is used for mutagenicity testing. Each tester strain contains a different type of mutation in the histidine operon. In addition to the histidine mutation, the standard tester strains contain other mutations that greatly increase their ability to detect mutagens. One mutation *(rfa*) causes partial loss of the lipopolysaccharide barrier that coats the bacteria and increases permeability to large molecules that do not penetrate the normal cell wall. The other mutation (*uvr*B) is a deletion of a gene coding for the DNA excision repair system, resulting in greatly increased sensitivity in detecting many mutagens. The deletion excising the *uvrB* gene extends through the bio-gene and consequently, these bacteria also require biotin for growth. The standard tester strains mostly used are TA97, TA98, TA100, TA102.

TA97 } Contains R-factor plasmid, pKM 101. This increases
TA98 } chemical and spontaneous mutagenesis by enhancing
TA100 } an error-prone DNA repair system.
TA102 } Contain multiple plasmid, pAQ1, which carries the *his*G428 Mutation and the tetracycline resistant gene.

Additionally,

TA100 - *his*G gene (encoding for the first enzyme of histidine biosynthesis) *his*G46 mutation. This mutation substitutes proline $^{-GGG-}$ for leucine $^{-GAG-}$ Therefore TA100, detects mutagens that cause base-pair substitutions primarily at one of these G-C pairs.

TA98 - *his*D gene (Coding for histidinol dehydrogenase) *his*D3052 mutation. Detects various frame-shift (FS) mutations. These FS mutations can stabilize the shifted pairing that often occurs in repetitive sequences or 'hot spots' of the DNA, resulting in a frame-

shift mutation which restores the correct reading frame for histidine synthesis. The *his* D3052 has the sequence $^{-CGCGCGCG-}$, 8 repetitive – GC residues near the site of a FS mutation in the *his*D gene. The mutation is reverted by i.e. 2-nitrosofluorene, daunomycin.

TA97 - *his*D6610 mutation, plus a second 'hot spot' of alternating -GC- base pairs near the run of the cytosines. It is sensitive to some of the mutagenes that revert TA98.

TA102 - *his*G gene contains the ochre mutation $^{-TAA-}$. This strain detects efficiently a variety of mutagens such as formaldehyde, glyoxal, hydroperoxides, bleomycin, X-rays, UV light.

5.13.4. Reagent List and Preparation

Oxoid Nutrient Broth No. 2

Bacto Difco Agar

NaCl

L-Histidine

D-Biotin

KCl

$MgCl_2.6H_2O$

NaH_2PO_4

Na_2HPO_4

NADP

G-6-PO_4

$MgSO_4.7H_2O$

K_2HPO_4

$NaHNH_4PO_4.4H_2O$

Citric acid monohydrate

Glucose

Daunomycin

Ampicillin

Crystal Violet

DMSO

Nutrient Broth (*autoclaved*)

- Oxoid nutrient broth - 1.25g
- dH_2O - 50ml

Nutrient Agar Plates (contains histidine) (*autoclaved*)

- Oxoid nutrient broth - 4.8g
- Bacto agar - 9.0g
- dH_2O - 600ml

Top Agar (*autoclaved*)

- Bacto agar - 0.6g
- NaCl - 0.5g
- dH_2O - 100ml

Vogel-Bonner Medium E (VB medium) (*autoclaved*)

- ddH_2O - 670ml
- $MgSO_4.7H_2O$ - 5g
- Citric acid monohydrate - 50g
- K_2HPO_4 or $K_2HPO_4.5H_2O$ - 250g or 327.59g
- $NaHNH_4PO_4.4H_2O$ - 78.5g

were added in the above order.

were added after each compound had dissolved.

Minimum Glucose Plates

- Bacto agar - 15g
- dH_2O - 910ml

The above-mentioned was autoclaved.

added 25X VB medium E - 40ml

added 40% glucose - 50ml

Histidine / Biotine Sol^{n} (*autoclaved*)

Per 250ml

- D-Biotin (FW 247.3) - 30.9mg
- L-Histidine - 24.0mg

0.1M Hitidine Sol^{n} (*autoclaved*)

- L-Histidine - 1.55g/100ml

0.5mM Biotin Sol^{n} (*autoclaved*)

- D-Biotin - 0.012g/100ml

0.1% Crystal violet Sol^{n}

- Crystal violet - 0.01g
- ddH_2O - 10ml

Daunomycin (daunorubicin hydrchloride)

- Daunomycin - 1mg / ml

Glucose-6-phosphate (G-6-P)

- G-6-P - 2.82g/10ml

Nicotine adenine dinucleotide phosphate (NADP) Sol^{n}

- NADP (FW 765.4) - 383mg / 5ml

1.65M KCl / 0.4M $MgCl_2$ Salt Sol^n (Per 100ml)

- KCl - 12.3g
- $MgCl_2.6H_2O$ - 8.14g

0.2M Sodium phosphate buffer (60ml A + 440ml B)

- 0.2M $NaH_2PO_4.H_2O$ - 13.8g/500ml……A
- 0.2M Na_2HPO_4 - 14.2g/500ml……B

S9 Mix (rat liver microsomal enzymes + co-factors)

- Purchased from Moltox (Molecular Toxicology Inc., Boone, USA).
- S9 Mix was diluted 1:3 in 0.15M KCl

5.13.5. Preparation of Liver Tissue for Ames Test

- 3g of liver tissue was homogenized in 9ml of KCL (0.15M)
  - 0.15M KCl was prepared by adding 74.56g KCl to 100ml of distilled water.
  - Preparation was then autoclaved.
- After homogenizing liver tissue, 1 ml of this homogenate was extracted and stored. This is known as the whole homogenate.
- The remaining homogenate was then centrifuged at 9000rpm for 10 minutes at 4°C.
- The resulting supernatant was retrieved and stored. This is known as the S9 fraction.
- The volume of S9 retrieved was measured and replaced with an equal volume of 0.15M KCl.
- The mixture was then homogenized. 1ml was then extracted. This is known as the nucleosomal homogenate.

- The remaining mixture was then transferred into Beckman tubes and ultracentrifuged at 40 000rpm for 1 hour at 4°C.
- The resulting supernatant was then removed and stored as the cytosolic fraction.
- The volume of supernatant removed was replaced with 0.15M KCl. The mixture was homogenized and stored as the microsomal fraction.

5.13.6. Characterization of TA97, TA98, TA100, TA102 strains (donated by Ames Lab, USA).

A. Upon receipt of discs impregnated with the *Salomonella* strains, each disc was dropped into separate tubes containing 10ml nutrient broth and incubated overnight at 37^{o}C. with shaking.

B. The overnight culture was plated on nutrient agar plates to obtain single colonies and incubated at 37^{o}C overnight. *(This is referred to as the master plate.)*

C. Six (6) culture tubes were filled with 10ml nutrient broth. Single colonies were transferred into each of the tubes and incubated overnight at 37^{o}C with shaking.

D The following markers were performed on each of the tubes and the tube that satisfied all criteria was selected. Where none was suitable a repeat was carried out using single colonies from step B.

5.13.6.1 Test for Histidine Requirement

- Requirement
  - Minimum glucose plates
  - 0.1M Histidine
  - 0.5M Biotin
  - dH_2O (autoclaved)
- Two circles were marked on the bottom of the culture plates and labeled H_2O & H/B. (Figure 15.13.6).
- A sterile loop was dipped into autoclaved ddH_2O and plated within the H_2O circle. Similarly, a loop-full of 0.1M Histidine was plated within the H/B circle ff by a loop-full of 0.5M Biotin.
- Finally a loop-full i.e. TA97 from one of the six tubes was plated within the ddH_2O circle and another within the H/B circle.
- The a/m procedure was repeated for two other minimum glucose plates. Thus, triplicates were produced for each of the 6 tubes.
- The whole procedure for each of the 6 tubes of TA98, TA100 & TA102 was repeated.
- The minimum glucose plates were incubated at 37^oC overnight.

5.13.6.2 rfa (Permeability) Test

- Requirement
  - Nutrient agar plates (NA)
  - Top agar
  - 0.1% Crystal violet sol^n
- The Top agar was placed in a water bath with temperature 45^oC.
- 2.5ml of Top agar was dispensed into culture tubes and capped.
- 0.1ml i.e. TA98 was added to each tube and vortexed for about 5sec.

- This was quickly poured onto the NA plate. The plate was gently swirled to allow even distribution.
- Work was done in triplicate.
- The above procedure was repeated for the other strains.
- An HPLC syringe was rinsed with HPLC MeOH. Using the syringe, 10µl of the crystal violet solution was drawn onto an autoclaved filter paper disc.
- The crystal violet-soaked disc was placed in the center of the plate (i.e. TA98 plate).
- For all 6 tubes of TA97, TA98, TA100, TA102 the above-mentioned procedure was repeated. Sterile filter paper discs were handled by flamed forceps.
- The Nutrient agar plates were incubated at 37^{o}C for 24hr (Figure 15.13.6).

5.13.6.3 *uvβ* Mutation Test

- Requirement - NA Plates
- Work was done in triplicates and plates labeled TA98, TA100 etc.
- A line was drawn under each plate (dividing it into two halves)
- A loop-full of i.e. TA 97 from tube 1 was streaked across the plate. In all 4-6 parallel streaks were made. Two streaks were made from each tube. Additionally, streaks were made at right angles to the dividing line. Samples from all 6 tubes of i.e. TA97 were treated in a similar manner.
- A piece of sterile cardboard or paper towel (sprayed with 70% EtOH) was placed across the plate along the vertical line that divided the plate.
- The plates were irradiated by a 15W UV lamp for 6sec at a vertical distance of about 33cm from above (Figure 15.13.6).
- Finally, the plates were incubated at 37^{o}C for 12-24hrs.

5.13.6.4 R-factor Test

- Requirement
  - Minimum glucose plates
  - Top agar
  - 0.5mM His/Bio Sol^{n}
- 10ml of His/Bio Sol^{n} was added to the Top agar held at 45^{o}C.
- 2.0ml of the Top agar (with His/Bio) was added to culture tubes (incubating at 37^{o}C).
- 0.1ml of i.e. TA98 (tube 1) was then added to each of the tubes containing the Top agar.
- This was vortexed for 3sec and quickly poured onto the Minimum glucose plate. The plate was swirled gently and the Top agar allowed to settle.
- Ampicillin discs (Bacto - sensitivity disc 10 µg 6363-33 DIFCO) was gently dropped onto the plates.
- The procedure was repeated for all 6 tubes of i.e. TA98, TA100, TA102 & TA97.
- Plates were incubated at 37^{o}C for 48 hr (Figure 15.13.6).

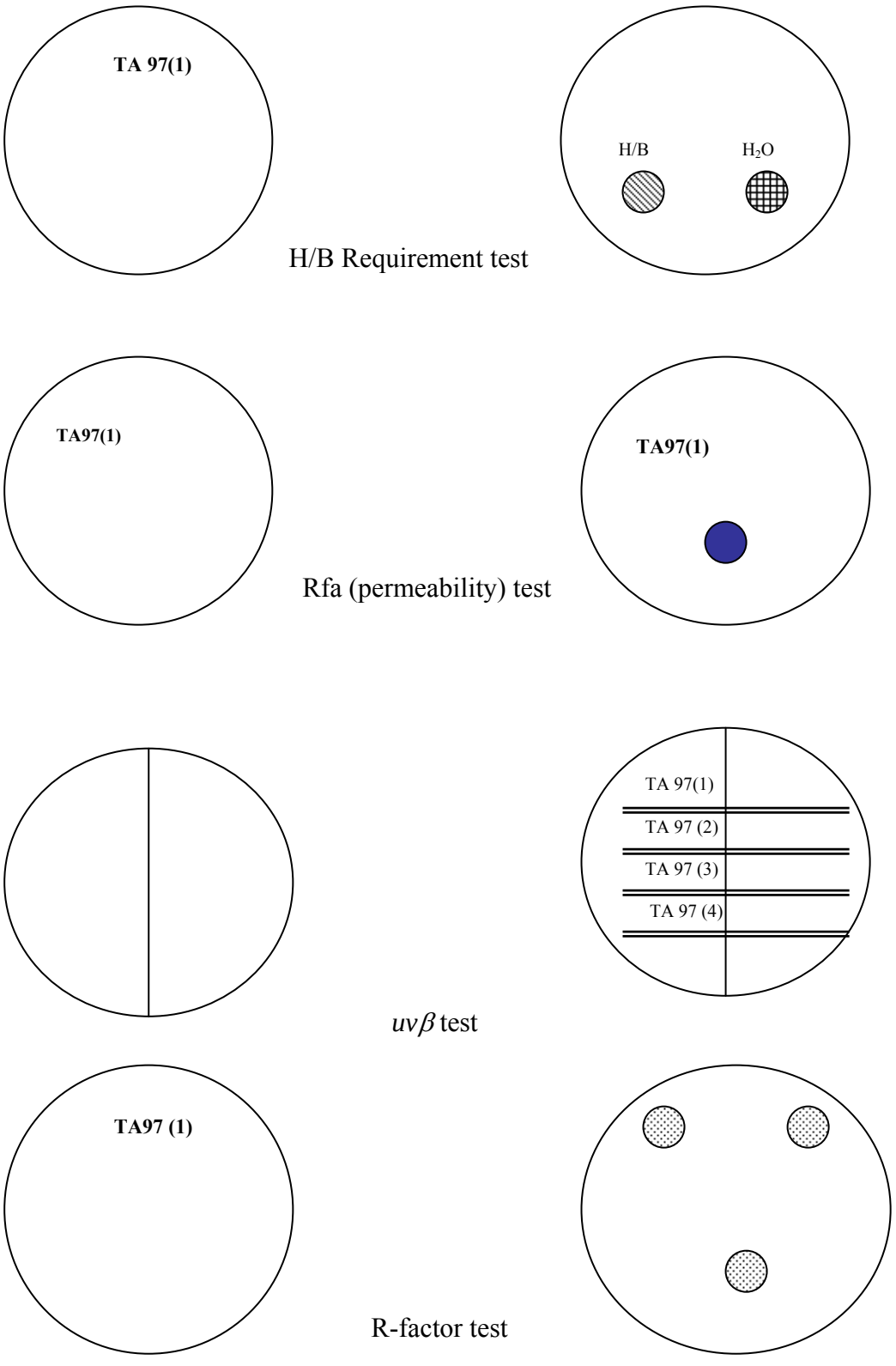

Figure 15.13.6 Characterization of *Salmonella* strains using the various markers.

5.13.6.5 Spontaneous Revertant Test

- Requirement
  - Nutrient agar plates
  - Top agar
  - 0.5mM Histidine/Biotin Sol^{n}
- Five plates were prepared for each of the 6 tubes from a particular strain i.e. TA97(1), TA97(2)……..TA97(6).
- The Top agar was incubated at 45^{o}C and the culture tubes at 37^{o}C.
- 2.5ml Top agar was dispensed into each (cupped) culture tube under sterile conditions.
  - 0.6ml of the tester strain i.e. TA97(1) was quickly pipetted and 0.1ml was dispensed into the five culture tubes.
- The culture tube was vortexed for 3sec. and quickly poured onto the Nutrient agar plate.
  - The labeled culture plate was gently swirled on a flat top and allowed to settle.
- The above procedure was repeated for all samples and culture plates were incubated at 37^{o}C for 48 hrs undisturbed.
  - Colonies (revertants against the background lawn) were counted (i.e. Figure 16*l*).
- For TA97, the acceptable range was: 90-180 colonies

  TA98, " 30-50 "

  TA100, " 120-200 "

  TA102, " 240-360 "

Finally, one tube from each *Salmonella typhimurium* strain that strictly adhered to all five conditions was selected. The selected tube was referred to as "master copies". Master copies were stored at 4^{o}C and used over the next few days. Master plates (first culture, 8.16.5 sec B) were stored at -70^{o}C for some few months. For long term storage the following procedure was followed:

- 50ml of Nutrient broth was prepared and autoclaved for each strain.
- The Nutrient broth was allowed to partially cool down. This was incubated for 30 min with continuous shaking at 37^{o}C.
- The 50ml Nutrient broth was inoculated with 1ml of the cultured bacteria from the selected tube and incubated for 12hrs, with continuous shaking at 37^{o}C.
- 0.09ml DMSO (filtered through a 0.22μm filter) was added per 1ml of culture and gently mixed. 1ml was then aliquot into 'nunc' tubes. This was stored at -70^{o}C for years.

5.13.6.6 Mutagenicity Test

- The procedure was the same as that described for the *Spontaneous revertant test.* However, 0.1ml of the suspected mutagenic substance was first added to the 2.0ml Top agar, followed by 0.1ml of the tester strain i.e. TA97.
- Test samples were challenged with 0.1ml S9 mix. This was added to the Top agar.

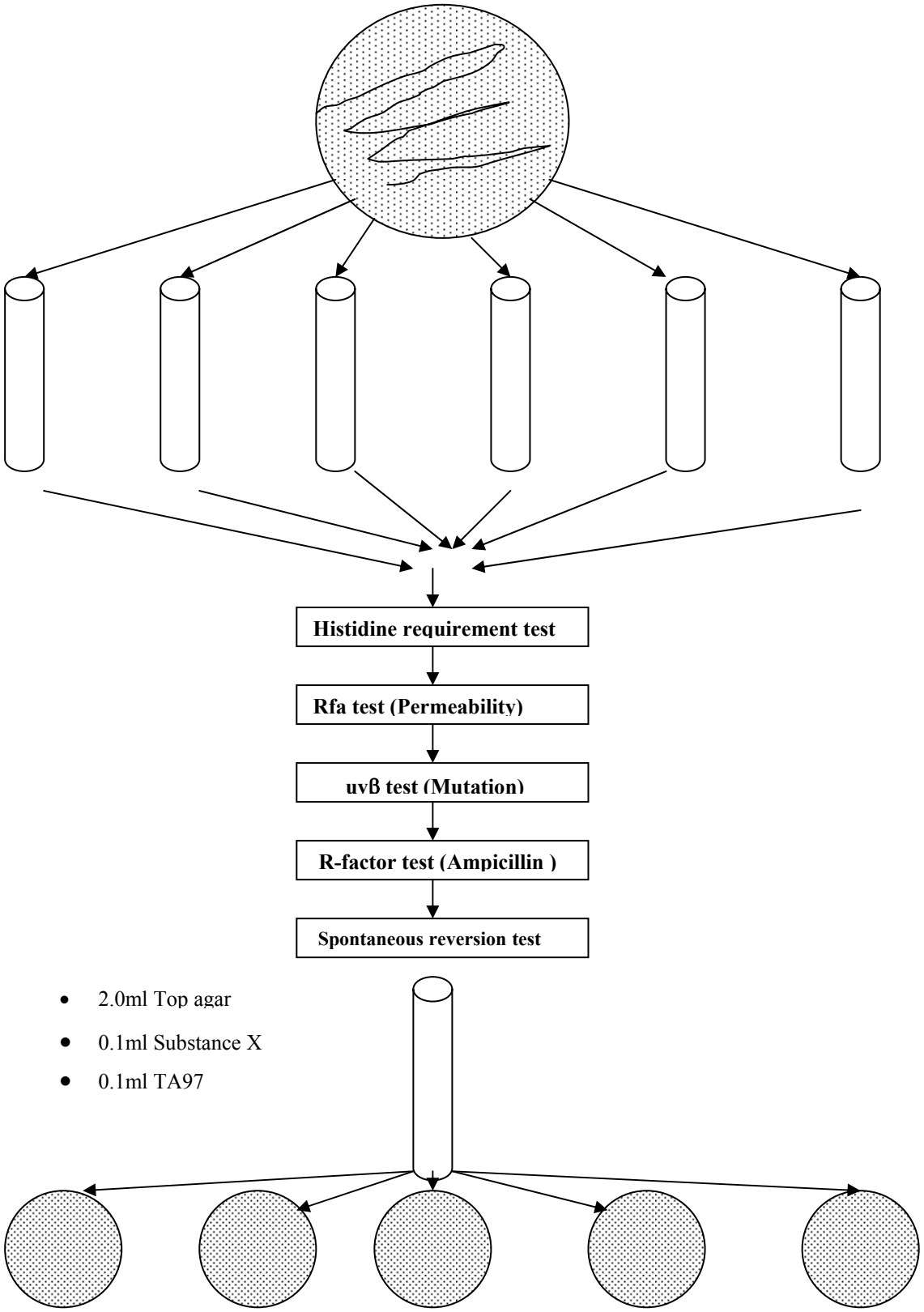

Figure 5.13.7. Summary of the steps involved in the characterization of the Salmonella tester strains.

5.14.Cytokines

5.14.1. Principle

The Bio-Plex cytokine reagent kit (BioRad, UK) is a suspension array system built around the following three core technologies:

1) The family of fluorescently dyed microspheres (beads) to which biomolecules are bound.
2) A flow cytometer with two lasers and associated optics to measure reactions that occur on the surface of the microspheres
3) A high-speed digital signal processor that efficiently manages the fluorescent output

The Bio-Plex suspension array system uses multiplexing technology that uses up to 100 colour-coded bead sets, each of which can be conjugated with a different specific reactant. Each reactant is specific for a different target molecule. Three different sets of colour-coated beads were used, each designated to IL-1β, IL-6 and IL-10 detection. The cytokine assays are designed in a capture sandwich immunoassay format. Antibodies specifically directed against the cytokine of interest are covalently coupled to a colour-coded 5.5 μm polystyrene bead. Antibody-coupled beads are allowed to react with a sample containing an unknown amount of cytokine, or with a standard solution containing a known amount of cytokine. A series of washes are performed to remove any unbound protein. Thereafter a biotinylated detection antibody specific for a different epitope on the cytokine is added to the beads. The result is the formation of a sandwich of antibodies around the cytokine. The reaction mixture is detected by the addition of streptavidin-phycoerythrin (strepatavidin-PE), which binds to the biotinylated detection antibodies. The constituents of each well are drawn up into the

flow-based Bio-Plex suspension array system, which identifies and quantitates each specific reaction based on bead colour and fluorescence. The magnitude of the reaction is measured using fluorescently labeled reporter molecules associated with each target protein. Unknown cytokine concentrations are automatically calculated by the Bio-Plex Manager software using a standard curve derived from a recombinant cytokine standard.

5.14.2. Reagents

Bio-Plex Cytokine Reagent Kit contains the following:

- Bio-Plex Assay Buffer
- Bio-Plex Wash Buffer
- Bio-Plex Detection Antibody Diluent
- Streptavidin PE (100x)
- Anti-cytokine Conjugated Beads (25X Concentration)
- Cytokine Detection Antibody (50X Concentration -70 µl)
- Cytokine Standard (2 vials, lyophilized)

Bio-Plex Rat Serum Diluent Kit:

- Bio-Plex Rat Serum Sample Diluent
- Bio-Plex Rat Serum Standard Diluent

Note: This assay was performed on a Bio-Plex Luminex 100 System

5.14.3. Reagent Preparation

All preparations were kept on ice throughout preparation procedures.

a) 1 volume of serum was diluted with 3 volumes of Bio-Plex sample diluent. (30µl sample was diluted with 90µl of diluent).

b) Reconstitution of the cytokine standard was performed as follows: A 30 second quick-spin centrifugation of the lyophilized standard was followed by reconstituting 1 tube of lyophilized cytokine standard with 500 µl of rat serum diluent. Brief mixing followed and the cytokine standard was stored on ice for 30 minutes.

c) Preparation of the standards: (Two sets of standards were prepared representing two sets of concentrations)

Table 5.14.3a. 1.95-32000 pg/ml Cytokine Standard Curve

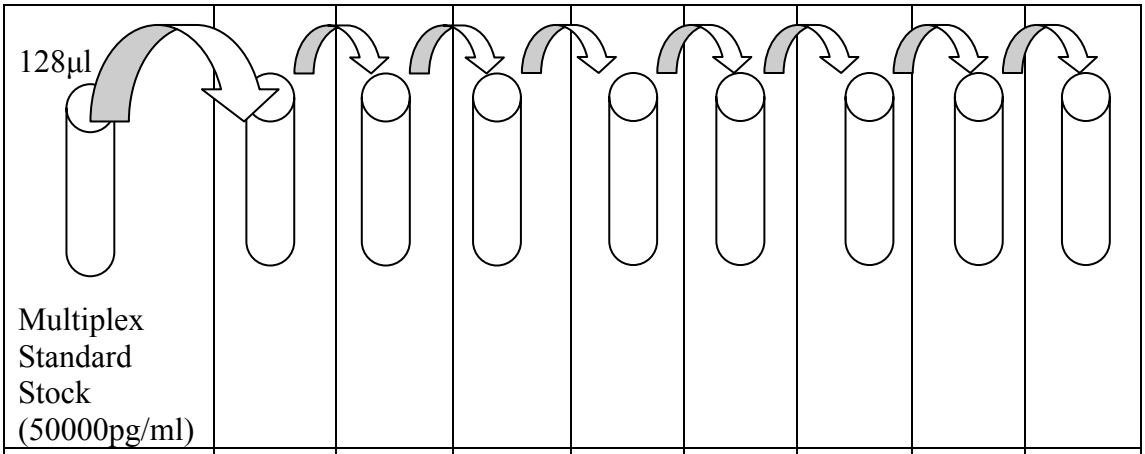 Multiplex Standard Stock (50000pg/ml)								
Concentration (pg/ml)	32000	8000	2000	500	125	31.3	7.8	1.95
Stock (µl)	128	50	50	50	50	50	50	50
Standard Diluent (µl)	72	150	150	150	150	150	150	150

Table 5.14.3b. 0.2-3200 pg/ml Cytokine Standard Curve

12.8µl 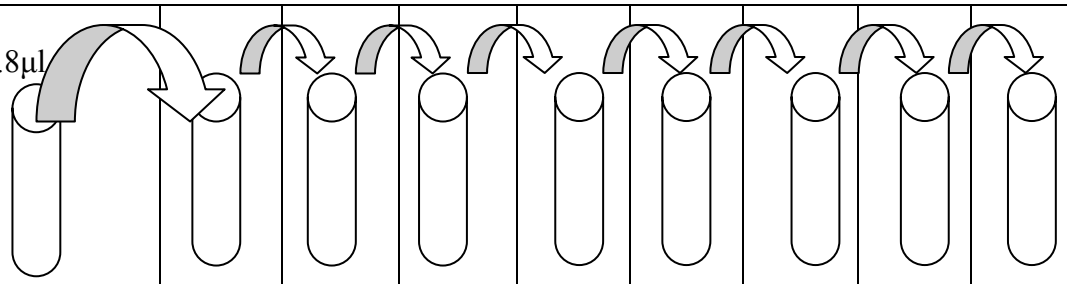 Multiplex Standard Stock (50000pg/ml)								
Concentration (pg/ml)	3200	800	200	50	12.5	3.13	0.78	0.2
Stock (µl)	12.8	50	50	50	50	50	50	50
Standard Diluent (µl)	187.2	150	150	150	150	150	150	150

d) Conjugated bead preparation: Beads were protected from light by covering with aluminum foil. The anti-cytokine conjugated beads were vortexed at a medium speed for 15-20 seconds. 240µl of the (25X) stock beads was added to 5760 µl of the Bio-Plex assay buffer to give a total volume of 6000 µl.

e) Detection antibody preparation: A 30 second quick spin centrifugation was performed on the detection antibody vial prior to pipetting, so as to collect the entire volume at the bottom of the vial. 120µl of the 50X stock detection antibody was added to 2880µl of the detection antibody diluent giving a total volume of 3000µl.

f) Streptavidin-PE Preparation: A 30 second quick spin centrifugation of the streptavidin-PE vial was performed prior to pipetting. 60µl of the (100X) streptavidin-PE was diluted with 5940µl of the Bio-Plex assay buffer giving a total volume of 6000µl. This solution was stored in the dark until ready for use.

5.14.4. Assay Procedure

The assay procedure is represented by the flow chart below.

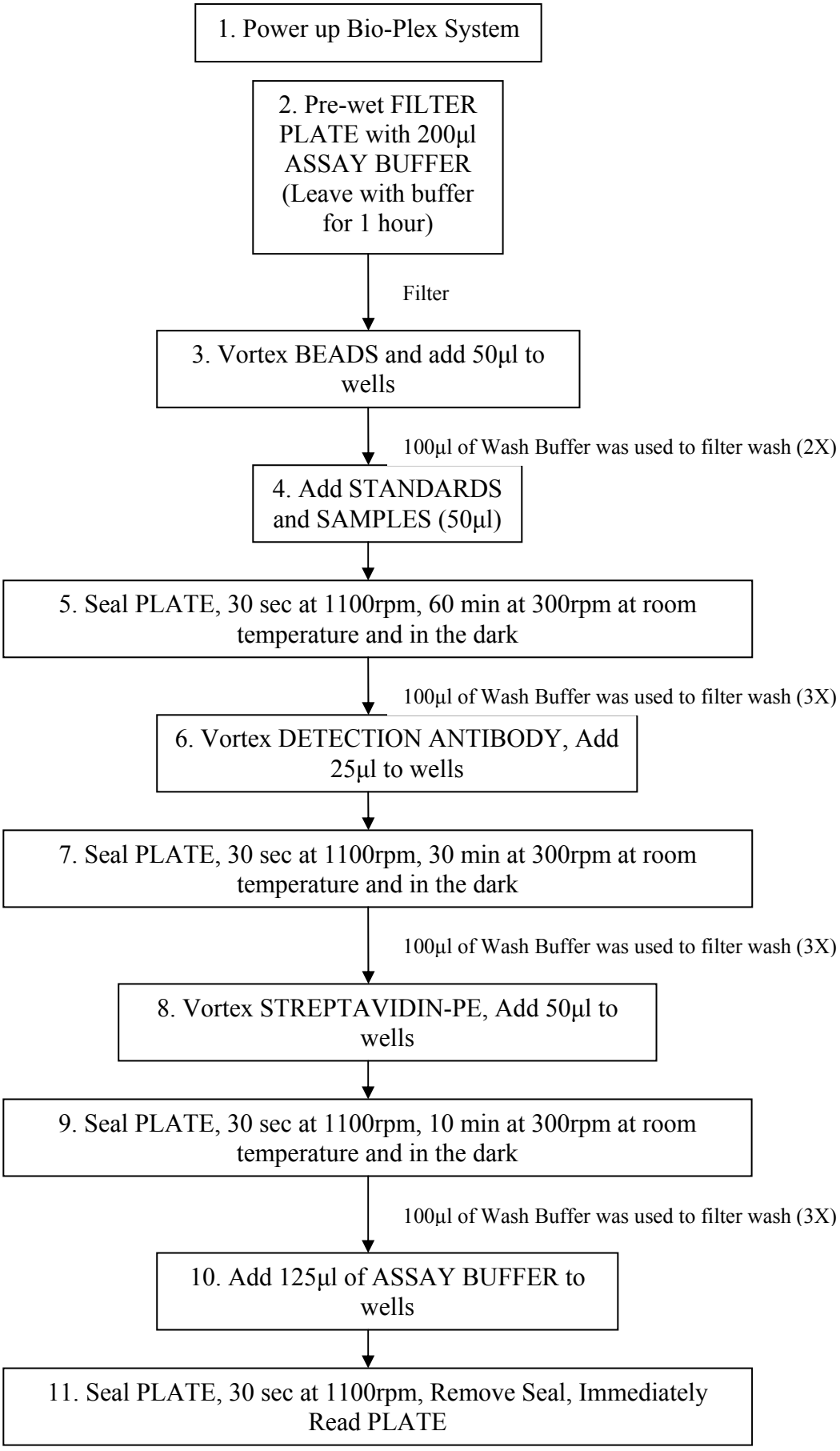
1. Power up Bio-Plex System
2. Pre-wet FILTER PLATE with 200µl ASSAY BUFFER (Leave with buffer for 1 hour)
Filter
3. Vortex BEADS and add 50µl to wells
100µl of Wash Buffer was used to filter wash (2X)
4. Add STANDARDS and SAMPLES (50µl)
5. Seal PLATE, 30 sec at 1100rpm, 60 min at 300rpm at room temperature and in the dark
100µl of Wash Buffer was used to filter wash (3X)
6. Vortex DETECTION ANTIBODY, Add 25µl to wells
7. Seal PLATE, 30 sec at 1100rpm, 30 min at 300rpm at room temperature and in the dark
100µl of Wash Buffer was used to filter wash (3X)
8. Vortex STREPTAVIDIN-PE, Add 50µl to wells
9. Seal PLATE, 30 sec at 1100rpm, 10 min at 300rpm at room temperature and in the dark
100µl of Wash Buffer was used to filter wash (3X)
10. Add 125µl of ASSAY BUFFER to wells
11. Seal PLATE, 30 sec at 1100rpm, Remove Seal, Immediately Read PLATE

5.14.5. Calculations

The assay was run on the Luminex 100 System. An example of data presentation generated by the software is shown below.

Type	Well	Outlier	Sample	FI	FI - Bkgd	Std Dev	%CV	Obs Conc	Exp Conc	(Obs/Exp) * 100
B	G11,H11	0		74	74	1.41	1.91			
S1	A1	1		---	---				32000	
S2	B1	0		24973	24899	0	0	6779	8000	85
S3	C1	0		15475	15401	0	0	2166	2000	108
S4	D1	0		4834	4760	0	0	518	500	104
S5	E1	0		1262	1188	0	0	121	125	96
S6	F1	0		371	297	0	0	30	31	94
S7	G1	0		144	70	0	0	8	8	97
S8	H1	0		81	7	0	0	2	2	91
S9	A2	0		20544	20470	0	0	3664	3200	115
S10	B2	0		6187	6113	0	0	681	800	85
S11	C2	0		2515	2441	0	0	255	200	127
S12	D2	0		557	483	0	0	48	50	96
S13	E2	0		226	152	0	0	15	12.5	123
S14	F2	0		93	19	0	0	3	3.1	91
S15	G2	0		72	-2	0	0	1	0.8	126
S16	H2	1		---	---				0.2	
X1	A3,B3	0	228	277	204	9	4.5	81.1		
X2	C3,D3	0	222	134	61	2	3.5	26.6		
X3	E3,F3	0	247	235	161	21	13.2	64.7		
X4	G3,H3	0	276	107	34	8	23.2	16.6		
X5	A4,B4	0	314	229	155	10	6.4	62.4		
X6	C4,D4	0	315	345	271	6	2.4	107.4		
X7	E4,F4	0	190	119	45	21	46.1	20.7		
X8	G4,H4	0	191	108	34	6	16.6	16.8		
X9	A5,B5	0	325	199	125	37	29.4	50.9		
X10	C5,D5	0	189	169	95	15	15.7	39.3		

5.15. Hydroxyproline

The following protocol was taken from Ruwart *et al.* (1989).

5.15.1. Reagents and Preparation

a) 6N HCl

b) 50% isopropanol

c) 0.84% chlormaine-T solution

d) Ehrlich's Solution: 1ml Ehrlich's Reagent + 4ml acetone

e) Hydroxyproline standard

5.15.2. Assay Procedure

- Liver tissue was homogenized in a weight to volume ratio of 3:1 in 6N HCl.
- This homogenate was then hydrolyzed at 110°C for 16 hours.
- The hydrosylate was then filtered.
- 25µl aliquotes of filtered hydrosylate were then dried in triplicate at 90°C.
- The sediment was then dissolved in 1.2ml of 50% isopropanol.
- 0.2ml of 0.84% chloramine-T solution was added.
- 1ml of Ehrlich's solution was added after 10 minutes.
- The mixture was then incubated at 50°C for 90 minutes, and allowed to cool thereafter at room temperature.
- The absorbencies of the samples were then read against a reagent blank at 558nm. Reagent blank contained the complete system without the added tissue.
- The concentration of hydroxyproline in each sample was determined from a standard curve generated from known quantities of hydroxyproline which had been hydrolyzed as above (Range of standard curve:0-100µM/g liver).

5.15.3. Calculations

- Absorbance values obtained were multiplied by the dilution factor of 4 and the following standard curve used to find the concentration of hydroxyproline.

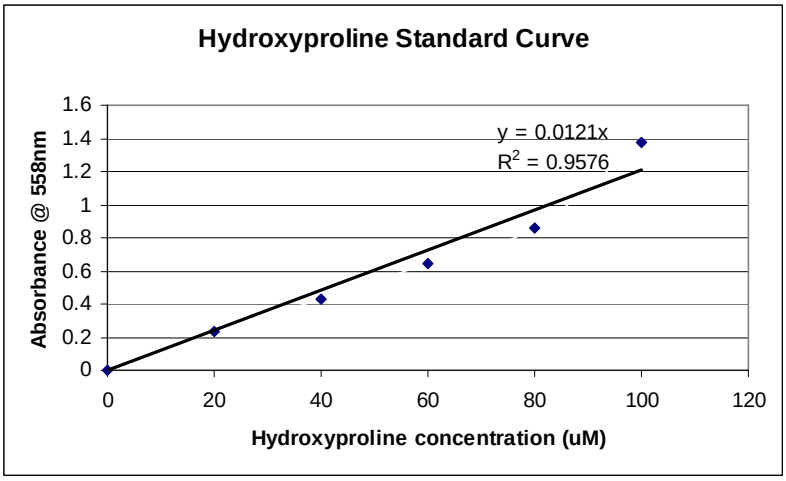

Fig. 5.15.3. Hydroxyproline Standard Curve

5.16. AFP and Haematological Differentials

AFP was determined using an auto-analyser (Advia Centaur) and kits from Bayer (Tarrytown, USA). Haematological differentials were determined using an auto-analyser (Cobas Integra 400) and kits from Roche Diagnostics (Indianapolis, USA). Haematological differentials measured include: haemoglobin concentration, white blood cell count (WBC), red blood cell count (RBC), Platelet count and mean platelet volume (MPV).

5.17. Statistics

Statistical Analysis was be performed by an independent student's t-test at the level of 0.05 for unpaired and paired data. A probability value of <0.05 was considered statistically significant. For multiple groups, analysis of variance was performed by Bonferroni (Dunn) Multiple comparison t-test. Two-way analysis of variance was used to determine the effect of time on parameters, with a Tukey post hoc test being used to determine specific group significance. Pearson's correlation was determined across groups. The GraphPad Instat software (San Diego, USA) was used to perform basic student's t-tests. The Statistica software by Statsoft Inc. (Tulsa, OK) was used to perform the analysis of variance and correlations.

6.0. Results

The focus of this study was to investigate the synergy and extent thereof between dietary iron overloading and AFB_1 in hepatocarcinogenesis in an animal model. In terms of presenting the acquired data, the focus will be on representing the synergy observed. Hence, data shown in the results section will contain only those which show synergy. Assays not showing synergy will be mentioned, and detailed representations thereof are available in the appendix. Synergy will be defined as a significant difference between the (Fe + AFB_1) group in comparison to the Fe and / or the AFB_1 groups. The extent of synergy will be described as a ratio calculated as follows:

$$\text{Fe group} + AFB_1 \text{ group} : \text{Fe} + AFB_1 \text{ group}$$

This ratio will be referred to as the extent of synergy ratio. A 1:1 ratio represents an additive effect, not considered synergistic. An additive effect is considered as being synergistic (1<1). A ratio of 1<1 ratio implies an additive and possible synergistic effect. This depicts that the combined diet of the two carcinogens has an additive or synergistic effect on the measured parameter. The results of all analyses are presented in figures and tables 6.1 to 6.19 in the results section, and figures A1.1(i) to A3.1(x) and tables A1.1(i) to A4.1(viii) in the appendix. The error bars in graphical presentations represent the standard deviation. Data is denoted as (mean ± standard deviation). The colour codes for the graphs illustrate the following groups:

- Control
- Iron
- Iron and Aflatoxin B_1
- Aflatoxin B_1

6.0.1. Indicators of Iron Overload and Liver Disease

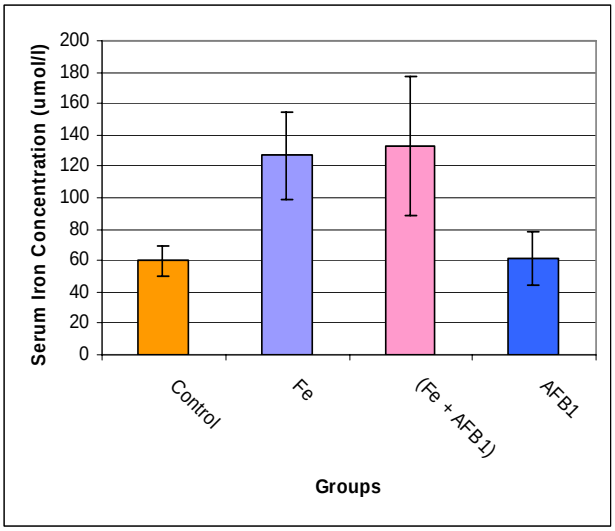

Figure 6.1. Bar Graph of Serum Iron Levels of Wistar Albino Rats at 12 months

Table 6.1. Bonferroni Dunn and T-Tests for Serum Iron at 12 months

Treatment Comparison	t	P-Value
Control vs. Fe	2.991	* P<0.05
Control vs. Fe + AFB_1	2.856	** P<0.01
Control vs. AFB_1	0.762	ns P>0.05
Fe vs. Fe + AFB_1	0.334	ns P>0.05
Fe vs. AFB_1	2.805	* P<0.05
Fe + AFB_1 vs. AFB_1	3.797	** P<0.01

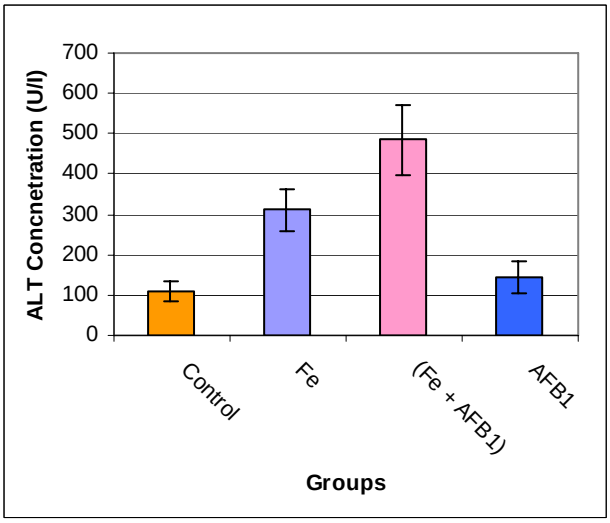

Figure 6.2. Bar Graph of Serum ALT Levels of Wistar Albino Rats at 12 months

Table 6.2. Bonferroni (Dunn) and t-tests for ALT at 12 months

Treatment Comparison	t	P-Value
Control vs. Fe	5.573	*** P<0.001
Control vs. Fe + AFB_1	11.881	*** P<0.001
Control vs. AFB_1	1.162	ns P>0.05
Fe vs. Fe + AFB_1	5.176	*** P<0.001
Fe vs. AFB_1	4.223	** P<0.01
Fe + AFB_1 vs. AFB_1	9.964	*** P<0.001

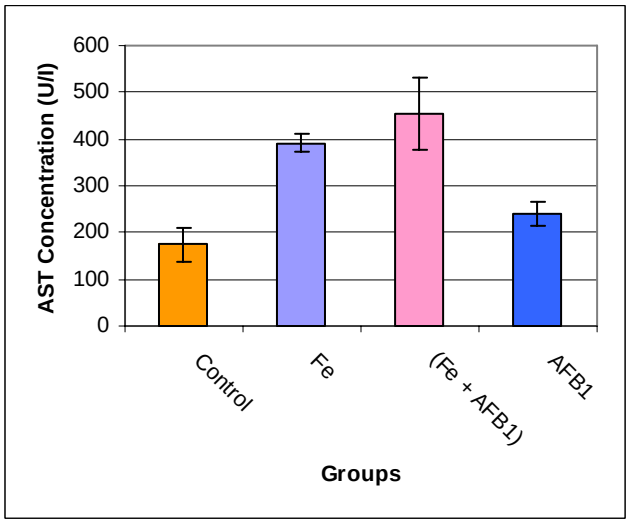

Figure 6.3. Bar Graph of Serum AST Levels of Wistar Albino Rats at 12 months

Table 6.3. Bonferroni (Dunn) and t-tests for AST at 12 months

Treatment Comparison	t	P-Value
Control vs. Fe	7.053	*** P<0.001
Control vs. Fe + AFB_1	10.432	*** P<0.001
Control vs. AFB_1	2.188	ns P>0.05
Fe vs. Fe + AFB_1	2.201	ns P>0.05
Fe vs. AFB_1	4.658	*** P<0.001
Fe + AFB_1 vs. AFB_1	7.482	*** P<0.001

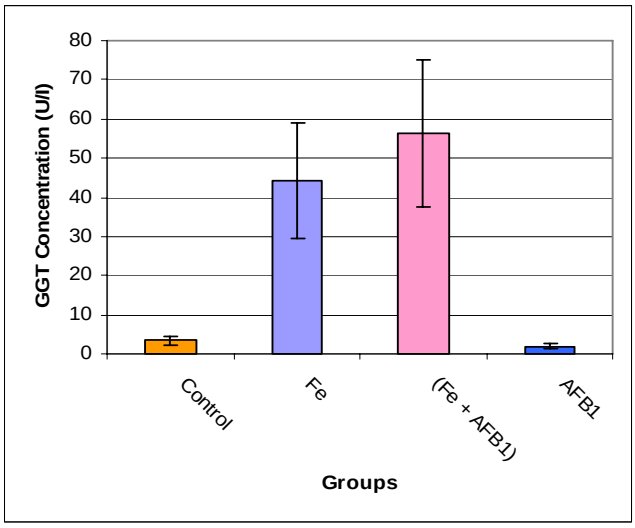

Figure 6.4. Bar Graph of Serum GGT Levels of Wistar Albino Rats at 6 months

Table 6.4. Bonferroni (Dunn) and t-tests for GGT at 6 months

Treatment Comparison	t	P-Value
Control vs. Fe	4.555	*** P<0.001
Control vs. Fe + AFB_1	7.027	*** P<0.001
Control vs. AFB_1	0.132	ns P>0.05
Fe vs. Fe + AFB_1	1.720	ns P>0.05
Fe vs. AFB_1	4.916	*** P<0.001
Fe + AFB_1 vs. AFB_1	7.698	*** P<0.001

6.0.2. Reactive Oxygen Species and Reactive Nitrogen Species

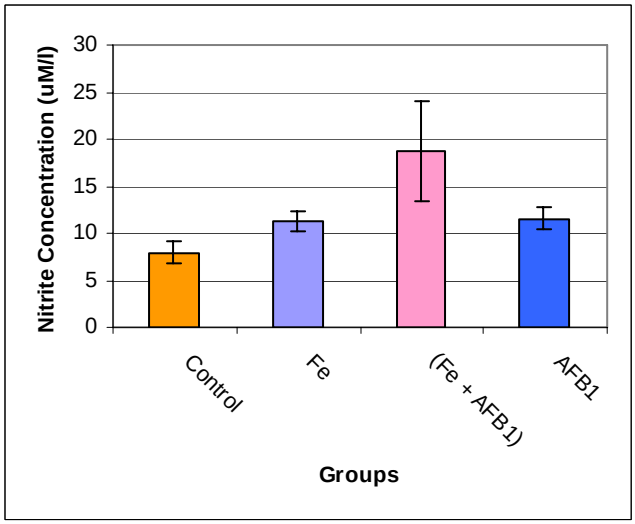

Figure 6.5. Bar Graph of Serum Nitrite Levels of Wistar Albino Rats at 6 months

Table 6.5. Bonferroni (Dunn) and t-tests for Serum Nitrite at 6 months

Treatment Comparison	t	P-Value
Control vs. Fe	1.317	ns P>0.05
Control vs. Fe + AFB_1	5.256	*** P<0.001
Control vs. AFB_1	1.428	ns P>0.05
Fe vs. Fe + AFB_1	3.618	** P<0.01
Fe vs. AFB_1	0.111	ns P>0.05
Fe + AFB_1 vs. AFB_1	3.480	** P<0.01

6.0.3. Indicators of Lipid Peroxidation

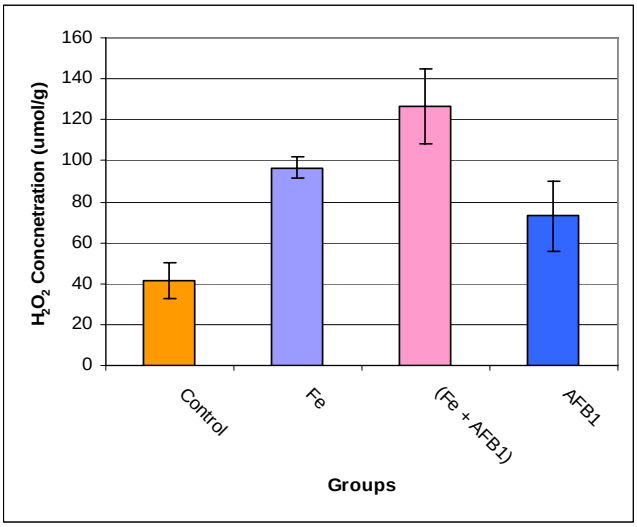

Figure 6.6. Bar Graph of Liver Lipid Peroxidation Levels of Wistar Albino Rats at 6 months

Table 6.6. Bonferroni (Dunn) and t-tests for Liver Liver Peroxidation at 6 months

Treatment Comparison	t	P-Value
Control vs. Fe	5.931	*** P<0.001
Control vs. Fe + AFB_1	10.747	*** P<0.001
Control vs. AFB_1	3.234	* P<0.05
Fe vs. Fe + AFB_1	4.055	** P<0.01
Fe vs. AFB_1	2.553	ns P>0.05
Fe + AFB_1 vs. AFB_1	6.786	*** P<0.001

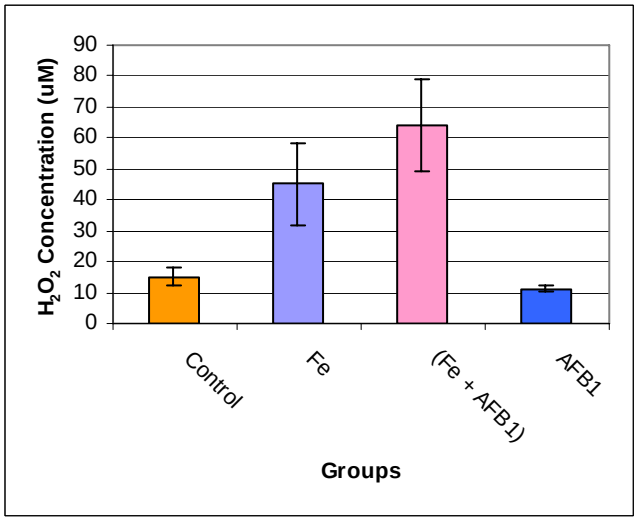

Figure 6.7. Bar Graph of Serum Lipid Peroxidation Levels of Wistar Albino Rats at 12 months

Table 6.7. Bonferroni (Dunn) and t-tests for Serum Lipid Peroxidation at 12 months

Treatment Comparison	t	P-Value
Control vs. Fe	3.816	** P<0.01
Control vs. Fe + AFB_1	7.868	*** P<0.001
Control vs. AFB_1	0.024	ns P>0.05
Fe vs. Fe + AFB_1	3.093	* P<0.05
Fe vs. AFB_1	3.623	** P<0.01
Fe + AFB_1 vs. AFB_1	7.225	*** P<0.001

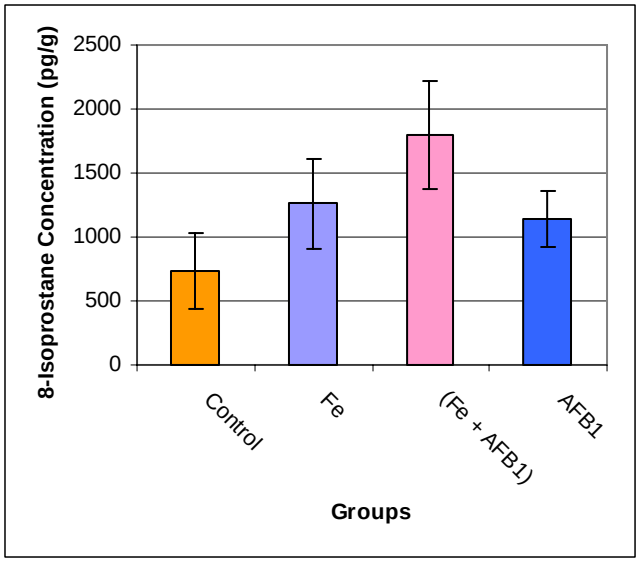

Figure 6.8. Bar Graph of Liver 8-Isoprostane Levels of Wistar Albino Rats at 12 months

Table 6.8. Bonferroni (Dunn) and t-tests for Liver 8-Isoprostane at 12 months

Treatment Comparison	t	P-Value
Control vs. Fe	2.202	ns P>0.05
Control vs. Fe + AFB_1	5.154	*** P<0.001
Control vs. AFB_1	2.560	ns P>0.05
Fe vs. Fe + AFB_1	2.713	ns P>0.05
Fe vs. AFB_1	0.471	ns P>0.05
Fe + AFB_1 vs. AFB_1	1.971	ns P>0.05

6.0.4 Indicators of DNA Changes

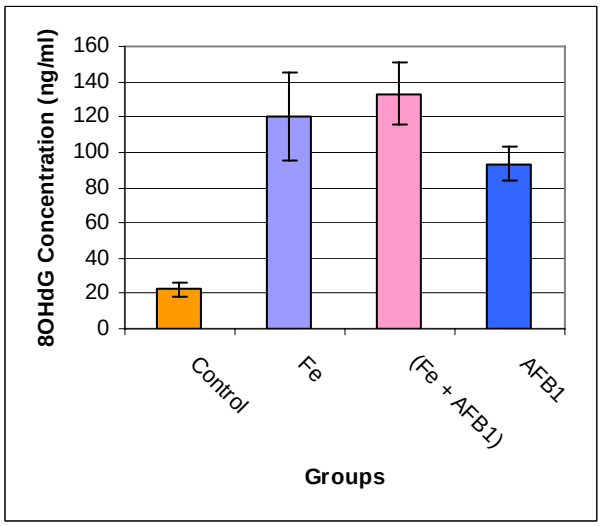

Figure 6.9. Bar Graph of Serum 8-Hydroxyguanosine Levels of Wistar Albino Rats at 6 months

Table 6.9. Bonferroni (Dunn) and t-tests for Serum 8OHdG at 6 months

Treatment Comparison	t	P-Value
Control vs. Fe	9.410	*** P<0.001
Control vs. Fe + AFB_1	13.160	*** P<0.001
Control vs. AFB_1	6.846	*** P<0.001
Fe vs. Fe + AFB_1	1.545	ns P>0.05
Fe vs. AFB_1	2.564	ns P>0.05
Fe + AFB_1 vs. AFB_1	4.709	*** P<0.001

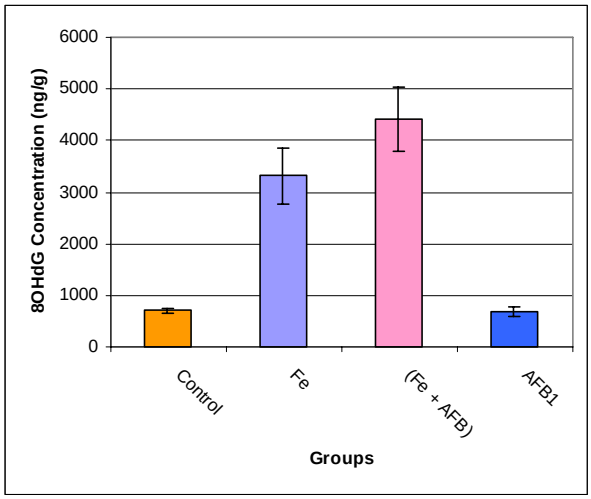

Figure 6.10. Bar Graph of Liver 8-Hydroxyguanosine Levels of Wistar Albino Rats at 6 months

Table 6.10. Bonferroni (Dunn) and t-tests for Liver 8OHdG at 6 months

Treatment Comparison	t	P-Value
Control vs. Fe	8.116	*** P<0.001
Control vs. Fe + AFB_1	14.294	*** P<0.001
Control vs. AFB_1	0.049	ns P>0.05
Fe vs. Fe + AFB_1	4.204	** P<0.01
Fe vs. AFB_1	8.166	*** P<0.001
Fe + AFB_1 vs. AFB_1	14.356	*** P<0.001

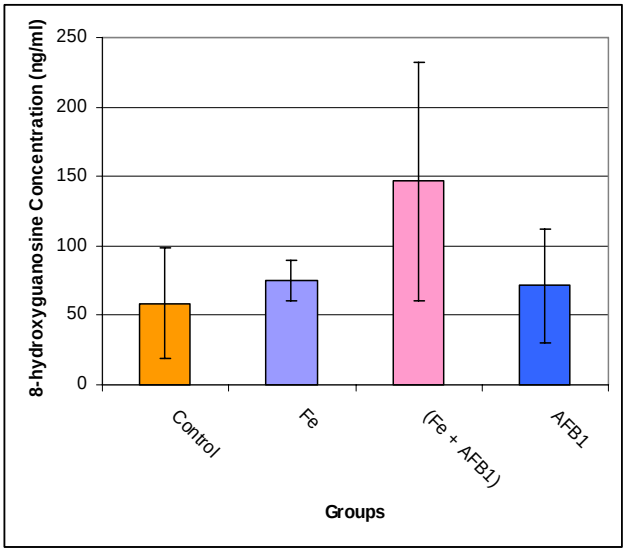

Figure 6.11. Bar Graph of Serum 8-hydroxyguanosine Levels of Wistar Albino Rats at 12 months

Table 6.11. Bonferroni (Dunn) and t-tests for Serum 8-Hydroxyguanosine at 12 months

Treatment Comparison	t	P-Value
Control vs. Fe	8.116	*** P<0.001
Control vs. Fe + AFB_1	14.294	*** P<0.001
Control vs. AFB_1	0.049	ns P>0.05
Fe vs. Fe + AFB_1	4.204	** P<0.01
Fe vs. AFB_1	8.166	*** P<0.001
Fe + AFB_1 vs. AFB_1	14.356	*** P<0.001

6.0.5. Indicators of Mutagenicity (Ames Test) *(These results represent fractions that were charged with the S9 mix)*

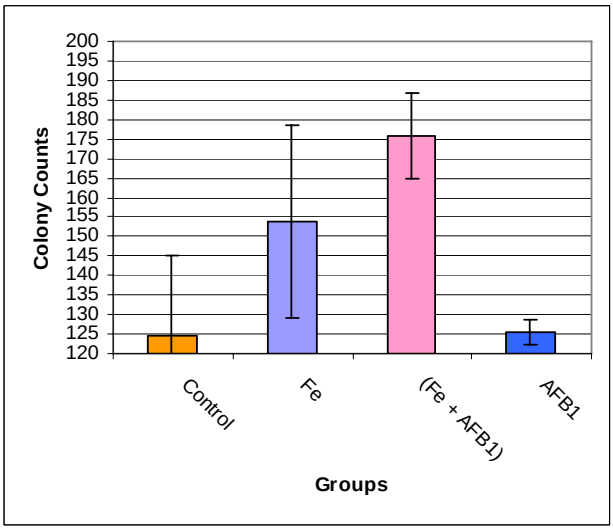

Figure. 6.12. Bar Graph Showing Spontaneous Revertant Colony Counts of TA100 from Whole Fraction of Wistar Albino Rat Liver Tissue at 12 months

Table 6.12. Bonferroni (Dunn) and t-tests for Salmonella typhimurium strain TA100 – Whole Fraction at 12 months

Treatment Comparison	t	P-Value
Control vs. Fe	2.700	ns P>0.05
Control vs. Fe + AFB_1	5.142	*** P<0.001
Control vs. AFB_1	0.152	ns P>0.05
Fe vs. Fe + AFB_1	2.184	ns P>0.05
Fe vs. AFB_1	2.422	ns P>0.05
Fe + AFB_1 vs. AFB_1	4.693	*** P<0.001

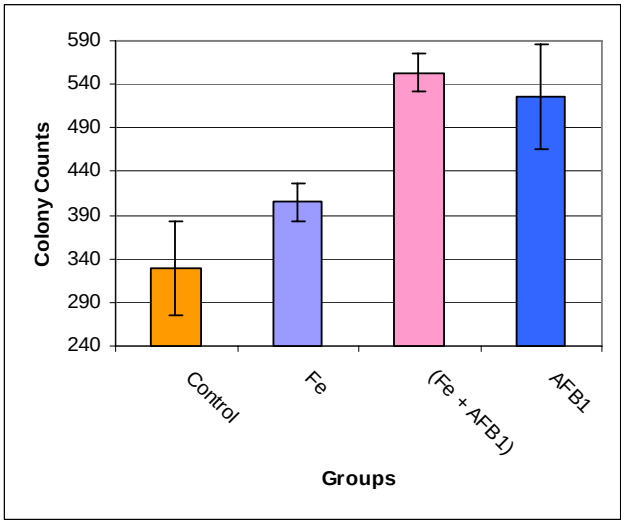

Figure. 6.13. Bar Graph Showing Spontaneous Revertant Colony Counts of TA102 from Nucleosomal Fraction of Wistar Albino Rat Liver Tissue at 12 months

Table 6.13. Bonferroni (Dunn) and t-tests for Salmonella typhimurium strain TA102 – Nucleosomal Fraction at 12 months

Treatment Comparison	t	P-Value
Control vs. Fe	2.165	ns P>0.05
Control vs. Fe + AFB_1	6.952	*** P<0.001
Control vs. AFB_1	5.135	*** P<0.001
Fe vs. Fe + AFB_1	4.581	*** P<0.001
Fe vs. AFB_1	3.071	* P<0.05
Fe + AFB_1 vs. AFB_1	0.995	ns P>0.05

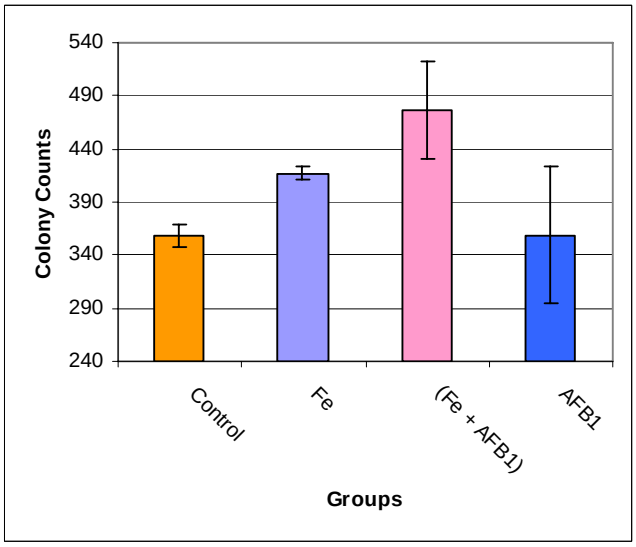

Figure. 6.14. Bar Graph Showing Spontaneous Revertant Colony Counts of TA102 from Cytosolic Fraction of Wistar Albino Rat Liver Tissue at 12 months

Table 6.14. Bonferroni (Dunn) and t-tests for Salmonella typhimurium strain TA102 – Cytosolic Fraction at 12 months

Treatment Comparison	t	P-Value
Control vs. Fe	2.165	ns P>0.05
Control vs. Fe + AFB_1	6.952	*** P<0.001
Control vs. AFB_1	5.135	*** P<0.001
Fe vs. Fe + AFB_1	4.581	*** P<0.001
Fe vs. AFB_1	3.071	* P<0.05
Fe + AFB_1 vs. AFB_1	0.995	ns P>0.05

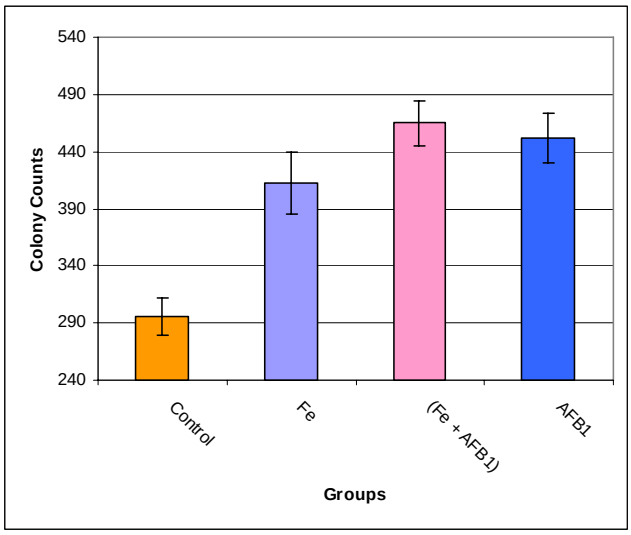

Figure. 6.15. Bar Graph Showing Spontaneous Revertant Colony Counts of TA102 from Microsomal Fraction of Wistar Albino Rat Liver Tissue at 12 months

Table 6.15. Bonferroni (Dunn) and t-tests for Salmonella typhimurium strain TA102 – Microsomal Fraction at 12 months

Treatment Comparison	t	P-Value
Control vs. Fe	5.883	*** P<0.001
Control vs. Fe + AFB_1	9.233	*** P<0.001
Control vs. AFB_1	0.424	ns P>0.05
Fe vs. Fe + AFB_1	2.788	ns P>0.05
Fe vs. AFB_1	5.185	*** P<0.001
Fe + AFB_1 vs. AFB_1	8.264	*** P<0.001

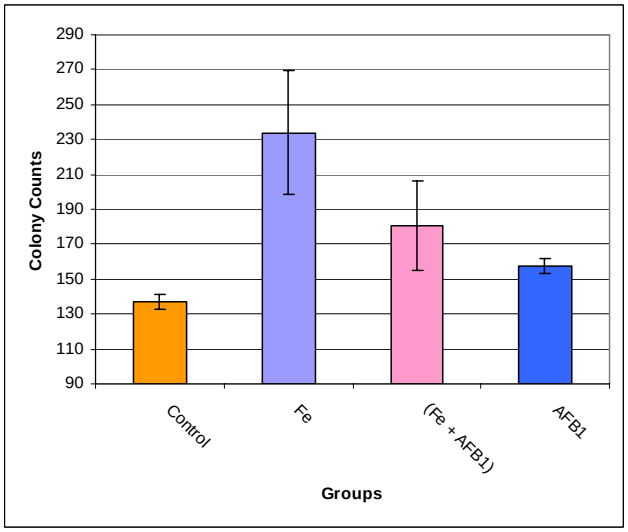

Figure. 6.16. Bar Graph Showing Spontaneous Revertant Colony Counts of TA97 from Whole Fraction of Wistar Albino Rat Liver Tissue at 12 months

Table 6.16. Bonferroni (Dunn) and t-tests for Salmonella typhimurium strain TA97 – Whole Homogenate at 12 months

Treatment Comparison	t	P-Value
Control vs. Fe	7.782	*** P<0.001
Control vs. Fe + AFB_1	4.511	** P<0.01
Control vs. AFB_1	1.637	ns P>0.05
Fe vs. Fe + AFB_1	4.013	** P<0.01
Fe vs. AFB_1	5.783	*** P<0.001
Fe + AFB_1 vs. AFB_1	2.486	ns P>0.05

6.0.6. Cytokine Indicators

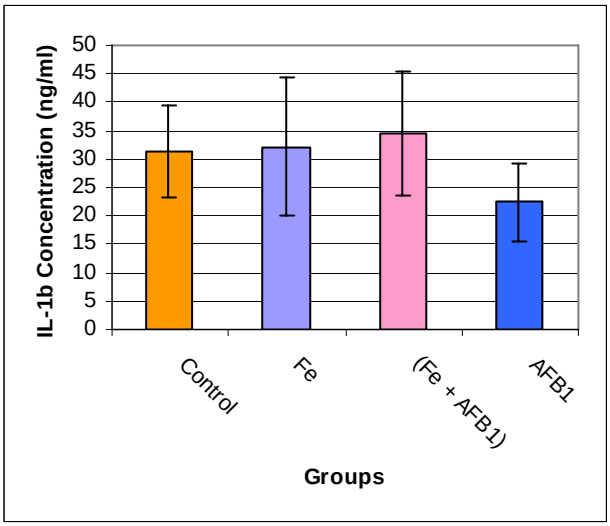

Figure. 6.17. Bar Graph of Interleukin-1β Levels of Wistar Albino Rats at 12 months

Table 6.17. Bonferroni (Dunn) and t-tests for Interleukin-1β at 12 months

Treatment Comparison	t	P-Value
Control vs. Fe	0.146	ns P>0.05
Control vs. Fe + AFB_1	0.609	ns P>0.05
Control vs. AFB_1	1.447	ns P>0.05
Fe vs. Fe + AFB_1	0.430	ns P>0.05
Fe vs. AFB_1	1.593	ns P>0.05
Fe + AFB_1 vs. AFB_1	2.381	ns P>0.05

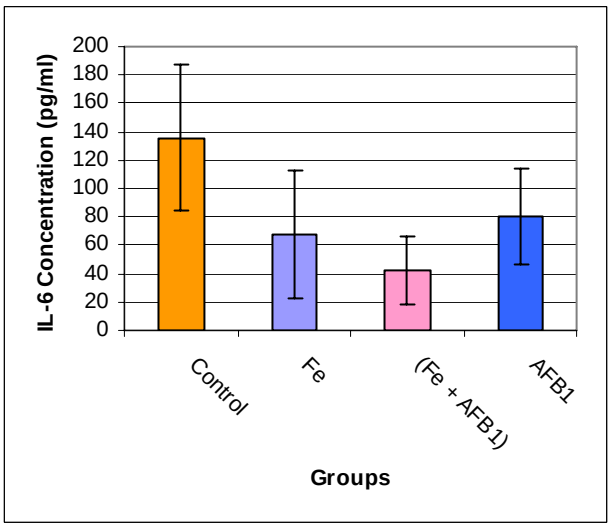

Figure. 6.18. Bar Graph of Interleukin-6 Levels of Wistar Albino Rats at 12 months

Table 6.18. Bonferroni (Dunn) and t-tests for Interleukin-6 at 12 months

Treatment Comparison	t	P-Value
Control vs. Fe	3.413	* P<0.05
Control vs. Fe + AFB_1	5.814	*** P<0.001
Control vs. AFB_1	2.802	ns P>0.05
Fe vs. Fe + AFB_1	1.571	ns P>0.05
Fe vs. AFB_1	0.610	ns P>0.05
Fe + AFB_1 vs. AFB_1	2.330	ns P>0.05

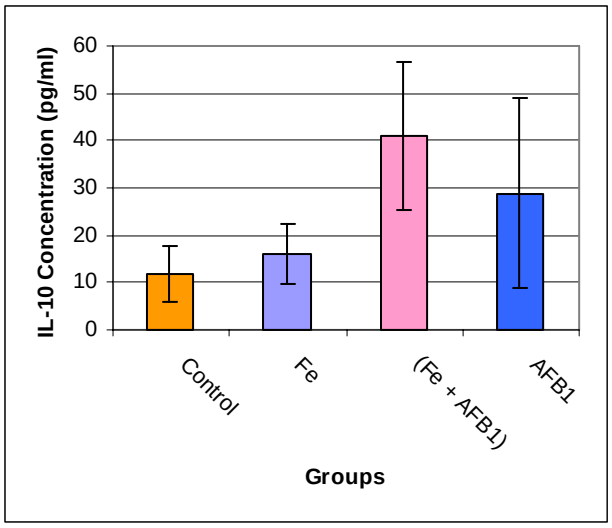

Figure. 6.19. Bar Graph of Interleukin-10 Levels of Wistar Albino Rats at 12 months

Table 6.19. Bonferroni (Dunn) and t-tests for Interleukin-10 at 12 months

Treatment Comparison	t	P-Value
Control vs. Fe	0.481	ns P>0.05
Control vs. Fe + AFB_1	4.126	** P<0.01
Control vs. AFB_1	1.943	ns P>0.05
Fe vs. Fe + AFB_1	3.532	** P<0.01
Fe vs. AFB_1	1.462	ns P>0.05
Fe + AFB_1 vs. AFB_1	1.728	ns P>0.05

6.1. Results of Assays Showing Synergy

6.1.1. Indicators of Iron Overload and Liver Disease

Figure 6.1 shows the serum iron levels of wistar albino rats at 12 months. The Fe fed groups showed to have the greatest serum iron levels, significantly higher than the control and AFB_1 groups. The relative serum iron concentrations (µmol/l) were: Control (59.7 ± 9.7); Fe (127.0 ± 28.0); Fe + AFB_1 (133.3 ± 44.1); AFB_1 (61.8 ± 17.1) (Appendix). The extent of synergy ratio was 1:0.7. Subsequent to a significant two-way ANOVA ($P<0.005$), a Tukey post-hoc test was used to determine significant time effects per group at an a priori p level of 0.05. Figure A3.1(i) (appendix) shows serum iron concentrations of wistar albino rats at the two time intervals. The Fe + AFB_1 is elevated significantly at 12 months.

Figure 6.2 shows the levels of serum ALT of wistar albino rats at 12 months. The iron fed groups had significantly elevated levels in comparison to the control group ($P<0.001$). The Fe +AFB_1 group levels was also significantly elevated in relation to

the Fe ($P<0.001$), and the AFB_1 groups ($P<0.001$). The Fe group levels were found to be elevated with respect to the AFB_1 group ($P<0.01$). The respective ALT concentrations (U/I) were: Control (107.5 ± 24.3); Fe (311.3 ± 44.2); Fe + AFB_1 (485.6 ± 87.2); AFB_1 (150.0 ± 35.4). The extent of synergy ratio was 1:1.05. The ALT levels of the Fe, Fe + AFB_1, and AFB_1 groups were all elevated at 12 months (Fig. A3.1(ii).) (Appendix).

Figure 6.3 shows the serum AST levels of wistar albino rats at 12 months. The iron fed groups showed AST levels greater than those of the control group and the AFB_1 group ($P<0.001$). The respective AST concentrations (U/I) were: Control (173.8 ± 35.6); Fe (391.8 ±16.5); Fe + AFB_1 (454.4 ± 75.2); AFB1 (241.4 ± 22.5). The extent of synergy ratio was 1:0.71. The AST levels of all four experimental groups were shown to be elevated at the 12 month time point (Fig. A3.1(iii)). (Appendix)

Figure 6.4 shows the serum GGT Levels of wistar albino rats at 6 months. The iron fed groups showed significantly higher GGT levels in comparison to the control group and the AFB_1 group ($P<0.001$) (Table 6.4). The relative GGT levels (U/I) were as follows: Control (3.1 ± 0.7); Fe (44.2 ± 14.6); Fe + AFB_1 (56.4 ± 18.7); AFB_1 (1.9 ± 0.8) (Appendix). The extent of synergy ratio was 1:1.22. No significant differences were found between the control and AFB_1 groups, or between the Fe and Fe + AFB_1 groups. The GGT concentration of the Fe + AFB_1 group was shown to be lowered at the 12 month time point in comparison to the 6 month levels (Fig. A3.1(iv).). (Appendix).

6.1.2. Reactive Oxygen Species and Reactive Nitrogen Species

Figure 6.5 shows the serum nitrite levels of wistar albino rats at 6 months. The Fe + AFB_1 groups showed to be significantly elevated in comparison with all three of the other groups. The p-values were as follows: Control vs.. Fe + AFB_1 ($P<0.001$); Fe vs. Fe + AFB_1 ($P<0.01$); AFB_1 vs. Fe + AFB_1 ($P<0.01$) (Table 6.7). The respective serum nitrite levels (μM/l) were as follows: Control (7.9 ± 1.1); Fe (17.3 ± 1.0); Fe + AFB_1 (18.8 ± 5.3); AFB_1 (11.6 ± 1.2). The extent of synergy ratio was 1:0.65.

6.1.3. Indicators of Lipid Peroxidation

Figure 6.6 shows the levels of liver lipid peroxidation of wistar albino rats at 6 months. All experimental groups were found to have higher LPO levels than the control group (Table 6.8). The Fe + AFB_1 was found to have the highest measure of LPO amongst groups (Table and figure 6.8.). The respective LPO concentrations (μmol/l) were as follows: Control (41.6 ± 8.8); Fe (96.6 ± 5.3); Fe + AFB_1 (126.6 ± 18.3); AFB_1 (72.9 ± 17.2). The extent of synergy ratio was 1:0.75. The control and Fe groups showed increased levels at the 12 month time point in comparison to the 6 month point (Fig A3.1(viii)) (Appendix).

Figure 6.7 shows the levels of serum LPO of wistar albino rats at 12 months. The iron fed groups showed the greatest elevations with respect to the control and AFB_1 groups. The Fe + AFB_1 group in particular had the highest levels (64.3 ± 14.8), and being significantly greater than the iron group ($P<0.05$). The respective serum LPO concentrations (μmol/l) of the groups were: Control (15.2 ± 2.6); Fe (45.0 ± 11.4); AFB_1 (15.0 ± 0.9). The extent of synergy ratio was 1:1.07. The Fe group showed a

decreased LPO concentration at the 12 month time point in comparison to the 6 month time point (Fig.A3.1(ix)) (Appendix).

Figure 6.8 shows the levels of 8-isoprostane in liver tissue of wistar albino rats at 12 months. The Fe + AFB_1 group is the only group showing significantly elevated levels in comparison to the control. The respective liver 8-isoprostane (pg/ml) levels were: Control (736 ± 208); Fe (1264 ± 272); Fe + AFB_1 (1773 ± 415); AFB_1 (1376 ± 554). The extent of synergy ratio was 1:0.67. Both the Fe-fed groups showed raised levels at the 12 month time point (Fig A3.1(vii)) (Appendix).

6.1.4. Indicators of DNA Changes

Figure 6.9 shows the levels of serum 8-hydroxyguanosine of wistar albino rats at 6 months. All experimental groups showed elevated levels in comparison to the control group ($P<0.001$). The Fe + AFB_1 group had levels significantly higher than the AFB_1 group ($P<0.001$). The respective serum 8-hydroxyguanosine concentrations (ng/ml) were as follows: Control (22.2 ± 4.1); Fe (120.2 ± 24.7); Fe + AFB_1 (133.3 ± 17.2); AFB_1 (93.5 ± 9.9). The extent of synergy ratio was 1:0.62.

Figure 6.10 show the levels of liver 8-hydroxyguanosine of wistar albino rats at 6 months. The iron fed groups show significant elevation in comparison to both control and AFB_1 groups ($P<0.001$). The Fe + AFB_1 group shows higher levels than those of the Fe group ($P<0.01$). The respective 8-hydroxyguanosine concentrations (ng/ml) in liver tissue were as follows: Control (702.4 ± 48.2); Fe (3323.6 ± 542.0); Fe + AFB_1 (4415.8 ± 617.0); AFB_1 (686.4 ± 80.4). The extent of synergy ratio was 1:1.1. The Fe-

fed groups showed increased levels at the 12 month time point (Fig. A3.1(x)). (Appendix)

Figure 6.11 shows the levels of serum 8-hydroxyguanosine of wistar albino rats at 12 months. The Fe-fed groups showed increased concentrations with respect to both the control and the AFB_1 groups ($P<0.001$). The Fe + AFB_1 group showed significantly greater concentrations than the Fe group ($P<0.01$). The respective 8-hydroxyguanosine levels (ng/ml) were: Control (58.8 ± 34.3); Fe (74.9 ± 12.6); Fe + AFB_1 (146.5 ± 85.4); AFB_1 (71.3 ± 41.2). The extent of synergy ratio was 1:1.

6.1.5. Indicators of Mutagenicity (Ames Test)

The preceding graphs show the results obtained from the Ames test after being challenged with the S9 enzymes. This challenge produced results showing a clearer differentiation between groups in terms of colony counts. Only the 12 month data showing synergy is shown, whilst the remaining data is discussed and respective graphs and statistical data are shown in the appendix.

Figure 6.12 shows the colony counts of spontaneous revertants of TA100 from the whole fraction of wistar albino rat liver homogenate at 12 months. The Fe + AFB_1 group showed to have increased counts in comparison to both the control and the AFB_1 group ($P<0.001$). The respective colony counts per group were: Control (125 ± 18); Fe (154 ± 22); Fe + AFB_1 (176 ± 21); AFB_1 (126 ± 3). The extent of synergy ratio was 1:0.63.

Figure 6.13 shows the colony counts of spontaneous revertants of TA102 from the nucleosomal fraction of wistar albino rat liver homogenate at 12 months. The AFB_1 fed groups showed elevated colony counts in comparison to both the control and Fe groups. The respective colony counts per group were: Control (329 ± 49); Fe (405 ± 20); Fe + AFB_1 (553 ± 83); AFB_1 (519 ± 58). The extent of synergy ratio was 1:0.6.

Figure 6.14 shows the colony counts of spontaneous revertants of TA102 from the cytosolic fraction of wistar albino rat liver homogenate at 12 months. The Fe + AFB_1 group is shown to be elevated in comparison to the control and AFB_1 groups ($P<0.001$). The respective colony counts per group were: Control (338 ± 9); Fe (417 ± 6); Fe + AFB_1 (485 ± 68); AFB_1 (345 ± 52). The extent of synergy ratio was 1:0.64.

Figure 6.15 shows the colony counts of spontaneous revertants of TA102 from the microsomal fraction of wistar albino rat liver homogenate at 12 months. The iron fed groups showed significantly elevated colony counts in comparison to both the control and AFB_1 groups ($P<0.001$). The respective colony counts per group were: Control (296 ± 170); Fe (412 ± 6); Fe + AFB_1 (463 ± 50); AFB_1 (305 ± 5). The extent of synergy ratio was 1:0.65.

Figure 6.16 shows the colony counts of spontaneous revertants of TA97 from the whole homogenate of wistar albino rat liver homogenate at 12 months. The iron fed groups showed to have elevated counts in comparison the control group. The Fe group had the highest counts in relation to all other groups, and in particular a higher count than that of the Fe + AFB_1 group ($P<0.01$). The respective colony counts per group were: Control (137 ± 4); Fe (234 ± 31); Fe + AFB_1 (188 ± 25); AFB_1 (158 ± 4). The extent of synergy ratio was 1:0.48.

6.1.6. Cytokine Indicators

Figure 6.17 shows the levels of interleukin-1β of wistar rats at 12 months. No significant differences were noted between experimental groups. The respective interleukin-1β (ng/ml) levels were: Control (31.3 ± 6.9); Fe (32.2 ± 10.4); Fe + AFB_1 (34.4 ± 10.9); AFB_1 (22.4 ± 6.9). The extent of synergy ratio was 1:0.63.

Figure 6.18 shows the levels of interleukin-6 of wistar rats at 12 months. Both the Fe ($P<0.05$) and the Fe + AFB_1 ($P<0.001$) groups have significantly lowered interleukin-6 concentrations with respect to the control group. The respective IL-6 concentrations (pg/ml) were: Control (135.6 ± 44.9); Fe (67.4 ± 39.2); Fe + AFB_1 (42.1 ± 24.0); AFB_1 (79.6 ± 33.8). The extent of synergy ratio was 1:0.3.

Figure 6.19 shows the levels of interleukin-10 of wistar rats at 12 months. The Fe + AFB_1 group is shown to have significantly elevated levels in comparison to both the control and Fe groups ($P<0.01$). The respective IL-10 concentrations (pg/ml) were: Control (12.0 ± 5.1); Fe (16.2 ± 5.4); Fe + AFB_1 (41.0 ± 15.7); AFB_1 (28.9 ± 17.3). The extent of synergy ratio was 1:0.91.

6.2. Correlations

6.2.1. Correlations at 6 months

Tables A4.1(i) to A4.1(iv) (Appendix) are the correlation matrices developed from the 6 month data. Highlighted data represents correlations significant at a 5% level. The matrix has been split into the four experimental groups for ease of reading. Table A4.1(i) shows the correlation matrix for 6 month data for the control group. ALT is significantly positively correlated with serum nitrite levels. Table A4.1(ii) shows the correlation matrix for the iron group. AST is positively correlated with serum nitrite

levels. ALT is negatively correlated to serum 8-Isoprostane and, liver nitrite levels are negatively correlated with superoxide production. Table A4.1(iii) shows the correlation matrix for the iron plus aflatoxin B_1 group. ALT show positive correlations with both hydroxyproline and liver 8-hydroxyguanosine levels. Serum nitrite levels show a positive correlation with liver lipid peroxidation. A4.1(iv) shows the correlation matrix for the aflatoxin B_1 group. ALT shows a positive correlation with GGT and liver lipid peoxidation, and a negative correlation with hydroxyproline and liver nitrite levels. GGT has a positive correlation with liver lipid peroxidation. Liver 8-hydroxyguanosine shows negative correlations with both serum lipid peroxidation and liver nitrite levels. Serum 8-isoprostane showed a negative correlation with hydroxyproline.

6.2.2. Correlations at 12 months.

Tables A4.1 (v) to A4.1 (viii) are the correlation matrices developed from the 12 month data. Highlighted data represents correlations significant at a 5% level. The matrix has been split into the four experimental groups for ease of reading. Table A4.1 (v) is a correlation matrix for the control group at 12 months. AST was found to be positively correlated to serum nitrite levels. ALT was positively correlated with liver 8-isoprostane and negatively with NTBI, RBC and MPV. MPV was also negatively correlated with liver nitrite levels. RBC was found to be positively correlated with MPV, and negatively correlated with WBC and TIBC. Hb was found to be positively correlated with both platelets and IL-1β.

Table A4.1 (vi) is a correlation matrix for the Fe group at 12 months. Serum 8-Isoprostane was shown to be prositively correlated with platelet counts, and NTBI. NTBI was also positively correlated with ferritin. ALT and AST were found to be

positively correlated with Hb and serum nitrite respectively. Liver lipid peroxidation was positively correlated with platelet counts and TIBC. Liver nitrite levels were positively correlated with serum 8-hydroxyguanosine levels and Hb, but negatively with MPV. In terms of the Ames test, the TA100 strain was found to be positively correlated with TA98.

Table A4.1 (vii) is a correlation matrix for the Fe + AFB_1 group at 12 months. The WB counts were shown to be positively correlated with serum 8-Isoprostane and ALT levels, but negatively so with serum 8-hydroxyguanosine. ALT was also shown to be positively correlated with liver 8-hydroxyguanosine levels. Serum 8-hydroxyguanosine was shown to be positively correlated with TIBC. Serum nitrite levels were shown to be positively correlated with serum lipid peroxidation levels and MPV and negatively with TA 102, whilst liver nitrite levels showed positive correlations with IL-10. The superoxide production was negatively correlated with IL-1β and MPV, but positively with TIBC and TA 102. TA 102 was also shown to be negatively correlated with TA98. RBC and Hb were shown to be positively correlated.

Table A4.1 (viii) is a correlation matrix for the AFB_1 group at 12 months. ALT was shown to be negatively correlated with WBC. AST showed a negative correlation with liver nitrite levels, but a positive correlation with serum lipid peroxidation levels. It followed that liver nitrite levels were negatively correlated with serum lipid peroxidation levels. Liver nitrite was also shown to be positively correlated with ferritin. Serum nitrite levels were shown to be negatively correlated with superoxide production and IL-10. GGT showed positive correlations with NTBI, IL-6 and IL-10.

RBc and Hb was also positively correlated. Within the Ames test, TA98 and TA100 were positively correlated.

6.3. Two-Way Analysis of Variance Results calculated between 6 and 12 month data.

The following assays were performed at both the 6 month and 12 month time points. Subsequent to a significant two-way ANOVA ($P<0.005$), a Tukey post-hoc test was used to determine significant time effects per group at an a priori p level of 0.05. The graphical representations are available in the appendix. Fig A3.1 (i) shows serum iron concentrations of wistar albino rats at the two time intervals. The Fe + AFB_1 is elevated significantly at 12 months. The ALT levels of the Fe, Fe + AFB_1, and AFB_1 groups were all elevated at 12 months (Fig. A3.1(ii)). The AST levels of all four experimental groups were shown to be elevated at the 12 month time point (Fig. A3.1(iii)). The GGT concentration of the Fe + AFB_1 group was shown to be lowered at the 12 month time point in comparison to the 6 month levels (Fig. A3.1(iv)). The superoxide production of the Fe + AFB_1 group was shown to be lowered at 12 months (Fig. A3.1(v)). The nitrite concentrations were elevated in all four experimental groups at 12 months (Fig. A3.1(vi)). The serum 8-isoprostane levels of both the control and AFB_1 groups were shown to be lowered at the 12 month time point (Fig. A3.1(vii)). The levels of liver lipid peroxidation were elevated in the control and Fe groups at 12 months (Fig. A3.1(viii)). The serum lipid peroxidation levels, were however only elevated in the Fe group at 12 months (Fig. A3.1(ix)). The liver 8-hydroxyguanosine concentrations of the Fe and Fe + AFB_1 groups were found to be significantly elevated at 12 months (Fig. A3.1(x)).

6.4. Results of Assays Not Showing Synergy

6.4.1. Indicators of Iron Overload and Liver Disease

(Figures and Statistical data for this section may be found in the Appendix).

6.4.1.1. Assays performed at 6 months

Figure A1.1(i) shows the serum iron levels of Wistar Albino Rats at 6 months. Experimental groups on the ferrocene diet showed significantly greater serum iron levels in comparison to the control group ($P<0.001$) (Table 6.1). The groups showed serum iron concentrations (μmol/l) as follows: Control (45.8 ± 9.3); Fe (95.2 ± 12.9); Fe + AFB_1 (87.8 ± 14.2); AFB_1 (37.6 ± 12.2) (Appendix). No differences were found between the AFB_1 and control group or the Fe and Fe + AFB_1 group.

Figure A1.1 (ii) shows the ALT levels of Wistar Albino rats at 6 months. The iron containing groups both showed higher ALT levels in comparison to the control group ($P<0.001$) and a lesser difference between themselves ($P<0.05$). The relative ALT levels (U/I) were as follows: Control (21.6 ± 6.5); Fe (91.8 ± 13.5); Fe + AFB_1 (72.3 ± 14.7); AFB_1 (26.3 ± 1.2). No significant differences were found between the AFB_1 and control group.

Figure A1.1 (iii) shows the AST levels of Wistar Albino Rats at 6 months. A high significant difference was found with the iron groups in comparison with the control and AFB_1 groups ($P<0.001$) (Table A1.1 (iii)). Significant differences were found between the control and Fe + AFB_1 groups as well as between Fe and Fe + AFB_1 ($P<0.05$). The relative AST levels (U/I) were as follows: Control (15.2 ± 2.5); Fe (30.0 ± 6.9); Fe + AFB_1 (22.7 ± 4.6); AFB_1 (16.1 ± 5.1) (Appendix). No significant differences were found between the control and Fe + AFB_1 groups and the AFB_1 and Fe + AFB_1 groups.

6.4.1.2. Assays performed at 12 months

Figure A2.1(ii) shows the ferritin levels of wistar albino rats at 12 months. The Fe + AFB_1 group showed to have decreased ferritin levels in comparison to the control and Fe groups ($P<0.05$). The respective Ferritin concentrations (ng/ml) were: Control (105.2 ± 23.5); Fe (107.5 ± 9.6); Fe + AFB_1 (79.4 ± 16.2); AFB_1 (80.9 ± 23.1) (Appendix).

Figure A2.1(iii) shows the TIBC of wistar albino rats at 12 months. No significant differences were found between experimental groups. The respective TIBC (μmol/l) for each group was: Control (67.5 ± 2.1); Fe (124.6 ± 13.9); Fe + AFB_1 (126.6 ± 108.6); AFB_1 (68.4 ± 18.9).

Figure A2.1(iv) shows the PSAT of wistar albino rats at 12 months. No significant differences were noted between experimental groups. The respective PSAT's (%) of groups was: Control (81.7 ± 26.8); Fe (96.5 ± 18.8); Fe + AFB_1 (97.9 ± 23.8); AFB_1 (78.2 ± 45.9).

Figure A2.1(v) show the levels of non-transferrin bound iron (NTBI) of wistar albino rats at 12 months. The iron fed groups showed significantly elevated NTBI level with respect to the control and AFB_1 groups ($P<0.001$). There were no differences between the iron fed groups themselves. The respective NTBI concentrations (μM) were: Control (6.6 ± 4.8); Fe (4.99 ± 9.13); Fe + AFB_1 (48.8 ± 17.71); AFB_1 (3.9 ± 4.55).

Figure A2.1(viii) shows GGT levels of wistar albino rats at 12 months. The iron fed groups showed significantly elevated GGT levels in relation to both the control and

AFB_1 groups. The respective group GGT levels were: Control (3.1 ± 0.6); Fe (27.4 ± 3.8); Fe + AFB_1 (22.5 ± 8.4); AFB1 (3.4 ± 1.0).

6.4.2. Reactive Oxygen Species and Reactive Nitrogen Species

6.4.2.1. Assays performed at 6 months

Figure A1.2(i) shows the superoxide anion levels of wistar albino rats at 6 months. No significant differences were found between any of the groups. The respective superoxide production (Max. O_2(mV/Neutr.)) values were as follows: Control (0.063 ± 0.022); Fe (0.051 ± 0.014); Fe + AFB_1 (0.058 ± 0.062); AFB_1 (0.101 ± 0.030).

Figure A1.2(ii) shows the liver nitrite levels of wistar albino rats at 6 months. No significant differences were found between the groups. The respective liver nitrite levels (μM) were as follows: Control (9.8 ± 1.7); Fe (10.7 ± 1.4); Fe + AFB_1 (12.8 ± 3.8); AFB_1 (14.2 ± 2.6).

6.4.2.2. Assays performed at 12 months

Figure A2.2(i) show the levels of superoxide production of wistar albino rats at 12 months. The AFB_1 group levels were significantly higher than those of the control, Fe and Fe + AFB_1 groups ($P<0.05$). The respective levels of superoxide production O_2 (mV)/Neutr.($x10^9$) were: Control (0.038 ± 0.038); Fe (0.028 ± 0.018); Fe + AFB_1 (0.061 ± .064); AFB_1 (0.168 ± 0.134).

Figure A2.2(ii) shows the nitrite levels in liver tissue of wistar albino rats at 12 months. No significant differences were found between experimental groups. The

respective liver nitrite levels (μM) were: Control (42.3 ± 3.8); Fe (42.8 ± 4.8); Fe + AFB_1 (43.8 ± 8.7); AFB_1 (39.8 ± 3.3).

Figure A2.2(iii) shows the serum nitrite levels of wistar albino rats at 12 months. The Fe group levels are shown to be elevated in comparison to the control ($P<0.01$) and AFB_1 ($P<0.05$) groups, but not in comparison to the Fe + AFB_1 group. The respective serum nitrite levels (μM) among groups was: Control (9.8 ± 2.0); Fe (21.0 ± 5.8); Fe + AFB_1 (15.2 ± 5.1); AFB_1 (11.3 ± 3.0).

6.4.3. Indicators of Lipid Peroxidation

6.4.3.1. Assays performed at 6 months

Figure A1.3(ii) shows the levels of serum lipid peroxidation in wistar albino rats at 6 months. The iron fed groups showed significantly elevated levels of H_2O_2 production in comparison to both the control group and the AFB_1 group ($P<0.001$) (Table 6.9). The respective LPO levels (μmol/l) among groups was as follows: Control (26.1 ± 6.6); Fe (69.9 ± 6.2); Fe + AFB_1 (60.8 ± 9.9); AFB_1 (33.1 ± 16.3).

Figure A1.3(iii) shows the levels of serum 8-isoprostane of wistar albino rats at 6 months. The iron fed groups showed to have higher serum 8-isoprostane levels than the control group. The Fe + AFB_1 groups showed to be most elevated against the control ($P<0.001$) and AFB_1 ($P<0.01$) groups respectively. The Fe group was elevated with respect to the control ($P<0.05$) and to the AFB_1 groups ($P<0.05$). The respective 8-Isoprostane concentrations (pg/ml) were as follows: Control (1969.8 ± 154.0); Fe (2259.7 ± 136.1); Fe + AFB_1 (2288.1 ± 150.4); AFB_1 (1985.0 ± 178.9). No

differences were noted between AFB_1 and the control groups, or the Fe and Fe + AFB_1 groups.

Figure A2.3(ii) shows the serum 8-isoprostane levels in wistar albino rats at 12 months. The iron fed groups showed significantly elevated levels in comparison to both the control group ($P<0.001$) and the AFB_1 group ($P<0.001$). The respective serum 8-isoprostane levels (pg/ml) were: Control (979 ± 253); Fe (2578 ± 333); Fe + AFB_1 (2444 ± 537); AFB_1 (1122 ± 193).

Figure A2.3(iii) shows the levels of liver lipid peroxidation of wisar albino rats at 12 months. The Fe + AFB_1 group showed the only significantly elevated levels in comparison to the control group ($P<0.01$). The respective lipid peroxidation levels (H_2O_2 μM/g) were: Control (332.8 ± 35.5); Fe (308.2 ± 12.6); Fe + AFB_1 (286.2 ± 21.60; AFB_1 (305.9 ± 16.8).

6.4.4. Indicators of DNA Changes

6.4.4.1. Assays performed at 12 months

Figure A2.4 (i) shows the levels of 8-hydroxyguanosine in liver tissue of wistar rats at 12 months. The iron fed groups showed significantly lowered liver 8-hydroxyguanosine levels in comparison to both the control and AFB_1 groups ($P<0.001$). The respective levels of 8-hydroxyguanosine (ng/ml) were: Control (1405 ± 79); Fe (5800 ± 941); Fe + AFB_1 (6635 ± 1366); AFB_1 (1815 ± 231).

6.4.5. Indicators of Mutagenicity (Ames Test)

6.4.5.1. Assays performed at 12 months

The following table shows all the colony counts obtained from using the four different S*almonella typhimirium* strains. The data showing significant differences has been depicted in the above figures and is included amongst the rest of the data below.

Table 6.4.5.1. Ames Mutagenicity Test

Salmonella typhimurium Strains									
		TA97		TA98		TA100		TA102	
Group	Liver Fraction	12 Months		12 Months		12 Months		12 Months	
		Mean	SD	Mean	SD	Mean	SD	Mean	SD
Control	(W)	137	4.5	39	2.1	125	20.5	295	15.0
	(N)	127	18.5	30	0.6	203	14.2	329	54.7
	(C)	116	21.9	22	5.2	190	22.5	358	10.6
	(S9)	80	18.9	29	4.4	124	15.0	331	52.3
	(M)	108	10.2	30	8.4	216	30.1	296	15.8
Fe	(W)	234	35.1	54	13.0	154	24.6	490	33.1
	(N)	286	40.3	29	11.8	204	27.2	405	22.3
	(C)	189	38.4	26	2.1	170	28.0	417	6.0
	(S9)	173	29.0	50	6.1	147	8.9	441	12.9
	(M)	152	20.2	29	6.7	182	22.6	412	26.9
Fe + AFB_1	(W)	181	25.8	39	7.8	176	11.1	399	16.4
	(N)	144	50.6	34	6.2	150	21.6	554	22.0
	(C)	123	25.9	21	5.0	180	6.6	476	46.5
	(S9)	185	17.1	51	9.9	153	18.5	502	24.7
	(M)	138	26.8	31	6.7	205	20.8	465	19.7
AFB_1	(W)	158	4.0	33	2.3	126	3.2	313	9.2
	(N)	131	8.7	27	3.8	183	18.1	525	60.2
	(C)	122	23.9	20	3.8	191	16.3	359	65.1
	(S9)	239	45.2	41	10.7	122	11.0	461	22.0
	(M)	131	34.7	33	8.0	198	47.9	452	21.8

Detailed results of the Ames mutagenicity test using *Salmonella typhimurium* strains TA97, TA98, TA100, and TA102. High-lighted areas indicate colony counts above 180, 50, 200 and 360 spontaneous revertants for TA97, TA98, TA100, and TA102 respectively. W = Whole liver homogenate; N = nucleosomal fraction; C = Cytosolic Fraction; S9 = Liver homogenate fraction at 9000rpm; M = Microsomal fraction.

6.4.6. Haematological Differentials

None of the haematological indices measures showed signs of synergy. The data acquired is however available in the appendix.

7.0. Discussion

The aim of this project was to ascertain the presence and the extent of synergy between the hepatocarcinogenicity of Fe overloading and aflatoxin B_1 exposure in an animal model. Through a series of investigations focusing on sequential steps associated with hepatocarcinogenesis, the synergistic relationship between these two toxins has been somewhat established.

The Fe profiling showed that Fe overload occurred within the Fe-fed groups. These groups showed raised serum Fe levels as well as a Fe content histology of 4+ at both the 6 and 12 month time points. In cases of Fe overloading, typical Fe profiling would involve increased serum Fe, ferritin, PSAT and NTBI along with a lowered TIBC (Sinniah, 1969; Walker et al., 1973; McNamara et al., 1999; Adams et al., 2000). The Fe profiling performed in the present study showed that Fe overloading did occur. The serum Fe and NTBI levels within the Fe-fed groups were raised, which is expected in cases of Fe overload (Fig. 6.1 & Fig A2.1(v)). Because ferrocene was used as the Fe delivery molecule, an atypical trend in TIBC and PSAT occurred. TIBC in the Fe-fed groups is expected to be lowered in Fe overloading, but is shown to be raised in this study (Fig.A2.1(iii)).The PSAT in the Fe-fed groups is uncharacteristically not greater, but statistically equal to that of the control group (Fig. A2.1(iv)). Ferrocene's mode of action in Fe overloading explains this atypical Fe profile. It has been shown that diets enriched with (3,5,5-trimethylhexanoyl)ferrocene (TMH-ferrocene) produce a severe experimental Fe overload in rats (Nielsen & Heinrich, 1993). After intestinal absorption, TMH-ferrocene Fe in the portal blood is transported to the liver independently from transferrin (Nielsen & Heinrich, 1993). It could be assumed that ferrocene itself, albeit not containing the same lipophilic character, would act in the same manner. As the ferrocene is delivered independently of transferrin, the TIBC would not be altered in any way. The Fe being introduced through the diet would not bind to

transferrin, and hence transferrin's Fe binding capacity would either remain normal or be slightly raised. PSAT is calculated by dividing the serum Fe by TIBC. Because the TIBC is raised, the PSAT is decreased. It is therefore evident that Fe overloading did occur in the present study in the subjects exposed to the Fe diet.

Liver disease indicators measured in this study include, ALT, AST and GGT. ALT is a more specific indicator if liver inflammation than AST. The level of ALT in blood is increased in conditions which hepatocytes are damaged and denatured. As cells are damaged, ALT leaks out into the bloodstream. At 6 months, the Fe-fed groups both showed higher ALT levels in comparison to the control group ($P<0.001$) and a lesser difference between themselves ($P<0.05$) (Fig. A1.1(ii)). At 12 months the same trend was noted, including a significant elevation of ALT in all groups over time, with the exception of the control group. Because both Fe and AFB_1 are known hepatotoxins, this was an expected outcome. The Fe + AFB_1 group showed significantly raised ALT levels in comparison to both the Fe and the AFB_1 groups. Although no difference is noted between the control and AFB_1 group, it is clear that the AFB_1 is increasing Fe's potential to raise ALT levels. This suggests that Fe may be the driving force in terms of liver damage, and AFB_1 a co-factor. The extent of synergy ratio was 1:1.05. This ratio was calculated using the following: Fe group + AFB_1 group : Fe + AFB_1 group. A ratio of 1:1 indicates an additive effect. At 12 months, an additive synergistic effect on ALT is noted in the Fe + AFB_1 group (485.6 ± 87.2 U/I) with reference to the Fe (311.3 ± 44.2 U/I) and AFB_1 (150.0 ± 35.4 U/I).

AST is less specific to liver disease than is ALT, since it is also produced in muscle tissue and can be raised in other conditions. In many liver inflammation cases however, ALT and AST activities are raised in a 1:1 ratio. At the 6 month time point, the Fe fed groups

showed increased AST levels in comparison to both the control and AFB_1 groups (Fig. A1.1(iii)). The Fe group had significantly higher AST than the Fe + AFB_1 group. At 12 months, however, the Fe + AFB_1 (454.4 ± 75.2 U/I) group showed the highest AST levels, although not significantly greater than the Fe group (391.8 ±16.5 U/I) (Fig.6.3.) Liver inflammation was occurring at this time point, as is collaborated by the ALT levels. AST showed signs of synergy, although not of an additive nature. The extent of synergy ratio was 1:0.71. The control group also showed an increase in AST over time, but not so with respect to ALT. AST has been shown to be elevated in the elderly (Inafuku & Nozaki, 2000), indicating that age may have been a contributing factor to the control group showing elevated AST levels, and hence a pre-existing baseline AST concentration. At 12 months, the rat model used would've surpassed adulthood.

While GGT is very useful in assisting in the diagnosis of liver disease, the enzyme is found in the cells lining secretory ducts. Therefore, it is raised in a number of inflammatory diseases and disorders including, pancreatitis, mononucleosis, hyperthyroidism and virtually any liver disease. At both the 6 month and 12 month time points, the Fe-fed groups showed raised GGT levels in comparison to both the control and AFB_1 groups. At the 6 month time point, the extent of synergy ratio was 1:1.22. An additive synergistic effective was therefore observed in terms of GGT activity. The graph showing GGT levels over the two time points show that GGT drops significantly amongst groups at the 12 month time point. GGT is considered a marker of acute liver damage, hence its levels are higher at 6 months than at 12 months. Because the development of liver inflammation in this study is of a chronic nature, GGT levels drop over time. At the 6 month time point GGT was shown to be positively correlated in the AFB_1 group with ALT, liver LPO, and liver 8OHdG levels at 6 months. GGT's positive correlation with ALT at 6 months and

lack thereof at 12 months, substantiates its use as a marker for acute liver inflammation. The positive correlations with liver LPO and 8OHdG are in accordance with their expected presence in liver damage.

In terms of cytokine indicators, this study showed that the joint administration of Fe and AFB_1 produced raised levels of the anti-inflammatory interleukin-10 (IL-10) and decreased levels of pro-inflammatory interleukin-6 (IL-6). The levels of pro-inflammatory interleukin-1β (IL-1β) were not affected by Fe, AFB_1 or their joint administration. In terms of IL-10, the extent of synergy ratio was 1:0.91, and hence a synergistic additive effect is noted. The Fe group produced a mean IL-10 concentration of 16.2pg/ml, the AFB_1 group 28.9pg/ml and the Fe + AFB_1 group, a concentration of 41pg/ml. Similar results were shown when the ingestion of AFB_1-contaminated feed in weaning piglets produced varying expressions of cytokine mRNA. (Marin *et al*., 2002). It was indicated that AFB_1 decreased the pro-inflammatory IL-1β and increased the anti-inflammatory IL-10. IL-10 is known to inhibit the synthesis of type 1 helper T cell (Th1)–derived cytokines, which includes IL-1β and IL-6 (Cortes & Kurzrock, 1997). The down-regulation of inflammatory cytokines such as IL-1β and IL-6 could be a consequence of the induction of IL-10. Hence an inverse relationship is noted between IL10 and IL-6. AFB_1 has been shown to markedly inhibit IL-6 production by lipopolysaccharide stimulated (LPS-stimulated) macrophages (Moon *et al.* 1999), which is in accordance with what was found in this study. IL-6 has been shown to decrease during dietary Fe overload (Olynyk & Clarke, 2001). It is evident that when jointly administered, Fe and AFB_1 would be expected to have a decreased IL-6, and since IL-6 and IL-10 have an inverse relationship, a raised IL-10. This is the observation made in the present study.

The present study did not, in contrast to Marin *et al.* (2002), find a significantly decreased IL-1β concentration in the AFB_1 group, although the tendency to be lower in the AFB_1 group in comparison to the other groups does exist. Although the incubation of AFB_1 reduced the amount of IL-1β mRNA in LPS-stimulated bovine monocytes, it was only observed at high concentrations of AFB_1 that non-specifically reduced steady-state transcription of actin mRNA (Kurtz & Czuprynski, 1992). The AFB_1 dosage used in the Kurtz & Czuprynski (1992) study was 10 μg/ml and it was perfomed *in vitro*. Therefore, the dosage cannot be directly equated to the *in vivo* nature of the current project. It is possible that a dosage of 250ug of AFB_1 over 10 days was not high enough to produce a significantly decreased IL-1β level.

It has been previously elucidated that both Fe overloading and AFB_1 ingestion causes a state of increased reactive oxygen and nitrogen species (Meneghini, 1997; Heinomen & Fisher, 1996). The link between oxidative stress and cancer has been well documented and is associated with the mutagenic potential of reactive forms of oxygen (Cerutti, 1994). The present study showed that serum nitrite levels at 6 months had an extent of synergy ratio of 1:0.65, not quite additive (Fig. 6.5). When administered individually, the serum nitrite concentrations of the Fe and the AFB_1 groups respectively were 11.3 and 11.6 μM/l, whilst the Fe + AFB_1 group had a level of 18.8 μM/l. . In terms of serum nitrite the Fe + AFB_1 group showed significantly elevated levels (Fig 6.5). This is accordingly reflected with the pattern noted with the lipid peroxidation graphs (Fig 6.6 & Fig 6.7). The serum nitrite pattern at 12 months is slightly different in that the Fe groups' levels are also elevated, but not significantly so with respect to the Fe + AFB_1 group. Although the AFB_1 group was not significantly increased, it suggests that AFB_1 is speeding up the potentially carcinogenic process in a time dependent process, in terms of Fe overloading. Nitric oxide

synthase 2 and hence nitric oxide is known to be increased in cases of HH (Marrogi *et al.*, 2001). AFB_1 ingestion in rats has been implicated with a slight reduction in nitric oxide concentration (Meki et al., 2001). The superoxide levels showed that the AFB_1 group had significantly raised levels (Fig. 2.2(i)). The superoxide graphs display the same pattern at the two time points, with the tendency being that the AFB_1 group had elevated levels, significantly so at the 12 month time point (Fig. 2.2(i)). A resultant synergistic effect is observed in the Fe + AFB_1 group in terms of serum nitrite, because the superoxide being produced by the AFB_1 is interacting with the nitric oxide produced from the Fe, and peroxynitrite is forming. The serum nitrite assay used is detecting the peroxynitrite. Peroxynitrite is a potent oxidant and cytotoxic ROS (Xia *et al*., 1996).

Lipid-containing structures, such as cell membranes and lipoproteins are well known targets of ROS, which can result in lipid peroxidation, a degenerative process that disturbs the structure or function of the target system. The induction of lipid peroxidation by AFB_1 and Fe overloading has been clearly elucidated by previous reports (Shen et al., 1994; Wu et al., 1990). It is noted that synergistic effects are seen initially in the liver at the 6-month time point (Fig. 6.6) and later in the serum (Fig 6.7) at the 12-month time point. This follows, considering that the tested substances are known hepatocarcinogens, that the liver would show the first signs of lipid peroxidation, and that the same trend would follow in the serum at a later stage. This explains what is seen in Fig A3.1 (viii). The drop in liver lipid peroxidation over time in the Fe group is not fully understood (Fig A3.1 (ix)), which is why the discussion was based on the serum results and not the liver homogenate.

At 12 months, the Fe group had a mean LPO concentration of 45 ± 11.4μM, the AFB_1 group 15 ± 0.9μM and the Fe + AFB_1 group 64.3 ± 14.8μM. An additive synergistic effect is observed, with an extent of synergy ratio of 1:1.07. An assay to detect 8-

Isoprostane was performed, and at 12 months, the liver 8-Isoprostane showed that the Fe + AFB_1 group had raised levels in comparison to the control group only. An extent of synergy ratio of 1:0.67 was observed, however no statistically significant differences were noted between groups. No synergy was observed. AFB_1 is unable to stimulate either arachidonic acid metabolism or initiate a respiratory burst of human leukocytes (Geissler & Henderson, 1988). In the event of free radical attack, arachidonic acid is oxidized to 8-isoprostane. It appears that this pathway is not involved in the genotoxic mechanisms of AFB_1, and therefore the driving force behind this assay's results is the presence of Fe and not AFB_1.

The presence of guanine analogue 8-hydroxyguanosine (8OHdG) has been found in both cases of Fe overloading and also in cases of AFB_1 exposure (Horvath *et al.,* 2001; Shen *et al.,* 1995). 8-OHdG is an abundant base modification in DNA whose levels increase with oxidative stress. The present study showed an interesting negative correlation between 8-isoprostane and 8OHdG. The metabolism of 8-isoprostane is liver dependent, and 8OHdG is a result of free radical attack which results in liver dysfunction. An increased 8OHdG would lead to liver dysfunction and would hence lead to impaired 8-isoprostane production. At 6 months, the 8OHdG levels produced within the groups showed that the Fe, AFB_1 and Fe + AFB_1 groups had raised levels (Fig. 6.9). An extent of synergy ratio of 1:0.62 was observed at this time point. 8OHdG measured from serum samples at 12 months (Fig. 6.10) showed an additive synergistic effect occurring, with an extent of synergy ratio of 1:1.1. It was observed in this study that the amount of 8OHdG present is increased between the two time points. An additive synergistic relationship therefore exists in terms of 8OHdG production, where the two compounds are producing these adducts at a

higher rate. This is consistent with the observation that oxidative stress is being boosted when these two carcinogens act together.

The Ames mutagenicity test is commonly used to determine whether a substance has mutagenic activity or not. A set of histidine-requiring strains is used for mutagenicity testing. Each tester strain is sensitive to different types of mutations. In this study, the following four tester strains were used, TA97, TA98, TA100 and TA102. TA97 is known to be sensitive to the same mutations which TA98 is sensitive to. In this study, TA97 failed to show any synergy, although the Fe group did produce high colony counts from this strain. Perhaps Fe's ability to induce free radical attacks caused TA97 nucleic acid mutations regardless of its specificity to other mutations. TA97 contains a 'hotspot' with alternating G-C base pairs. It is suggested that 8-OHdG adducts would form within this region when under free radical attack, hence triggering TA97 spontaneous revertants. The AFB_1 group and Fe + AFB_1 did not cause a significantly altered spontaneous reversion rate in this strain.

TA98 detects various frame-shift mutations, and TA100 detects mutagens that cause base-pair substitutions primarily at one of the G-C pairs. The TA98 and TA100 strains have the broadest specificity. Interestingly, this study shows a positive correlation between these two strains at the 12 month point. TA98 has previously been used to understand the mutagenicity of AFB_1, and its use lead to the elucidation that the key structure to AFB_1 mutagenicity is a bisfuran ring moiety (Wong et al., 1977). These strains are also known to be sensitive to polycyclic aromatic hydrocarbons (Perez et al., 2003), 40% of which makes up the ferrocene molecule. The assumption that TA98 would be sensitive to mutagenicty caused by both carcinogens would hence be substantiated. TA98 showed that the Fe-fed

groups had raised colony counts with respect to the control group, but no synergistic effect was noted, regardless of activation with S9 enzymes. This finding is not well understood. TA100 results show that when administered simultaneously, the Fe + AFB_1 group had elevated colony counts in comparison to the AFB_1 group (Fig. 6.12). In terms of AFB_1, it seems as though a slight synergistic effect is observed. An extent of synergy ratio of 1:0.63 was observed.

TA102 detects efficiently a variety of mutagens such as formaldehyde, hydroperoxides, bleomycin and is predominantly used to detect mutations generated through oxidative stress (Stayos *et al.*, 2004). Knowing that both Fe and AFB_1 are ROS/RNS inducers, it is understood why the results of TA102 colony counts show signs of synergy. The nuceleosomal (Fig.6.13), microsomal (Fig.14) and cytosolic (Fig.6.15) fractions particularly illustrate this point. The extent of synergy ratios for these fractions respectively was 1:0.6; 1:0.64; 1:0.65. When both carcinogens are administered, the result shows an increase in colony counts. This is expected because it is known that both carcinogens used are capable of eliciting ROS/RNS production. The results shown by testing with the TA102 strain are substantiated by the synergy shown by the serum nitrite, lipid peroxidation and 8OHdG assays. These measures are all increased in conjunction with an increased presence of ROS/RNS, and all show raised levels when both Fe and AFB_1 are administered. With respect to oxidative stress, it would seem that a collective additive synergistic relationship is observed between Fe and AFB_1.

8.0. Conclusion

Hepatocarcinogenesis is a disease of multifactorial etiology and involves a multistep process involving different genetic alterations that ultimately lead to malignant

transformation of hepatocytes. Oxidative stress is one of the major pathways involved in this transformation. Fe overload predominantly promotes hepatic carcinogenesis through DNA damage and lipid peroxidation attributed to oxidative stress. AFB_1 is renown for exerting it hepatotoxic effects through the formation of guanyl adducts, but more recently also for its ability to enhance ROS/RNS production. To obtain a carcinogenic level of oxidative stress requires a multistep process. The generation of ROS/RNS, ultimately leads to LPO, DNA destruction and consequent malignant transformation. Examples of these steps were analyzed in the present study, and an additive synergistic relationship has been shown in terms of ALT, GGT, IL-10, lipid hydroperoxides, 8OHdG formation and nitrite production. The Ames mutagenicity TA102 tester strain, sensitive to oxidative stress, showed synergy, although not of an additive nature. It may seem that the effect of AFB_1 is debatable, based on the fact that in some of the presented parameters, the AFB_1 group was not significantly different to the control group. It is important to note that in some of these parameters there was a significant difference between the Fe group and the Fe + AFB_1 group. The implication of which is that the presence of AFB_1 is increasing the activity of Fe as a carcinogen, thereby acting as a co-carcinogen. Examples of such parameters illustrating this are presented in the results section including serum ALT, serum nitrite, liver and serum lipid peroxidation, liver and serum 8-hydroxyguanosine, some of the mutagenicity assays, and interleukin-10. Further markers of oxidative stress and lipid peroxidation need to be utilized to substantiate these findings. The use of liver histology, in particular with reference to Fe-free foci development, gamma GT production, AFP presence and other signs of hepatocarcinogenesis and tumour formation are necessary to substantiate these findings further. The mechanisms behind this synergy need to be analyzed and elaborated upon in further studies.

Appendix A

A. Appendix to Results

A1. Analysis of Variance Results for 6 Month Data

A1.1. Indicators of Iron Overload and Liver Disease

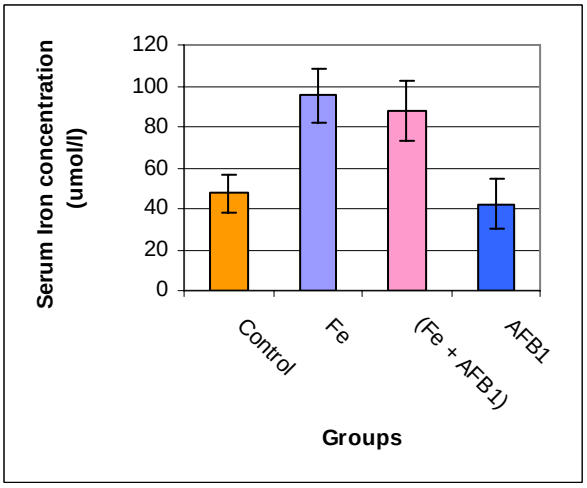

Table A1.1(i). Bonferroni Dunn and T-Tests for Serum Iron at 6 months

Treatment Comparison	t	P-Value
Control vs. Fe	2.043	ns P>0.05
Control vs. Fe + AFB_1	2.856	* P<0.05
Control vs. AFB_1	0.762	ns P>0.05
Fe vs. Fe + AFB_1	0.334	ns P>0.05
Fe vs. AFB_1	2.805	ns P>0.05
Fe + AFB_1 vs. AFB_1	3.797	** P<0.01

Figure A1.1(i). Bar Graph of Serum Iron Levels of Wistar Albino Rats at 6 months

A1.1i) ANOVA Data of Serum Iron at 6 months.

Group	Number of points	Mean	Standard Deviation	Standard Error of Mean	Median	Max	Min	95% Confidence Interval	
								From	To
Control	7	45.8	9.3	3.5	50.1	32.3	56.9	37.2	54.4
Fe	6	95.2	12.9	5.3	92.9	79.6	114.0	81.7	108.8
Fe + AFB_1	17	87.8	14.2	3.5	92.7	69.0	118.2	80.5	95.0
AFB_1	5	37.6	12.2	5.4	39.2	25.7	55.5	22.5	52.7

A1.1i) Intermediate Calculations. ANOVA Table (Serum Iron at 6 months)

Source of variation	Degrees of freedom	Sum of squares	Mean square
Treatments (between columns)	3	18129	6043.1
Residuals (within columns)	31	5192.1	167.49
Total	34	23321	

F = 36.081 =(MStreatment/MSresidual)

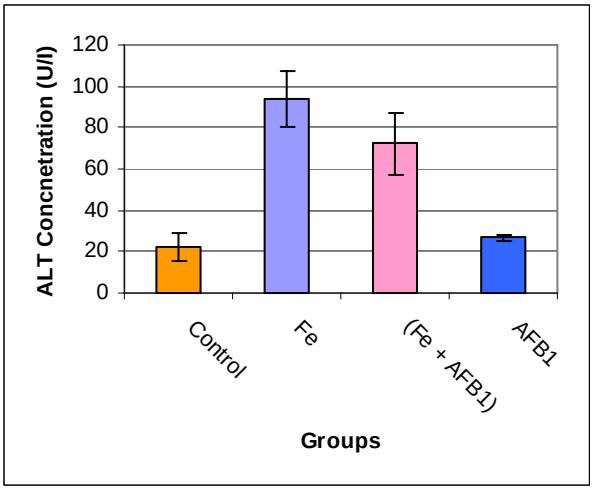

Table A1.1(ii). Bonferroni (Dunn) and t-tests for ALT at 6 months

Treatment Comparison	t	P-Value
Control vs. Fe	9.959	*** P<0.001
Control vs. Fe + AFB_1	8.602	*** P<0.001
Control vs. AFB_1	0.639	ns P>0.05
Fe vs. Fe + AFB_1	3.302	* P<0.05
Fe vs. AFB_1	8.856	*** P<0.001
Fe + AFB_1 vs. AFB_1	7.296	*** P<0.001

Figure A1.1ii). Bar Graph of ALT Levels of Wistar Albino Rats at 6 months

A1.1ii) ANOVA Data of ALT at 6 months.

Group	Number of points	Mean	Standard Deviation	Standard Error of Mean	Median	Max	Min	95% Confidence Interval	
								From	To
Control	6	21.6	6.5	2.6	20.0	16.0	34.1	14.8	28.4
Fe	6	91.8	13.5	5.5	88.1	81.0	114.8	77.6	106.0
Fe + AFB_1	15	72.3	14.7	3.8	75.2	45.0	92.7	64.2	80.5
AFB_1	5	26.3	1.2	0.5	26.6	25.2	27.9	24.9	27.8

A1.1. ii) Intermediate Calculations. ANOVA Table (ALT at 6 months)

Source of variation	Degrees of freedom	Sum of squares	Mean square
Treatments (between columns)	3	22816	7605.4
Residuals (within columns)	28	4168.0	148.86
Total	31	26984	

F = 51.092 =(MStreatment/MSresidual)

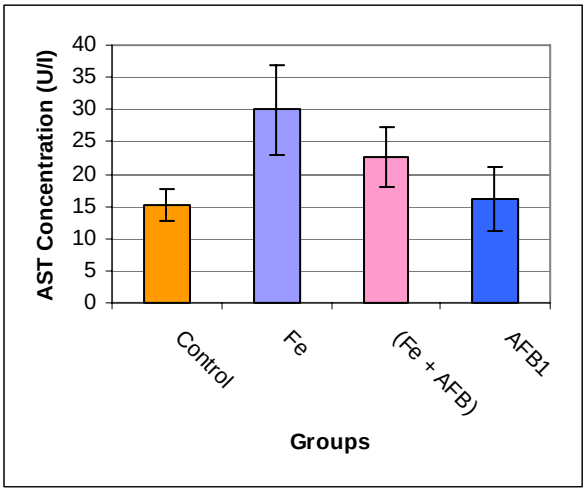

Figure A1.1(iii) Bar Graph of AST Levels of Wistar Albino Rats at 6 months

Table A1.1(iii). Bonferroni (Dunn) and t-tests for AST at 6 months

Treatment Comparison	t	P-Value
Control vs. Fe	4.915	*** P<0.001
Control vs. Fe + AFB_1	2.944	* P<0.05
Control vs. AFB_1	0.268	ns P>0.05
Fe vs. Fe + AFB_1	3.066	* P<0.05
Fe vs. AFB_1	4.635	*** P<0.001
Fe + AFB_1 vs. AFB_1	2.613	ns P>0.05

A1.1(iii) ANOVA Data of AST at 6 months.

Group	Number of points	Mean	Standard Deviation	Standard Error of Mean	Median	Max	Min	95% Confidence Interval	
								From	To
Control	5	15.2	2.5	1.1	14.6	12.3	18.5	12.2	18.3
Fe	6	30.0	6.9	2.8	28.8	20.6	41.1	22.7	37.3
Fe + AFB_1	16	22.7	4.6	1.2	23.2	15.1	30.5	20.3	25.2
AFB_1	5	16.1	5.1	2.3	15.7	8.6	22.2	9.8	22.4

A1.1(iii) Intermediate Calculations. ANOVA Table (AST at 6 months)

Source of variation	Degrees of freedom	Sum of squares	Mean square
Treatments (between columns)	3	793.72	264.57
Residuals (within columns)	28	687.15	24.541
Total	31	1480.9	

F = 10.781 =(MStreatment/MSresidual)

A1.1 (iv) ANOVA Data of GGT at 6 months. (Figure 6.4 in Results)

Group	Number of points	Mean	Standard Deviation	Standard Error of Mean	Median	Max	Min	95% Confidence Interval	
								From	To
Control	5	3.1	0.7	0.2	3.2	2.1	3.9	2.2	3.9
Fe	6	44.2	14.6	5.9	45.8	25.5	60.2	28.9	59.5
Fe + AFB_1	17	56.4	18.7	4.5	49.8	28.7	89.9	46.8	66.0
AFB_1	6	1.9	0.8	0.3	1.6	1.2	3.2	1.1	2.7

A1.1. (iv) Intermediate Calculations. ANOVA Table (GGT at 6 months)

Source of variation	Degrees of freedom	Sum of squares	Mean square
Treatments (between columns)	3	19857	6619.0
Residuals (within columns)	30	6671.6	222.39
Total	33	26529	

F = 29.764 =(MStreatment/MSresidual)

A1.2. Reactive Oxygen Species and Reactive Nitrogen Species

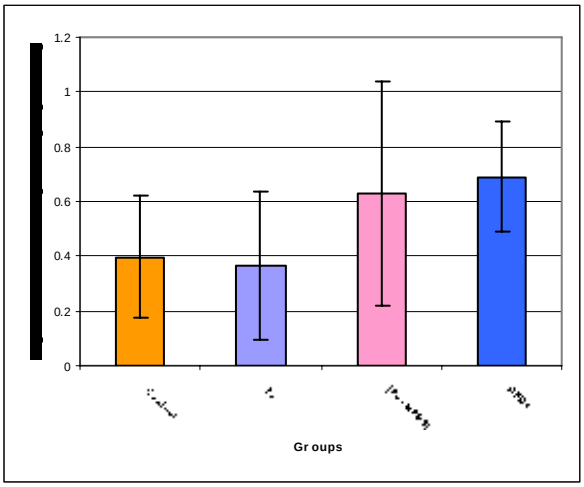

Figure A1.2(i). Bar Graph of Superoxide Anion Levels in Whole Blood of Wistar Albino Rats at 6 months

Table A1.2(i). Bonferroni (Dunn) and t-tests for Superoxide Anion in Whole Blood at 6 months

Treatment Comparison	t	P-Value
Control vs. Fe	0.397	ns P>0.05
Control vs. Fe + AFB_1	0.211	ns P>0.05
Control vs. AFB_1	1.226	ns P>0.05
Fe vs. Fe + AFB_1	0.282	ns P>0.05
Fe vs. AFB_1	1.623	ns P>0.05
Fe + AFB_1 vs. AFB_1	1.735	ns P>0.05

A1.2(i) ANOVA Data of Superoxide Anion in Whole Blood at 6 months.

Group	Number of points	Mean	Standard Deviation	Standard Error of Mean	Median	Max	Min	95% Confidence Interval	
								From	To
Control	5	0.063	0.022	0.010	0.066	0.031	0.085	0.036	0.090
Fe	5	0.051	0.014	0.006	0.051	0.032	0.068	0.033	0.068
Fe + AFB_1	17	0.058	0.062	0.015	0.043	0.011	0.285	0.026	0.090
AFB_1	5	0.101	0.030	0.013	0.101	0.062	0.132	0.064	0.138

A1.2 (i) Intermediate Calculations. ANOVA Table (Superoxide Anion in Whole Blood at 6 months)

Source of variation	Degrees of freedom	Sum of squares	Mean square
Treatments (between columns)	3	0.008460	0.002820
Residuals (within columns)	28	0.06772	0.002419
Total	31	0.07618	

F = 1.166 =(MStreatment/MSresidual)

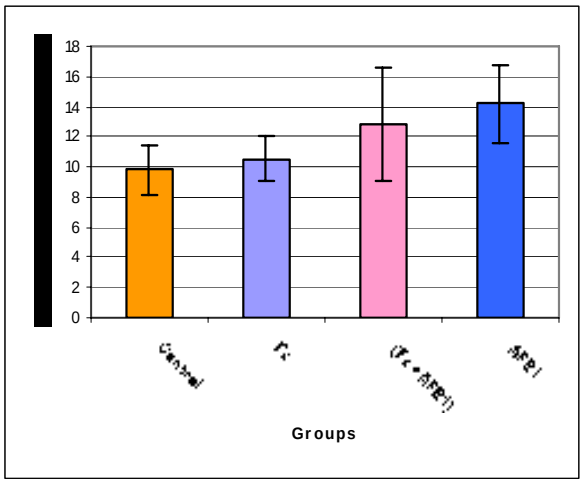

Figure A1.2 (ii). Bar Graph of Liver Nitrite Levels of Wistar Albino Rats at 6 months

Table A1.2(ii). Bonferroni (Dunn) and t-tests for Liver Nitrite Levels at 6 months

Treatment Comparison	t	P-Value
Control vs. Fe	0.476	ns P>0.05
Control vs. Fe + AFB_1	2.079	ns P>0.05
Control vs. AFB_1	2.337	ns P>0.05
Fe vs. Fe + AFB_1	1.374	ns P>0.05
Fe vs. AFB_1	1.782	ns P>0.05
Fe + AFB_1 vs. AFB_1	0.841	ns P>0.05

A1.2(ii) ANOVA Data of Liver Nitrite at 6 months.

Group	Number of points	Mean	Standard Deviation	Standard Error of Mean	Median	Max	Min	95% Confidence Interval	
								From	To
Control	6	9.8	1.7	0.69	9.5	7.6	12.0	8.0	11.6
Fe	5	10.7	1.4	0.62	11.1	8.5	12.3	8.9	12.4
Fe + AFB_1	17	12.8	3.8	0.92	11.4	7.9	22.5	10.9	14.8
AFB_1	5	14.2	2.6	1.18	13.3	11.7	17.7	10.9	17.4

A1.2(ii) Intermediate Calculations. ANOVA Table (Liver Nitrite at 6 months)

Source of variation	Degrees of freedom	Sum of squares	Mean square
Treatments (between columns)	3	72.964	24.321
Residuals (within columns)	29	278.45	9.602
Total	32	351.42	

F = 2.533 =(MStreatment/MSresidual)

A1.2(iii) ANOVA Data of Serum Nitrite at 6 months (Figure 6.5 in Results).

Group	Number of points	Mean	Standard Deviation	Standard Error of Mean	Median	Max	Min	95% Confidence Interval	
								From	To
Control	5	7.9	1.1	0.5	8.6	6.3	8.9	6.5	9.3
Fe	5	11.3	1.0	0.5	11.9	9.7	12.2	10.0	12.6
Fe + AFB_1	17	18.8	5.3	1.3	18.0	10.6	30.9	16.1	21.5
AFB_1	5	11.6	1.2	0.5	11.1	10.6	13.5	10.2	13.0

A1.2(iii) Intermediate Calculations. ANOVA Table (Serum Nitrite at 6 months)

Source of variation	Degrees of freedom	Sum of squares	Mean square
Treatments (between columns)	3	620.28	206.76
Residuals (within columns)	28	463.08	16.538
Total	31	1083.4	

F = 12.502 =(MStreatment/MSresidual)

A.1.3. Indicators of Lipid Peroxidation

A1.3(i) ANOVA Data of Liver Lipid Peroxidation at 6 months (Figure 6.6 in Results).

Group	Number of points	Mean	Standard Deviation	Standard Error of Mean	Median	Max	Min	95% Confidence Interval	
								From	To
Control	5	41.6	8.8	3.9	46.2	31.1	50.1	30.7	52.5
Fe	6	96.6	5.3	2.1	98.6	86.9	100.4	91.1	102.1
Fe + AFB_1	15	126.6	18.3	4.7	119.9	108.6	180.6	116.4	136.7
AFB_1	5	72.9	17.2	7.7	77.1	44.1	89.1	51.6	94.3

A1.3(i) Intermediate Calculations. ANOVA Table (Liver Lipid Peroxidation at 6 months)

Source of variation	Degrees of freedom	Sum of squares	Mean square
Treatments (between columns)	3	31304	10435
Residuals (within columns)	27	6329.5	234.43
Total	30	37634	

F = 44.512 =(MStreatment/MSresidual)

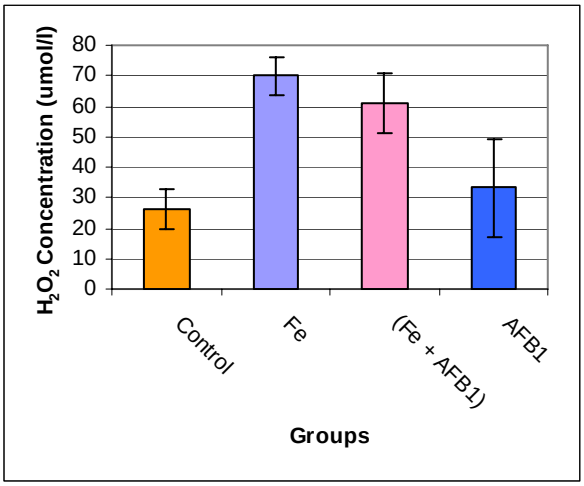

Figure A1.3(ii). Bar Graph of Serum Lipid Peroxidation Levels of Wistar Albino Rats at 6 months

Table A1.3(ii). Bonferroni (Dunn) and t-tests Serum Lipid Peroxidation Levels at 6 months

Treatment Comparison	t	P-Value
Control vs. Fe	6.725	*** P<0.001
Control vs. Fe + AFB_1	6.512	*** P<0.001
Control vs. AFB_1	1.071	ns P>0.05
Fe vs. Fe + AFB_1	1.724	ns P>0.05
Fe vs. AFB_1	5.654	*** P<0.001
Fe + AFB_1 vs. AFB_1	5.200	*** P<0.001

A1.3(ii) ANOVA Data of Serum Lipid Peroxidation at 6 months.

Group	Number of points	Mean	Standard Deviation	Standard Error of Mean	Median	Max	Min	95% Confidence Interval	
								From	To
Control	5	26.1	6.6	3.0	22.9	27.7	37.6	17.9	34.4
Fe	5	69.9	6.2	2.8	68.5	63.8	80.2	62.3	77.6
Fe + AFB_1	15	60.8	9.9	2.6	58.5	50.8	88.2	55.3	66.3
AFB_1	5	33.1	16.3	7.3	28.8	18.5	61.1	12.9	53.3

A1.3(ii) Intermediate Calculations. ANOVA Table (Liver Lipid Peroxidation at 6 months)

Source of variation	Degrees of freedom	Sum of squares	Mean square
Treatments (between columns)	3	7892.6	2630.9
Residuals (within columns)	26	2758.3	106.09
Total	29	10651	

F = 24.799 =(MStreatment/MSresidual)

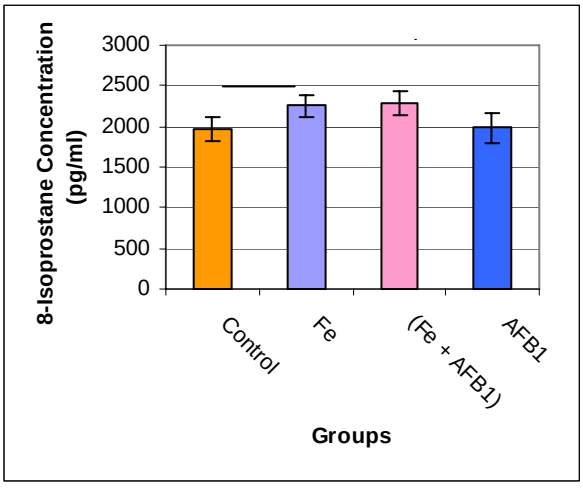

Figure A1.3(iii) Bar Graph of Serum 8-Isoprostane Levels of Wistar Albino Rats at 6 months

Table A1.3(iii). Bonferroni (Dunn) and t-tests of Serum 8-Isoprostane Levels at 6 months

Treatment Comparison	t	P-Value
Control vs. Fe	3.283	* P<0.05
Control vs. Fe + AFB_1	4.383	*** P<0.001
Control vs. AFB_1	0.164	ns P>0.05
Fe vs. Fe + AFB_1	0.392	ns P>0.05
Fe vs. AFB_1	2.966	* P<0.05
Fe + AFB_1 vs. AFB_1	3.897	** P<0.01

A1.3(iii) ANOVA Data of Serum 8-Isoprostane at 6 months.

Group	Number of points	Mean	Standard Deviation	Standard Error of Mean	Median	Max	Min	95% Confidence Interval	
								From	To
Control	6	1969.8	154.0	62.9	1977.5	1738	2213	1808	2131
Fe	6	2259.7	136.1	55.6	2300.0	2005	2377	2116	2402
Fe + AFB_1	17	2288.1	150.4	36.5	2300.0	2061	2552	2210	2365
AFB_1	5	1985.0	178.9	80.0	1898.0	1816	2262	1762	2207

A1.3(iii) Intermediate Calculations. ANOVA Table (Serum 8-Isoprostane at 6 months)

Source of variation	Degrees of freedom	Sum of squares	Mean square
Treatments (between columns)	3	691758	230586
Residuals (within columns)	30	701432	23381
Total	33	1393190	

F = 9.862 =(MStreatment/MSresidual)

A1.4. Indicators of Collagen Expression

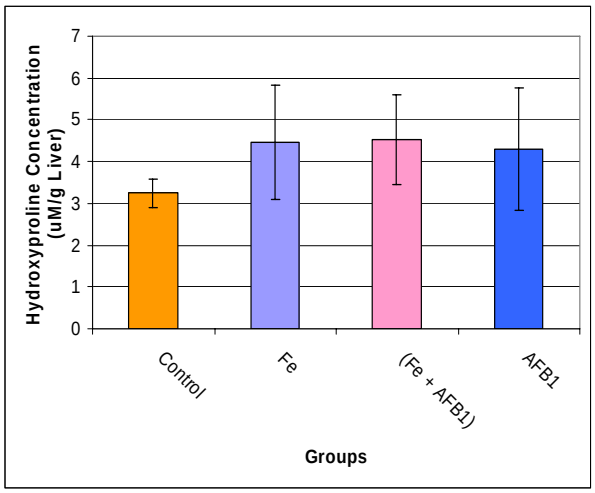

Figure A1.4(i) Bar Graph of Liver Hydroxyproline Levels of Wistar Albino Rats at 6 months

Table A1.4(i). Bonferroni (Dunn) and t-tests of Liver Hydroxyproline Levels at 6 months

Treatment Comparison	t	P-Value
Control vs. Fe	1.684	ns P>0.05
Control vs. Fe + AFB_1	2.177	ns P>0.05
Control vs. AFB_1	1.492	ns P>0.05
Fe vs. Fe + AFB_1	0.114	ns P>0.05
Fe vs. AFB_1	0.192	ns P>0.05
Fe + AFB_1 vs. AFB_1	0.349	ns P>0.05

A1.4(i) ANOVA Data of Hydroxyproline at 6 months.

Group	Number of points	Mean	Standard Deviation	Standard Error of Mean	Median	Max	Min	95% Confidence Interval	
								From	To
Control	5	3.3	0.3	0.2	3.4	2.73	3.60	2.83	3.68
Fe	5	4.5	1.4	0.6	4.1	2.74	6.16	2.75	6.15
Fe + AFB_1	15	4.5	1.1	0.3	4.8	2.74	6.32	3.92	5.11
AFB_1	5	4.3	1.5	0.7	5.1	2.40	5.48	2.49	6.13

A4.1(i) Intermediate Calculations. ANOVA Table (Hydroxyproline at 6 months)

Source of variation	Degrees of freedom	Sum of squares	Mean square
Treatments (between columns)	3	6.235	2.078
Residuals (within columns)	26	32.756	1.260
Total	29	38.991	

F = 1.650 =(MStreatment/MSresidual)

A1.5. Indicators of DNA Changes

A1.5(i) ANOVA Data of Liver 8-OHdG at 6 months (Figure 6.10 in Results).

Group	Number of points	Mean	Standard Deviation	Standard Error of Mean	Median	Max	Min	95% Confidence Interval	
								From	To
Control	5	702.4	48.2	21.6	709.0	641	750	643	762
Fe	5	3323.6	542.0	242.4	3190.0	2575	3874	2651	3997
Fe + AFB_1	17	4415.8	617.0	149.6	4293.0	3433	5951	4099	4733
AFB_1	5	686.4	80.2	35.9	713.0	558	750	587	786

A1.5 (i) Intermediate Calculations. ANOVA Table (Liver 8-OHdG at 6 months)

Source of variation	Degrees of freedom	Sum of squares	Mean square
Treatments (between columns)	3	8.754E+07	2.918E+07
Residuals (within columns)	28	7300724	260740
Total	31	9.484E+07	

F = 111.92 =(MStreatment/MSresidual)

A1.5(ii) ANOVA Data of Serum 8-OHdG at 6 months (Figure 6.9 in Results).

Group	Number of points	Mean	Standard Deviation	Standard Error of Mean	Median	Max	Min	95% Confidence Interval	
								From	To
Control	5	22.2	4.1	1.8	20.0	18.1	26.6	17.1	27.3
Fe	5	120.2	24.7	11.1	118.8	95.6	150.7	89.5	151.0
Fe + AFB_1	16	133.3	17.2	4.3	141.9	90.5	150.7	124.1	142.4
AFB_1	5	93.5	9.9	4.4	90.1	81.2	104.0	81.2	105.8

A1.5(ii) Intermediate Calculations. ANOVA Table (Serum 8-OHdG at 6 months)

Source of variation	Degrees of freedom	Sum of squares	Mean square
Treatments (between columns)	3	48809	16270
Residuals (within columns)	27	7330.8	271.51
Total	30	56140	

F = 59.923 =(MStreatment/MSresidual)

A2. Analysis of Variance Results for 12 Month Data

A2.1(i) ANOVA Data of Serum Iron at 12 months (Figure 6.1 in Results).

Group	Number of points	Mean	Standard Deviation	Standard Error of Mean	Median	Max	Min	95% Confidence Interval	
								From	To
Control	5	59.7	9.7	4.4	62.0	45.8	70.0	47.9	72.1
Fe	5	127.0	28.0	12.5	118.7	98.8	173.7	92.2	161.8
Fe + AFB_1	16	133.3	44.1	11.0	129.0	86.7	263.0	109.8	156.7
AFB_1	5	61.8	17.1	7.7	57.2	41.1	3.4	40.6	83.1

A2.1(i) Intermediate Calculations. ANOVA Table (Serum Iron at 12 months)

Source of variation	Degrees of freedom	Sum of squares	Mean square
Treatments (between columns)	3	34176	11392
Residuals (within columns)	27	33866	1254.3
Total	30	68041	

F = 9.082 =(MStreatment/MSresidual)

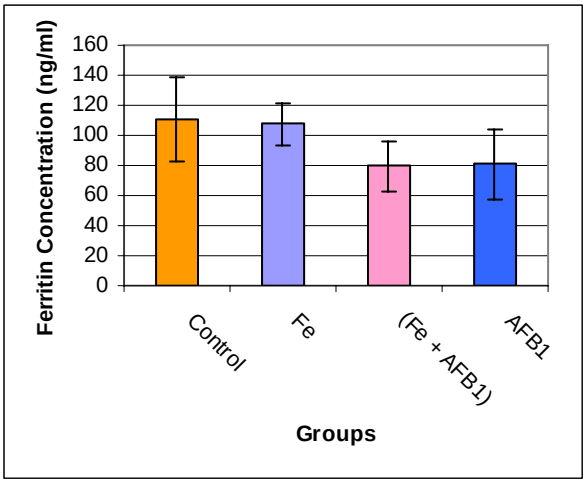

Figure A2.1(ii). Bar Graph of Ferritin Levels of Wistar Albino Rats at 12 months

Table A2.1(ii). Bonferroni (Dunn) and t-tests of Liver Ferritin Levels at 6 months

Treatment Comparison	t	P-Value
Control vs. Fe	0.205	ns P>0.05
Control vs. Fe + AFB_1	2.878	* P<0.05
Control vs. AFB_1	2.169	ns P>0.05
Fe vs. Fe + AFB_1	3.135	* P<0.05
Fe vs. AFB_1	2.374	ns P>0.05
Fe + AFB_1 vs. AFB_1	0.165	ns P>0.05

A2.1(ii) ANOVA Data of Ferritin at 12 months.

Group	Number of points	Mean	Standard Deviation	Standard Error of Mean	Median	Max	Min	95% Confidence Interval	
								From	To
Control	5	105.2	23.5	10.5	111.0	64.3	123.9	76.1	134.4
Fe	5	107.5	9.6	4.3	108.0	92.0	117.4	95.6	119.5
Fe + AFB_1	18	79.4	16.2	3.8	80.1	37.7	101.4	71.3	87.4
AFB_1	5	80.9	23.1	10.3	84.7	54.3	112.0	52.2	109.5

A2.1(ii) Intermediate Calculations. ANOVA Table (Ferritin at 12 months)

Source of variation	Degrees of freedom	Sum of squares	Mean square
Treatments (between columns)	3	4983.2	1661.1
Residuals (within columns)	29	9154.0	315.65
Total	32	14137	

F = 5.262 =(MStreatment/MSresidual)

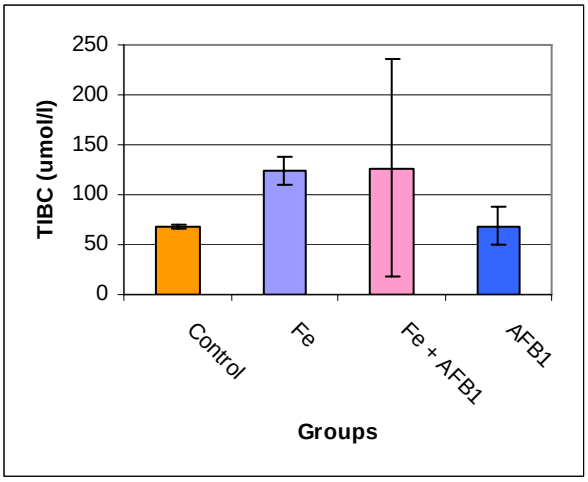

Figure A2.1(iii) Bar Graph of Total Iron Binding Capacity (TIBC) of Wistar Albino Rats at 12 months

Table A2.1(iii). Bonferroni (Dunn) and t-tests of Total Iron Binding Capacity (TIBC)at 6 months

Treatment Comparison	t	P-Value
Control vs. Fe	0.205	ns P>0.05
Control vs. Fe + AFB_1	2.878	* P<0.05
Control vs. AFB_1	2.169	ns P>0.05
Fe vs. Fe + AFB_1	3.135	* P<0.05
Fe vs. AFB_1	2.374	ns P>0.05
Fe + AFB_1 vs. AFB_1	0.165	ns P>0.05

A2.1(iii) ANOVA Data of Total Iron Binding Capacity (TIBC) at 12 months.

Group	Number of points	Mean	Standard Deviation	Standard Error of Mean	Median	Max	Min	95% Confidence Interval	
								From	To
Control	5	67.5	2.13	0.96	67.5	64.2	70.1	64.87	70.18
Fe	5	124.6	13.92	6.23	124.6	105.3	143.7	107.30	141.86
Fe + AFB_1	12	126.6	108.64	31.36	98.9	65.9	466.6	57.56	195.62
AFB_1	5	68.4	18.91	8.46	64.2	47.1	98.0	44.95	91.89

A2.1(iii) Intermediate Calculations. ANOVA Table (Total Iron Binding Capacity (TIBC) at 12 months)

Source of variation	Degrees of freedom	Sum of squares	Mean square
Treatments (between columns)	3	21219	7073.0
Residuals (within columns)	23	132058	5741.6
Total	26	153277	

F = 1.232 =(MStreatment/MSresidual)

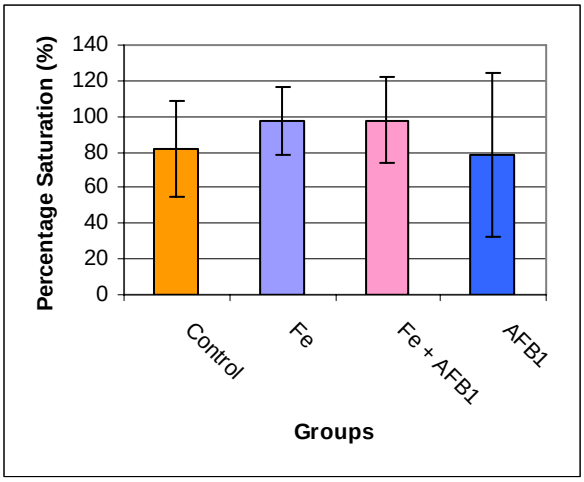

Figure A2.1(iv) Bar Graph of Percentage Saturation of Iron (PSAT) of Wistar Albino Rats at 12 months

Table A2.1(iv). Bonferroni (Dunn) and t-tests for Percentage Saturation of Iron (PSAT) at 12 months

Treatment Comparison	t	P-Value
Control vs. Fe	0.205	ns P>0.05
Control vs. Fe + AFB_1	2.878	* P<0.05
Control vs. AFB_1	2.169	ns P>0.05
Fe vs. Fe + AFB_1	3.135	* P<0.05
Fe vs. AFB_1	2.374	ns P>0.05
Fe + AFB_1 vs. AFB_1	0.165	ns P>0.05

A2.1(iv) ANOVA Data of Percentage Saturation of Iron (PSAT)at 12 months.

Group	Number of points	Mean	Standard Deviation	Standard Error of Mean	Median	Max	Min	95% Confidence Interval	
								From	To
Control	5	81.7	26.8	12.0	91.4	36.4	105.6	48.4	114.9
Fe	5	96.5	18.8	8.4	98.1	68.2	120.9	73.2	119.8
Fe + AFB_1	12	97.9	23.8	6.9	107.3	56.4	132.4	82.8	113.0
AFB_1	5	78.2	45.9	20.5	62.3	35.0	130.1	21.3	135.1

A2.1(iv) Intermediate Calculations. ANOVA Table (Percentage Saturation of Iron (PSAT) at 12 months)

Source of variation	Degrees of freedom	Sum of squares	Mean square
Treatments (between columns)	3	1979.3	659.75
Residuals (within columns)	23	18909	822.14
Total	26	20888	

F = 0.8025 =(MStreatment/MSresidual)

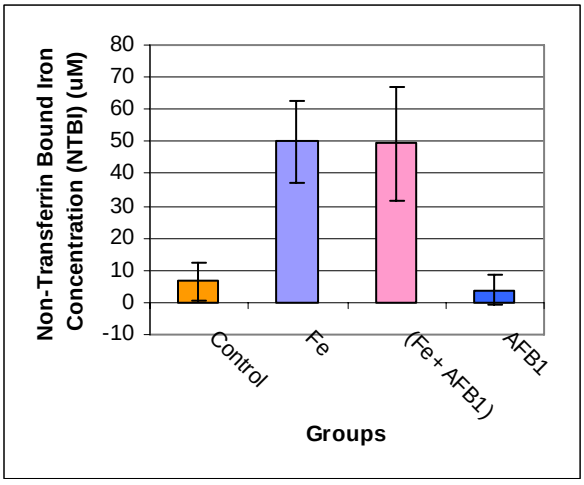

Figure A2.1(v) Bar Graph of Non-Transferrin Bound Iron (NTBI) of Wistar Albino Rats at 12 months

Table A2.1(v). Bonferroni (Dunn) and t-tests for Non-Transferrin Bound Iron (NTBI) at 12 months

Treatment Comparison	t	P-Value
Control vs. Fe	6.992	*** P<0.001
Control vs. Fe + AFB_1	8.416	*** P<0.001
Control vs. AFB_1	0.426	ns P>0.05
Fe vs. Fe + AFB_1	0.216	ns P>0.05
Fe vs. AFB_1	7.418	*** P<0.001
Fe + AFB_1 vs. AFB_1	8.941	*** P<0.001

A2.1(v) ANOVA Data of Non-Transferrin Bound Iron (NTBI)at 12 months.

Group	Number of points	Mean	Standard Deviation	Standard Error of Mean	Median	Max	Min	95% Confidence Interval	
								From	To
Control	5	6.6	4.18	1.87	6.4	0.90	12.70	1.37	11.75
Fe	5	49.9	9.13	4.09	50.0	36.10	1.70	38.58	61.26
Fe + AFB_1	16	48.8	17.71	4.43	45.6	23.40	7.50	39.40	58.27
AFB_1	5	3.9	4.55	2.03	0.7	0.40	9.10	-1.73	9.57

A2.1(v) Intermediate Calculations. ANOVA Table (NTBI at 12 months)

Source of variation	Degrees of freedom	Sum of squares	Mean square
Treatments (between columns)	3	13051	4350.2
Residuals (within columns)	27	5191.5	192.28
Total	30	18242	

F = 22.624 =(MStreatment/MSresidual)

A2.1(vi) ANOVA Data of ALT at 12 months.

Group	Number of points	Mean	Standard Deviation	Standard Error of Mean	Median	Max	Min	95% Confidence Interval	
								From	To
Control	6	107.5	24.3	9.9	103.5	81.0	150.0	82.0	133.0
Fe	5	311.3	44.2	19.8	311.3	256.0	375.0	256.4	366.1
Fe + AFB_1	9	485.6	87.2	29.1	452.0	370.3	608.0	418.6	552.6
AFB_1	5	150.0	35.4	15.8	170.0	93.0	177.0	106.1	193.9

A2.1(vi) Intermediate Calculations. ANOVA Table (ALT at 12 months)

Source of variation	Degrees of freedom	Sum of squares	Mean square
Treatments (between columns)	3	644187	214729
Residuals (within columns)	21	76563	3645.9
Total	24	720751	

F = 58.897 =(MStreatment/MSresidual)

A2.1(vii) ANOVA Data of AST at 12 months.

Group	Number of points	Mean	Standard Deviation	Standard Error of Mean	Median	Max	Min	95% Confidence Interval	
								From	To
Control	6	173.8	35.6	14.6	160.0	144.0	33.0	136.4	211.2
Fe	5	391.8	16.5	7.4	391.8	367.0	411.0	371.3	412.2
Fe + AFB_1	9	454.4	75.2	25.1	455.0	342.3	14.0	396.6	512.2
AFB_1	5	241.4	22.5	10.1	232.0	222.0	279.8	213.5	269.4

A2.1(vii) Intermediate Calculations. ANOVA Table (AST at 12 months)

Source of variation	Degrees of freedom	Sum of squares	Mean square
Treatments (between columns)	3	343798	114599
Residuals (within columns)	21	54682	2603.9
Total	24	398480	

F = 44.010 =(MStreatment/MSresidual)

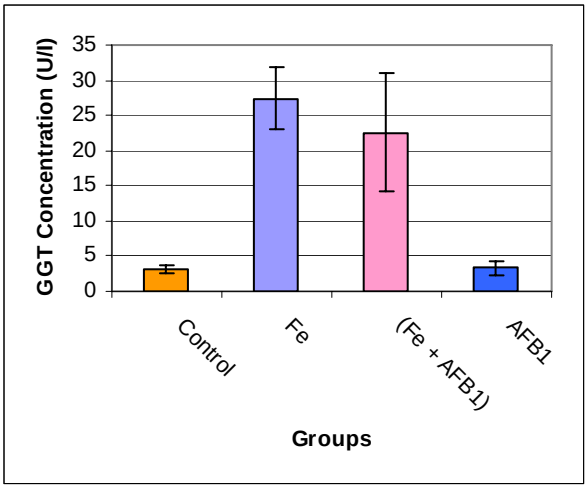

Figure A2.1(viii) Bar Graph of GGT Levels of Wistar Albino Rats at 12 months

Table A2.1(viii) Bonferroni (Dunn) and t-tests for GGT at 12 months

Treatment Comparison	t	P-Value
Control vs. Fe	5.920	*** P<0.001
Control vs. Fe + AFB_1	5.888	*** P<0.001
Control vs. AFB_1	0.065	ns P>0.05
Fe vs. Fe + AFB_1	1.471	ns P>0.05
Fe vs. AFB_1	5.855	*** P<0.001
Fe + AFB_1 vs. AFB_1	5.807	*** P<0.001

A2.1(viii) ANOVA Data of GGT at 12 months.

Group	Number of points	Mean	Standard Deviation	Standard Error of Mean	Median	Max	Min	95% Confidence Interval	
								From	To
Control	5	3.1	0.6	0.3	3.5	2.49	3.64	2.40	3.81
Fe	5	27.4	3.8	1.7	27.4	22.04	32.68	22.67	32.10
Fe + AFB_1	17	22.5	8.4	2.0	23.0	7.28	39.87	18.24	26.82
AFB_1	5	3.4	1.0	0.4	3.1	2.49	4.98	2.17	4.57

A2.1(viii) Intermediate Calculations. ANOVA Table (GGT at 12 months)

Source of variation	Degrees of freedom	Sum of squares	Mean square
Treatments (between columns)	3	2951.2	983.75
Residuals (within columns)	28	1177.6	42.056
Total	31	4128.8	

F = 23.391 =(MStreatment/MSresidual)

A2.2. Reactive Oxygen Species and Reactive Nitrogen Species

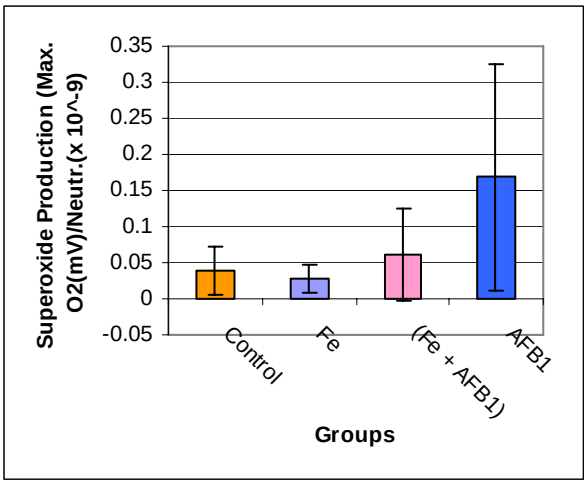

Figure A2.2(i). Bar Graph of Superoxide Production Levels of Wistar Albino Rats at 12 months

Table A2.2(i) Bonferroni (Dunn) and t-tests for Superoxide Anion at 12 months

Treatment Comparison	t	P-Value
Control vs. Fe	0.220	ns P>0.05
Control vs. Fe + AFB_1	0.619	ns P>0.05
Control vs. AFB_1	2.865	* P<0.05
Fe vs. Fe + AFB_1	0.893	ns P>0.05
Fe vs. AFB_1	3.085	* P<0.05
Fe + AFB_1 vs. AFB_1	2.943	* P<0.05

A2.2(i) ANOVA Data of Superoxide Production at 12 months.

Group	Number of points	Mean	Standard Deviation	Standard Error of Mean	Median	Max	Min	95% Confidence Interval	
								From	To
Control	5	0.038	0.038	0.017	0.03	0.00	0.10	-0.009	0.085
Fe	5	0.028	0.018	0.008	0.03	0.00	0.05	0.006	0.050
Fe + AFB_1	17	0.061	0.064	0.016	0.04	0.00	0.23	0.028	0.093
AFB_1	5	0.168	0.134	0.060	0.17	0.02	0.35	0.002	0.334

A2.2(i) Intermediate Calculations. ANOVA Table (Superoxide Production at 12 months)

Source of variation	Degrees of freedom	Sum of squares	Mean square
Treatments (between columns)	3	0.06342	0.02114
Residuals (within columns)	28	0.1441	0.005148
Total	31	0.2076	

F = 4.106 =(MStreatment/MSresidual)

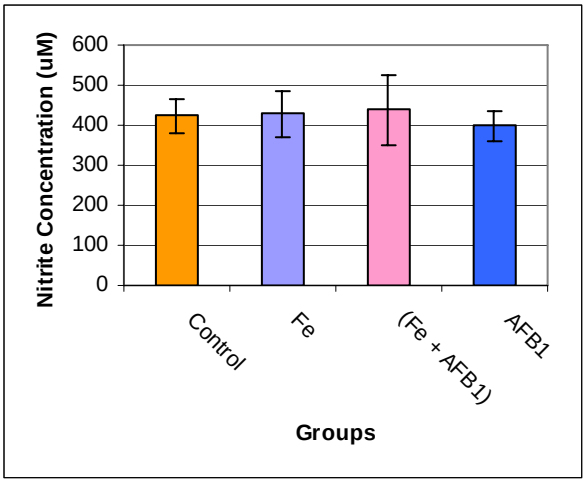

Figure A2.2(ii). Bar Graph of Liver Nitrite Levels of Wistar Albino Rats at 12 months

Table A2.2(ii). Bonferroni (Dunn) and t-tests for Liver Nitrite Concentration at 12 months

Treatment Comparison	t	P-Value
Control vs. Fe	0.098	ns P>0.05
Control vs. Fe + AFB_1	0.422	ns P>0.05
Control vs. AFB_1	0.551	ns P>0.05
Fe vs. Fe + AFB_1	0.299	ns P>0.05
Fe vs. AFB_1	0.649	ns P>0.05
Fe + AFB_1 vs. AFB_1	1.111	ns P>0.05

A2.2(ii) ANOVA Data of Liver Nitrite Levels at 12 months.

Group	Number of points	Mean	Standard Deviation	Standard Error of Mean	Median	Max	Min	95% Confidence Interval	
								From	To
Control	5	42.3	3.8	1.60	42.32	38.0	46.8	37.9	46.8
Fe	5	42.8	4.8	2.13	44.88	34.5	45.9	36.8	48.7
Fe + AFB_1	18	43.8	8.7	2.05	41.08	36.8	73.0	39.5	48.2
AFB_1	5	39.8	3.3	1.47	39.84	36.6	43.5	35.8	44.0

A.2.2(ii) Intermediate Calculations. ANOVA Table (Liver Nitrite Levels at 12 months)

Source of variation	Degrees of freedom	Sum of squares	Mean square
Treatments (between columns)	3	64.087	21.362
Residuals (within columns)	29	1464.9	50.513
Total	32	1529.0	

F = 0.4229 =(MStreatment/MSresidual)

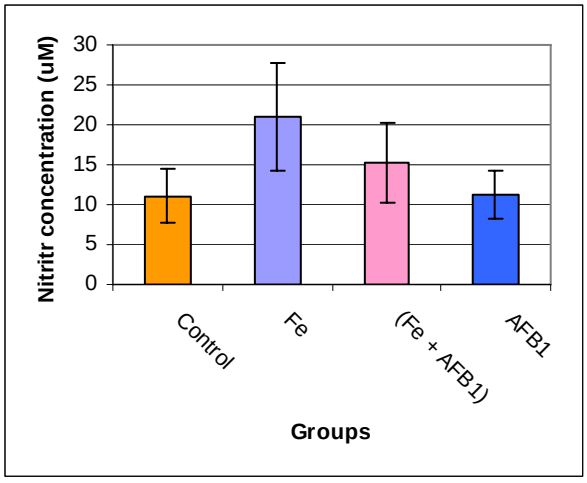

Figure A2.2(iii) Bar Graph of Serum Nitrite Levels of Wistar Albino Rats at 12 months

Table A2.2(iii). Bonferroni (Dunn) and t-tests for Serum Nitrite Concentration at 12 months

Treatment Comparison	t	P-Value
Control vs. Fe	3.548	** P<0.01
Control vs. Fe + AFB_1	2.092	ns P>0.05
Control vs. AFB_1	0.479	ns P>0.05
Fe vs. Fe + AFB_1	2.420	ns P>0.05
Fe vs. AFB_1	3.255	* P<0.05
Fe + AFB_1 vs. AFB_1	1.652	ns P>0.05

A2.2(iii) ANOVA Data of Serum Nitrite Levels at 12 months.

Group	Number of points	Mean	Standard Deviation	Standard Error of Mean	Median	Max	Min	95% Confidence Interval	
								From	To
Control	4	9.8	2.0	1.0	9.8	8.0	11.6	6.6	13.0
Fe	5	21.0	5.8	2.6	18.7	15.9	31.0	13.8	28.3
Fe + AFB_1	18	15.2	5.1	1.2	12.4	9.8	24.3	12.7	17.8
AFB_1	5	11.3	3.0	1.4	10.4	9.1	16.6	7.6	15.1

A2.2(iii) Intermediate Calculations. ANOVA Table (Serum Nitrite Levels at 12 months)

Source of variation	Degrees of freedom	Sum of squares	Mean square
Treatments (between columns)	3	357.55	119.18
Residuals (within columns)	28	621.95	22.212
Total	31	979.50	

F = 5.366 =(MStreatment/MSresidual)

A2.3. Indicators of Lipid Peroxidation

A2.3(i) ANOVA Data of Liver 8-Isoprostane Levels at 12 months.

Group	Number of points	Mean	Standard Deviation	Standard Error of Mean	Median	Max	Min	95% Confidence Interval	
								From	To
Control	5	736	208	93	737	525	1073	478	995
Fe	6	1264	272	111	1250	969	1765	978	1550
Fe + AFB_1	17	1773	415	101	1881	1033	2398	1560	1986
AFB_1	5	1376	554	248	1129	957	2308	689	2065

A2.3(i) Intermediate Calculations. ANOVA Table (Liver 8-Isoprostane Levels at 12 months)

Source of variation	Degrees of freedom	Sum of squares	Mean square
Treatments (between columns)	3	4548381	1516127
Residuals (within columns)	29	4531985	156275
Total	32	9080366	

F = 9.702 =(MStreatment/MSresidual)

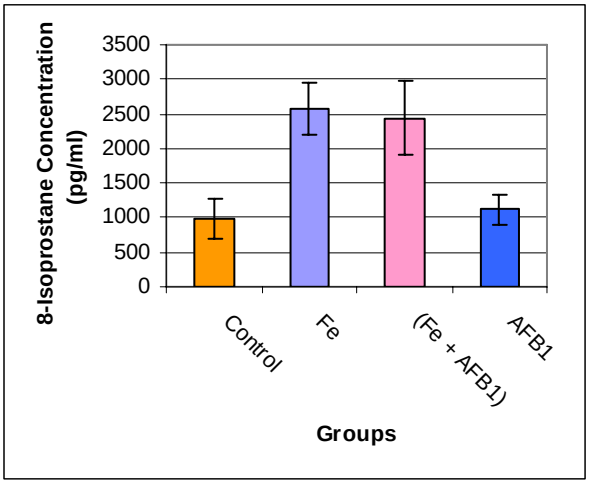

Table A2.3(ii). Bonferroni (Dunn) and t-tests for Serum 8-Isoprostane Levels at 12 months

Treatment Comparison	t	P-Value
Control vs. Fe	5.596	***P<0.001
Control vs. Fe + AFB_1	6.482	***P<0.001
Control vs. AFB_1	0.498	ns P>0.05
Fe vs. Fe + AFB_1	0.597	ns P>0.05
Fe vs. AFB_1	5.098	***P<0.001
Fe + AFB_1 vs. AFB_1	5.853	***P<0.001

Figure A2.3(ii) Bar Graph of Serum 8-Isoprostane Levels of Wistar Albino Rats at 12 months

A2.3(ii) ANOVA Data of Serum 8-Isoprostane Levels at 12 months.

Group	Number of points	Mean	Standard Deviation	Standard Error of Mean	Median	Max	Min	95% Confidence Interval	
								From	To
Control	5	979	253	113	921	741	1403	666	1293
Fe	5	2578	333	149	2588	2057	2979	2164	2992
Fe + AFB_1	20	2444	537	120	2540	1033	3135	2192	2695
AFB_1	5	1122	193	86	1121	853	1350	882	1361

A2.3(ii) Intermediate Calculations. ANOVA Table (Serum 8-Isoprostane Levels at 12 months)

Source of variation	Degrees of freedom	Sum of squares	Mean square
Treatments (between columns)	3	1.452E+07	4841337
Residuals (within columns)	31	6325580	204051
Total	34	2.085E+07	

F = 23.726 =(MStreatment/MSresidual)

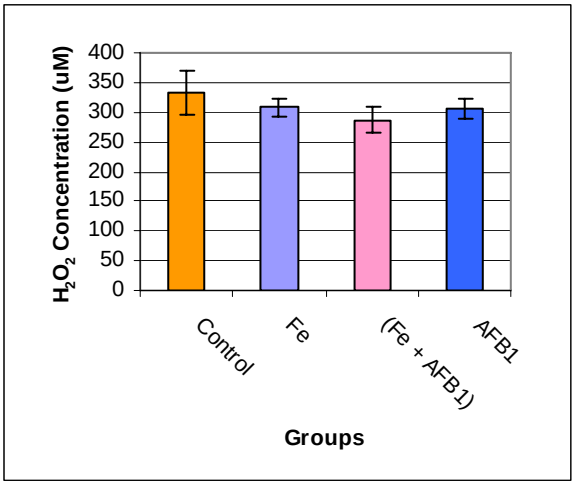

Figure A2.3(iii) Bar Graph of Liver Lipid Peroxidation Levels of Wistar Albino Rats at 12 months

Table A2.3(iii) Bonferroni (Dunn) and t-tests for Liver Lipid Peroxidation at 12 months

Treatment Comparison	t	P-Value
Control vs. Fe	1.727	ns P>0.05
Control vs. Fe + AFB_1	4.118	** P<0.01
Control vs. AFB_1	1.885	ns P>0.05
Fe vs. Fe + AFB_1	1.945	ns P>0.05
Fe vs. AFB_1	0.158	ns P>0.05
Fe + AFB_1 vs. AFB_1	1.747	ns P>0.05

A2.3(iii) ANOVA Data of Liver Lipid Peroxidation Levels at 12 months.

Group	Number of points	Mean	Standard Deviation	Standard Error of Mean	Median	Max	Min	95% Confidence Interval	
								From	To
Control	5	332.8	35.5	15.9	326.8	297.5	369.6	288.7	376.9
Fe	5	308.2	12.6	5.6	308.0	293.2	326.1	292.6	323.8
Fe + AFB_1	19	286.2	21.6	5.0	283.2	241.8	335.4	275.7	296.6
AFB_1	5	305.9	16.8	7.5	304.6	281.8	328.9	285.1	326.8

A2.3(iii) Intermediate Calculations. ANOVA Table (Liver Lipid Peroxidation Levels at 12 months)

Source of variation	Degrees of freedom	Sum of squares	Mean square
Treatments (between columns)	3	9506.0	3168.7
Residuals (within columns)	30	15232	507.74
Total	33	24738	

F = 6.241 =(MStreatment/MSresidual)

A2.3(iv) ANOVA Data of Serum Lipid Peroxidation Levels at 12 months.

Group	Number of points	Mean	Standard Deviation	Standard Error of Mean	Median	Max	Min	95% Confidence Interval	
								From	To
Control	5	15.2	2.6	1.2	15.2	12.0	18.8	11.9	18.4
Fe	5	45.0	11.4	5.1	41.4	36.0	64.5	30.9	59.2
Fe + AFB_1	18	64.3	14.8	3.5	63.5	37.9	101.3	57.0	71.7
AFB_1	4	15.0	0.9	0.5	15.3	13.6	15.6	13.5	16.5

A2.3(iv) Intermediate Calculations. ANOVA Table (Serum Lipid Peroxidation Levels at 12 months)

Source of variation	Degrees of freedom	Sum of squares	Mean square
Treatments (between columns)	3	14599	4866.4
Residuals (within columns)	28	4280.0	152.86
Total	31	18879	

F = 31.836 =(MStreatment/MSresidual)

A2.4. Indicators of DNA Change

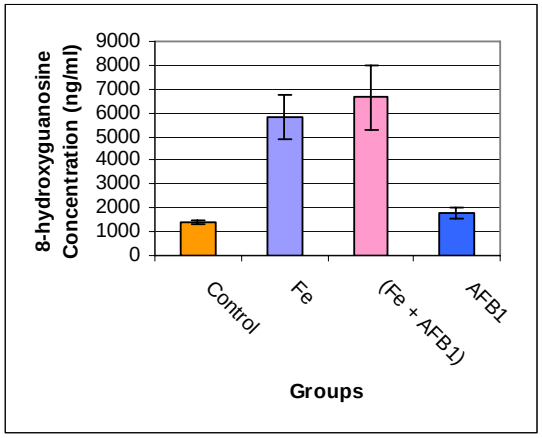

Figure A2.4(i) Bar Graph of Liver 8-hydroxyguanosine Levels of Wistar Albino Rats at 12 months

Table A2.4(i) Bonferroni (Dunn) and t-tests for Liver 8-Hydroxyguanosine at 12 months

Treatment Comparison	t	P-Value
Control vs. Fe	6.340	*** P<0.001
Control vs. Fe + AFB_1	9.380	*** P<0.001
Control vs. AFB_1	0.592	ns P>0.05
Fe vs. Fe + AFB_1	1.498	ns P>0.05
Fe vs. AFB_1	5.749	*** P<0.001
Fe + AFB_1 vs. AFB_1	8.644	*** P<0.001

A2.4(i) ANOVA Data of Liver 8-Hydroxyguanosine Levels at 12 months.

Group	Number of points	Mean	Standard Deviation	Standard Error of Mean	Median	Max	Min	95% Confidence Interval	
								From	To
Control	5	1405	79	35	1405	1290	1500	1307	1503
Fe	5	5800	941	421	6000	4300	6900	4632	6968
Fe + AFB_1	17	6635	1366	331	6200	5100	9400	5933	7338
AFB_1	5	1815	231	104	1815	1550	2050	1528	2102

A2.4(i) Intermediate Calculations. ANOVA Table (Liver 8-Hydroxyguanosine Levels at 12 months)

Source of variation	Degrees of freedom	Sum of squares	Mean square
Treatments (between columns)	3	1.639E+08	5.462E+07
Residuals (within columns)	28	3.364E+07	1201351
Total	31	1.975E+08	

F = 45.467 =(MStreatment/MSresidual)

A2.4(ii) ANOVA Data of Serum 8-Hydroxyguanosine Levels at 12 months.

Group	Number of points	Mean	Standard Deviation	Standard Error of Mean	Median	Max	Min	95% Confidence Interval	
								From	To
Control	5	58.8	34.3	15.4	58.8	21.0	100.6	16.2	101.4
Fe	5	74.9	12.6	5.7	79.7	53.2	84.4	59.2	90.6
Fe + AFB_1	17	146.5	85.4	20.7	112.8	41.0	360.8	102.6	190.4
AFB_1	5	71.3	41.2	18.4	80.1	14.6	126.5	20.2	122.5

A2.4(ii) Intermediate Calculations. ANOVA Table (Serum 8-Hydroxyguanosine Levels at 12 months)

Source of variation	Degrees of freedom	Sum of squares	Mean square
Treatments (between columns)	3	49391	16464
Residuals (within columns)	28	128895	4603.4
Total	31	178286	

F = 3.576 =(MStreatment/MSresidual)

A2.5. Indicators of Mutagenicity (Ames Test)

Where one of the *Salmonella typhimirium* strains used showed a very similar pattern in its whole homogenate, the other homogenate's data was omitted to avoid redundancy, and only the whole homogenate shown. Where there were significant differences in homogenates, the statistical data is shown.

The TA97 strain is only represented here as the whole fraction. All other fractions thereof showed almost identical patterns between groups and it was thought redundant to present that data.

A2.5(i) ANOVA Data of Ames Test TA97-Whole Fraction Colony Counts at 12 months.

Group	Number of points	Mean	Standard Deviation	Standard Error of Mean	Median	Max	Min	95% Confidence Interval	
								From	To
Control	6	137	4	1.7	138	132	141	133	141
Fe	6	234	31	12.8	224	205	273	201	267
Fe + AFB_1	9	188	25	8.5	189	138	236	169	208
AFB_1	5	158	4	1.6	157	154	162	154	163

A2.5(i) Intermediate Calculations. ANOVA Table (TA97-Whole Fraction Colony Counts at 12 months)

Source of variation	Degrees of freedom	Sum of squares	Mean square
Treatments (between columns)	3	31506	10502
Residuals (within columns)	22	10255	466.15
Total	25	41761	

F = 22.529 =(MStreatment/MSresidual)

A2.5(ii) ANOVA Data of Ames Test TA98-Whole Fraction Colony Counts at 12 months.

Group	Number of points	Mean	Standard Deviation	Standard Error of Mean	Median	Max	Min	95% Confidence Interval	
								From	To
Control	6	39.333	1.862	0.7601	40	37	41	37	41
Fe	6	54.000	11.628	4.747	47	46	69	42	66
Fe + AFB_1	5	43.800	10.281	4.598	40	37	62	31	57
AFB_1	6	33.333	2.066	0.8433	32	32	36	31	36

A2.5(ii) Intermediate Calculations. ANOVA Table (TA98-Whole Fraction Colony Counts at 12 months)

Source of variation	Degrees of freedom	Sum of squares	Mean square
Treatments (between columns)	3	1366.2	455.40
Residuals (within columns)	19	1137.5	59.867
Total	22	2503.7	

F = 7.607 =(MStreatment/MSresidual)

A2.5(iii) ANOVA Data of Ames Test TA98-S9 Fraction Colony Counts at 12 months.

Group	Number of points	Mean	Standard Deviation	Standard Error of Mean	Median	Max	Min	95% Confidence Interval	
								From	To
Control	6	29	4	2	27	26	34	24.9	33.1
Fe	6	49	6	2	50	42	54	42.9	54.4
Fe + AFB_1	9	48	16	5	43	21	71	35.9	61.0
AFB_1	5	43	10	4	37	33	53	30.6	54.6

A2.5(iii) Intermediate Calculations. ANOVA Table (TA98-S9 Fraction Colony Counts at 12 months)

Source of variation	Degrees of freedom	Sum of squares	Mean square
Treatments (between columns)	3	1635.9	545.30
Residuals (within columns)	22	2726.8	123.94
Total	25	4362.7	

F = 4.400 =(MStreatment/MSresidual)

A2.5(iv) ANOVA Data of Ames Test TA100 - Whole Fraction Colony Counts at 12 months.

Group	Number of points	Mean	Standard Deviation	Standard Error of Mean	Median	Max	Min	95% Confidence Interval	
								From	To
Control	6	125	18	8	136	101	137	105.4	143.9
Fe	6	154	22	9	151	131	180	130.9	177.1
Fe + AFB_1	9	176	21	7	169	147	211	159.2	192.1
AFB_1	5	126	3	1	127	122	128	123.3	129.5

A2.5(iv) Intermediate Calculations. ANOVA Table (TA100 - Whole Fraction Colony Counts at 12 months)

Source of variation	Degrees of freedom	Sum of squares	Mean square
Treatments (between columns)	3	12652	4217.3
Residuals (within columns)	22	7792.5	354.21
Total	25	20444	

F = 11.906 =(MStreatment/MSresidual)

A2.5(v) ANOVA Data of Ames Test TA102 - Whole Fraction Colony Counts at 12 months.

Group	Number of points	Mean	Standard Deviation	Standard Error of Mean	Median	Max	Min	95% Confidence Interval	
								From	To
Control	6	358	9	4	361	347	367	349	368
Fe	6	417	6	2	420	410	422	411	423
Fe + AFB_1	6	439	111	45	425	305	572	323	556
AFB_1	6	451	24	10	467	420	467	426	477

A2.5(iv) Intermediate Calculations. ANOVA Table (TA102 - Whole Fraction Colony Counts at 12 months)

Source of variation	Degrees of freedom	Sum of squares	Mean square
Treatments (between columns)	3	30667	10222
Residuals (within columns)	20	65179	3258.9
Total	23	95846	

F = 3.137 =(MStreatment/MSresidual)

A2.5(v) ANOVA Data of Ames Test TA102 - Nucleosomal Fraction Colony Counts at 12 months.

Group	Number of points	Mean	Standard Deviation	Standard Error of Mean	Median	Max	Min	95% Confidence Interval	
								From	To
Control	6	329	49	20	357	266	363	277.6	379.7
Fe	6	405	20	8	398	388	430	384.7	425.9
Fe + AFB_1	9	553	83	28	531	457	698	489.4	617.5
AFB_1	5	519	58	26	551	456	567	447.1	591.7

A2.5(v) Intermediate Calculations. ANOVA Table (TA102 - Nucleosomal Fraction Colony Counts at 12 months)

Source of variation	Degrees of freedom	Sum of squares	Mean square
Treatments (between columns)	3	217631	72544
Residuals (within columns)	22	82788	3763.1
Total	25	300419	

F = 19.278 =(MStreatment/MSresidual)

A2.5(vi) ANOVA Data of Ames Test TA102 - Cytosolic Fraction Colony Counts at 12 months.

Group	Number of points	Mean	Standard Deviation	Standard Error of Mean	Median	Max	Min	95% Confidence Interval	
								From	To
Control	6	358	9	4	361	347	367	348.7	368.0
Fe	6	417	6	2	420	410	422	411.3	423.4
Fe + AFB_1	6	485	68	28	467	419	572	413.4	556.9
AFB_1	5	345	52	23	342	305	431	281.1	49.0

A2.5(vi) Intermediate Calculations. ANOVA Table (TA102 – Cytosolic Fraction Colony Counts at 12 months)

Source of variation	Degrees of freedom	Sum of squares	Mean square
Treatments (between columns)	3	70512	23504
Residuals (within columns)	19	34560	1818.9
Total	22	105072	

F = 12.922 =(MStreatment/MSresidual)

A2.5(vii) ANOVA Data of Ames Test TA102 - Microsomal Fraction Colony Counts at 12 months.

Group	Number of points	Mean	Standard Deviation	Standard Error of Mean	Median	Max	Min	95% Confidence Interval	
								From	To
Control	6	296	17	7	295	278	315	278.6	313.4
Fe	6	412	30	12	415	378	444	381.3	443.4
Fe + AFB_1	9	463	50	17	448	413	569	424.3	501.1
AFB_1	5	305	5	2	303	302	314	298.4	311.2

A2.5(vii) Intermediate Calculations. ANOVA Table (TA102 – Microsomal Fraction Colony Counts at 12 months)

Source of variation	Degrees of freedom	Sum of squares	Mean square
Treatments (between columns)	3	138258	46086
Residuals (within columns)	22	25806	1173.0
Total	25	164065	

F = 39.289 =(MStreatment/MSresidual)

Table 2.5.A. Ames Mutagenicity Test (With added S9 Enzymes)

Salmonella typhimurium Strains									
		TA97		TA98		TA100		TA102	
Group	Liver Fraction	12 Months		12 Months		12 Months		12 Months	
		Mean	SD	Mean	SD	Mean	SD	Mean	SD
Control	(W)	137	4.5	39	2.1	125	20.5	295	15.0
	(N)	127	18.5	30	0.6	203	14.2	329	54.7
	(C)	116	21.9	22	5.2	190	22.5	358	10.6
	(S9)	80	18.9	29	4.4	124	15.0	331	52.3
	(M)	108	10.2	30	8.4	216	30.1	296	15.8
Fe	(W)	234	35.1	54	13.0	154	24.6	490	33.1
	(N)	286	40.3	29	11.8	204	27.2	405	22.3
	(C)	189	38.4	26	2.1	170	28.0	417	6.0
	(S9)	173	29.0	50	6.1	147	8.9	441	12.9
	(M)	152	20.2	29	6.7	182	22.6	412	26.9
Fe + AFB_1	(W)	181	25.8	39	7.8	176	11.1	399	16.4
	(N)	144	50.6	34	6.2	150	21.6	554	22.0
	(C)	123	25.9	21	5.0	180	6.6	476	46.5
	(S9)	185	17.1	51	9.9	153	18.5	502	24.7
	(M)	138	26.8	31	6.7	205	20.8	465	19.7
AFB_1	(W)	158	4.0	33	2.3	126	3.2	313	9.2
	(N)	131	8.7	27	3.8	183	18.1	525	60.2
	(C)	122	23.9	20	3.8	191	16.3	359	65.1
	(S9)	239	45.2	41	10.7	122	11.0	461	22.0
	(M)	131	34.7	33	8.0	198	47.9	452	21.8

Detailed results of the Ames mutagenicity test using *Salmonella typhimurium* strains TA97, TA98, TA100, and TA102. High-lighted areas indicate colony counts above 180, 50, 200 and 360 spontaneous revertants for TA97, TA98, TA100, and TA102 respectively. W = Whole liver homogenate; N = nucleosomal fraction; C = Cytosolic Fraction; S9 = Liver homogenate fraction at 9000rpm; M = Microsomal fraction.

Table 2.5.B. Ames Mutagenicity Test (Without added S9 Enzymes)

(No significant differences were found between groups. All P-values were greater than 0.05)

Salmonella typhimurium Strains									
		TA97		TA98		TA100		TA102	
Group	Liver Fraction	12 Months		12 Months		12 Months		12 Months	
		Mean	SD	Mean	SD	Mean	SD	Mean	SD
Control	(W)	112	7.8	32	1.8	133	18.1	189	20.4
	(N)	102	9.0	26	3.3	189	11.7	256	19.7
	(C)	105	13.2	20	3.8	192	27.7	278	33.4
	(S9)	83	4.5	17	2.1	122	14.2	299	17.5
	(M)	120	11.0	27	3.7	159	30.2	222	31.9
Fe	(W)	145	12.8	39	4.0	154	16.3	255	37.2
	(N)	201	23.4	27	4.8	221	20.5	326	18.5
	(C)	165	40.3	23	0.8	171	30.1	359	17.9
	(S9)	172	25.8	32	1.1	174	22.6	366	11.0
	(M)	122	8.7	27	7.1	213	27.8	400	47.6
Fe + AFB_1	(W)	100	6.8	33	3.7	176	21.6	322	28.7
	(N)	148	2.3	31	3.3	156	26.6	452	53.8
	(C)	129	10.7	21	2.4	122	12.5	412	18.3
	(S9)	123	24.6	44	0.9	153	15.0	487	34.5
	(M)	111	11.7	28	0.7	121	14.6	456	44.1
AFB_1	(W)	132	47.9	30	1.3	126	17.4	289	40.2
	(N)	118	7.8	21	4.0	205	40.6	368	47.8
	(C)	106	27.4	25	5.1	156	17.4	321	12.3
	(S9)	182	17.3	36	0.4	106	22.5	378	19.3
	(M)	144	0.6	32	3.1	157	13.0	391	51.6

Detailed results of the Ames mutagenicity test using *Salmonella typhimurium* strains TA97, TA98, TA100, and TA102. High-lighted areas indicate colony counts above 180, 50, 200 and 360 spontaneous revertants for TA97, TA98, TA100, and TA102 respectively. W = Whole liver homogenate; N = nucleosomal fraction; C = Cytosolic Fraction; S9 = Liver homogenate fraction at 9000rpm; M = Microsomal fraction.

A2.6. Cytokine Indicators

A2.6(i) ANOVA Data of Interleukin-1β Levels at 12 months.

Group	Number of points	Mean	Standard Deviation	Standard Error of Mean	Median	Max	Min	95% Confidence Interval	
								From	To
Control	5	31.3	6.9	3.1	31.3	20.7	39.3	22.8	39.9
Fe	5	32.2	10.4	4.7	32.2	19.6	47.7	19.3	45.2
Fe + AFB_1	15	34.4	10.9	2.8	34.8	16.6	53.4	28.4	40.4
AFB_1	5	22.4	6.9	3.1	20.7	15.2	30.1	13.8	31.0

A2.6(i) Intermediate Calculations. ANOVA Table (Interleukin-1β Levels at 12 months)

Source of variation	Degrees of freedom	Sum of squares	Mean square
Treatments (between columns)	3	541.79	180.60
Residuals (within columns)	26	2470.8	95.031
Total	29	3012.6	

F = 1.900 =(MStreatment/MSresidual)

A2.6(ii) ANOVA Data of Interleukin-6 Levels at 12 months.

Group	Number of points	Mean	Standard Deviation	Standard Error of Mean	Median	Max	Min	95% Confidence Interval	
								From	To
Control	5	135.6	44.9	20.1	135.6	69.4	195.9	79.9	191.3
Fe	5	67.4	39.2	17.5	67.4	23.5	129.2	18.7	116.1
Fe + AFB_1	17	42.1	24.0	5.8	39.8	4.2	83.3	29.8	54.5
AFB_1	5	79.6	33.8	15.1	69.4	47.5	135.5	37.6	121.6

A2.6(ii) Intermediate Calculations. ANOVA Table (Interleukin-6 Levels at 12 months)

Source of variation	Degrees of freedom	Sum of squares	Mean square
Treatments (between columns)	3	34837	11612
Residuals (within columns)	28	27970	998.93
Total	31	62807	

F = 11.625 =(MStreatment/MSresidual)

A2.6(iii) ANOVA Data of Interleukin-10 Levels at 12 months.

Group	Number of points	Mean	Standard Deviation	Standard Error of Mean	Median	Max	Min	95% Confidence Interval	
								From	To
Control	5	12.0	5.1	2.3	12.0	6.3	18.2	5.7	18.3
Fe	5	16.2	5.4	2.4	16.2	9.1	23.0	9.5	22.9
Fe + AFB_1	16	41.0	15.7	3.9	32.4	23.0	70.0	32.7	49.4
AFB_1	5	28.9	17.3	7.8	23.0	15.7	58.5	7.4	50.4

A2.6(iii) Intermediate Calculations. ANOVA Table (Interleukin-10 Levels at 12 months)

Source of variation	Degrees of freedom	Sum of squares	Mean square
Treatments (between columns)	3	4528.4	1509.5
Residuals (within columns)	27	5096.9	188.77
Total	30	9625.3	

F = 7.996 =(MStreatment/MSresidual)

A2.7. Haematology Differentials

A2.7(i) ANOVA Data of Haemoglobin Concentration at 12 months.

Group	Number of points	Mean	Standard Deviation	Standard Error of Mean	Median	Max	Min	95% Confidence Interval	
								From	To
Control	5	15.1	0.88	0.39	15.0	14.1	16.3	14.0	16.2
Fe	5	14.5	0.12	0.06	14.5	14.3	14.6	14.3	14.7
Fe + AFB_1	17	13.6	1.73	0.42	14.0	7.6	15.1	12.7	14.5
AFB_1	5	14.5	0.77	0.34	14.5	13.7	15.7	13.6	15.5

Table A2.7(i) Bonferroni (Dunn) and t-tests for Haemoglobin Concentration at 12 months

Treatment Comparison	t	P-Value
Control vs. Fe	0.6411	ns P>0.05
Control vs. Fe + AFB_1	2.112	ns P>0.05
Control vs. AFB_1	0.6411	ns P>0.05
Fe vs. Fe + AFB_1	1.314	ns P>0.05
Fe vs. AFB_1	0.000	ns P>0.05
Fe + AFB_1 vs. AFB_1	1.314	ns P>0.05

A2.7(i) Intermediate Calculations. ANOVA Table (Haemoglobin Concentration at 12 months)

Source of variation	Degrees of freedom	Sum of squares	Mean square
Treatments (between columns)	3	10.867	3.622
Residuals (within columns)	28	53.403	1.907
Total	31	64.270	

F = 1.899 =(MStreatment/MSresidual)

A2.7(ii) ANOVA Data of White Blood Cell (WBC) Count at 12 months.

Group	Number of points	Mean	Standard Deviation	Standard Error of Mean	Median	Max	Min	95% Confidence Interval	
								From	To
Control	5	7.8	4.7	2.12	8.6	1.8	14.4	1.9	13.7
Fe	5	19.5	3.7	1.65	20.0	14.7	23.0	14.9	24.1
Fe + AFB_1	17	11.0	4.0	0.96	11.5	2.7	18.2	8.9	13.0
AFB_1	5	10.9	2.5	1.13	10.0	7.8	13.5	7.7	14.0

Table A2.7(ii) Bonferroni (Dunn) and t-tests for White Blood Cell Count at 12 months

Treatment Comparison	t	P-Value
Control vs. Fe	4.757	*** P<0.001
Control vs. Fe + AFB_1	1.605	ns P>0.05
Control vs. AFB_1	1.242	ns P>0.05
Fe vs. Fe + AFB_1	4.308	** P<0.01
Fe vs. AFB_1	3.515	** P<0.01
Fe + AFB_1 vs. AFB_1	0.061	ns P>0.05

A2.7(ii) Intermediate Calculations. ANOVA Table (White Blood Cell (WBC) Count at 12 months)

Source of variation	Degrees of freedom	Sum of squares	Mean square
Treatments (between columns)	3	388.43	129.48
Residuals (within columns)	28	419.11	14.968
Total	31	807.53	

F = 8.650 =(MStreatment/MSresidual)

A2.7(iii) ANOVA Data of Red Blood Cell (RBC) Count at 12 months.

Group	Number of points	Mean	Standard Deviation	Standard Error of Mean	Median	Max	Min	95% Confidence Interval	
								From	To
Control	5	8.3	0.66	0.30	8.25	7.64	9.34	7.47	9.11
Fe	5	7.0	0.28	0.13	7.00	6.55	7.29	6.60	7.31
Fe + AFB_1	17	6.7	0.96	0.23	6.94	3.50	7.78	6.16	7.14
AFB_1	5	7.6	0.59	0.27	7.37	6.97	8.52	6.87	8.34

Table A2.7(iii) Bonferroni (Dunn) and t-tests for Red Blood Cell Count at 12 months		
Treatment Comparison	t	P-Value
Control vs. Fe	2.623	ns P>0.05
Control vs. Fe + AFB_1	4.000	** P<0.01
Control vs. AFB_1	1.347	ns P>0.05
Fe vs. Fe + AFB_1	0.7386	ns P>0.05
Fe vs. AFB_1	1.276	ns P>0.05
Fe + AFB_1 vs. AFB_1	2.325	ns P>0.05

A2.7(iii) Intermediate Calculations. ANOVA Table (Red Blood Cell (RBC)) Count at 12 months

Source of variation	Degrees of freedom	Sum of squares	Mean square
Treatments (between columns)	3	11.878	3.959
Residuals (within columns)	28	18.158	0.6485
Total	31	30.036	

F = 6.105 =(MStreatment/MSresidual)

A2.7(iv) ANOVA Data of Platelet Count at 12 months.

Group	Number of points	Mean	Standard Deviation	Standard Error of Mean	Median	Max	Min	95% Confidence Interval	
								From	To
Control	5	88.6	53.2	23.8	85.0	16.0	162.0	22.6	154.7
Fe	5	231.2	138.1	61.7	235.0	90.0	407.0	59.8	402.6
Fe + AFB_1	17	196.7	206.4	50.1	158.0	59.0	943.0	90.5	302.8
AFB_1	5	433.4	334.1	149.4	345.0	81.0	868.0	18.7	848.1

Table A2.7(iv) Bonferroni (Dunn) and t-tests for Platelet Count at 12 months		
Treatment Comparison	t	P-Value
Control vs. Fe	1.082	ns P>0.05
Control vs. Fe + AFB_1	1.019	ns P>0.05
Control vs. AFB_1	2.617	ns P>0.05
Fe vs. Fe + AFB_1	0.3260	ns P>0.05
Fe vs. AFB_1	1.535	ns P>0.05
Fe + AFB_1 vs. AFB_1	2.234	ns P>0.05

A2.7(iv) Intermediate Calculations. ANOVA Table (Platelet Count) at 12 months

Source of variation	Degrees of freedom	Sum of squares	Mean square
Treatments (between columns)	3	323777	107926
Residuals (within columns)	28	1215341	43405
Total	31	1539118	

F = 2.486 =(MStreatment/MSresidual)

A2.7(v) ANOVA Data of Mean Platelet Volume at 12 months.

Group	Number of points	Mean	Standard Deviation	Standard Error of Mean	Median	Max	Min	95% Confidence Interval	
								From	To
Control	5	7.1	1.06	0.47	7.3	5.40	8.30	5.79	8.41
Fe	5	7.3	0.54	0.24	7.2	6.80	8.20	6.63	7.97
Fe + AFB_1	16	7.4	0.54	0.14	7.3	6.60	8.60	7.12	7.68
AFB_1	5	7.2	0.73	0.33	7.0	6.50	8.40	6.27	8.09

Table A2.7(v) Bonferroni (Dunn) and t-tests for Mean Platelet Volume at 12 months

Treatment Comparison	t	P-Value
Control vs. Fe	0.4716	ns P>0.05
Control vs. Fe + AFB_1	0.8551	ns P>0.05
Control vs. AFB_1	0.1887	ns P>0.05
Fe vs. Fe + AFB_1	0.2729	ns P>0.05
Fe vs. AFB_1	0.2830	ns P>0.05
Fe + AFB_1 vs. AFB_1	0.6222	ns P>0.05

A2.7(v) Intermediate Calculations. ANOVA Table (Mean Platelet Volume) at 12 months

Source of variation	Degrees of freedom	Sum of squares	Mean square
Treatments (between columns)	3	0.4123	0.1374
Residuals (within columns)	27	12.137	0.4495
Total	30	12.550	

F = 0.3057 =(MStreatment/MSresidual)

A3.1. Two-Way Analysis of Variance Results calculated between 6 and 12 month data.

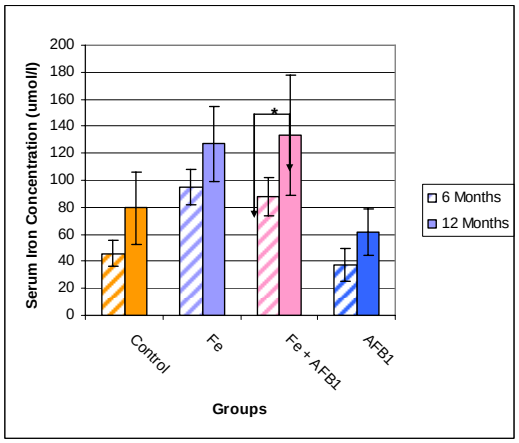

Fig. A3.1(i) Bar Graph of Serum Iron Levels of Wistar Albino Rats at 6 and 12 Month Intervals

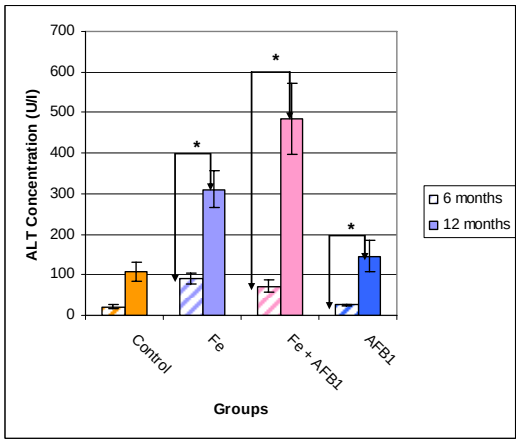

Fig. A3.1(ii) Bar Graph of Serum ALT Concentration in Wistar Albino Rats at 6 and 12 Month Intervals

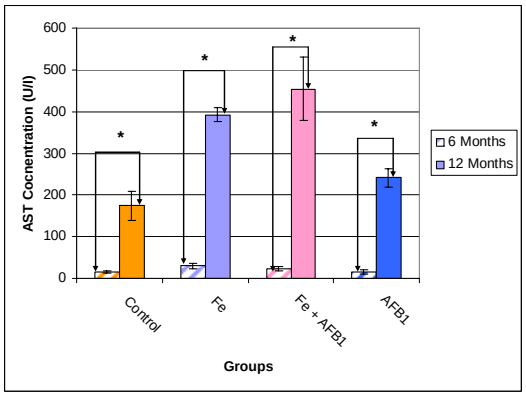

Fig. A3.1(iii) Bar Graph of Serum AST Concentration of Wistar Albino Rats at 6 and 12 Month Intervals

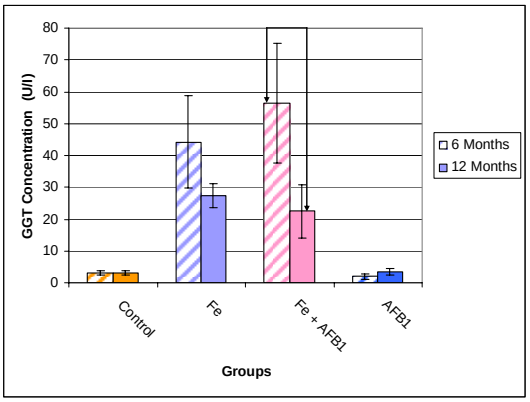

Fig. A3.1(iv) Bar Graph of GGT Concentration of Wistar Albino Rats at 6 and 12 Month Intervals

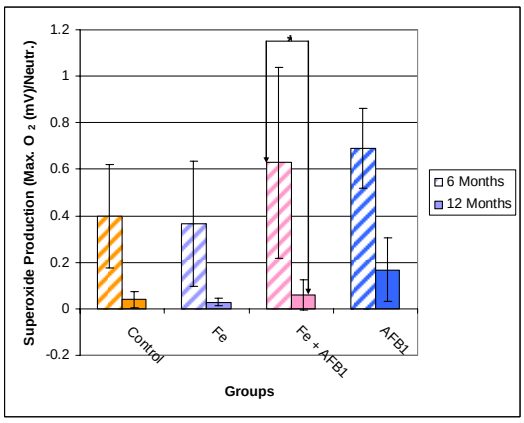

Fig. A3.1(v) Bar Graph of Superoxide Anion Production in Wistar Albino Rats at 6 and 12 Month Intervals

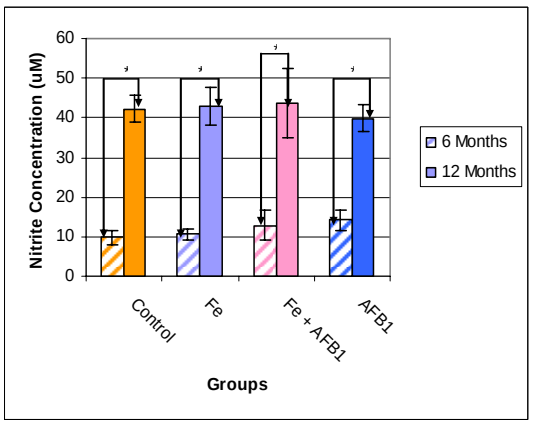

Fig. A3.1(vi) Bar Graph of Liver Nitrite Concentration of Wistar Albino Rat at 6 and 12 Month Intervals

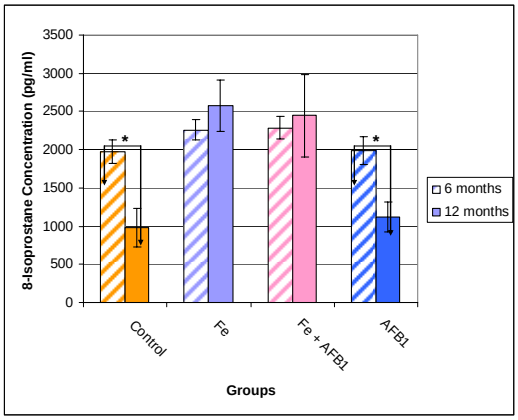

Fig. A3.1(vii) Bar Graph of Serum 8-Isoprostane Concentration in Wistar Albino Rats at 6 and 12 Month Intervals

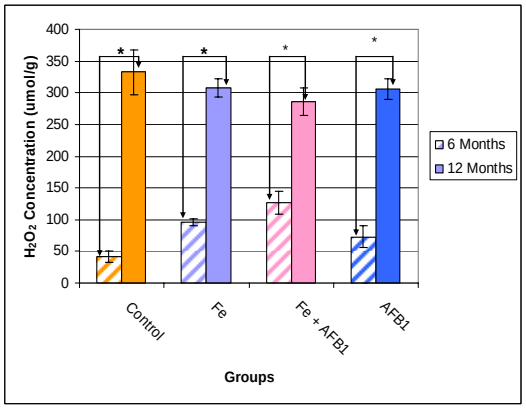

Fig. A3.1(viii) Bar Graph of Liver Lipid Peroxidation of Wistar Albino Rats at 6 and 12 Month Intervals

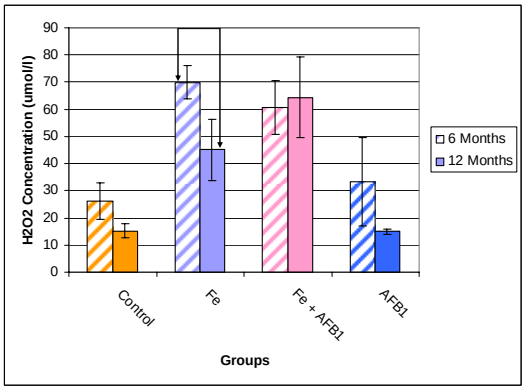

Fig. A3.1(ix)Bar Graph of Serum Lipid Peroxidation of Wistar Albino Rats at 6 and 12 Months

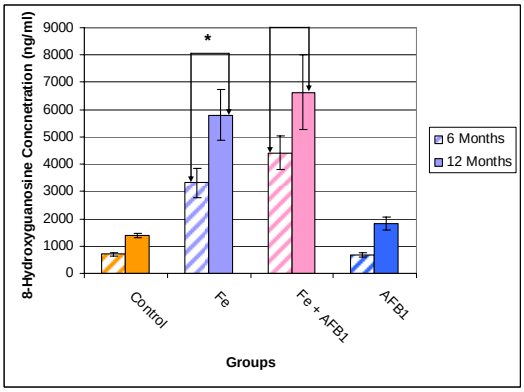

Fig. A3.1(x) Bar Graph of Liver 8-Hydroxyguanosine Concentration of Wistar Albino Rats at 6 and 12 months

A4.1 Correlation Tables

A4.1(i) to A4.1(iv) represent correlation tables at 6 months. A4.1(v) to A4.1(viii) represent correlation tables at 12 months.

Table A4.1(i) Correlation Matrix of 6 Month Data
Highlighted Correlations are Significant at p<0.05

Group: Control

	Hydroxy-proline	GGT	AST	ALT	Serum 8- IsoP	Liver 8OHdG	Serum LPO	Liver Nitrite	Serum Nitrite	Superoxide Anion	Liver LPO
Hydroxyproline	1.00	-0.30	-0.70	-0.85	0.26	-0.41	-0.80	0.50	0.65	-0.27	0.33
GGT	-0.30	1.00	0.71	0.28	0.24	0.55	-0.14	0.33	-0.01	0.68	0.79
AST	-0.70	0.71	1.00	0.41	0.24	0.31	0.30	-0.41	0.00	0.81	0.30
ALT	-0.85	0.28	0.41	1.00	-0.66	0.36	0.86	-0.06	**-0.88**	-0.14	-0.32
8 Isoprostane	0.26	0.24	0.24	-0.66	1.00	0.30	-0.72	-0.02	0.67	0.76	0.52
Liver 8OHdG	-0.41	0.55	0.31	0.36	0.30	1.00	-0.07	0.20	-0.46	0.38	0.31
Serum LPO	-0.80	-0.14	0.30	0.86	-0.72	-0.70	1.00	-0.43	-0.72	-0.28	-0.69
Liver Nitrite	0.50	0.33	-0.41	-0.06	-0.20	0.20	-0.43	1.00	-0.10	-0.31	0.56
Serum Nitrite	0.65	-0.01	0.00	**-0.88**	0.67	-0.46	-0.72	-0.10	1.00	0.43	0.46
Superoxide	-0.27	0.68	0.81	-0.14	0.76	0.38	-0.28	-0.31	0.43	1.00	0.59
Liver LPO	0.33	0.79	0.30	-0.32	0.52	0.31	-0.69	0.56	0.46	0.59	1.00

Table A4.1(ii) Correlation Matrix of 6 Month Data
Highlighted Correlations are Significant at p<0.05

Group: Iron

	Hydroxy-proline	GGT	AST	ALT	Serum 8- IsoP	Liver 8OHdG	Serum LPO	Liver Nitrite	Serum Nitrite	Superoxide Anion	Liver LPO
Hydroxyproline	1.00	-0.10	-0.59	0.02	-0.55	-0.56	-0.47	-0.13	-0.65	-0.18	0.58
GGT	-0.10	1.00	0.38	0.16	-0.20	0.85	-0.76	-0.83	0.06	0.83	0.62
AST	-0.59	0.38	1.00	-0.35	0.17	0.76	-0.17	0.14	**0.87**	0.05	-0.37
ALT	0.62	0.16	-0.35	1.00	**-0.98**	-0.22	-0.27	-0.48	-0.18	0.34	0.31
8 Isoprostane	-0.55	-0.20	0.17	**-0.98**	1.00	0.11	0.30	0.43	0.00	-0.33	-0.23
Liver 8OHdG	-0.56	0.85	0.76	-0.22	0.11	1.00	-0.45	-0.48	0.17	0.64	0.15
Serum LPO	-0.47	-0.76	-0.17	-0.27	0.30	-0.45	1.00	0.58	0.24	-0.39	-0.82
Liver NO	-0.13	-0.83	0.14	-0.48	0.43	-0.48	0.58	1.00	0.31	**-0.94**	-0.74
Serum NO	-0.65	0.60	**0.87**	-0.18	0.00	0.50	0.24	0.31	1.00	-0.05	-0.71
Superoxide	-0.18	0.83	0.05	0.34	-0.33	0.64	-0.39	**-0.94**	-0.05	1.00	0.50
Liver LPO	0.58	0.62	-0.37	0.31	-0.23	0.15	-0.82	-0.74	-0.71	0.50	1.00

Table A4.1(iii) Correlation Matrix of 6 Month Data
Highlighted Correlations are Significant at p<0.05

Group: Iron and Aflatoxin B1

	Hydroxy-proline	GGT	AST	ALT	Serum 8- IsoP	Liver 8OHdG	Serum LPO	Liver Nitrite	Serum Nitrite	Superoxide Anion	Liver LPO
Hydroxyproline	1.00	0.51	0.27	**0.96**	-0.60	0.80	0.03	-0.05	-0.31	-0.66	-0.23
GGT	0.51	1.00	-0.39	0.71	-0.65	0.85	0.38	0.16	0.62	-0.74	0.53
AST	0.27	-0.39	1.00	0.08	0.47	0.04	-0.61	-0.42	-0.54	0.46	-0.19
ALT	**0.96**	0.71	0.08	1.00	-0.74	**0.92**	0.07	0.11	-0.09	-0.80	-0.08
8 Isoprostane	-0.60	-0.65	0.47	-0.74	1.00	-0.70	-0.09	-0.66	0.01	0.99	0.26
Liver 8OHdG	0.80	0.85	0.40	**0.92**	-0.70	1.00	-0.05	-0.16	0.42	0.54	0.18
Serum LPO	0.03	0.38	0.61	0.07	0.09	-0.05	1.00	-0.43	0.48	-0.16	0.42
Liver NO	-0.05	0.16	-0.42	0.11	-0.66	0.23	-0.43	1.00	-0.05	-0.57	-0.38
Serum NO	-0.31	0.62	-0.54	-0.09	0.01	0.18	0.48	-0.05	1.00	-0.07	**0.92**
Superoxide	-0.66	-0.74	0.46	-0.80	0.99	-0.77	-0.16	-0.57	-0.07	1.00	0.14
Liver LPO	-0.23	0.53	-0.19	-0.08	0.26	0.18	0.42	-0.38	**0.92**	0.16	1.00

Table A4.1(iv) Correlation Matrix of 6 Month Data
Highlighted Correlations are Significant at p<0.05

Group: Aflatoxin B1

	Hydroxy-proline	GGT	AST	ALT	Serum 8- IsoP	Liver 8OHdG	Serum LPO	Liver Nitrite	Serum Nitrite	Superoxide Anion	Liver LPO
Hydroxyproline	1.00	0.10	-0.79	**-0.95**	**-0.96**	-0.10	0.30	-0.07	-0.40	-0.12	0.40
GGT	0.10	1.00	-0.65	**0.96**	-0.14	0.76	-0.49	-0.76	-0.70	0.56	**0.90**
AST	-0.79	-0.65	1.00	-0.67	0.74	-0.26	-0.09	0.40	0.74	-0.37	-0.87
ALT	**-0.95**	**0.96**	-0.67	1.00	-0.16	0.82	-0.55	**-0.88**	-0.84	0.60	**0.90**
8 Isoprostane	**-0.96**	-0.14	0.74	-0.16	1.00	0.00	-0.15	0.10	0.25	0.33	-0.33
Liver 8OHdG	-0.10	0.76	-0.26	0.82	0.00	1.00	**-0.93**	**-0.96**	-0.54	0.22	0.50
Serum LPO	0.30	-0.49	-0.09	-0.55	-0.15	**-0.93**	1.00	0.83	0.23	0.05	-0.14
Liver NO	-0.07	-0.76	0.40	**-0.88**	0.10	**-0.96**	0.83	1.00	0.73	-0.36	-0.62
Serum NO	-0.40	-0.70	0.74	-0.84	0.25	-0.54	0.23	0.73	1.00	-0.74	-0.87
Superoxide	-0.12	0.56	-0.37	0.60	0.33	0.22	0.05	-0.36	-0.74	1.00	0.70
Liver LPO	0.40	**0.90**	-0.87	**0.90**	-0.33	0.50	-0.14	-0.76	-0.70	0.56	1.00

Table A4.1(v)
Correlation Matrix of 12 Month Data
Highlighted Correlations are Significant at p<0.05
Group: Control (Part 1)

	Serum 8-IsoP	Liver 8IsoP	ALT	AST	Liver 8OHdG	Serum 8OHdG	Liver LPO	Serum LPO	Liver NO	Serum NO	Super-oxide	GGT	Ferritin	NTBI
Serum 8IsoP	1	1	1	1	0.5	-0.16	-0.96	0.7	-0.83	-0.9	-0.37	-1	0.34	-0.96
Liver 8IsoP	0.99	1	**1**	1	0.3	-0.01	-0.91	0.5	-0.91	-1	-0.22	-1	-0.97	-0.19
ALT	0.98	**1**	1	1	0.3	0.02	-0.9	0.5	-0.92	-1	-0.19	-1	0.09	**-1**
AST	0.95	1	1	1	0.2	0.15	-0.84	0.4	-0.96	**-1**	-0.6	-0.9	0.79	-0.65
Liver 8OHdG	0.47	0.3	0.3	0.2	1	-0.95	-0.68	1	0.1	-1	-0.99	-0.6	-0.17	0.99
Serum 8OHdG	-0.16	0	0	0.1	-0.9	1	0.42	-0.9	-0.41	-0.2	0.98	0.3	-0.23	-0.96
Liver LPO	-0.96	-0.9	-0.9	-0.8	-0.7	0.42	1	-0.8	0.66	0.8	0.6	1	1	0.04
Serum LPO	0.66	0.5	0.5	0.4	1	-0.85	-0.83	1	-0.13	-0.4	-0.94	-0.7	0.7	0.67
Liver NO	-0.83	-0.9	-0.9	-1	0.1	-0.41	0.66	-0.1	1	1	-0.21	0.8	-0.3	0.97
Serum NO	-0.94	-1	-1	**1**	-0.1	-0.019	0.81	-0.4	0.97	1	0.02	0.9	0.39	0.9
Superoxide	-0.37	-0.2	-0.2	-0.1	-1	0.98	0.6	-0.9	-0.21	0	1	0.5	0.8	-0.65
GGT	-0.99	-1	-1	-0.9	-0.6	0.27	0.99	-0.7	0.77	0.9	0.47	1	0.97	0.19
IL-1b	0.89	0.9	1	1	0	0.31	-0.73	0.2	-0.99	-1	0.1	-0.8	-0.8	-0.56
IL-6	-0.72	-0.6	-0.6	-0.5	-0.9	0.8	0.88	-1	0.22	0.4	-0.25	-1	0.5	-0.89
IL-10	0.56	0.7	0.7	0.8	-0.5	0.73	-0.32	-0.3	-0.92	-0.8	0.91	0.8	0.48	-0.9
Serum Fe	0.32	0.2	0.1	0	1	-0.99	-0.56	0.9	0.25	0	0.57	-0.5	-0.63	0.81
TIBC	-0.54	-0.4	-0.4	-0.3	-1	0.92	0.74	-1	-0.1	0.2	**-1**	-0.4	0.98	-0.25
WBC	-0.34	0.12	0.87	0.7	-0.64	0.35	0.59	-0.72	-0.75	0.71	-0.24	-0.58	-0.86	0.56
RBC	0.5	0.23	**-0.92**	-0.63	0.34	-0.44	-0.74	0.8	-0.7	0.09	0.63	0.47	-0.43	0.93
Hb	0.27	-0.17	-0.59	-0.64	0.15	-0.92	-0.04	0.65	-0.82	0.01	0.45	0.33	-0.25	0.98
Platelets	-0.9	0.01	-0.63	-0.53	0	-0.89	-0.2	0.7	-0.74	0.68	-0.33	-0.66	-0.84	0.59
MPV	0.6	0.24	**-0.93**	-0.53	0.29	-0.39	-0.82	0.82	**-0.98**	-0.05	-0.23	-0.28	-0.19	0.99
TA97	0.56	0.29	-0.75	-0.02	-0.35	-0.65	-0.76	0.88	0.51	0.7	-0.28	-0.5	-0.69	-0.68
TA98	0.9	-0.33	0.07	-0.03	0.53	0.51	-0.01	-0.21	-0.01	0.92	-0.31	-0.67	-0.98	-0.15
TA100	0.27	-0.34	-0.36	-0.19	0.54	0.14	-0.32	0.25	0.13	0.93	-0.3	-0.68	-1	-0.04
TA102	0.3	-0.33	-0.44	-0.22	0.53	0.06	-0.38	0.34	0.69	0.55	-0.24	-0.39	-0.47	-0.86
Ferritin	0.34	-0.97	0.09	0.79	-0.17	-0.23	1	0.7	-0.3	0.39	0.8	0.97	1	-0.05
NTBI	-0.96	-0.19	**-1**	-0.65	0.99	-0.96	0.04	0.67	0.97	0.9	-0.65	0.19	-0.05	1

Table A4.1(v) Correlation Matrix of 12 Month Data
Highlighted Correlations are Significant at p<0.05
Group: Control (Part 2)

	IL-1b	IL-6	IL-10	Serum Fe	TIBC	WBC	RBC	Hb	Platelets	MPV	TA97	TA98	TA100	TA102
Serum 8IsoP	0.9	-0.7	0.56	0.32	-0.5	-0.34	0.5	-0.27	-0.9	0.6	0.56	0.9	0.27	0.3
Liver 8IsoP	0.9	-0.6	0.68	0.17	-0.4	0.12	0.23	-0.17	0.01	0.24	0.29	-0.33	-0.34	-0.33
ALT	1	-0.6	0.7	0.14	-0.4	0.87	**-0.92**	-0.59	-0.63	**-0.93**	-0.75	0.07	-0.36	-0.44
AST	1	-0.5	0.79	0.01	-0.3	0.7	-0.63	-0.64	-0.53	-0.53	-0.02	-0.03	-0.19	-0.22
Liver 8OHdG	0	-0.9	-0.47	0.99	-1	-0.64	0.34	0.15	0	0.29	-0.35	0.53	0.54	0.53
Serum 8OHdG	0.3	0.8	0.73	-0.99	0.9	0.35	-0.44	-0.92	-0.89	-0.39	-0.65	0.51	0.14	0.06
Liver LPO	-0.7	0.9	-0.32	-0.56	0.7	0.59	-0.74	-0.04	-0.2	-0.82	-0.76	-0.01	-0.32	-0.38
Serum LPO	0.2	-1	-0.26	0.92	-1	-0.72	0.8	0.65	0.7	0.82	0.88	-0.21	0.25	0.34
Liver NO	-1	0.2	-0.92	0.25	0	-0.75	-0.7	-0.82	-0.74	**-0.98**	0.51	-0.01	-0.13	0.69
Serum NO	-1	0.4	-0.81	0.03	0.2	0.71	0.09	0.01	0.68	-0.05	0.7	0.92	0.93	0.55
Superoxide	0.1	0.9	0.57	**1**	1	-0.24	0.63	0.45	-0.33	-0.23	-0.28	-0.31	-0.3	-0.24
GGT	-0.8	0.8	-0.46	-0.42	0.6	-0.58	0.47	0.33	-0.66	-0.28	-0.5	-0.67	-0.68	-0.39
IL-1b	1	-0.3	0.88	-0.15	-0.1	0.47	0.94	**0.99**	0.43	0.84	-0.74	-0.3	-0.18	-0.87
IL-6	0.9	1	0.17	-0.89	1	-0.26	-0.76	-0.87	-0.25	-0.87	0.9	0.54	0.43	0.97
IL-10	-0.3	0.2	1	-0.61	0.4	-0.49	-0.81	-0.69	-0.39	-0.21	0.08	-0.23	-0.29	0.2
Serum Fe	0.9	-0.9	-0.61	1	-1	-0.14	0.8	0.81	-0.19	0.49	-0.95	-0.78	-0.71	-0.93
TIBC	-0.2	1	0.4	-0.97	1	-0.39	**-0.89**	-0.25	-0.25	-0.91	-0.37	-0.38	-0.67	-0.71
WBC	0.47	-0.26	-0.49	-0.14	-0.39	1	**-0.89**	-0.65	-0.82	0.88	-0.21	0.14	0.34	0.34
RBC	0.94	-0.76	-0.81	0.8	-0.89	**-0.89**	1	0.47	0.53	**0.98**	0.58	-0.02	0.31	0.37
Hb	**0.99**	-0.87	-0.69	0.81	-0.25	-0.65	0.47	1	**0.98**	0.36	0.52	-0.7	-0.42	-0.35
Platelets	0.43	-0.25	-0.39	-0.19	-0.25	-0.82	0.53	**0.98**	1	0.43	0.65	-0.76	-0.45	-0.37
MPV	0.84	-0.87	-0.21	0.49	-0.91	0.88	**0.98**	0.36	0.43	1	0.63	0.08	0.43	0.49
TA97	-0.74	0.9	0.08	-0.95	-0.37	-0.21	0.58	0.52	0.65	0.63	1	-0.44	-0.01	0.09
TA98	-0.3	0.54	-0.23	-0.78	-0.38	0.14	-0.02	-0.7	-0.76	0.08	-0.44	1	0.89	0.84
TA100	-0.18	0.43	-0.29	-0.71	-0.67	0.34	0.31	-0.42	-0.45	0.43	-0.01	0.89	1	1
TA102	-0.87	0.97	0.2	-0.93	-0.71	0.34	0.37	-0.35	-0.37	0.49	0.09	0.84	1	1
Ferritin	-0.8	0.5	0.48	-0.63	0.98	-0.86	-0.43	-0.25	-0.84	-0.19	-0.69	-0.98	-1	-0.47
NTBI	-0.56	-0.89	-0.9	0.81	-0.25	0.56	0.93	0.98	0.59	0.99	-0.68	-0.15	-0.04	-0.86

Table A4.1(vi) Correlation Matrix of 12 Month Data
Highlighted Correlations are Significant at p<0.05
Group: Iron (Part 1)

	Serum 8-IsoP	Liver 8IsoP	ALT	AST	Liver 8OHdG	Serum 8OHdG	Liver LPO	Serum LPO	Liver NO	Serum NO	Super-oxide	GGT	Ferritin	NTBI
Serum 8IsoP	1	0.62	0.53	0.33	-0.53	0.92	-0.42	-0.74	-0.93	0.62	0.13	-0.44	-0.83	**0.95**
Liver 8IsoP	0.62	1	-0.3	-0.5	-1	0.9	0.4	-1	0.9	-0.2	0.9	-1	0.22	0.26
ALT	0.53	-0.3	1	1	0.4	0.2	-1	0.2	0.2	1	-0.8	0.5	-0.13	0.24
AST	0.33	-0.5	1	1	0.6	-1	-1	0.4	0	**0.9**	-0.9	0.7	0.13	0.02
Liver 8OHdG	-0.53	-1	0.4	0.6	1	-0.81	-0.54	0.96	-0.81	0.33	-0.91	0.99	0.73	-0.76
Serum 8OHdG	0.92	0.9	0.2	-1	-0.81	1	-0.05	-0.94	**1**	0.28	0.5	-0.75	-0.59	0.9
Liver LPO	-0.42	0.4	-1	-1	-0.54	-0.05	1	-0.3	-0.1	-1	0.8	-0.6	0.07	-0.12
Serum LPO	-0.74	-1	0.2	0.4	0.96	-0.94	-0.3	1	-0.94	0.06	-0.76	0.93	0.6	-0.15
Liver NO	0.93	0.9	0.2	0	-0.81	**1**	-0.1	-0.94	1	0.29	0.49	-0.74	-0.63	0.92
Serum NO	0.62	-0.2	1	**0.9**	0.33	0.28	-1	0.06	0.29	1	-0.69	0.43	-0.41	0.34
Superoxide	0.13	0.9	-0.8	-0.9	-0.91	0.5	0.8	-0.76	0.49	-0.69	1	-0.95	-0.6	0.24
GGT	-0.44	-1	0.5	0.7	0.99	-0.75	-0.6	0.93	-0.74	0.43	-0.95	1	0.74	-0.41
IL-1b	-0.18	0.7	-0.9	-1	0.74	0.21	1	-0.53	0.2	-0.88	0.95	-0.8	-0.41	0.09
IL-6	-0.05	0.8	-0.9	-1	-0.82	0.33	0.9	-0.63	0.32	-0.81	0.98	-0.9	-0.48	0.2
IL-10	0.84	0.9	0	-0.2	-0.9	0.98	0.1	-0.99	0.98	0.11	0.64	-0.9	-0.96	0.92
Serum Fe	-0.96	-0.8	-0.3	-0.1	0.75	-0.99	0.2	0.9	-1	-0.38	-0.4	0.7	0.44	-0.81
TIBC	-0.45	0.4	-1	-1	-0.52	-0.07	**1**	-0.27	-0.09	-0.2	**0.83**	-0.6	0.45	-0.09
WBC	0.26	-0.76	-0.38	0.42	-0.14	-0.09	-0.2	-0.37	0.38	0.78	-0.33	-0.37	-0.25	0.58
RBC	0.78	-0.47	-0.03	-0.04	0.09	0.19	0.49	-0.78	0.45	-0.57	-0.22	-0.46	-0.87	0.56
Hb	0.23	0.17	**0.9**	-0.96	0.77	0.79	0.82	0.01	**0.95**	0.26	0.24	0.2	-0.88	1
Platelets	**0.92**	0.34	0.24	-0.41	0.09	0.2	**0.92**	-0.81	0.24	0.39	-0.65	-0.75	-0.4	0.52
MPV	0.54	-0.57	0.41	-0.45	0.52	0.6	0.59	-0.44	**-0.98**	-0.33	-0.39	-0.18	0.82	-0.99
TA97	-0.94	-0.43	-0.08	0.26	0.07	-0.03	-0.84	0.87	-0.25	0.84	0.1	0.3	0.7	-0.28
TA98	0.09	-0.25	-0.7	0.71	-0.56	-0.54	-0.46	-0.27	-0.89	0.07	-0.17	0.08	0.99	-0.94
TA100	-0.72	-0.39	-0.48	0.64	-0.31	-0.39	-0.94	0.55	-0.75	0.37	-0.09	0.18	0.99	-0.8
TA102	-0.45	-0.37	-0.63	0.74	-0.45	-0.05	-0.84	0.26	-0.87	-0.62	-0.3	-0.16	0.61	-0.91
Ferritin	-0.83	0.22	-0.13	0.13	0.73	-0.59	0.07	0.6	-0.63	-0.41	-0.6	0.74	1	-0.88
NTBI	**0.95**	0.26	0.24	0.02	-0.76	0.9	-0.12	-0.15	0.92	0.34	0.24	-0.41	**0.98**	1

Table A4.1(vi) Correlation Matrix of 12 Month Data
Highlighted Correlations are Significant at p<0.05
Group: Iron (Part 2)

	IL-1b	IL-6	IL-10	Serum Fe	TIBC	WBC	RBC	Hb	Platelets	MPV	TA97	TA98	TA100	TA102
Serum 8IsoP	-0.18	-0.05	0.84	-0.96	-0.45	0.26	0.78	0.23	0.92	0.54	-0.94	0.09	-0.72	-0.45
Liver 8IsoP	0.7	0.8	0.9	-0.8	0.4	-0.76	-0.47	0.17	0.34	-0.57	-0.43	-0.25	-0.39	-0.37
ALT	-0.9	-0.9	0	-0.3	-1	-0.38	-0.03	**0.9**	0.24	0.41	-0.08	-0.7	-0.48	-0.63
AST	-1	-1	-0.2	-0.1	-1	0.42	-0.04	-0.96	-0.41	-0.45	0.26	0.71	0.64	0.74
Liver 8OHdG	-0.74	-0.82	-0.9	0.75	-0.52	-0.14	0.09	0.77	0.09	0.52	0.07	-0.56	-0.31	-0.45
Serum 8OHdG	0.21	0.33	0.98	-0.99	-0.07	-0.09	0.19	0.79	0.2	0.6	-0.03	-0.54	-0.39	-0.5
Liver LPO	1	0.9	0.1	0.2	**1**	-0.2	0.49	0.82	**0.92**	0.59	-0.84	-0.46	-0.94	-0.84
Serum LPO	-0.53	-0.63	-0.99	0.9	-0.27	-0.37	-0.78	0.01	-0.81	-0.44	0.87	-0.27	0.55	0.26
Liver NO	0.2	0.32	0.98	-1	-0.09	0.38	0.45	**0.95**	0.24	**-0.98**	-0.25	-0.89	-0.75	-0.87
Serum NO	-0.88	-0.81	0.11	-0.38	-0.2	0.78	-0.57	0.26	0.39	-0.33	0.84	0.07	0.37	-0.62
Superoxide	0.95	0.98	0.64	-0.4	0.83	-0.33	-0.22	0.24	-0.65	-0.39	0.1	-0.17	-0.09	-0.3
GGT	-0.8	-0.9	-0.9	0.7	-0.6	-0.37	-0.46	0.2	-0.75	-0.18	0.3	0.08	0.18	-0.16
IL-1b	1	0.99	0.38	-0.11	0.96	-0.75	-0.67	-0.76	-0.92	0.65	0.33	0.76	0.68	0.64
IL-6	0.99	1	0.49	-0.23	0.92	0.8	0.18	0.9	0.58	-0.92	0.17	-0.7	-0.45	1
IL-10	0.38	0.49	1	-0.04	0.28	0.28	0.43	-0.12	0.68	0.27	-0.31	-0.01	-0.13	0.25
Serum Fe	-0.11	-0.23	-0.4	1	0.42	0.42	-0.89	-0.15	-0.02	0.4	0.99	0.47	0.72	-0.27
TIBC	0.96	0.92	0.28	0.42	1	0.77	0.02	0.58	0.87	-0.55	0.37	-0.36	-0.12	-0.76
WBC	-0.75	0.8	0.28	0.42	0.77	1	0.02	0.6	0.9	-0.6	0.4	-0.4	-0.1	-0.8
RBC	-0.67	0.18	0.43	-0.89	0.02	0.02	1	0.56	0.39	-0.44	-0.92	-0.8	-0.93	-0.19
Hb	-0.76	0.9	-0.12	-0.15	0.58	0.6	0.56	1	0.52	0.99	0.28	0.94	-0.8	-0.91
Platelets	-0.92	0.58	0.68	-0.02	0.87	0.9	0.39	0.52	1	-0.42	-0.03	-0.45	-0.34	-0.53
MPV	0.65	-0.92	0.27	0.4	-0.55	-0.6	-0.44	0.99	-0.42	1	0.17	0.89	0.72	0.94
TA97	0.33	0.17	-0.31	0.99	0.37	0.4	-0.92	0.28	-0.03	0.17	1	0.58	0.8	-0.14
TA98	0.76	-0.7	-0.01	0.47	-0.36	-0.4	-0.8	0.94	-0.45	0.89	0.58	1	**0.95**	0.72
TA100	0.68	-0.45	-0.13	0.72	-0.12	-0.1	-0.93	-0.8	-0.34	0.72	0.8	**0.95**	1	0.48
TA102	0.64	1	0.25	-0.72	-0.76	-0.8	-0.19	-0.91	-0.53	0.94	-0.14	0.72	0.45	1
Ferritin	-0.41	-0.48	-0.96	0.44	0.45	-0.25	-0.87	-0.88	-0.4	0.82	0.7	0.99	0.99	0.61
NTBI	0.09	0.2	0.92	-0.81	-0.09	0.58	0.56	1	0.52	-0.99	-0.28	-0.94	-0.8	-0.91

Table A4.1(vii) Correlation Matrix of 12 Month Data
Highlighted Correlations are Significant at p<0.05
Group: Iron and Aflatoxin B_1 (Part 1)

	Serum 8-IsoP	Liver 8IsoP	ALT	AST	Liver 8OHdG	Serum 8OHdG	Liver LPO	Serum LPO	Liver NO	Serum NO	Super-oxide	GGT	Ferritin	NTBI
Serum 8IsoP	1	-1	1	-0.3	1	0.8	-0.3	-0.5	-0.7	-0.6	1	1	-0.64	0.07
Liver 8IsoP	-1	1	-1	0.09	**-1**	-0.72	0.46	0.39	0.59	0.41	-0.9	-0.96	0.37	0.05
ALT	1	-1	1	-0.17	**1**	0.78	-0.38	-0.47	-0.66	-0.49	0.93	0.98	-0.27	-0.16
AST	-0.3	0.09	-0.17	1	-0.15	-0.75	-0.84	0.95	0.85	0.95	-0.52	-0.36	-0.45	-0.41
Liver 8OHdG	1	**-1**	**1**	-0.15	1	0.57	0.62	-0.5	-0.64	-0.46	0.92	0.98	0.13	0.64
Serum 8OHdG	0.8	-0.72	0.78	-0.75	0.57	1	0.3	-0.9	-1	-0.9	1	0.9	0.49	0.53
Liver LPO	0.3	0.46	-0.38	-0.84	0.62	0.3	1	-0.63	-0.44	-0.62	-0.02	-0.19	0.06	-0.61
Serum LPO	-0.5	0.39	-0.47	0.95	-0.5	-0.9	-0.63	1	0.97	**1**	-0.76	-0.64	0.53	0.55
Liver NO	-0.7	0.59	-0.66	0.85	-0.64	-1	-0.44	0.97	1	0.98	-0.89	-0.8	0.39	0.21
Serum NO	-0.6	0.41	-0.49	0.95	-0.46	-0.9	-0.62	**1**	0.98	1	-0.77	-0.65	0.09	-0.13
Superoxide	1	-0.9	0.93	-0.52	0.92	1	-0.02	-0.76	-0.89	-0.77	1	1	0.43	0.07
GGT	1	-0.96	0.98	-0.36	0.98	0.9	-0.19	-0.64	0.8	-0.65	1	1	0.21	0.63
IL-1b	-1	0.9	-0.93	0.52	-0.92	-1	0.03	0.76	0.89	0.77	**-1**	-1	-0.37	-0.23
IL-6	-0.9	0.8	-0.85	0.66	-0.84	-1	-0.16	0.86	0.96	0.87	-1	-0.9	0.09	-0.34
IL-10	-0.7	0.59	-0.66	0.85	-0.64	-1	-0.44	0.97	**1**	0.98	-0.9	-0.8	-0.08	0.09
Serum Fe	0.1	-0.26	0.17	0.94	0.2	-0.5	-0.98	0.79	0.62	0.78	-0.2	0	0.05	-0.21
TIBC	0.9	-0.87	0.91	-0.56	0.9	**1**	0.3	-0.79	-0.91	-0.8	**1**	1	-0.17	-0.03
WBC	**0.91**	-0.8	**0.99**	0.71	-0.84	**-0.92**	-0.12	-0.32	-0.52	-0.58	0.5	0.85	-0.08	0.02
RBC	0.33	0.38	-0.6	-0.47	-0.21	0.38	-0.55	0.45	-0.25	0.29	-0.38	0.41	-0.63	-0.17
Hb	0.86	0.83	-0.67	-0.52	0.63	0.7	0.1	0.29	-0.28	0.22	0.31	0.46	-0.45	0.02
Platelets	0.82	0.79	-0.61	-0.53	0.56	0.68	0.03	0.29	-0.24	-0.17	0.1	0.59	-0.71	-0.35
MPV	0.56	0.67	-0.44	0.08	0.29	0.42	0.28	0.79	0.32	**0.99**	**-1**	-0.51	-0.04	-0.02
TA97	0.56	0.51	-0.66	0.07	0.87	0.33	0.77	-0.01	-0.59	-0.91	0.87	0.86	-0.13	-0.25
TA98	-0.02	0.05	0.22	-0.35	-0.63	0.18	-0.81	0.57	0.14	0.97	-0.98	-0.44	0.25	-0.15
TA100	0.39	0.22	-0.59	-0.26	0.85	0.29	0.51	-0.52	0.5	0.6	0.66	-0.17	-0.37	-0.19
TA102	0.53	0.51	0.68	0.16	-0.52	-0.54	-0.29	-0.49	-0.28	-0.98	**0.99**	0.48	-0.34	-0.25
Ferritin	-0.64	0.37	-0.27	-0.45	0.13	0.49	0.06	0.53	0.39	0.09	0.43	0.21	1	0.24
NTBI	0.07	0.05	-0.16	-0.41	0.64	0.53	-0.61	0.55	0.21	-0.13	0.07	0.63	0.24	1

Table A4.1(vii) Correlation Matrix of 12 Month Data
Highlighted Correlations are Significant at p<0.05
Group: Iron and Aflatoxin B_1 (Part 2)

	IL-1b	IL-6	IL-10	Serum Fe	TIBC	WBC	RBC	Hb	Platelets	MPV	TA97	TA98	TA100	TA102
Serum 8IsoP	-1	-0.9	-0.7	0.1	0.9	**0.91**	0.33	0.86	0.82	0.56	0.56	-0.02	0.39	0.53
Liver 8IsoP	0.9	0.8	0.59	-0.26	-0.87	-0.8	0.38	0.83	0.79	0.67	0.51	0.05	0.22	0.51
ALT	-0.93	-0.85	-0.66	0.17	0.91	**0.99**	-0.6	-0.67	-0.61	-0.44	-0.66	0.22	-0.59	0.68
AST	0.52	0.66	0.85	0.94	-0.56	0.71	-0.47	-0.52	-0.53	0.08	0.07	-0.35	-0.26	0.16
Liver 8OHdG	-0.92	-0.84	-0.64	0.2	0.9	-0.84	-0.21	0.62	0.56	0.29	0.87	-0.63	0.85	-0.52
Serum 8OHdG	-1	-1	-1	-0.5	**1**	**-0.92**	0.38	0.7	0.68	0.42	0.33	0.18	0.29	-0.54
Liver LPO	0.03	-0.16	-0.44	-0.98	0.3	-0.12	-0.55	0.1	0.03	0.28	0.77	-0.81	0.51	-0.29
Serum LPO	0.76	0.86	0.97	0.79	-0.79	-0.32	0.45	0.29	0.29	0.79	-0.01	0.57	-0.52	-0.49
Liver NO	0.89	0.96	**1**	0.62	-0.91	-0.52	-0.25	-0.28	-0.24	0.32	-0.59	0.14	0.5	-0.28
Serum NO	0.77	0.87	0.98	0.78	-0.8	-0.58	0.29	0.22	-0.17	**0.99**	-0.91	0.97	-0.6	**-0.98**
Superoxide	**-1**	-1	-0.9	-0.2	**1**	0.5	-0.38	-0.31	0.1	**-1**	0.87	-0.98	0.66	**0.99**
GGT	-1	-0.9	-0.8	0	1	0.85	0.41	0.46	0.59	-0.51	0.86	-0.44	-0.17	0.48
IL-1b	1	1	0.9	0.2	1	-0.26	-0.4	-0.39	-0.15	-0.15	-0.17	-0.33	0.84	0.18
IL-6	1	1	1	0.4	-1	-0.63	-0.12	-0.17	-0.27	0.59	-0.79	0.44	0.21	-0.56
IL-10	0.9	1	1	-0.73	-0.39	-0.39	-0.5	-0.51	-0.67	-0.14	-0.06	0.11	-0.45	0.13
Serum Fe	0.2	0.4	-0.75	1	0.17	0.2	0.81	0.78	0.61	0.72	-0.36	0.56	-0.26	-0.73
TIBC	1	-1	-0.39	0.17	1	0.6	0.61	0.66	0.89	-0.44	0.85	-0.5	0.12	0.41
WBC	-0.26	-0.63	-0.39	0.2	0.6	1	0.6	0.6	0.8	-0.4	0.8	-0.48	0.2	0.39
RBC	-0.4	-0.12	-0.5	0.81	0.61	0.6	1	**1**	0.86	0.44	0.11	0.36	-0.46	-0.47
Hb	-0.39	-0.17	-0.51	0.78	0.66	0.6	**1**	1	0.9	0.38	0.18	0.29	-0.42	-41
Platelets	-0.15	-0.27	-0.67	0.61	0.89	0.8	0.86	0.9	1	-0.02	0.52	-0.15	-0.01	0
MPV	-0.15	0.59	-0.14	0.72	-0.44	-0.4	0.44	0.38	-0.02	1	-0.84	0.97	-0.65	-1
TA97	-0.17	-0.79	-0.06	-0.36	0.85	0.8	0.11	0.18	0.52	-0.84	1	-0.83	0.36	0.82
TA98	-0.33	0.44	0.11	0.56	-0.5	-0.48	0.36	0.29	-0.15	0.97	-0.83	1	-0.79	**-0.97**
TA100	0.84	0.21	-0.45	-0.26	0.12	0.2	-0.46	-0.42	-0.01	-0.65	0.36	-0.79	1	0.67
TA102	0.18	-0.56	0.13	-0.73	0.41	0.39	-0.47	-0.42	0	-1	0.82	**-0.97**	0.67	1
Ferritin	-0.37	0.09	-0.08	0.05	-0.17	-0.08	-0.63	-0.45	-0.71	-0.04	-0.13	0.25	-0.37	-0.34
NTBI	-0.23	-0.34	0.09	-0.21	-0.03	0.02	-0.17	0.02	-0.35	-0.02	-0.25	-0.15	-0.19	-0.25

Table A4.1(viii) Correlation Matrix of 12 Month Data
Highlighted Correlations are Significant at p<0.05
Group: Aflatoxin B_1 (Part 1)

	Serum 8-IsoP	Liver 8IsoP	ALT	AST	Liver 8OHdG	Serum 8OHdG	Liver LPO	Serum LPO	Liver NO	Serum NO	Super-oxide	GGT	Ferritin	NTBI
Serum 8IsoP	1	-0.8	-0.96	-0.21	-0.9	0.42	0.02	-0.16	0.21	-0.66	0.6	0.51	0.13	0.79
Liver 8IsoP	-0.8	1	0.59	0.76	0.98	0.21	-0.61	0.72	-0.76	0.08	0	0.1	-0.89	-0.06
ALT	-0.96	0.59	1	-1	0.7	-0.7	0.3	-0.1	0.1	0.8	-0.8	-0.7	0.24	-0.9
AST	-0.21	0.76	-1	1	0.6	0.8	-1	1	**-1**	-0.6	0.7	0.7	0.44	-0.23
Liver 8OHdG	-0.9	0.98	0.7	0.6	1	0.01	-0.44	0.57	-0.61	0.28	-0.21	-0.1	-0.17	-0.5
Serum 8OHdG	0.42	0.21	-0.7	0.8	0.01	1	-0.9	0.8	-0.8	-1	1	1	-0.59	0.89
Liver LPO	0.02	-0.61	0.3	-1	-0.44	-0.9	1	-0.99	0.98	0.74	-0.79	-0.85	0.41	-0.41
Serum LPO	-0.16	0.72	-0.1	**1**	0.57	0.8	-0.99	1	**-1**	-0.64	0.69	0.76	-0.71	0.45
Liver NO	0.21	-0.76	0.1	**-1**	-0.61	-0.8	0.98	**-1**	1	0.6	-0.7	-0.7	**0.98**	-0.55
Serum NO	-0.66	0.08	0.8	-0.6	0.28	-1	0.74	-0.64	0.6	1	**-1**	-1	-0.46	0
Superoxide	0.6	0	-0.8	0.7	-0.21	1	-0.79	0.69	-0.7	**-1**	1	0.53	0.23	0.32
GGT	0.51	0.1	-0.7	0.7	-0.1	1	-0.85	0.76	-0.7	-1	0.53	1	-0.62	**0.95**
IL-1b	0.98	-0.91	-0.9	-0.4	-0.98	0.2	0.23	-0.37	0.4	-0.5	0.82	0.64	-0.13	0.61
IL-6	0.88	-0.42	-1	0.3	-0.59	0.8	-0.46	0.33	-0.3	-0.9	-0.61	0.03	-0.22	**0.98**
IL-10	0.71	-0.14	-0.9	0.5	-0.34	0.9	-0.7	0.59	-0.5	**-1**	-0.03	-0.58	-0.39	**0.99**
Serum Fe	0.83	-0.33	-1	0.4	-0.51	0.9	-0.55	0.42	-0.4	-1	-0.5	0.28	-0.49	0.92
TIBC	-0.03	-0.58	0.3	-1	-0.4	-0.9	1	-0.98	1	0.8	-0.38	0.58	0.05	-0.2
WBC	0.02	-0.08	**-0.89**	-0.15	0.65	-0.13	-0.33	0.05	0.54	-0.59	-0.38	0.58	0.34	0.58
RBC	0.23	-0.33	0.87	0.49	0.12	0.61	0.64	0.15	0.73	-74	-0.54	-0.44	0.54	0.17
Hb	0.4	-0.19	-0.31	0.02	0.74	0.32	0.05	0.19	0.67	-67	-0.5	-0.52	0.5	0.1
Platelets	0.38	0.07	-0.43	-0.16	0.62	0.27	-0.03	0.28	-0.58	0.51	0.46	-0.51	-0.22	-0.67
MPV	-1	-0.02	-0.86	-0.42	0.03	-0.71	-0.73	-0.39	-0.14	-0.62	0.43	0.92	0.76	-0.27
TA97	0.78	-0.15	0.75	-0.31	-0.49	-0.19	-0.17	-0.52	-1	0.78	-0.23	-0.12	-0.92	0.52
TA98	-0.9	-0.2	0.15	0.75	0.1	0.32	0.55	0.31	-0.4	0.8	-0.3	-0.27	-0.97	0.54
TA100	-0.92	-0.28	0.01	0.79	0.26	0.32	0.53	0.33	-0.02	0.8	-0.33	-0.32	-0.97	0.55
TA102	0.92	-0.3	-0.03	0.79	0.3	0.32	0.52	0.33	0.37	-0.14	-0.38	-0.87	0.05	-0.05
Ferritin	0.13	-0.89	0.24	0.44	-0.17	-0.59	0.41	-0.71	**0.98**	-0.46	0.23	-0.62	1	-0.39
NTBI	0.79	-0.06	-0.9	-0.23	-0.5	0.89	-0.41	0.45	-0.55	0	0.32	**0.95**	-0.39	1

Table A4.1(viii) Correlation Matrix of 12 Month Data
Highlighted Correlations are Significant at p<0.05
Group: Aflatoxin B_1 (Part 2)

	IL-1b	IL-6	IL-10	Serum Fe	TIBC	WBC	RBC	Hb	Platelets	MPV	TA97	TA98	TA100	TA102
Serum 8IsoP	0.98	0.88	0.71	0.83	-0.03	0.02	0.23	0.4	0.38	-1	0.78	-0.9	-0.92	0.92
Liver 8IsoP	-0.91	-0.42	-0.14	-0.33	-0.58	-0.08	-0.33	-0.19	0.07	-0.02	-0.15	-0.2	-0.28	-0.3
ALT	-0.9	-1	-0.9	-1	0.3	**-0.89**	0.87	-0.31	-0.43	-0.86	0.75	0.15	0.01	-0.03
AST	-0.4	0.3	0.5	0.4	-1	-0.15	0.49	0.02	-0.16	-0.42	-0.31	0.75	0.79	0.79
Liver 8OHdG	-0.98	-0.59	-0.34	-0.51	-0.4	0.65	0.12	0.74	0.62	0.03	-0.49	0.1	0.26	0.3
Serum 8OHdG	0.2	0.8	0.9	0.9	-0.9	-0.13	0.61	0.32	0.27	-0.71	-0.19	0.32	0.52	0.32
Liver LPO	0.23	-0.46	-0.7	-0.55	1	-0.33	0.64	0.05	-0.03	-0.73	-0.17	0.55	0.53	0.52
Serum LPO	-0.37	0.33	0.59	0.42	-0.98	0.05	0.15	0.19	0.28	-0.39	-0.52	0.31	0.33	0.33
Liver NO	0.4	-0.3	-0.5	-0.4	1	0.54	0.73	0.67	-0.58	-0.14	-1	-0.4	-0.02	0.37
Serum NO	-0.5	-0.9	**-1**	-1	0.8	-0.59	-0.74	-0.67	0.51	-0.62	0.78	0.8	0.8	-0.14
Superoxide	0.82	-0.61	-0.03	-0.05	-0.38	-0.38	-0.54	-0.5	0.46	0.43	-0.23	-0.3	-0.33	-0.38
GGT	0.64	0.03	-0.58	0.28	-0.58	0.58	-0.44	-0.52	-0.51	0.92	-0.12	0.27	-0.32	-0.87
IL-1b	1	-0.06	-0.57	0.52	-0.13	-0.13	-0.91	-0.9	0.16	0.35	0.31	0.2	0.17	-0.75
IL-6	-0.06	1	-0.76	0.81	0.55	0.5	-0.29	-0.37	-0.65	-0.18	0.79	0.76	0.75	-0.42
IL-10	-0.57	-0.76	1	-0.94	-0.53	-0.48	0.75	0.82	0.58	-0.26	-0.72	-0.61	-0.57	0.9
Serum Fe	0.52	0.81	-0.94	1	0.27	0.3	-0.8	-0.84	-0.35	-0.09	0.92	0.84	0.82	-0.72
TIBC	-0.13	0.55	-0.53	0.27	1	0.3	0.11	-0.08	-0.99	0.63	0	-0.09	-0.12	-0.54
WBC	-0.13	0.5	-0.48	0.3	0.3	1	0.1	-0.15	-0.78	0.6	0.5	-0.04	-0.22	-0.64
RBC	-0.91	-0.29	0.75	-0.8	0.11	0.1	1	**0.99**	-0.08	-0.06	-0.68	-0.59	-0.56	0.75
Hb	-0.9	-0.37	0.82	-0.84	-0.02	-0.15	**0.99**	1	0.04	-0.14	-0.68	-0.57	-0.54	0.82
Platelets	0.16	-0.65	0.58	-0.35	-0.99	-0.78	-0.08	0.04	1	-0.53	-0.11	-0.03	0	0.53
MPV	0.35	-0.18	-0.26	-0.09	0.63	0.6	-0.06	-0.14	-0.53	1	-0.47	-0.61	-0.64	-0.61
TA97	0.31	0.79	-0.72	0.92	0	0.5	-0.68	-0.68	-0.11	-0.47	1	0.99	0.98	-0.39
TA98	0.2	0.76	-0.61	0.84	-0.09	-0.04	-0.59	-0.57	-0.03	-0.61	0.99	1	**1**	-0.24
TA100	0.17	0.75	-0.57	0.82	-0.12	-0.22	-0.56	-0.54	0	-0.64	0.98	**1**	1	-0.2
TA102	-0.75	-0.42	0.9	-0.72	-0.54	-0.64	0.75	0.82	0.53	-0.61	-0.39	-0.24	-0.2	1
Ferritin	-0.13	-0.22	-0.39	-0.49	0.05	0.34	0.54	0.5	-0.22	0.76	-0.92	-0.97	-0.97	0.05
NTBI	0.61	**0.98**	**0.99**	0.92	-0.2	0.58	0.17	0.1	-0.67	-0.27	0.52	0.54	0.55	-0.05

Appendix B

Biosafety Committee Certificate

UNIVERSITY OF THE WITWATERSRAND, JOHANNESBURG

Office of the Deputy Registrar (Academic and Research)
(R14/16)

MEMORANDUM

Date: 10 June 2004

To: Mr G Asare
Molecular Hepatology Research Unit
Dept of Medicine
Medical School

From: Mr I Burns
Research Office (ext.71231)

E-mail: 132AIB @ witsvmb.wits.ac.za

Interaction between dietary iron overload and Aflotoxin B_1 in hepatocarcinogenisis using experimental animals

The memo serves to confirm that, at its meeting on 29 March 2004, the University's Biosafety Committee considered your protocol for the above project. You were asked by the Chairman to expand on five points in your application. This you did on or about 30 April. The Committee is now satisfied with your revised protocol and the work may therefore proceed.

Reports

Please report on the progress of the study to the Biosafety Committee not later than 1 July 2005, or sooner in the event of any unforeseen serious adverse events. The Committee may then extend its period of approval, withdraw it, or require amendments before allowing you to proceed further, as it sees fit.

Inspection

The University Safety Officer, or any duly appointed person nominated by her, may from time to time inspect your laboratory to ensure compliance with current Health and Safety legislation. Please offer your full co-operation over any such inspection.

I am sending you a duplicate copy of this memo – please sign it and return it to me.

Memo received and contents noted: _____ Principal Investigator

cc Mr DJagibhan, University Safety Officer

MSWord/lain0015/IBCAppl

Ethics Clearance Certificate

AESC 3

STRICTLY CONFIDENTIAL

UNIVERSITY OF THE WITWATERSRAND, JOHANNESBURG

ANIMAL ETHICS SCREENING COMMITTEE

CLEARANCE CERTIFICATE NO:

2004	16	5

APPLICANT: Professor MC Kew

DEPARTMENT: Department of Medicine

PROJECT TITLE: Interaction Between Dietary Iron Overload and Aflatoxin B1 and Alcohol in Hepatocarcinogenesis Using Experimental Animals

Species	Number	Expiry Date
Rats	300 male and or female	June 2006

i) Approval is hereby given for the experiment described in the above application.

The use of these animals is subject to AESC Guidelines for the use and care of animals, is limited to the procedures specified in the application form, and to:

APPROVED subject to:

- approval for the study being granted by the **University Biosafety Committee**
- weighing each animal weekly and making the weight records available to the CAS staff
- discussing the husbandry and care of the with the CAS Director

SIGNED D. A. Gray DATE: 29 June 2004
(Chairman: ~~Animal~~ Ethics Screening Committee)

ii) I am satisfied that the persons listed in this application are competent to perform the procedures therein, in terms of Section 23(1)(c) of the Veterinary and Para-veterinary Professions Act (19 of 1982)

SIGNED D. A. Gray DATE: 29 June 2004
~~P/~~(Registered Veterinarian)

NOTE:

First-time users of the CAS should contact the Director of the CAS in order to familiarise themselves with the facilities available, and the procedures required by the CAS for the carrying out of experiments.

Modifications and Extension to Experiment

AESC 5/2003 This form is also available on disk (Word Perfect 6 or MSWord 97)

Please note that only typewritten applications will be accepted. Should additional space be required for section "i" and/or "j", please use the back of this form.

ANIMAL ETHICS SCREENING COMMITTEE

MODIFICATIONS AND EXTENSIONS TO EXPERIMENTS

a. Name: Prof. MC. Kew

b. Department: Molecular Hepatology Research Unit.

c. Experiment to be modified / extended

AESC NO: 2004 | 16 | 5

d. Project Title: Interaction between dietary iron overload and Aflatoxin B, in hepatocarcinogenisis using an experimental rat model.

e. Number and species of animals **originally approved**: 300 WISTAR RATS.

f. Number of additional animals **previously allocated** on M&Es: /

g. Total number of animals **allocated** to the experiment to date: 300

h. Number of animals **used** to date: 300

i. Specific modification / extension requested:
Blood sampling from tail vein from 30 animals. (1ml) to be done by Mr. L. Sinclair (CAS).

j. Motivation for modification / extension:
To check α-fetoprotein prior to euthanasia.

Date: 13.6.05 Signature: M.C. Kew

RECOMMENDATIONS:

Approved: inclusion of blood screening of up to 30 rats.

Date: 14/06/05 Signature: A. Gray
Chairman, AESC

November 2000

References:

Adams P, Brissot P, Powell LW. (2000) EASL International Consensus Conference on Haemochromatosis. *J Hepatol* 33(3):485-504.

Adamson RH, Correa P, Sieber SM, McIntire KR, Dalgard DW. (1976) Carcinogenicity of aflatoxin B1 in rhesus monkeys: two additional cases of primary liver cancer. *J Natl Cancer Inst.* Jul;57(1):67-78.

Aguilar F, Harris CC, Sun T, Hollstein M, Cerutti P. (1994) Geographic variation of p53 mutational profile in nonmalignant human liver. *Science.* May 27;264(5163):1317-9.

Aisen P, Listowsky I. (1980) Iron transport and storage proteins. *Annu Rev Biochem*. 49:357-93. Review.

Alexopoulos CJ, Mims CW, Blackwell MI. (1996) In: Alexopouols CJ. *Introductory Mycology.* John Wiley and Sons, Inc, New York.

Al-Refaie FN, Wicken DG, Wonke B, Kontoghiorghes GJ, Hoffbrand AV (1992) Serum non-transferrin-bound iron in beta-thalassaemia major patients treated with desferrioxamine and L_1. *Br. J. Haematol.* 82: 431-6.

Ameredes BT, Zamora R, Sethi JM, Liu HL, Kohut LK, Gligonic AL, Choi AM, Calhoun WJ. (2005) Alterations in nitric oxide and cytokine production with airway inflammation in the absence of IL-10. *J Immunol.* Jul 15;175(2):1206-13.

Ames BN, Gold LS, Willett WC. (1995) The causes and prevention of cancer. *Proc Natl Acad Sci U S A.* Jun 6;92(12):5258-65. Review.

Amstad P, Levy A, Emerit I, Cerutti P. (1984) Evidence for membrane-mediated chromosomal damage by aflatoxin B_1 in human lymphocytes. *Carcinogenesis.* Jun;5(6):719-23.

Appleton BS, Campbell TC. (1982) Inhibition of aflatoxin-initiated preneoplastic liver lesions by low dietary protein. *Nutr Cancer*. 3(4):200-6.

Arezzini B, Lunghi B, Lungarella G, Concetta G (2003). Iron overload enhances the development of experimental liver cirrhosis in mice. *Int J Bioch and Cell Biol*. 35: 486-495.

Asare GA, Paterson AC, Kew MC, Khan S, Mossanda KS. (2006a) Iron-free neoplastic nodules and hepatocellular carcinoma without cirrhosis in Wistar rats fed a diet high in iron. *J Pathol*. Jan; 208(1):82-90.

Asare GA, Mossanda KS, Kew MC, Paterson AC, Kahler-Venter CP, Siziba K. (2006b) Hepatocellular carcinoma caused by iron overload: a possible mechanism of direct hepatocarcinogenicity. *Toxicology*. Feb 15; 219(1-3):41-52. Epub 2005 Dec 6.

Atroshi F, Biese I, Saloniemi H, Ali-Vehmas T, Saari S, Rizzo A, Veijalainen P. (2000) Significance of apoptosis and its relationship to antioxidants after ochratoxin A administration in mice. *J Pharm Pharm Sci*. Sep-Dec;3(3):281-91.

Aust SD, Morehouse LA, Thomas CE. (1985) Role of metals in oxygen radical reactions. *J Free Radic Biol Med.* 1(1):3-25. Review.

Bacon BR, Healey JF, Brittenham GM, Park CH, Nunnari J, Tavill AS *et al.,* (1986) Hepatic microsomal function in rats with chronic dietary iron overload. *Gastroenterology* 90:1844-53.

Bacon BR, Tavill AS, Brittenham GM, Park CH, Recknagel RO (1983). Hepatic lipid peroxidation in rats with chronic iron overload. *J.Clin. Invest.* 71:429-39.

Bailey EA, Iyer RS, Stone MP, Harris TM, Essigmann JM. (1996) Mutational properties of the primary aflatoxin B_1-DNA adduct. Proc Natl Acad Sci U S A. Feb 20; 93(4):1535-9.

Bali PK, Zak O, Aisen P. (1991) A new role for the transferrin receptor in the release of iron from transferrin. *Biochemistry* Jan 15;30(2):324-8.

Baranano DE, Wolosker H, Bae BI, Barrow RK, Snyder SH, Ferris CD. (2000) A mammalian iron ATPase induced by iron. *J Biol Chem.* May 19;275(20):15166-73.

Barbacid M. (1990) ras oncogenes: their role in neoplasia. *Eur J Clin Invest*. Jun;20(3):225-35. Review.

Bauer-Hofmann R, Buchmann A, Wright AS, Schwarz M. (1990) Mutations in the Ha-ras proto-oncogene in spontaneous and chemically induced liver tumours of the CF1 mouse. *Carcinogenesis* Oct;11(10):1875-7.

Beardall JM, Miller JD (1994) Diseases in humans with mycotoxins as possible causes, in: Miller JD, Trenholm HL (Eds), Mycotoxins in Grain: Compounds Other Than Aflatoxins, Eagan Press, St. Paul, MN, pp. 487-539.

Beckman JS, Beckman TW, Chen J, Marshall PA, Freeman BA. (1990) Apparent hydroxyl radical production by peroxynitrite: implications for endothelial injury from nitric oxide and superoxide. *Proc Natl Acad Sci* USA 87: 1620-4.

Becognee AK, Mobio TA, Ennamany R, Fleurat-Lessard F, Shier WT, Badria F, Creppy EE. (1998) Cytotoxicity of fumonisin B_1: implication of lipid peroxidation and inhibition of protein and DNA syntheses. *Arch Toxicol*. Mar;72(4):233-6.

Bennett JW, Klich M., (2003). Mycotoxins. *Clin Microbiol Rev*. 16(3):497-516.

Bennett JW, Klich M. (2003) Mycotoxins. *Clin Microbiol Rev*. Jul;16(3):497-516. Review.

Bennett RA, Essigmann JM, Wogan GN. (1981) Excretion of an aflatoxin-guanine adduct in the urine of aflatoxin B1-treated rats. *Cancer Res*. Feb;41(2):650-4.

Benson AB 3rd. (1993) Oltipraz: a laboratory and clinical review. *J Cell Biochem Suppl*. 17F:278-91. Review.

Boelsterli UA, Wolf A, Goldlin C. (1993) Oxygen free radical production mediated by cocaine and its ethanol-derived metabolite, cocaethylene, in rat hepatocytes. *Hepatology* Nov;18(5):1154-61.

Boix-Ferrero J, Pellin A, Blesa R, Adrados M, Llombart-Bosch A. (1999) Absence of p53 gene mutations in hepatocarcinomas from a Mediterranean area of Spain. A study of 129 archival tumour samples. *Virchows Arch.* Jun; 434(6):497-501.

Bolton MG, Munoz A, Jacobson LP, Groopman JD, Maxuitenko YY, Roebuck BD, Kensler TW. (1993) Transient intervention with oltipraz protects against aflatoxin-induced hepatic tumorigenesis. *Cancer Res.* Aug 1; 53(15):3499-504.

Bothwell T, Abrahams C, Bradlow BA, Charlton RW (1965). Idiopathic and Bantu hemochromatosis. *Arch Path* 79:163.

Bothwell TH and Isaacson C (1962). Siderosis in the Bantu. A comparison of incidence in males and females. *Br Med J* 1:522.

Bothwell TH, Brandlow BA (1960). Siderosis in the Bantu. A combined histopathological and chemical study. *Arch Pathol*. 70:279-292.

Bothwell TH, Seftel H, Jacobs P, Torrance JD, Baumslag N (1964). Iron overload in Bantu subjects. Studies on the availability of iron in Bantu beer. *Am J Clin.* Jan;14:47-51.

Bradbear RA, Bain C, Siskind V, Schofield FD, Webb S, Axelsen EM, Halliday JW, Bassett ML, Powell LW (1985) Cohort study of internal malignancy in genetic hemochromaosis and other chronic non-alcoholic liver diseases. *J Natl Cancer Inst*. 75:81-84.

Brage A, Tome S, Figueruela B, Abdulkader I, Martinez J, Varo E. (2002) Hepatoma in a 40-year old male with hereditary hemochromatosis in the absence of cirrhosis. Implications of molecular diagnosis. *Rev Esp Enferm Dig*. Aug; 94(8):493-9. English, Spanish.

Bridle KR, Crawford DH, Fletcher LM, Smith JL, Powell LW, Ramm GA. (2003) Evidence for a sub-morphological inflammatory process in the liver in haemochromatosis. *J Hepatol.* Apr;38(4):521-5.

Britton RS (1996): Metal-induced hepatotoxicity. *Seminars in liver disease*: Vol 16. No. 1:3-12.

Britton RS, Leicester KL, Bacon BR. (2002) Iron toxicity and chelation therapy. *Int J Hematol.* Oct;76(3):219-28. Review.

Britton RS, O'Neill R, Bacon BR (1990). Chronic dietary overload in rats. *Hepatology* 11:789-804.

Britton RS, O'Neill R, Bacon BR (1991): Chronic dietary iron overload in rats results in impaired calcium sequestration by hepatic mitochondria and microsomes. *Gastroenterology* 101: 806-11.

Brody T. (1999) Nutritional Biochemistry. 2nd edition. San Diego: Academic Press.

Brown JP, Hewick RM, Hellstrom I, Hellstrom KE, Doolittle RF, Dreyer WJ. (1982) Human melanoma-associated antigen p97 is structurally and functionally related to transferrin. *Nature.* Mar 11; 296(5853):171-3.

Buchanan WM (1966). Siderosis in Rhodesian Africans. *Central Afr J Med* 12:199

Buchanan WM (1967). Bantu siderosis with special reference to Rhodesian Africans. University College of Rhodesia Faculty of Medicine Research Series. Vol 1. Salisbury: University College of Rhodesia, 5-30.

Buchanan WM (1969) Bantu siderosis- A review. *Central Afr J Med* 15:105.

Buckley GB (1994). Reactive oxygen metabolites and reperfusion injury: aberrant triggering of reticuloendothelial function. *Lancet* 344: 934-936.

Buege JA and Aust SD (1978). Microsomal lipid peroxidation. *Methods Enzymol*. 302-310.

Buetler TM, Slone D, Eaton DL. (1992) Comparison of the aflatoxin B1-8,9-epoxide conjugating activities of two bacterially expressed alpha class glutathione S-transferase isozymes from mouse and rat. *Biochem Biophys Res Commun.* Oct 30;188(2):597-603.

Bulger EM, Helton WS. (1998) Nutrient antioxidants in gastrointestinal diseases. *Gastroenterol Clin North Am*. Jun;27(2):403-19. Review.

Busby Jr.WF, Wogan GN (1985) Aflatoxins, in: Searle CE (Ed.), Chemical Carcinogens, 2nd ed, American Chemical Society, Washington, DC pp. 945-1136.

Busby WF, Jr and Wogan GN (1984) Aflatoxins. In Searle, C (ed.) Chemical Carcinogens. American Chemical Society, Washington, DC, pp. 945-1136.

BusbyWF and Wogan GN. (1985) Aflatoxins, in: CE Searle (Ed.), Chemical Carcinogens, 2nd edition, American Chemical Society, Washington, DC pp. 945-1136.

Cairo G, Pietrangelo A. (2000) Iron regulatory proteins in pathobiology. *Biochem J.* Dec 1; 352 Pt 2:241-50. Review.

Cao G, Alessio HM, and Cutler RG (1993). Oxygen-radical absorbance capacity assay for antioxidants. *Free Radic. Biol. Med.* 14:303-311.

Cerutti PA. (1994). Oxy-radicals and cancer. *Lancet;* 344:862-863.

Cheeseman KH (1993). Lipid peroxidation and cancer. In *DNA and Free Radicals*. Ed. Halliwell B and Aruoma OI, pp 109-144, Ellis Horwood: London.

Chisolm GM (1991). Cytotoxicity of oxidized lipoproteins. *Current Opinions In Lipodology*. 2: 311-316.

Ciechanover A, Schwartz AL, Dautry-Varsat A, Lodish HF. (1983) Kinetics of internalization and recycling of transferrin and the transferrin receptor in a human hepatoma cell line. Effect of lysosomotropic agents. *J Biol Chem.* Aug 25;258(16):9681-9.

Cighetti G, Duca L, Bortone L, Sala S, Nava I, Fiorelli G, Cappellini MD. (2002) Oxidative status and malondialdehyde in beta-thalassaemia patients. *Eur J Clin Invest.* Mar; 32 Suppl 1:55-60.

College of American Pathologists (CAP). Chemistry Survey (1997) Sets C3, C4, C5, C6, C7, C8a Participant Summary 1997 CAP, April Northfield, IL.

Cortes J, Kurzrock R. (1997) Interleukin-10 in non-Hodgkin's lymphoma. *Leuk Lymphoma.* Jul; 26(3-4):251-9. Review.

Coulombe RA, Jr. (1994) Non-hepatic disposition and effects of aflatoxin B1, in: DL Eaton, JD Groopman (Eds)., The Toxicology of Aflatoxins: Human Health, Veterinary, and Agricultural Significance, Academic Press, San Diego pp. 137-148.

Coulombe, RA, Jr., (1994). Non-hepatic disposition and effects of aflatoxin B1, in: Eaton DL, Groopman JD (Eds.), The Toxicology of Aflatoxins: Human Health, Veterinary, and Agricultural Significance, Academic Press, San Diego, pp. 89-101.

Croy RG, Wogan GN. (1981) Temporal patterns of covalent DNA adducts in rat liver after single and multiple doses of aflatoxin B1. *Cancer Res.* Jan; 41(1):197-203.

Curnutte JT and Babior BM (1987). Chronic granulomatous disease. *Advances in Human Genetics*. 16: 229-245.

Dana F, Becherer PR, Bacon BR. (1994) Hepatits C virus: what recent studies can tell us. *Postgrad Med.* 95(6):121-30.

Dautry-Varsat A, Ciechanover A, Lodish HF. (1983) pH and the recycling of transferrin during receptor-mediated endocytosis. *Proc Natl Acad Sci U S A.* Apr; 80(8):2258-62.

Davidson NE, Egner PA, Kensler TW. (1990) Transcriptional control of glutathione S-transferase gene expression by the chemoprotective agent 5-(2-pyrazinyl)-4-methyl-1,2-dithiole-3-thione (oltipraz) in rat liver. *Cancer Res.* Apr 15;50(8):2251-5.

De Luca C, Filosa A, Grandinetti M, Maggio F, Lamba M, Passi S. (1999) Blood antioxidant status and urinary levels of catecholamine metabolites in beta-thalassemia. *Free Radic Res.* Jun; 30(6):453-62.

Dean RT, Fu S, Stocker R, Davies MJ. (1997) Biochemistry and pathology of radical-mediated protein oxidation. *Biochem J.* May 15;324 (Pt 1):1-18. Review.

Dekkers JC, van Doornen LJP, Kemper HCG. (1996) The Role of Antioxidant Vitamins and Enzymes in the Prevention of Exercise-Induced Muscle Damage. *Sports Med.* 21: 213-238.

Deugnier Y, Guyander D, Crantock L, Lopez J, Turlin B, Yaouand J, Jouanolle H et al (1993) Primary liver cancer in genetic hemochromatosis: a clinical, pathological and pathogenic study of 54 cases. *Gastroenterology* 104:228-234.

Deugnier Y, Turlin B. (2001) Iron and hepatocellular carcinoma. *J Gastroenterol Hepatol*. May;16(5):491-4. Review.

Dienier UL, Cole RJ, Sanders TH, Payne GA, Lee SL, Klich ML., (1987). Epidemiology of aflatoxin formation by Aspergillus flavus. *Ann. Rev. Phytopathol*. 25:249-270.

Dix TA and Aitkens J (1993). Mechanisms and biological relevance of lipid peroxidation. *Chemical Research In Toxicology.* 6: 2-18.

Donato F, Tagger A, Gelatti U, Parrinello G, Boffetta P, Albertini A, Decarli A, Trevisi P, Ribero ML, Martelli C, Porru S, Nardi G. (2002) Alcohol and hepatocellular carcinoma: the effect of lifetime intake and hepatitis virus infections in men and women. *Am J Epidemiol. Feb 15;155(4):323-31*.

Duflot A, Hollstein M, Mehrotra R, Trepo C, Montesano R, Cova L. (1994) Absence of p53 mutation at codon 249 in duck hepatocellular carcinomas from the high incidence area of Qidong (China). *Carcinogenesis.* Jul;15(7):1353-7.

Dugyala RR, Sharma RP. (1996) The effect of aflatoxin B_1 on cytokine mRNA and corresponding protein levels in peritoneal macrophages and splenic lymphocytes. *Int J Immunopharmacol*. Oct;18(10):599-608.

Eaton DL and Gallagher EP. (1994). Mechanisms of aflatoxin carcinogenesis. *Annu Rev Pharmacol Toxicol.* 34:135-72. Review.

Eaton DL, Gallagher EP (1994) Mechanisms of aflatoxin carcinogenesis. *Annu Rev Pharmacol Toxicol.* 34:135-72. Review.

Eaton DL, Gallagher EP. (1994) Mechanisms of aflatoxin carcinogenesis. *Annu Rev Pharmacol Toxicol.* 34:135-72. Review.

Eaton DL, Groopman JD (Eds). (1994) The Toxicology of Aflatoxins, Human Health, Veterinary, and Agricultural Significance, Academic Press, San Diego.

Edling JE, Britton RS, Grisham MB, bacon BR (1990) Increased unwinding of hepatic double-stranded DNA in rats with chronic dietary iron overload. *Gastroenterology* 98:A585.

Egyed A. (1988) Carrier mediated iron transport through erythroid cell membrane. *Br J Haematol.* Apr;68(4):483-6.

Eisenstein RS, Ross KL. (2003) Novel roles for iron regulatory proteins in the adaptive response to iron deficiency. *J Nutr*. May;133(5 Suppl 1):1510S-6S. Review.

Essigmann JM, Croy RG, Bennett RA, Wogan GN. (1982) Metabolic activation of aflatoxin B_1: patterns of DNA adduct formation, removal, and excretion in relation to carcinogenesis. *Drug Metab Rev*. 13(4):581-602. Review.

Essigmann JM, Green CL, Croy RG, Fowler KW, Buchi GH, Wogan GN. (1983) Interactions of aflatoxin B_1 and alkylating agents with DNA: structural and functional studies. *Cold Spring Harb Symp Quant Biol*. 47 Pt 1:327-37.

Esterbauer H. (1993) Cytotoxicity and genotoxicity of lipid-oxidation products. *Am J Clin Nutr*. May; 57(5 Suppl):779S-785S; discussion 785S-786S. Review.

Feder JN, Penny DM, Irrinki A, Lee VK, Lebron JA, Watson N, Tsuchihashi Z, Sigal E, Bjorkman PJ, Schatzman RC. (1998) The hemochromatosis gene product complexes with the transferrin receptor and lowers its affinity for ligand binding. *Proc Natl Acad Sci U S A*. Feb 17; 95(4):1472-7.

Floyd RA. (1983) Direct demonstration that ferrous ion complexes of di- and triphosphate nucleotides catalyze hydroxyl free radical formation from hydrogen peroxide. Arch Biochem Biophys. Aug;225(1):263-70.

Foster PL, Eisenstadt E, Miller JH. (1983) Base substitution mutations induced by metabolically activated aflatoxin B_1. *Proc Natl Acad Sci U S A*. May; 80(9):2695-8.

Frenkel K, Gleichauf C. (1991) Hydrogen peroxide formation by cells treated with a tumor promoter. *Free Radic Res Commun*. 12-13 Pt 2:783-94.

Frenkel K. (1992) Carcinogen-mediated oxidant formation and oxidative DNA damage. *Pharmacol Ther*. 53(1):127-66. Review.

Frigerio R, Mela Q, Passiu G, Cacace E, La Nasa G, Perpignano G *et al*; (1984). Iron overload and lysosomal stability in β-thalassaemia intermedia and trait: correlation between serum ferritin and serun N-acetyl-β-D - glucosaminidase levels. *Scand J Haematol* 33:252-5.

Gan S, Skipper PL, Peng X, Groopman JD, Chen J, Wogan GN, Tannenbaum SR (1988) Serum albumin adducts in the molecular epidemiology of aflatoxin carcinogenesis: correlation with aflatoxin B1 intake and urinary excretion of aflatoxin m1. *Carcinogenesis* 9, 1323-1325.

Garner RC, Wright CM. (1973) Induction of mutations in DNA-repair deficient bacteria by a liver microsomal metabolite of aflatoxin B_1. *Br J Cancer*. Dec;28(6):544-51.

Garrick MD, Gniecko K, Liu Y, Cohan DS, Garrick LM. (1993) Transferrin and the transferrin cycle in Belgrade rat reticulocytes. *J Biol Chem.* Jul 15;268(20):14867-74.

Gaziano JM, Hatta A, Flynn M, Johnson EJ, Krinsky NI, Ridker PM, Hennekens CH, and Frei B (1995). Supplementation with beta-carotene *in vivo* and *in vitro* does not inhibit low density lipoprotein oxidation. *Atherosclerosis* 112:187-195.

Geissler FT, Henderson WR. (1988) Inability of aflatoxin B_1 to stimulate arachidonic acid metabolism in human polymorphonuclear and mononuclear leukocytes. *Carcinogenesis.* Jul; 9(7):1135-8.

Ghosh RC, Chauhan HV, Roy S. (1990) Immunosuppression in broilers under experimental aflatoxicosis. *Br Vet J*. Sep-Oct; 146(5):457-62.

Goldfarb AH. (1999) Nutritional antioxidants as therapeutic and preventative modalities in exercise-induced muscle damage. *Can. J. Appl. Physiol*. 24:249-266.

Gordeuk VK (1992). Hereditary and nutritional iron overload. *Baillière's Clin Haematol* 5:169-186.

Gordeuk VR, Boyd RD, Brittenham GM (1986). Dietary iron overload persists in rural sub-Saharan Africa. *Lancet* 1:1310.

Govoni G, Gros P. (1998) Macrophage NRAMP1 and its role in resistance to microbial infections. *Inflamm Res.* Jul; 47(7):277-84. Review.

Granger DN (1988). Role of xanthine oxidase and granulocytes in ischaemia reperfusion injury. *Am J Physiol*. 255: H1269-H1275.

Griess P. (1879) Bemerkungen zu der abhandlung der HH Weselsky und Benedikt "Ueber einige azoverbindungen." *Chem. Ber*. 12, 426.

Groopman JD, Cain LG, Kensler TW., (1988). Aflatoxin exposure in human populations: measurements and relationship to cancer. *Crit Rev Toxicol*. 19(2):113-45. Review.

Groopman JD, Cain LG, Kensler TW. (1988) Aflatoxin exposure in human populations: measurements and relationship to cancer. *Crit Rev Toxicol*. 19(2):113-45. Review.

Groopman JD, Roebuck BD, Kensler TW. (1992) Molecular dosimetry of aflatoxin DNA adducts in humans and experimental rat models. *Prog Clin Biol Res*. 374:139-55. Review.

Gurtoo HL, Bejba N. (1974) Hepatic microsomal mixed function oxygenase: enzyme multiplicity for the metabolism of carcinogens to DNA-binding metabolites. *Biochem Biophys Res Commun*. Nov 27; 61(2):735-42.

Gurtoo HL, Dave CV. (1975) In vitro metabolic conversion of aflatoxins and benzo(alpha)pyrene to nucleic acid-binding metabolites. *Cancer Res.* Feb;35(2):382-9.

Gutteridge JMC. (1993) Free radicals in disease processes: a complication of cause and consequence. *Free Radic Res Commun* 19: 141-58.

Gutteridge JMC. (1983) Antioxidant properties of caeruloplasmin towards iron and copper dependent oxygen radical formation. *FEBS Lett* 157:30-40.

Halliwell B and Gutteridge JM (1992). Biologically relevant metal ion-dependent hydroxyl radical generation. An update. *FEBS Lett*, Jul 27;307(1):108-12.

Halliwell B and Gutteridge JMC (1989). Free Radicals in Biology and Medicine. 2nd ed. Oxford University Press.

Halliwell B and Gutteridge JMC (1990). Role of free radicals and catalytic metal ions in human disease: an overview. *Methods Enzymol* 186:1-85.

Handelman GJ and Pryor WA (1999). Evaluation of antioxidant status in humans. In: Antioxidant status, diet, nutrition and health. (Papas AM ed), pp. 37-62. CRC Press, Boca Raton, FL.

Harford JB, Rouault TA, Huebers HA and Klausner RD. (1994) Molecular mechanisms of iron metabolism. In The Molecular Basis of Blood Diseases, G.Stamataoyannopoulos, A.W. Nienhuis, P.W. Majerus and H. Varmus, eds. (Philadelphia: WB. Saunders Co.) pp. 351-378.

Harlan, UK (2000). Price List 2000. pg 11.

Harris CC, Hollstein M. (1993) Clinical implications of the p53 tumor-suppressor gene. *N Engl J Med*. Oct 28;329(18):1318-27. Review.

Harrison SA, Bacon BR. (2005) Relation of hemochromatosis with hepatocellular carcinoma: epidemiology, natural history, pathophysiology, screening, treatment, and prevention. *Med Clin North Am*. Mar; 89(2):391-409. Review.

Hayes GR, Enns CA, Lucas JJ. (1992) Identification of the O-linked glycosylation site of the human transferrin receptor. Glycobiology. Aug; 2(4):355-9.

Hayes JD, Judah DJ, Neal GE, Nguyen T. (1992) Molecular cloning and heterologous expression of a cDNA encoding a mouse glutathione S-transferase Yc subunit possessing high catalytic activity for aflatoxin B1-8,9-epoxide. *Biochem J. Jul* 1; 285 (Pt 1):173-80.

Heinonen JT, Fisher R, Brendel K, Eaton DL. (1996) Determination of aflatoxin B_1 biotransformation and binding to hepatic macromolecules in human precision liver slices. *Toxicol Appl Pharmacol*. Jan;136(1):1-7.

Hellerbrand C, Poppl A, Hartmann A, Scholmerich J, Lock G. (2003) HFE C282Y heterozygosity in hepatocellular carcinoma: evidence for an increased prevalence. *Clin Gastroenterol Hepatol*. Jul;1(4):279-84.

Heubers HA, Finch CA (1987) The physiology of transferrin and transferrin receptors. *Physiological Reviews* 67, 520.

Higginson J, Gerritsen T, Walker ARP (1953). Siderosis in the Bantu of southern Africa. *Am J Pathol* 29:779.

Hinton DM, Myers MJ, Raybourne RA, Francke-Carroll S, Sotomayor RE, Shaddock J, Warbritton A, Chou MW. (2003) Immunotoxicity of aflatoxin B_1 in rats: effects on lymphocytes and the inflammatory response in a chronic intermittent dosing study. *Toxicol Sci*. Jun;73(2):362-77. Epub 2003 Apr 15.

Hirota N and Williams G (1979). The sensitivity and heterogencity of histochemical markers for altered foci involved in liver carcinogenesis. *Am J Pathol* 95:317-328.

Hollstein M, Sidransky D, Vogelstein B, Harris CC. (1991) p53 mutations in human cancers. *Science*. Jul 5; 253(5015):49-53. Review.

Horvath ME, Faux SP, Blazovics A, Feher J (2001) Lipid and DNA oxidative damage in experimentally induced hepatic porphyria in C57BL/10ScSn mice. *Z Gastroenterol.* Jun;39(6):453-5, 458.

Houglum K, Filip M, Witztum JL and Chojkier M (1990). Malondialdehyde and 4-Hydroxynonal protein adducts in plasma and liver of rats with iron overload. *J Clin Invest* 86:1991-1998.

Hruszkewycz AM (1988). Evidence of mitochondrial DNA damage by lipid peroxidation. *Biochem Biophys Res Commun* 153: 191-7.

Hsieh DPH, Wong ZA, Wong JJ, Michas C, Ruebner BH (1977). Comparitive metabolism of aflatoxin. In Mycotoxins in Human and Animal Health (JV Rodricks, CW Hesseltine, and MA Mehlman, Ed). Pp. 37-50. Park Forest South, IL: Pathotox Publishers.

Hsieh DPH. Genotoxicity of mycotoxins, in :PL. Chambers, P. Gebring, F. Sakai (Eds.), New Concenpts and Developments in Toxicology, Elsevier, New York, 1986, pp. 251-259.

Hultcrantz R, Arborgh B, Wroblewski R, Ericsson JL. (1980) Studies on the rat liver following iron overload. *Acta Pathol Microbiol Scand [A]*. Nov;88(6):341-53.

Iancu TC and Shiloh H (1994). Morphological observations in iron overload: an update. *Adv Exp Med Biol* 356: 255-65.

Iancu TC, Ward RJ and Peters TJ (1987). Ultrastructural observation in the carbonyl iron-fed rat; an animal model for hemochromatosis. *Virchows Arch B* 53:208-217.

Imlay JA, Chin SM, Linn S (1988). Toxic DNA damage by hydrogen peroxide through the Fenton reaction in vivo and *in vitro*. *Science* 240:640-2.

Inafuku T, Nozaki H. (2000) [Liver function of the most elderly patients] [Article in Japanese] *Rinsho Byori.* Mar;48(3):227-32.

International Agency for Research on Cancer (IARC)., (1993). IARC monographs on the evaluation of carcinogenic risks to humans. Some naturally occurring substances: Food items and constituents, hetercyclic aromatic amines and mycotoxins, Vol. 56, IARC, Lyon, France, pp. 41-524.

Irvin TR, Wogan GN. (1984) Quantitation of aflatoxin B_1 adduction within the ribosomal RNA gene sequences of rat liver DNA. *Proc Natl Acad Sci U S A.* Feb; 81(3):664-8.

Ivan M, Kondo K, Yang H, Kim W, Valiando J, Ohh M, Salic A, Asara JM, Lane WS, Kaelin WG Jr. (2001) HIFalpha targeted for VHL-mediated destruction by proline hydroxylation: implications for O_2 sensing. *Science*. Apr 20;292(5516):464-8. Epub 2001 Apr 5.

Jaakkola P, Mole DR, Tian YM, Wilson MI, Gielbert J, Gaskell SJ, Kriegsheim Av, Hebestreit HF, Mukherji M, Schofield CJ, Maxwell PH, Pugh CW, Ratcliffe PJ. (2001) Targeting of HIF-alpha to the von Hippel-Lindau ubiquitylation complex by O_2-regulated prolyl hydroxylation. *Science*. Apr 20;292(5516):468-72. Epub 2001 Apr 5.

Jakab GJ, Hmieleski RR, Zarba A, Hemenway DR, Groopman JD. (1994) Respiratory aflatoxicosis: suppression of pulmonary and systemic host defenses in rats and mice. *Toxicol Appl Pharmacol*. Apr; 125(2):198-205.

Jialal I, Fuller CJ, Huet BA (1995). Effect of alpha-tocopherol supplementation on LDL oxidation. *Arterioscler Thromb Vasc Biol*. Feb;15(2)190-8.

Jing SQ, Trowbridge IS. (1987) Identification of the intermolecular disulfide bonds of the human transferrin receptor and its lipid-attachment site. *EMBO J. Feb;* 6(2):327-31.

Kaczmarski MJ, Wojicicki J, Samochowiee L, Dutkiewicz, Synch Z. (1999). The influence of exogenous antioxidants and physical exercise on some parameters associated with production and removal of free radicals. *Pharmazie* 54: 303-306.

Karlsson J. (1997) Introduction to Nutraology and Radical Formation, In: Antioxidants and Exercise, Illinois: Human kinetics Press pp. 1-143.

Katiyar S, Dash BC, Thakur V, Guptan RC, Sarin SK, Das BC. (2000) p53 tumor suppressor gene mutations in hepatocellular carcinoma patients in India. *Cancer.* Apr 1;88(7):1565-73.

Kensler TW, Egner PA, Davidson NE, Roebuck BD, Pikul A, Groopman JD. (1986) Modulation of aflatoxin metabolism, aflatoxin-N7-guanine formation, and hepatic tumorigenesis in rats fed ethoxyquin: role of induction of glutathione S-transferases. *Cancer Res*. Aug;46(8):3924-31.

Kensler TW, Egner PA, Dolan PM, Groopman JD, Roebuck BD. (1987) Mechanism of protection against aflatoxin tumorigenicity in rats fed 5-(2-pyrazinyl)-4-methyl-1,2-dithiol-3-thione (oltipraz) and related 1,2-dithiol-3-thiones and 1,2-dithiol-3-ones. *Cancer Res*. Aug 15;47(16):4271-7.

Kensler TW, Groopman JD, Eaton DL, Curphey TJ, Roebuck BD. (1992) Potent inhibition of aflatoxin-induced hepatic tumorigenesis by the monofunctional enzyme inducer 1,2-dithiole-3-thione. *Carcinogenesis*. Jan;13(1):95-100.

Kew MC (1994). Epidemiology of Hepatocellular Carcinoma. *Viral hepatitis and Liver Diseases* 681-684.

Kew MC, Yu MC, Kedda MA, Coppin A, Sarkin A, Hodkinson J. (1997) The relative roles of hepatitis B and C viruses in the etiology of hepatocellular carcinoma in southern African blacks. *Gastroenterology Jan;112(1):184-7.*

Kew MC. (2003) Synergistic interaction between aflatoxin B_1 and hepatitis B virus in hepatocarcinogenesis. *Liver Int. Dec.* 23(6):405-9. *Review.*

Kirk GD, Camus-Randon AM, Mendy M, Goedert JJ, Merle P, Trepo C, Brechot C, Hainaut P, Montesano R. (2000) Ser-249 p53 mutations in plasma DNA of patients with hepatocellular carcinoma from The Gambia. *J Natl Cancer Inst*. Jan 19; 92(2):148-53.

Klausner RD, Van Renswoude J, Ashwell G, Kempf C, Schechter AN, Dean A, Bridges KR. (1983) Receptor-mediated endocytosis of transferrin in K562 cells. *J Biol Chem.* Apr 25; 258(8):4715-24.

Knowdley KV (2004) Iron, Hemochromatosis, and Hepatocellular Carcinoma. Gastroenterology 127:S79-S86.

Knutson MD, Handelman GY and Viteri FE (2000). Methods for measuring ethane and pentane in expired air from rats and humans. *Free Radic. Biol. Med.* 28:514-519.

Kuhn LC, McClelland A, Ruddle FH. (1984) Gene transfer, expression, and molecular cloning of the human transferrin receptor gene. *Cell*. May;37(1):95-103.

Kuo PC, Slivka A. (1994) Nitric oxide decreases oxidant-mediated hepatocyte injury. J *Surg Res*. Jun;56(6):594-600.

La Russo NF (1989) Hepatic lysosomes in intracellular digestion and biliary secretion. In: Forte JG (eds) Handbook of physiology. The gastrointestinal system III. Bethesda, *American Physiological Society* pp. 677-91.

Lee P, Peng H, Gelbart T, Wang L, Beutler E (2005) Regulation of hepcidin transcription by interleukin-1 and interleukin-6. *Proc Natl Acad Sci U S A.* Feb 8;102(6):1906-10.

Lemmer ER, Gelderblom WC, Shephard EG, Abel S, Seymour BL, Cruse JP, Kirsch RE, Marasas WF, Hall PM. (1999) The effects of dietary iron overload on fumonisin B_1-induced cancer promotion in the rat liver. *Cancer Lett.* Nov 15;146(2):207-15.

Leon M, Kew MC. (1995) Analysis of ras gene mutations in hepatocellular carcinoma in southern African blacks. *Anticancer Res*. May-Jun;15(3):859-61.

Levine RL, Garland D, Oliver CN, Amici A, Climent I, Lenz AG, Ahn BW, Shaltiel S and Stadtman ER (1990). Determination of carbonyl content in oxidatively modified proteins. *Methods Enzymol.* 186:464-478.

Link G, Pinson A, Hershko C (1994). Ability of the orally effective iron chelators dimethyl- and diethyl-hydroxypyrid-4-one and of deferoxamine to restore sarcolemmal thiolic enzyme activity in iron loaded heart cells. *Blood* 83:2692-7.
Loechler EL, Teeter MM, Whitlow MD. (1988) Mapping the binding site of aflatoxin B_1 in DNA: molecular modeling of the binding sites for the N(7)-guanine adduct of aflatoxin B_1 in different DNA sequences. *J Biomol Struct Dyn*. Jun; 5(6):1237-57.

Loechler EL. (1994) Mechanisms by which aflatoxins and other bulky carcinogens induce mutations, in: DL Eaton, JD Groopman (Eds.), the toxicology of Aflatoxins: human Health, Veterinary, and Agricultural significance, Academic Press, San Diego pp. 149-178.

Low H, Grebing C, Lindgren A, Tally M, Sun IL, Crane FL. (1987) Involvement of transferrin in the reduction of iron by the transplasma membrane electron transport system. *J Bioenerg Biomembr*. Oct;19(5):535-49.

MacPhail AP, Derman DP, Bothwell TH, Torrance JD, Charlton RW, Du Plessi JP, Visagie ME (1979a). Serum ferritin concentrations in black miners. *S Afr Med J* 55: 758.

MacPhail AP, Simmon MO, Torrance JD, Bothwell TH, Isaacson C (1979b). Changing patterns of dietary iron overload in black South Africans. *Am J Clin Nutr* 32: 1272.

Mandishona E, McPhail AP, Gordeuk VR *et al*., (1998). Dietary iron overload as a risk factor for hepatocellular carcinoma in black Africans. *Hepatology* 27:1563.

Marin DE, Taranu I, Bunaciu RP, Pascale F, Tudor DS, Avram N, Sarca M, Cureu I, Criste RD, Suta V, Oswald IP. (2002) Changes in performance, blood parameters, humoral and cellular immune responses in weanling piglets exposed to low doses of aflatoxin. *J Anim Sci.* May;80(5):1250-7.

Maron DM and Ames BN (1983). Revised methods for the Salmonella mutagenicity test. *Mutat Research*, May; 113 (3-4):173 –215.

Massey TE. (1996). Cellular and molecular targets I pulmonary chemical carcinogenesis: studies with aflatoxin B_1. *Can. J. Physiol. Pharmacol*. 74: 621-628.

Maxuitenko YY, MacMillan DL, Kensler TW, Roebuck BD. (1993) Evaluation of the post-initiation effects of oltipraz on aflatoxin B1-induced preneoplastic foci in a rat model of hepatic tumorigenesis. *Carcinogenesis*. Nov;14(11):2423-5.

Mazurier J, Metz-Boutigue MH, Jolles J, Spik G, Montreuil J, Jolles P. (1983) Human lactotransferrin: molecular, functional and evolutionary comparisons with human serum transferrin and hen ovotransferrin. *Experientia*. Feb 15;39(2):135-41.

McCord JM, Day ED Jr. (1978) Superoxide-dependent production of hydroxyl radical catalyzed by iron-EDTA complex. *FEBS Lett.* Feb 1;86(1):139-42.

McKie AT, Marciani P, Rolfs A, Brennan K, Wehr K, Barrow D, Miret S, Bomford A, Peters TJ, Farzaneh F, Hediger MA, Hentze MW, Simpson RJ. (2000) A novel duodenal iron-regulated transporter, IREG1, implicated in the basolateral transfer of iron to the circulation. *Mol Cell.* Feb;5(2):299-309.

McLaren GD, Muir WA, Kellermeyer RW. (1983) Iron overload disorders: natural history, pathogenesis, diagnosis, and therapy. *Crit Rev Clin Lab Sci*. 19(3):205-66. Review.

McLean M, Dutton MF. (1995) Cellular interactions and metabolism of aflatoxin: an update. *Pharmacol Ther*. Feb;65(2):163-92. Review.

McNamara L, MacPhail AP, Mandishona E, Bloom P, Paterson C, Rouault TA, Gordeuk VR. (1999) Non-transferrin-bound iron and hepatic dysfunction in African dietary iron overload. *Journal of Gastroenterology and Hepatology 14, 126-132.*

Meki AR, Abdel-Ghaffar SK, El-Gibaly I. (2001) Aflatoxin B_1 induces apoptosis in rat liver: protective effect of melatonin. *Neuro Endocrinol Lett*. Dec;22(6):417-26.

Mello Filho AC, Meneghini R (1984). *In vivo* formation of single strand breaks in DNA by hydrogen peroxide is mediated by the Haber-Weiss reaction. *Biochem Biophys Acta* 781:56-63.

Meneghini R. (1997) Iron homeostasis, oxidative stress, and DNA damage. *Free Radic Biol Med* 23:783-792.

Metz-Boutigue MH, Jolles J, Mazurier J, Schoentgen F, Legrand D, Spik G, Montreuil J, Jolles P. Human lactotransferrin: amino acid sequence and structural comparisons with other transferrins. *Eur J Biochem*. 1984 Dec 17; 145(3):659-76.

Meyer DJ, Harris JM, Gilmore KS, Coles B, Kensler TW, Ketterer B. (1993) Quantitation of tissue- and sex-specific induction of rat GSH transferase subunits by dietary 1,2-dithiole-3-thiones. *Carcinogenesis*. Apr; 14(4):567-72.

Miller DM, Buettner GR and Aust SD (1990). Transition Metals as Catalyst of autooxidation reactions. *Free Rad Biol & Med*. 8:95-108.

Miller DM, Stuart BP, Crowell WA. (1978) Aflatoxicosis in swine: Its effects on immunity and relationship to salmonellosis. *J. Am. Ass. Vet. Lab. Dign*. 21:135-146.

Mocchegiani E, Corradi A, Santarelli L, Tibaldi A, DeAngelis E, Borghetti P, Bonomi A, Fabris N, Cabassi E. (1998) Zinc, thymic endocrine activity and mitogen responsiveness (PHA) in piglets exposed to maternal aflatoxicosis B_1 and G_1. *Vet Immunol Immunopathol.* Apr 16; 62(3):245-60.

Moon EY, Rhee DK, Pyo S. (1999) In vitro suppressive effect of aflatoxin B_1 on murine peritoneal macrophage functions. *Toxicology.* Apr 15;133(2-3):171-9.

Morel F, Fardel O, Meyer DJ, Langouet S, Gilmore KS, Meunier B, Tu CP, Kensler TW, Ketterer B, Guillouzo A. (1993) Preferential increase of glutathione S-transferase class alpha transcripts in cultured human hepatocytes by phenobarbital, 3-methylcholanthrene, and dithiolethiones. *Cancer Res*. Jan 15;53(2):231-4.

Morrow DJ, Hill EK, Burk RF, Nammour TM, Badr KF and Roberts LJ (1990). A series of prostaglandin F2-like compounds are produced in vivo in humans by a non-cyclooxygenase, free radical-catalyzed mechanism. *Proc. Natl. Acad. Sci. USA* 87:9383-9387.

Morrow JD and Roberts LJ (1996). The isoprostanes: current knowledge and direction for future research. *Biochemical Pharmacology* 51: 1-9.

Nair J, Carmichael PL, Fernando RC, Phillips DH, Strain AJ, Bartsch H. (1998) Lipid peroxidation-induced etheno-DNA adducts in the liver of patients with the genetic metal storage disorders Wilson's disease and primary hemochromatosis. *Cancer Epidemiol Biomarkers Prev*. May;7(5):435-40.

Nielsen P, Heinrich HC. (1993) Metabolism of iron from (3,5,5-trimethylhexanoyl)ferrocene in rats. A dietary model for severe iron overload. *Biochem Pharmacol.* Jan 26;45(2):385-91.

Niranjan BG, Bhat NK, Avadhani NG. (1982) Preferential attack of mitochondrial DNA by aflatoxin B1 during hepatocarcinogenesis. *Science.* Jan 1;215(4528):73-5.

Nourooz-Zadeh K Gopaul NK, Barrow S, Mallet AI and Anggärd EE (1995). Analysis of F_2-isoprostanes as indicators of non-enzymatic lipid peroxidation *in vivo* by gas chromatography-mass spectroscopy: development of a solid phase extraction procedure. *J. Chromatography* B667: 199-208.

Nourooz-Zadeh J, Javad Tajaddini-Sarma DI, and Simon P. Wolff; (1994). Measurement of plasma hydroperoxide concentration by the ferrous oxidation – xylenol assay in conjuction with triphenylphosphine. Analytical Biochemistry 220, 403-409

Nunez MT, Gaete V, Watkins JA, Glass J. (1990) Mobilization of iron from endocytic vesicles. The effects of acidification and reduction. *J Biol Chem*. Apr 25;265(12):6688-92.

O'Connell MJ, Ward RJ, Baum H, Peters TJ. (1985) The role of iron in ferritin- and haemosiderin-mediated lipid peroxidation in liposomes. *Biochem J*. Jul 1; 229(1):135-9.

Olynyk JK, Clarke SL. (2001) Iron overload impairs pro-inflammatory cytokine responses by Kupffer cells. *J Gastroenterol Hepatol*. Apr; 16(4):438-44.

Paterson S, Armstrong NJ, Iacopetta BJ, McArdle HJ, Morgan EH. (1984) Intravesicular pH and iron uptake by immature erythroid cells. *J Cell Physiol*. Aug;120(2):225-32.

Peters TJ, O' Connel MJ Ward RJ (1985) Role of free radical mediated lipid peroxidation in the pathogenesis of hepatic damage by lysosomal disruption. In: Poli G, Cheeseman KH, Dianzani MU, Slater TF (eds) free radicals in liver injury. Oxford, IRL Press pp. 107-15.

Pietrangelo A, Rocchi E, Schiaffonati L, Ventura E, Cairo G (1990). Liver gene expression during chronic dietary iron overload in rats. *Hepatology* 11:798-804.

Ponka P. (1997) Tissue-specific regulation of iron metabolism and heme synthesis: distinct control mechanisms in erythroid cells. *Blood*. Jan 1;89(1):1-25. Review.

Qian GS, Ross RK, Yu MC, Yuan JM, Gao YT, Henderson BE, Wogan GN, Groopman JD. (1994) A follow-up study of urinary markers of aflatoxin exposure and liver cancer risk in Shanghai, People's Republic of China. *Cancer Epidemiol Biomarkers Prev*. Jan-Feb; 3(1):3-10.

Qian GS, Ross RK, Yu MC, Yuan JM, Gao YT, Henderson BE, Wogan GN, Groopman JD. (1994) A follow-up study of urinary markers of aflatoxin exposure and liver cancer risk in Shanghai, People's Republic of China. *Cancer Epidemiol Biomarkers Prev*. Jan-Feb; 3(1):3-10.

Raisuddin S, Singh KP, Zaidi SI, Paul BN, Ray PK. (1993) Immunosuppressive effects of aflatoxin in growing rats. Mycopathologia. Dec; 124(3):189-94.

Ramos CL, Pou S and Rosen GM (1995). Effects of antiinflamatory drugs on myoloperoxidase-dependent hydroxyl radical generation by human neutrophils. *Biochemical Pharmacology*. 19:1079-1084.

Rashid A, Wang JS, Qian GS, Lu BX, Hamilton SR, Groopman JD. (1999) Genetic alterations in hepatocellular carcinomas: association between loss of chromosome 4q and p53 gene mutations. *Br J Cancer*. Apr;80(1-2):59-66.

Reilly MP, Barry P, Lawson JA, Fitzgerald GA (1998). Eicosanoids and isoeicosanoids: index of cellular function and oxidative stress. *The J Nutr* Vol. 128 No. 2 Feb 434S –438S

Reitman S, Frankel S (1957) A colorimetric method for the determination of serum glutamic oxalacetic and glutamic pyruvic transaminases. *Am J Clin Pathol.* Jul;28(1):56-63.

Rizzo AF, Atroshi F, Ahotupa M, Sankari S, Elovaara E. (1994) Protective effect of antioxidants against free radical-mediated lipid peroxidation induced by DON or T-2 toxin. Zentralbl Veterinarmed A. Mar;41(2):81-90.

Roberts LJ and Morrow JD (1997). The generation and actions of isoprostanes. *Biochim Biophys Acta* 1345:121-135.

Roebuck BD, Liu YL, Rogers AE, Groopman JD, Kensler TW. (1991) Protection against aflatoxin B1-induced hepatocarcinogenesis in F344 rats by 5-(2-pyrazinyl)-4-methyl-1,2-dithiole-3-thione (oltipraz): predictive role for short-term molecular dosimetry. *Cancer Res*. Oct 15;51(20):5501-6.

Roebuck BD. (2004) Hyperplasia, partial hepatectomy, and the carcinogenicity of aflatoxin B1. J Cell Biochem. Feb 1;91(2):243-9. Review.

Ross RK, Yuan JM, Yu MC, Wogan GN, Qian GS, Tu JT, Groopman JD, Gao YT, Henderson BE. (1992) Urinary aflatoxin biomarkers and risk of hepatocellular carcinoma. *Lancet.* Apr 18;339(8799):943-6.

Ross RK, Yuan JM, Yu MC, Wogan GN, Qian GS, Tu JT, Groopman JD, Gao YT, Henderson BE. (1992) Urinary aflatoxin biomarkers and risk of hepatocellular carcinoma. *Lancet.* Apr 18; 339(8799):943-6.

Ruwart MJ, Wilkinson KF, Rush BD, Vidmar TJ, et al., (1989) The Integrated Value of Serum Procollagen III Pepetide over Time Predicts Hepatic Hydroxyproline Content and Stainable Collagen in a Model of Dietary Cirrhosis in the Rat. *Hepatology* Vol.10, No. 5, pp.801-806.

Sabbioni G, Skipper PL, Buchi G, Tannenbaum SR. (1987) Isolation and characterization of the major serum albumin adduct formed by aflatoxin B1 in vivo in rats. *Carcinogenesis*. Jun;8(6):819-24.

Santella RM (1999). Immunological methods for detection of carcinogen-DNA damage in humans. *Cancer Epidemiol. Biomarkers Prev*. 8:733-739.

Santella RM, Zhang YJ, Chen CJ, Hsieh LL, Lee CS, Haghighi B, Yang GY, Wang LW, Feitelson M. (1993) Immunohistochemical detection of aflatoxin B1-DNA adducts and hepatitis B virus antigens in hepatocellular carcinoma and nontumorous liver tissue. *Environ Health Perspect.* Mar;99:199-202.

Schaaper RM, Kunkel TA, Loeb LA. (1983) Infidelity of DNA synthesis associated with bypass of apurinic sites. *Proc Natl Acad Sci U S A.* Jan; 80(2):487-91.

Schneider C, Kurkinen M, Greaves M. (1983) Isolation of cDNA clones for the human transferrin receptor. *EMBO J.* 2(12):2259-63.

Schrager TF, Newberne PM, Pikul AH, Groopman JD. (1990) Aflatoxin-DNA adduct formation in chronically dosed rats fed a choline-deficient diet. *Carcinogenesis*. Jan;11(1):177-80.

Selden C, Owen M, Hopkins JM, Peters TJ. (1980) Studies on the concentration and intracellular localization of iron proteins in liver biopsy specimens from patients with iron overload with special reference to their role in lysosomal disruption. *Br J Haematol*. Apr;44(4):593-603.

Seymour CA and Peters TJ (1978). Organelle pathology in primary and secondary haemochromatosis with special reference to lysosomal changes. *Br. J Haematol* 40: 239-59.

Shen HM, Ong CN, LeeBL, Shi CY. (1995) Aflatoxin-B1-induced 8-hydroxy-deoxyguanosine formation in rat hepatic DNA. *Carcinogenesis* 16: 419-422.

Shen HM, Ong CN. (1996) Mutations of the p53 tumor suppressor gene and ras oncogenes in aflatoxin hepatocarcinogenesis. *Mutat Res*. Oct;366(1):23-44. Review.

Shen HM, Shi CY, Lee HP, Ong CN. (1994) Aflatoxin B1-induced lipid peroxidation in rat liver. *Toxicol Appl Pharmacol;* 127(1):145-150.

Shimizu Y, Zhu JJ, Han F, Ishikawa T, Oda H. (1999) Different frequencies of p53 codon-249 hot-spot mutations in hepatocellular carcinomas in Jiang-su province of China. *Int J Cancer*. Jul 19;82(2):187-90.

Silvotti L, Petterino C, Bonomi A, Cabassi E. (1997) Immunotoxicological effects on piglets of feeding sows diets containing aflatoxins. *Vet Rec*. Nov 1;141(18):469-72.

Sinniah R, Doggart JR, Neill DW. (1969) Diurnal variations of the serum iron in normal subjects and in patients with haemochromatosis. *Br J Haematol*. Oct;17(4):351-8.

Sipe DM, Murphy RF. 1991) Binding to cellular receptors results in increased iron release from transferrin at mildly acidic pH. *J Biol Chem*. (May 5;266(13):8002-7.

Sivakumar V, Thanislass J, Niranjali S, Devaraj H. (2001) Lipid peroxidation as a possible secondary mechanism of sterigmatocystin toxicity. *Hum Exp Toxicol*. Aug;20(8):398-403.

Sjodin T, Westing YH, Apple FS. (1990) Biochemical mechanisms for oxygen free radical formation during exercise. *Sports Med*. 10: 236-254.

Smela ME, Currier SS, Bailey EA, Essigmann JM. (2001) The chemistry and biology of aflatoxin B(1): from mutational spectrometry to carcinogenesis. *Carcinogenesis.* Apr;22(4):535-45. Review.

Sodergren E, Cederberg J, Basu S and Vessby B (2000). Vitamin E supplementation decreases basal levels of F(2)-isoprostanes and prostaglandins F(2alpha) in rats. *J. Nutr.* 130:10-14.

Sodum RS, Chung FL. (1989) Structural characterization of adducts formed in the reaction of 2,3-epoxy-4-hydroxynonanal with deoxyguanosine. *Chem Res Toxicol*. Jan-Feb;2(1):23-8.

Sokol RJ, Devereaux MW, O'Brien K, Khandwala RA, Loehr JP (1993). Abnormal hepatic mitochondrial respiration and cytochrome c oxidase activity in rats with long-term copper overload. *Gastroenterology* 105:178-187.

Sorenson WG, Jones W, Simpson J an Davidson JI. (1984) Aflatoxin in respirable airborne peanut dust. Journal of Toxicology and Environmental Health, Vol 14, pp. 525-533.

Souza MF, Tome AR, Rao VS. (1999) Inhibition by the bioflavonoid ternatin of aflatoxin B_1-induced lipid peroxidation in rat liver. *J Pharm Pharmacol*. Feb;51(2):125-9.

Stagos D, Kouris S, Kouretas D. (2004) Plant phenolics protect from bleomycin-induced oxidative stress and mutagenicity in *Salmonella typhimurium* TA102. *Anticancer Res*. Mar-Apr;24(2B):743-5.

Stanley LA, Mandel HG, Riley J, Sinha S, Higginson FM, Judah DJ, Neal GE. (1999) Mutations associated with in vivo aflatoxin B1-induced carcinogenesis need not be present in the in vitro transformations by this toxin. *Cancer Lett.* Apr 1;137(2):173-81.

Stewart BW, Kleihues P, eds. (2003) World Cancer Report. Lyon:IARC Press.

Strachan AS (1929). Hemochromatosis and Hemochromatosis in southern African Natives with a Comment on the Etiology of Hemochromatosis. MD Thesis. Glasgow, UK, University of Glasgow.

Strohmeyer G, Niederau C, Stremmel W. (1988) Survival and causes of death in hemochromatosis. Observations in 163 patients. *Ann N Y Acad Sci*. 526:245-57.

Swarts JC, Swarts DM, Maree DM, Neuse EW, La Madeleine C, Van Lier JE. (2001) Polyaspartamides as water-soluble drug carriers. Part 1: Antineoplastic activity of ferrocene-containing polyaspartamide conjugates. *Anticancer Res*. May-Jun;21(3B):2033-7.

Szasz G. (1976) Reaction-rate method for gamma-glutamyltransferase activity in serum. *Clin Chem*. Dec;22(12):2051-5.

Tashiro F, Morimura S, Hayashi K, Makino R, Kawamura H, Horikoshi N, Nemoto K, Ohtsubo K, Sugimura T, Ueno Y. (1986) Expression of the *c-Ha-ras* and *c-myc* genes in aflatoxin B_1-induced hepatocellular carcinomas. *Biochem Biophys Res Commun*. Jul 31;138(2):858-64.

Tector AJ, Olynyk JK, Britton RS, Janney CG, O'Neill R, Bacon BR (1995). Hepatic mitochondrial oxidative metabolism and lipid peroxidation in iron loaded rats fed ethanol. *J. Lab. Clin. Med*. 126:597-602.

Thorstensen K, Romslo I. (1988) Uptake of iron from transferrin by isolated rat hepatocytes. A redox-mediated plasma membrane process? *J Biol Chem*. Jun 25;263(18):8844-50.

Tiniakos D, Spandidos DA, Kakkanas A, Pintzas A, Pollice L, Tiniakos G. (1989) Expression of *ras* and *myc* oncogenes in human hepatocellular carcinoma and non-neoplastic liver tissues. *Anticancer Res*. May-Jun;9(3):715-21.

Top S, Vessieres A, Leclercq G, Quivy J, Tang J, Vaissermann J, Huche M, Jaouen G. (2003) Synthesis, biochemical properties and molecular modelling studies of organometallic specific estrogen receptor modulators (SERMs), the ferrocifens and hydroxyferrocifens: evidence for an antiproliferative effect of hydroxyferrocifens on both hormone-dependent and hormone-independent breast cancer cell lines. *Chemistry*. Nov 7;9(21):5223-36.

Towner RA, Qian SY, Kadiiska MB, Mason RP (2003) In vivo Identification of Aflatoxin-Induced Free Radicals in Rat Bile. *Free Radical Biology & Medicine. 35:10:1330-1340.*

Trinder D, Oates PS, Thomas C, Sadleir J, Morgan EH. (2000) Localisation of divalent metal transporter 1 (DMT1) to the microvillus membrane of rat duodenal enterocytes in iron deficiency, but to hepatocytes in iron overload. *Gut*. Feb;46(2):270-6.

van Renswoude J, Bridges KR, Harford JB, Klausner RD. (1982) Receptor-mediated endocytosis of transferrin and the uptake of fe in K562 cells: identification of a nonlysosomal acidic compartment. *Proc Natl Acad Sci U S A*. Oct;79(20):6186-90.

Vashisht Gopal YN, Jayaraju D, Kondapi AK. (2000) Topoisomerase II poisoning and antineoplastic action by DNA-nonbinding diacetyl and dicarboxaldoxime derivatives of ferrocene. *Arch Biochem Biophys*. Apr 1;376(1):229-35.

Vautier G, Bomford AB, Portmann BC, Metivier E, Williams R, Ryder SD. (1999) p53 mutations in british patients with hepatocellular carcinoma: clustering in genetic hemochromatosis. *Gastroenterology*. Jul;117(1):154-60.

Vernet M and Le Gall J-Y (1998) Transferrin Saturation and Screening of Genetic Hemochromatosis. *Clinical Chemistry* 44:360-362.

Vernet-Nyssen M. (1983) Is commercial serum suitable for quality control of serum total iron-binding capacity? [Letter]. *Clin Chem* 29:573-574.

Voet D, Voet JG. (1995) Biochemistry 2nd. (Rose N., ed.), John Wiley & Sons, Inc. New York.

Vulpe CD, Kuo YM, Murphy TL, Cowley L, Askwith C, Libina N, Gitschier J, Anderson GJ. (1999) Hephaestin, a ceruloplasmin homologue implicated in intestinal iron transport, is defective in the sla mouse. *Nat Genet*. Feb; 21(2):195-9.

Walker ARP and Arvidsson UB (1953). Iron 'overload' in the South African Bantu. *Trans Roy Soc Trop Med Hyg* 47:536.

Walker RJ, Beamish MR, Jacobs A, Williams R. (1973) Serum ferritin as a measure of body iron in primary idiopathic haemochromatosis. *Gut*. May;14(5):420-1.

Waller RL, Glende EA Jr. Recknagel RO (1983). Carbon tetrachloride and bromotrichloromethane toxicity. Dual role of covalent binding of metabolic cleavage products and lipid peroxidation in depression of microsomal calcium sequestration. *Biochem Pharmacol* 32:1613-7.

Wang JS, Busby WF Jr, Wogan GN. (1995) Formation and persistence of DNA adducts in organs of CD-1 mice treated with a tumorigenic dose of fluoranthene. *Carcinogenesis*. Nov;16(11):2609-16.

Wang JS, Groopman JD. (1999) DNA damage by mycotoxins. *Mutat Res.* Mar 8;424(1-2):167-81. Review.

Wang P, Chaudry IH.(1996) Mechanism of hepatocellular dysfunction during hyperdynamic sepsis. Am J Physiol. May;270(5 Pt 2):R927-38. Review.

Wayner DD, Burton GW, Ingold KU and Locke S. (1985). Quantitative measurement of the total peroxyl radical-trapping antioxidant capacity of human blood plasma by controlled peroxidation. The important contribution made by plasma proteins. *FEBS Lett.* 187:33-37.

Weiss G, Houston T, Kastner S, Johrer K, Grunewald K, Brock JH. (1997) Regulation of cellular iron metabolism by erythropoietin: activation of iron-regulatory protein and upregulation of transferrin receptor expression in erythroid cells. *Blood.* Jan 15;89(2):680-7.

Williams J, Elleman TC, Kingston IB, Wilkins AG, Kuhn KA. (1982) The primary structure of hen ovotransferrin. *Eur J Biochem*. Feb;122(2):297-303.

Winterbourn CC, and Buss IH (1999). Protein carbonyl measurement by enzyme-linked immunosorbent assay. *Methods Enzymol.* 300:106-111.
Wogan GN (1989) Molecular and cellular events associated with aflatoxin-induced hepatocarcinogenesis. *Pure Appl. Chem*. 61, 1-6.

Wogan GN. (1992). Aflatoxins as risk factors for hepatocellular carcinoma in humans. *Cancer Res.* 52,2114s-2118s.

Wogan GN. (1992) Aflatoxin carcinogenesis: interspecies potency differences and relevance for human risk assessment. *Prog Clin Biol Res*. 374:123-37. Review.

Wogan GN. (1975) Mycotoxins. Annu Rev Pharmacol. 15:437-51. Review.

Wolff SP (1994). Ferrous ion oxidation in presence of ferric ion indicator xylenol orange for measurement of hydroperoxides. *Methods in Enzymol.* 233:182-288.

Wong JJ, Hsieh DP. (1976) Mutagenicity of aflatoxins related to their metabolism and carcinogenic potential. *Proc Natl Acad Sci U S A.* Jul;73(7):2241-4.

Wong JJ, Singh R, Hsieh DP.(1977) Mutagenicity of fungal metabolites related to aflatoxin biosynthesis. *Mutat Res.* Sep;44(3):447-50.

Wong SH, Knight JA, Hopfer SM, Zaharia Q, Leach CN Jr., and Sunderman FW Jr. (1987). Lipoperoxides in plasma as measured by liquid-chromatographic separation of malondialdehyde-thiobarbituric acid adducts. *Clin. Chem*. 33:214-220.

Wu WH, Meydani M, Meydani SN, Burklund PM, Blumberg JB, Munro HN. (1990) Effect of dietary iron overload on lipid peroxidation, prostaglandin synthesis and lymphocyte proliferation in young and old rats. *J Nutr. Mar;120(3):280-9.*

Xia Y, Dawson VL, Dawson TM, Snyder SH, Zweier JL. (1996) Nitric oxide synthase generates superoxide and nitric oxide in arginine-depleted cells leading to peroxynitrite-mediated cellular injury. *Proc Natl Acad Sci U S A.* Jun 25;93(13):6770-4.

Yamashiro DJ, Tycko B, Fluss SR, Maxfield FR. (1984) Segregation of transferrin to a mildly acidic (pH 6.5) para-Golgi compartment in the recycling pathway. *Cell.* Jul;37(3):789-800.

Yang M, Zhou H, Kong RY, Fong WF, Ren LQ, Liao XH, Wang Y, Zhuang W, Yang S. (1997) Mutations at codon 249 of p53 gene in human hepatocellular carcinomas from Tongan, China. *Mutat Res.* Nov 19;381(1):25-9.

Yeh FS, Yu MC, Mo CC, Luo S, Tong MJ, Henderson BE. (1989) Hepatitis B virus, aflatoxins, and hepatocellular carcinoma in southern Guangxi, China. *Cancer Res*. May 1;49(9):2506-9.

Yip R, Dallman PR. (1996) Iron. In: Ziegler EE, Filer LJ, eds. Present Knowledge in Nutrition. 7th edition. Washington DC: ILSI Press pp. 277-292.

Yu FL. (1983) Preferential binding of aflatoxin B_1 to the transcriptionally active regions of rat liver nucleolar chromatin in vivo and in vitro. *Carcinogenesis.* 4(7):889-93.
Yu J, Ehrlich KC, Cary JW, Bhatnagar D, Cleveland TE, Payne GA, Linz JE, Woloshuk CP, Bennet JW. (2004) Clustered pathway genes in aflatoxin biosynthesis and contamination of crops. *Appl Environ Microbiol.* 70;1253-1262.

Yu MW, Lien JP, Liaw YF, Chen CJ. (1996) Effects of multiple risk factors for hepatocellular carcinoma on formation of aflatoxin B1-DNA adducts. *Cancer Epidemiol Biomarkers Prev.* Aug;5(8):613-9.

Zak O, Trinder D, Aisen P. (1994) Primary receptor-recognition site of human transferrin is in the C-terminal lobe. *J Biol Chem*. Mar 11; 269(10):7110-4.

Fig 3.1 Taken from:Stock Photography [http://www.denniskunkel.com/index.asp]

Fig 3.2 Taken from: Food Safety [http://www.nri.org/images/foodsafety1.jpg]

Figure 3.3 from: Griffiths AJF, Miller JH, Suzuki DT, Lewontin RC, Gelbart WM. An Introduction to Genetic Analysis, Seventh Edition. (2000) Folchetti N. (Ed.), New York, WH Freeman and company Library of Congress Cataloging-in-Publication Data.